PN-AAW-343
48219

DESIGN OF SOLAR **HOT WATER** SYSTEMS FOR JAMAICA

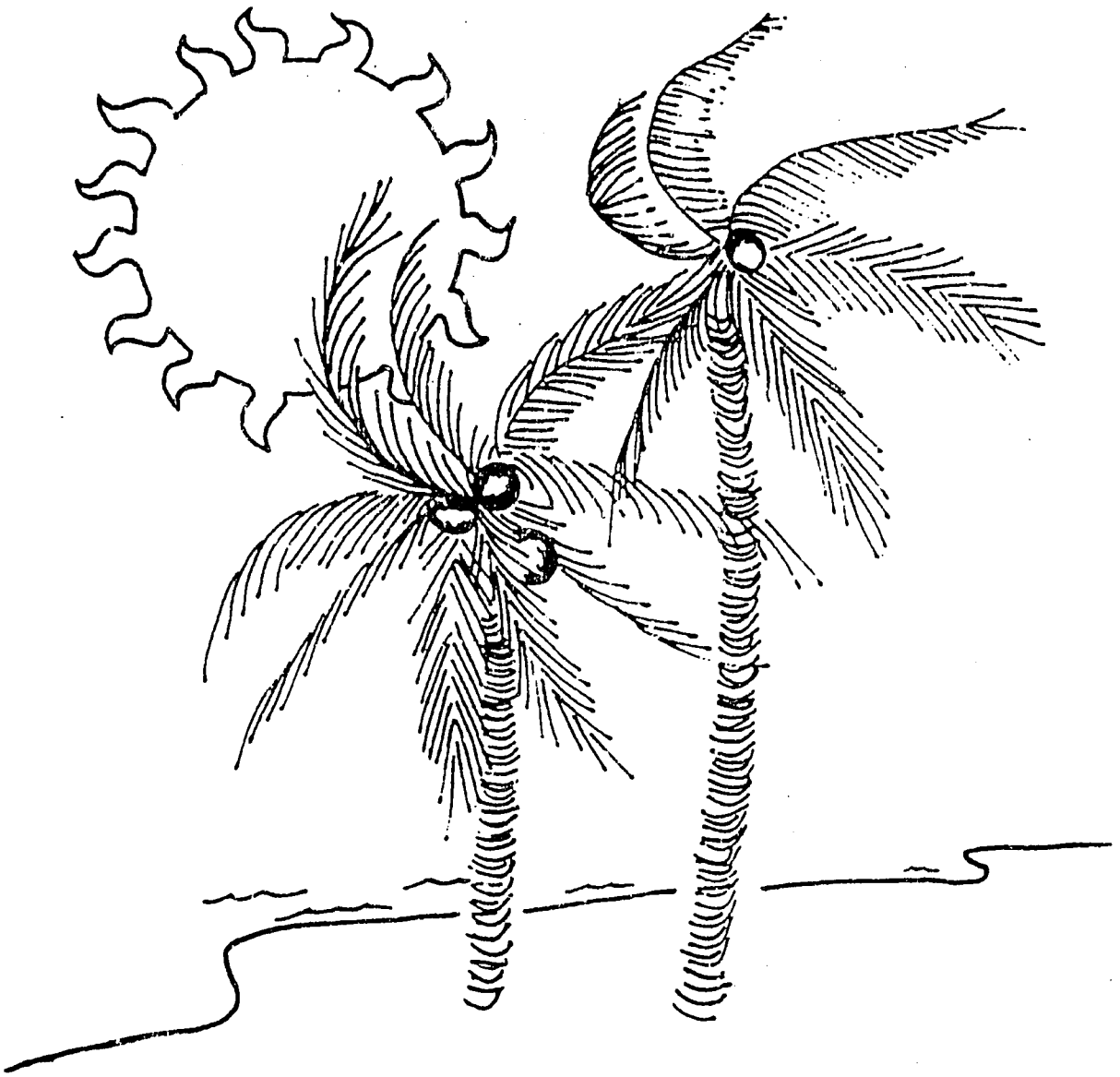

DESIGN OF SOLAR HOT WATER SYSTEMS FOR JAMAICA

Prepared for
Ministry of Mining and Energy
2, St. Lucia Avenue
Kingston, 5, Jamaica

USAID/GOJ ENERGY ASSISTANCE PROJECT

Prepared By
Charles J. Cromer, P.E.

May 23, 1983

V

TABLE OF CONTENTS

	Page
INTRODUCTION	i
MODULE 1: THE SOLAR RESOURCE:.....	1-1
The Nature Of Solar Radiation.	1-2
Radiation On A Horizontal Surface.	1-2
Liu and Jordan method.	1-4
Klein, Duffie, and Beckman method.	1-4
Radiation On A Tilted Surface.	1-7
Determination of K_T .	1-10
Historical data.	1-11
References (Module 1).	1-14
List of symbols.	1-15
Conversion factors.	1-16
Insolation tables	1-17
Paper 1-1 (Estimation by Rainfall)	1-51
MODULE 2: SITING THE COLLECTOR ARRAY.....	2-1
The Solar Window.	2-2
Bennett Sun Angle Chart.	2-4
Collector Orientation.	2-8
MODULE 3: COLLECTOR TYPES AND CONSTRUCTION:.....	3-1
Types Of Collectors.	3-2
Flatplate collectors.	3-4
Flatplate collector Materials.	3-7
High temperature collectors.	3-11
Heat Flow.	3-13
Conduction.	3-13
Convection.	3-13
Radiation.	3-15
General Principles (flat plate).	3-16
Heat Losses From Collector.	3-17
Solar Energy Absorption.	3-20
Selective Surfaces.	3-23
MODULE 4: TESTING OF COLLECTORS:.....	4-1
ASHRAE Standard 93-77.	4-2
Heat Recovery Factor.	4-4
Collector Temperature Patterns.	4-5
Collector Efficiency.	4-6
Collector characteristics.	4-7
Collector Performance Ratings.	4-11
The Incident Angle Modifier.	4-13
The cosine effect.	4-15
K for various collectors	4-17
Collector Time Constant	4-18
References (Module 4)	4-19
Paper 4-1 (Performance of Collector Type)	4-20

TABLE OF CONTENTS (CONTINUED)

MODULE 5: SIZING THE SOLAR ARRAY:..... 5-1
The Hot Water Load 5-2
Sizing The Tank 5-4
Finding Solar Panel Requirement 5-4
Sizing To Solar Fraction 5-5
F-Chart 5-5
Simplified Sizing Procedure 5-8
References (Module 5) 5-16

MODULE 6: TYPES OF SOLAR HOT WATER SYSTEMS:..... 6-1
Thermosiphon 6-2
Forced Circulation 6-2
Integral Or Breadbox 6-5
Photovoltaic Circulated 6-6
Pumped With Heat Exchanger 6-7
Pumped Drainback 6-8
Pumped Draindown 6-10

MODULE 7: PLUMBING MULTIPLE TANKS:..... 7-1
Preheat, Series, Parallel 7-2
Thermosiphon Tank Assembly 7-5
Pumped Tank Assembly 7-6

MODULE 8: TYPES OF CONTROLS AND CONTROLLERS:..... 8-1
Control Types 8-2
Photovoltaic Control Sizing 8-5
Paper 5-1 (PV Match With Circulating Pump) 8-8
PV And Pump I-V Charts 8-13

MODULE 9: PLUMBING MULTIPLE COLLECTOR ARRAYS:..... 9-1
Piping Large Arrays 9-2
Piping Between Collectors 9-7
Collector-To-Storage Runs 9-7
Hangers And Supports 9-10
Forces On The Collector Array 9-13
Special Array Considerations For Thermosiphon Systems 9-15
References(Module 9) 9-17

TABLE OF CONTENTS (CONT.)

MODULE 10: SIZING THE PIPE AND CIRCULATION PUMP:..... 10-1
- Pumps 10-2
  - Flow rate through the collector 10-3
- Pipe 10-4
- Air Vents 10-6
- Heat Exchangers 10-6
- Pressure/Temperature Relief Valves 10-6
- Insulation On Piping 10-7
- Special Piping Considerations For Thermosiphon 10-7
- Pump And Pipe Tables 10-11
- Paper 10-1 (Collector Flowrate) 10-17

MODULE 11: SOLAR INSTRUMENTATION:..... 11-1
- Advantages and Problems of Laboratory Monitoring 11-2
- Advangages and Problems of Field Monitoring 11-3
- Levels of Instrumentation 11-4
- Instrumentation Diagram 11-6
- Btu Meters 11-7
- References (Module 11) 11-12

APPENDIX A: SOLAR SYSTEM SIZING FOR JAMAICA - F-chart:..... A-1

APPENDIX B: A NOTE ON PIPE INSULATION:..... B-1

APPENDIX C: SIMPLIFIED SOLAR COLLECTOR TEST PROCEDURE:..... D-1

Introduction:

The engineering and design of a solar hot water system involves seven major steps: 1) Determine the solar resource and location for the array. 2) Determine the required hot water load for the installation. 3) Determine the size of solar array needed to meet the load. 4) Determine the size of storage needed to meet the load. 5) Diagram the collector array, tank location and piping runs. 6) Size & select the pump(s) (for pumped systems) 7) Finish detailed drawings.

This manual places emphasis on the technical aspects of design and engineering of solar hot water systems for Jamaica. More basic installation information on solar systems is provided by the manual: Solar Water Heater Installation and Operation, C.J. Cromer, 1983, which is the text developed for use with a vocational level solar installers training course. This text is available through the Ministry of Mining and Energy.

The design engineer should be knowledgeable of the information provided in the above mentioned text, as well as the information provided in this manual. Some of the information is common to both manuals, however this manual deals primarily with the calculation of the parameters needed for the selection of proper system components. The completion of step 7, the assembly of these components into detailed drawings, also requires knowledge of proper installation practices and techniques covered in the "Installation and Operation" manual.

MODULE 1: THE SOLAR RESOURCE

OBJECTIVE

The objective of this module is for the trainee to be able to determine the radiation on a tilted collector surface by using the charts and figures presented in this module.

THE NATURE OF SOLAR RADIATION

The energy from the sun is derived from thermonuclear reactions in its core. This energy makes its way to the sun's exterior layers from which it is radiated into interplanetary space. The radiation consists of particulate radiation and electromagnetic radiation. The particulate radiation consists of electrons and protons and is commonly referred to as the "solar wind". The electromagnetic radiation is what is commonly referred to as "solar radiation" and it is this radiation that partially penetrates the earth's atmosphere and is utilized in a solar heating or cooling system. This solar radiation varies inversely with distance from the sun. Since the earth's distance from the sun varies by only about three percent during the course of the year, the amount of solar radiation reaching the upper limits of the earth's atmosphere is essentially constant. This is referred to as the "solar constant" and is defined as the solar radiation received on a unit area of surface per unit time perpendicular to the radiation at the earth's mean distance from the sun. Recent measurements of the solar constant have indicated that its value should be 1353 watts per square meter (429 Btu per square foot per hour, 4871 kJ per square meter per hour, or 1.940 calories per square centimeter per minute). (Ref. 1)

The amount of radiation on a surface perpendicular to the solar radiation at the mean distance of the earth from the sun is essentially constant, but the amount of solar radiation that reaches the surface of the earth will vary with respect to latitude and time of year. It is necessary that this "solar weather" be known in order to design a solar system.

RADIATION ON A HORIZONTAL SURFACE

Hottel and Whiller (Ref. 2,3) first developed a comprehensive approach to a generalized, long-term description of solar weather. Using their "utilizability" method, it is possible to separate the treatment of solar radiation data from the physical and geometrical characteristics of a particular collector. It is not sufficient, for purposes of predicting detailed collector performance, to use only long-term daily or monthly averages of solar radiation. Hourly fluctuations of radiation about these average values must be taken into account. This is accomplished by using hourly radiation data for a particular location over a period of several years to establish a set of radiation distribution and Θ curves.

The Θ or "utilizability function is of central importance and accounts statistically for the effect of fluctuations in solar weather on collector performance. By use of the utilizability function, account is taken of the fact that only a certain average fraction of the incident radiation on a collector can be "utilized", i.e., converted to usable heat at a given collector plate temperature, etc.

Utilizability is inherently taken into account when collector performance is calculated using these hourly radiation values as an input parameter and the heat delivered in the form of hot water as the output. The specific performance equation of the collector must be used to do this calculation. This calculation and a discussion of panel performance is covered by Modules 4 and 5. For now we will limit our discussion to the determination of the monthly average daily total radiation.

9

LIU AND JORDAN METHOD

The ϕ-curves of Hottel and Whillier are site-specific; a set of distribution and ϕ-curves must be generated for each location using solar radiation over a three to five year period. Liu and Jordan (Ref. 4, 5) showed that the long-term solar weather at any location can be characterized surprisingly well by just two site-specific parameters:

$\overline{H}$ - monthly average daily total radiation on a horizontal surface

$\overline{K}_T = \overline{H}/\overline{H}_o$

where $\overline{H}_o$ is the extraterrestrial daily radiation on a horizontal surface, calculated from the equations of solar geometry for the 16th day of each month.

The term, $\overline{K}_T$, introduced by Liu and Jordan, can be considered as a "cloudiness index" which, together with $\overline{H}$, characterizes the solar weather for a particular month. A large value of $\overline{K}_T$ indicates sunny and rather uniform clear weather. A small value indicates cloudy, more fluctuating weather. In most cases, $\overline{K}_T$ is found to lie in the range from about 0.3 up to 0.75.

$\overline{K}_T$ is of importance in characterizing a collector's performance, because it provides a measure of direct to diffuse radiation which in turn is used to estimate solar radiation on a tilted surface. However, Liu and Jordan used $\overline{H}_o$ found for the 16th day of each month. A more often used definition of $\overline{K}_T$ was developed by Klein, Duffie, and Beckman at the Universty of Wisconsin.

KLEIN, DUFFIE, AND BECKMAN METHOD

The Liu and Jordan approach has been modified by Klein, Duffie, and Beckman. (Ref. 6) In this approach, $\overline{K}_T$ is defined as the ratio between the monthly average daily total radiation on a horizontal surface and the mean daily extraterrestrial radiation, $\overline{H}_o$, where $\overline{H}_o$ may be calculated from the equation:

$$\overline{H}_o = \frac{1}{\Delta t} \int_0^{\Delta t} \frac{24}{\pi} I_{sc}\left(1 + 0.033 \cos\left(\frac{360\, n}{365}\right)\right)$$

$$\left[\cos\phi \cos\delta \sin\omega_s + \omega_s \frac{2\pi}{360} \sin\phi \sin\delta\right] dt$$

where Δt = 1 month, I_{sc} is the solar constant, ϕ is the latitude, δ is the solar declination, and ω_s is the sunset hour angle. This is described on the following sketch.

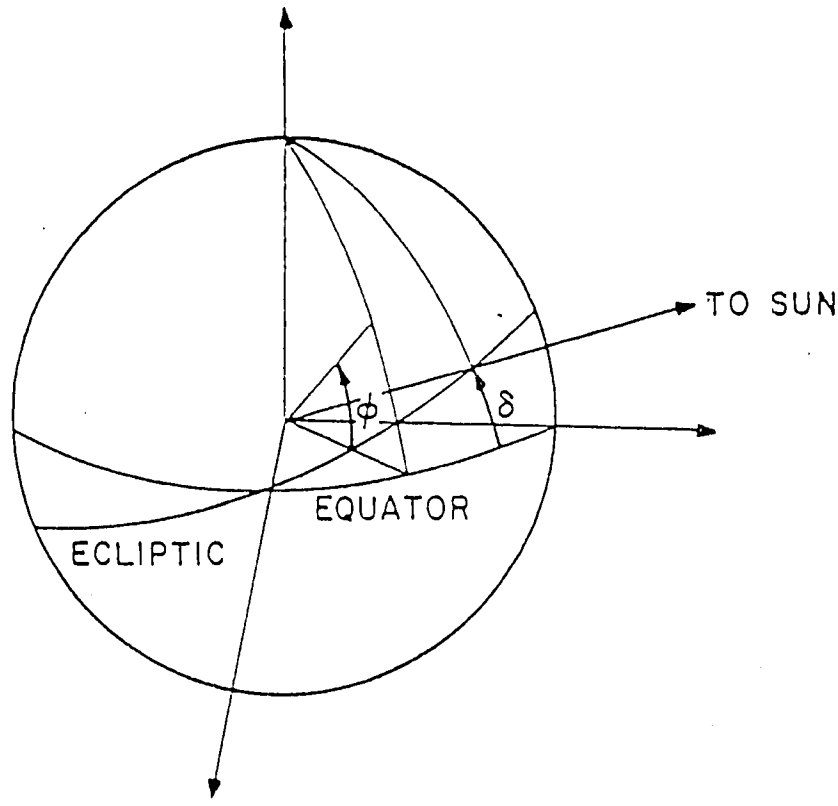

Since the spin axis of the earth is tilted relative to the ecliptic plane, as shown on the sketch, the amount of radiation on a horizontal

surface of given area will vary with respect to the time of year. This is illustrated on the sketches below:

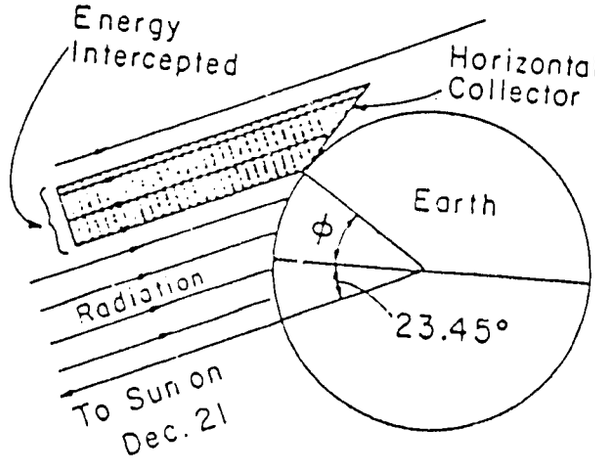

(a) Radiation on a Horizontal Collector

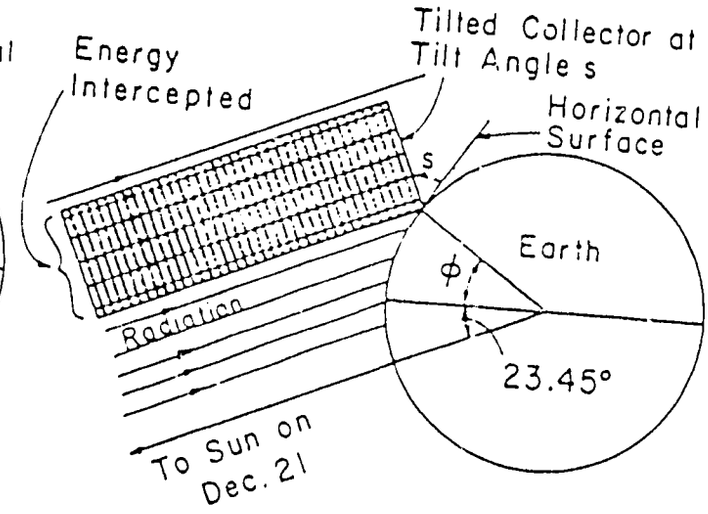

(b) Radiation on a Collector Tilted Perpendicular to the Radiation

The declination varies with time of year according to the approximate equation:

$$\delta = 23.45 \sin \left[360 \frac{284 + n}{365}\right] \quad \text{(Degrees)}$$

where n is the day of the year (n = 1 for January 1).

The sunset hour angle is given by:

$$\cos \omega_s = -\tan \phi \ \tan \delta.$$

The average daily insolation on a horizontal surface at a given latitude for a given month may be calculated by using the above equations. This has been done for you for several latitudes for the months of the year. This is provided as Table 1-2. A computer program in Microsoft Basic is provided as Figure 1 that will calculate H_o for any latitude and month.

RADIATION ON A TILTED SURFACE

Radiation measurements are made worldwide on $\bar{H}$, the radiation on the surface of the earth in the horizontal plane. When $\bar{H}$ is known, then $\bar{K}_T$ may be calculated by: $\bar{K}_T = \bar{H}/\bar{H}_o$. For estimating purposes, values for $\bar{H}$ may be taken from contour maps(see Figure 1-2) showing mean solar radiation, but in many areas these are not fully developed. However, it may be possible to get a good estimate of $\bar{K}_T$ from other measured data. For now, lets look at the effect of tilt.

In order to determine the performance of flat-plate collectors, it is required that the average daily radiation on a tilted surface, $\bar{H}_T$, be known. This may be expressed by $\bar{H}_T = \bar{R}\bar{H} = \bar{R}\bar{K}_T\bar{H}_o$, where $\bar{R}$ is defined as the ratio of the average daily radiation on a tilted surface to that on a horizontal surface for each month. There are several methods for calculating $\bar{R}$, all of which give slightly different results but do not strongly affect the calculations of long-term performance of flat-plate collectors.

One method, proposed by Liu and Jordan, is to express $\bar{R}$ by:

$$\bar{R} = \left(1 - \frac{\bar{D}}{\bar{H}}\right) R_D + \frac{\bar{D}}{\bar{H}} \left(\frac{1 + \cos s}{2}\right) + \rho \left(\frac{1 - \cos s}{2}\right)$$

where $\bar{D}/\bar{H}$ is obtained from:

$$\bar{D}/\bar{H} = 1.3903 - 4.0273\ \bar{K}_T + 5.541\ \bar{K}_T^{\,2} - 3.108\ \bar{K}_T^{\,3}$$

Also,

$$R_D = \frac{\cos(\phi - s)\cos\delta\ \sin\omega_s' + \omega_s'\sin(\phi - s)\sin\delta}{\cos\phi\ \cos\delta\ \sin\omega_s + \omega_s\ \sin\phi\ \sin\delta}$$

where

$$\omega_s' \triangleq [\arccos(-\tan\phi\ \tan\delta),\ \arccos(-\tan(\phi - s)\tan\delta]$$

In the above equations,

s is the collector tilt angle from the horizontal

ρ is ground reflectance

$\bar{D}$ is average daily diffuse radiation for each month

R_D is ratio of the average daily beam radiation on the tilted surface to that on a horizontal surface for each month.

Notice $\bar{D}/\bar{H}$ is a function of $\bar{K}_T$. This was the important relationship developed by Liu and Jordan(ref 4).

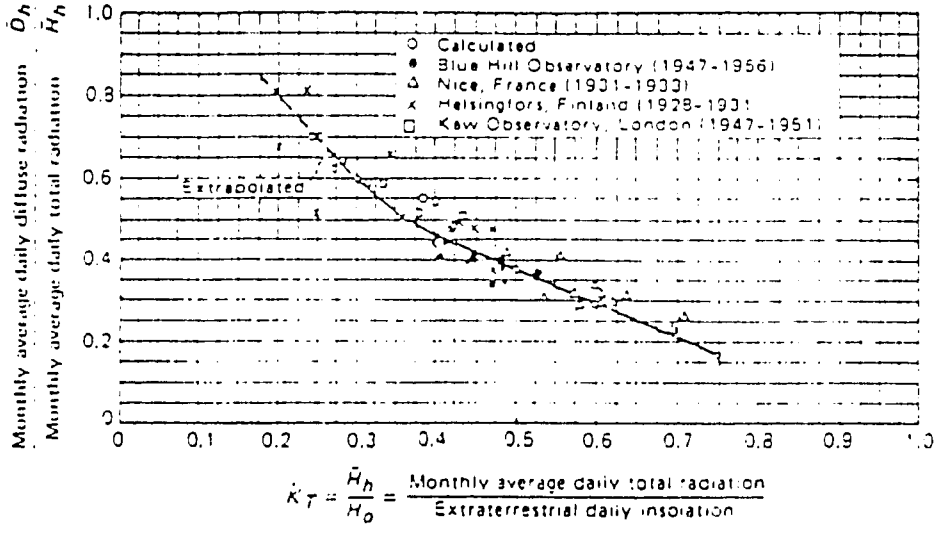

Also notice that if an average reflectance value is assumed, the other variables are latitude, tilt and declination. Thus for a fixed latitude, and given tilt, the relationship between $\bar{K}_T$ and $\bar{R}$ can be found for each month of the year. This has been done for you in Figures 1-8 through Figure 1-10.

Since $\bar{H}_T = \bar{R}\,\bar{K}_T\,\bar{H}_0$ we can determine monthly average $\bar{H}_T$ values for given tilts if we know $\bar{K}_T$.

Tilt for Direct Normal Radiation at Solar Noon:

A flat plate collector panel can be tilted such that it presents a normal surface to the solar noon direct beam radiation. Any tilt angle, s, is defined as the included angle from the horizontal surface to the plane of the collector. Direct normal tilt s_N at noon is a function of the declination angle and the latitude.

$s_N =$ where

= latitude and is negative below the equator and positive above the equator. As shown earlier, can be found by the equation:

$$= 23.45 \sin 360 \frac{284 + n}{365} \quad \text{(degrees)}$$

where n is the Julian date (Jan 1st = 1, December 31st = 365).

Though direct normal does not always find the tilt for maximum insolation, for areas with $\bar{K}_T$ above 0.35 the error is usually small.

The following Table provides the declination angle and direct normal tilt angle for 18°N latitude for the mid day of each month (16th).

TABLE OF DECLINATIONS

Date	Day of Year	Declination, (Degrees)	= 18°N Direct Normal Tilt
Jan. 16	16	-21.10	39.1
Feb. 16	47	-12.95	30.95
Mar. 16	75	- 2.42	20.42
Apr. 16	106	9.78	8.22
May 16	136	19.03	-1.03
June 16	167	23.35	-5.35
July 16	197	21.35	-3.35
Aug. 16	228	13.45	4.55
Sept. 16	259	1.81	16.19
Oct. 16	289	-9.97	27.97
Nov. 16	320	-19.38	37.38
Dec. 16	350	-23.37	41.37

Determination of K_T

Lopez and Soderstrom of the Center for Energy and Environment Research at the Universty of Puerto Rico have developed a linear fit correlation between annual rainfall and annual $\overline{K}_T$ at 94% with a standard error in $\overline{K}_T$ of .018. (See Paper 1-1)

The equation is;

$$\overline{K}_T = 0.659 - 0.000886\ R$$

where R = rainfall measured in cm.

It is also found that the annual $\overline{K}_T$ is quite constant throughout the year, probably because the moderate rainy season, with slightly higher cloud cover, occurs during the summer when $\overline{H}_0$ is higher. Such a relationship provides a means by which insolation values may be estimated for countries in the Caribbean.

The Climatology branch of the Jamaican Meteorological Society found a good correlation (.32-.75) between rainfall and mean hours of sunshine (Ref 7). Though hours of sunshine are not suitable to provide amounts of radiation because the recorders may vary in their minimum threshold that is considered sunlight (70 to 280 w/m^2); nevertheless the good correlation supports the use of rainfall as a measure of $\overline{K}_T$ for Jamaica. (See Figure 1-10)

Figure 1-11 provides a contour map of Jamaica providing average daily horizontal radiation calculated using the rainfall method and mean 30 year rainfall values of 1931 thru 1960 (Ref. 7) (Figure 1-11).

Figure 1-12 through 1-24 provide annual and monthly rainfall distributions that can be used to obtain monthly estimates of insolation using the rainfall method.

Historical Data:

The best method for calculating the sunlight available on a tilted plane is to use actual historical data. These are limited for Jamaica. The only historical data available to the author at the time of writing is provided as Table 1-4 through 1-7 (Ref 8). It has been suggested that the data for Norman Manley Airport and Bodles are consistantly high due to problems with the data collection equipment.

Jamaica is in the process of developing a good base of insolation data-both diffuse and direct components. When this becomes available, the solar engineer is advised to adjust his calculations accordingly.

Example:

Find the daily average radiation in December on a solar panel sloped 20° to the south, located in Montego Bay (lat 18°N).

Solution 1:

The contour map (Figure 1-5) provides the site receives just under the 400 cal/cm^2 perday line - assume 380 cal/cm^2 perday. Thus,

380 cal/cm^2 perday = 1.5081 Btu/cm^2 perday

1400 Btu/ft^2 perday = $\bar{H}$

From Table 1-3 $\bar{H}_o$ = 2343 $\bar{K}_T = \frac{1400}{2343} = .60$

From Figure 1-7 $\bar{R}$ = 1.28 thus

$\bar{H}_T = \bar{H}\,\bar{R}$ = 1792 Btu/ft^2 per December day

on the sloped surface.

Solution 2:

Figure 1-24 shows MoBay along the 3 inch contour.

3.0 in x 2.54 cm/in = 7.62 cm/mo

7.62 cm/mo x 12 mo/yr = 91.44 cm/yr.

$\bar{K}_T = .659 - (91.44 \times 8.86 \times 10^{-4})$

$\bar{K}_T = .659 - .081 = .578$

From Figure 1-7 $\bar{R}$ = 1.273

$\bar{H}_T = \bar{R}\,\bar{H}_o\,\bar{K}_T = 1.273 \times 2343 \times .578$

$\bar{H}_T$ = 1724 Btu/ft^2.day

Solution 3:

Historical data, Table 1-6 shows for Smithfield, not far from MoBay, as

$\bar{H} = 1302$, so $\bar{K}_T = \frac{1302}{2343} = .556$

from Figure 1-7, $\bar{R}$ = 1.265

$\bar{H}_T = \bar{H}\,\bar{R} = 1302 \times 1.265 = 1647$

Solution 1:

Using the same historical data from Table 1-6, interpolating between 18^0 and 25^0 to 20^0:

$$\frac{2}{7}(1647 - 1573) + 1573 = 1594$$

REFERENCES

1. Duffie, J.A. and Beckman, W.A., Solar Energy Thermal Processes, John Wiley and Sons, New York, New York, 1974.

2. Hottel, H.C. and Whillier, A., Evaluation of Flat-Plate Collector Performance. Transactions of the Conference on the Use of Solar Energy: The Scientific Basis, II, Part 1, Section A, 74-104 (1955).

3. Whillier, A., Solar Energy Collection and Its Utilization for House Heating. D. Sc. Thesis in Mechanical Engineering, M.I.T., Cambridge, Massachusetts (1953).

4. Liu, B.Y.H. and Jordan, R.C., "A Rational Procedure for Predicting a Long-Term Average Performance of Flat-Plate Collectors", Solar Energy, Vol. 17, No. 2, 1963.

5. Liu, B.Y.H. and Jordan, R.C.,"The Interrelationship and Characteristic Distribution of Direct, Diffuse and Total Solar Radiation." Solar Energy, Vol. 4, No. 3, pp. 1-19, 1960.

6. Klein, S.A., Beckman, W.A., and Duffie, J.A., "A Design Procedure for Solar Heating Systems". Presented at the International Solar Energy Society Meeting, Los Angeles, California, July/August 1975.

7. The Climate of Jamaica, The Climatology Branch of the Jamaican Meteorological Service, First Edition, 1973.

8. George, K.; Kreider, J., and Nuney, A.; Design, Construction and Installation Manual for Solar Water Heating Systems in Jamaica and the West Indies; March 1977; Ministry of Mining and Natural Resources Kingstons, Jamaica.

9. Solar Heating of Residential Buildings, U.S. Department of Commerce, Economic Development Administration, October, 1977.

LIST OF SYMBOLS

$\bar{D}$	Average daily diffuse radiation for a month
$\bar{H}$	Monthly average daily total radiation on a horizontal surface, Btu/(day)(ft^2)
H_o	Extraterrestrial daily radiation on a horizontal surface for the 16th day of the month, Btu/(day)(ft^2)
$\bar{H}_o$	Monthly averaged value of extraterrestrial radiation on a horizontal surface, Btu/(day)(ft^2)
$\bar{H}_T$	Radiation on a tilted surface averaged over a day, Btu/(day)(ft^2)
$\bar{K}_T$	Fraction of solar energy which penetrates through the earth's atmosphere on daily average
n	Number of days from January 1
$\bar{R}$	Fraction of average daily radiation on tilted surface compared with a horizontal surface
R_D	Ratio of the average daily beam radiation on a tilted surface to that on a horizontal surface
S	Collector tilt angle from horizontal, degrees
T	Temperature, °F
t	Time variable
ω_s	Sunset hour angle, degrees from solar noon
δ	Position of the sun relative to the equatorial plane at solar noon, degrees
ϕ	Latitude angle, degrees (north plus)
ρ	Reflectivity of material or ground surface

TABLE 1-1

CONVERSION FACTORS

Energy (radiant energy)

From To	J = Ws	kcal	Wh	BTU
J = Ws	1	238.8×10^{-6}	277.8×10^{-6}	947.8×10^{-6}
kcal	4.184×10^{3}	1	1.162	3.968
Wh	3.600×10^{3}	859.8×10^{-3}	1	3.410
BTU	1.054×10^{3}	252.0×10^{-3}	292.9×10^{-3}	1

Energy density (irradiation)

From To	ly=cal cm^{-2}	Jm^{-2}	Wh m^{-2}	BTU ft^{-2}
ly = cal cm^{-2}	1	41.84×10^{3}	11.63	3.6867
J m^{-2}	23.89×10^{-6}	1	277.8×10^{-6}	88.11×10^{-6}
Wh m^{-2}	85.93×10^{-3}	3.60×10^{3}	1	316.82×10^{-3}
BTU ft^{-2}	271.25×10^{-3}	11.35×10^{3}	3.152	1

Power density (irradiance)

From To	ly min^{-1}	Wm^{-2}	BTU$min^{-1}ft^{-2}$	BTU $h^{-1}ft^{-2}$
ly min^{-1}	1	697.3	3.688	221.2
Wm^{-2}	1.434×10^{-3}	1	5.285×10^{-3}	317.21×10^{-3}
BTU $min^{-1}ft^{-2}$	271.1×10^{-3}	189.2	1	59.97
BTU $h^{-1}ft^{-2}$	4.5208×10^{-3}	3.152	16.68×10^{-3}	1

Example

To convert BTU $h^{-1}ft^{-2}$ to Wm^{-2} multiply by 3.152, e.g. 100 BTU $h^{-1}ft^{-2}$ is equal to 315.2 Wm^{-2}.

Table 1-2

```
>RUN
LATITUDE? 17.5
MONTH? JANUARY

DAILY RATES:  BTU/SQ FT, (MJ/SQ M)

 2374.51 ( 26.9484 )          2378.15 ( 26.9897 )
 2382.07 ( 27.0342 )          2386.27 ( 27.0819 )
 2390.75 ( 27.1327 )          2395.5 ( 27.1866 )
 2400.52 ( 27.2436 )          2405.81 ( 27.3036 )
 2411.36 ( 27.3666 )          2417.17 ( 27.4325 )
 2423.24 ( 27.5014 )          2429.56 ( 27.5731 )
 2436.13 ( 27.6477 )          2442.95 ( 27.725 )
 2450 ( 27.8051 )             2457.29 ( 27.8879 )
 2464.82 ( 27.9732 )          2472.57 ( 28.0612 )
 2480.54 ( 28.1517 )          2488.73 ( 28.2446 )
 2497.13 ( 28.34 )            2505.74 ( 28.4376 )
 2514.54 ( 28.5376 )          2523.55 ( 28.6398 )
 2532.74 ( 28.7441 )          2542.11 ( 28.8505 )
 2551.67 ( 28.9589 )          2561.39 ( 29.0693 )
 2571.28 ( 29.1815 )          2581.33 ( 29.2956 )
 2591.54 ( 29.4114 )
MONTHLY DAILY AVERAGE 2466.48 ( 27.7922 )
READY
```

```
>RUN
LATITUDE? 17.5
MONTH? FEBRUARY

DAILY RATES:  BTU/SQ FT, (MJ/SQ M)

 2601.88 ( 29.5258 )          2612.37 ( 29.6479 )
 2622.99 ( 29.7684 )          2633.74 ( 29.8904 )
 2644.6 ( 30.0137 )           2655.58 ( 30.1383 )
 2666.67 ( 30.2641 )          2677.85 ( 30.391 )
 2689.12 ( 30.5189 )          2700.48 ( 30.6473 )
 2711.92 ( 30.7776 )          2723.42 ( 30.9082 )
 2734.99 ( 31.0395 )          2746.62 ( 31.1714 )
 2758.29 ( 31.3039 )          2770.01 ( 31.4369 )
 2781.76 ( 31.5702 )          2793.53 ( 31.7038 )
 2805.33 ( 31.8377 )          2817.14 ( 31.9717 )
 2828.95 ( 32.1058 )          2840.77 ( 32.2399 )
 2852.57 ( 32.3739 )          2864.36 ( 32.5077 )
 2876.13 ( 32.6413 )          2887.87 ( 32.7745 )
 2899.58 ( 32.9073 )          2911.24 ( 33.0397 )

MONTHLY DAILY AVERAGE 2753.92 ( 31.2543 )
READY
```

```
>RUN
LATITUDE? 17.5
MONTH? MARCH

DAILY RATES:  BTU/SQ FT, (MJ/SQ M)

 2922.85 ( 33.1715 )          2934.41 ( 33.3027 )
 2945.91 ( 33.4332 )          2957.34 ( 33.5629 )
 2968.69 ( 33.6918 )          2979.97 ( 33.8197 )
 2991.16 ( 33.9467 )          3002.26 ( 34.0727 )
 3013.26 ( 34.1976 )          3024.16 ( 34.3213 )
 3034.95 ( 34.4438 )          3045.63 ( 34.565 )
 3056.19 ( 34.6848 )          3066.63 ( 34.8033 )
 3076.95 ( 34.9203 )          3087.12 ( 35.0358 )
 3097.17 ( 35.1498 )          3107.07 ( 35.2622 )
 3116.83 ( 35.373 )           3126.44 ( 35.4821 )
 3135.9 ( 35.5894 )           3145.21 ( 35.695 )
 3154.35 ( 35.7998 )          3163.34 ( 35.9008 )
 3172.16 ( 36.0009 )          3180.81 ( 36.0991 )
 3189.3 ( 36.1954 )           3197.61 ( 36.2898 )
 3205.76 ( 36.3822 )          3213.72 ( 36.4726 )
 3221.51 ( 36.561 )
MONTHLY DAILY AVERAGE 3081.76 ( 34.975 )
READY
```

```
>RUN
LATITUDE? 17.5
MONTH? APRIL

DAILY RATES:  BTU/SQ FT, (MJ/SQ M)

 3229.12 ( 36.6474 )          3236.56 ( 36.7317 )
 3243.81 ( 36.814 )           3250.88 ( 36.8943 )
 3257.77 ( 36.9725 )          3264.48 ( 37.0486 )
 3271 ( 37.1226 )             3277.34 ( 37.1946 )
 3283.5 ( 37.2645 )           3289.48 ( 37.3324 )
 3295.28 ( 37.3982 )          3300.9 ( 37.4619 )
 3306.33 ( 37.5236 )          3311.59 ( 37.5833 )
 3316.67 ( 37.641 )           3321.57 ( 37.6966 )
 3326.3 ( 37.7503 )           3330.86 ( 37.802 )
 3335.24 ( 37.8518 )          3339.46 ( 37.8995 )
 3343.51 ( 37.9455 )          3347.39 ( 37.9896 )
 3351.11 ( 38.0319 )          3354.68 ( 38.0723 )
 3358.08 ( 38.1109 )          3361.33 ( 38.1479 )
 3364.42 ( 38.1829 )          3367.37 ( 38.2164 )
 3370.18 ( 38.2482 )          3372.84 ( 38.2784 )

MONTHLY DAILY AVERAGE 3312.64 ( 37.5952 )
READY
```

Table 1-2 (Cont.)

```
>RUN
LATITUDE? 17.5
MONTH? MAY

DAILY RATES:  BTU/SQ FT, (MJ/SQ M)

 3375.36 ( 38.307 )          3377.74 ( 38.334 )
 3379.99 ( 38.3596 )         3382.11 ( 38.3836 )
 3384.11 ( 38.4063 )         3385.98 ( 38.4275 )
 3387.73 ( 38.4474 )         3389.37 ( 38.466 )
 3390.89 ( 38.4833 )         3392.31 ( 38.4994 )
 3393.62 ( 38.5143 )         3394.84 ( 38.5291 )
 3395.95 ( 38.5407 )         3396.97 ( 38.5523 )
 3397.9 ( 38.5628 )          3398.74 ( 38.5724 )
 3399.51 ( 38.5811 )         3400.19 ( 38.5888 )
 3400.8 ( 38.5957 )          3401.33 ( 38.6018 )
 3401.8 ( 38.6071 )          3402.2 ( 38.6116 )
 3402.54 ( 38.6155 )         3402.82 ( 38.6187 )
 3403.04 ( 38.6212 )         3403.22 ( 38.6232 )
 3403.35 ( 38.6246 )         3403.43 ( 38.6255 )
 3403.46 ( 38.626 )          3403.46 ( 38.626 )
 3403.42 ( 38.6255 )
MONTHLY DAILY AVERAGE 3395.42 ( 38.5347 )
READY
```

```
>RUN
LATITUDE? 17.5
MONTH? JUNE

DAILY RATES:  BTU/SQ FT, (MJ/SQ M)

 3403.35 ( 38.6247 )         3403.25 ( 38.6235 )
 3403.11 ( 38.622 )          3402.95 ( 38.6202 )
 3402.77 ( 38.6181 )         3402.56 ( 38.6158 )
 3402.34 ( 38.6132 )         3402.1 ( 38.6105 )
 3401.84 ( 38.6075 )         3401.57 ( 38.6044 )
 3401.28 ( 38.6012 )         3400.98 ( 38.5978 )
 3400.68 ( 38.5943 )         3400.36 ( 38.5908 )
 3400.04 ( 38.5871 )         3399.71 ( 38.5834 )
 3399.38 ( 38.5796 )         3399.04 ( 38.5758 )
 3398.7 ( 38.5719 )          3398.36 ( 38.568 )
 3398.01 ( 38.5641 )         3397.66 ( 38.5601 )
 3397.3 ( 38.5561 )          3396.95 ( 38.552 )
 3396.59 ( 38.5479 )         3396.22 ( 38.5438 )
 3395.86 ( 38.5397 )         3395.49 ( 38.5354 )
 3395.11 ( 38.5312 )         3394.73 ( 38.5266 )

MONTHLY DAILY AVERAGE 3399.81 ( 38.5822 )
READY
```

```
>RUN
LATITUDE? 17.5
MONTH? JULY

DAILY RATES:  BTU/SQ FT, (MJ/SQ M)

 3394.34 ( 38.5224 )         3393.94 ( 38.5179 )
 3393.54 ( 38.5133 )         3393.12 ( 38.5086 )
 3392.69 ( 38.5037 )         3392.25 ( 38.4987 )
 3391.79 ( 38.4935 )         3391.32 ( 38.4881 )
 3390.82 ( 38.4825 )         3390.31 ( 38.4766 )
 3389.77 ( 38.4705 )         3389.2 ( 38.4641 )
 3388.61 ( 38.4574 )         3387.99 ( 38.4503 )
 3387.33 ( 38.4429 )         3386.64 ( 38.4351 )
 3385.91 ( 38.4268 )         3385.14 ( 38.418 )
 3384.33 ( 38.4088 )         3383.47 ( 38.399 )
 3382.55 ( 38.3887 )         3381.59 ( 38.3777 )
 3380.57 ( 38.3662 )         3379.49 ( 38.3539 )
 3378.35 ( 38.3409 )         3377.14 ( 38.3272 )
 3375.86 ( 38.3127 )         3374.51 ( 38.2974 )
 3373.09 ( 38.2812 )         3371.58 ( 38.2642 )
 3369.99 ( 38.2461 )
MONTHLY DAILY AVERAGE 3385.07 ( 38.4173 )
READY
```

```
>RUN
LATITUDE? 17.5
MONTH? AUGUST

DAILY RATES:  BTU/SQ FT, (MJ/SQ M)

 3368.32 ( 38.2271 )         3366.56 ( 38.2071 )
 3364.7 ( 38.186 )           3362.74 ( 38.1639 )
 3360.69 ( 38.1405 )         3358.53 ( 38.1161 )
 3356.27 ( 38.0904 )         3353.89 ( 38.0634 )
 3351.41 ( 38.0352 )         3348.8 ( 38.0056 )
 3346.08 ( 37.9747 )         3343.23 ( 37.9423 )
 3340.25 ( 37.9086 )         3337.15 ( 37.8734 )
 3333.91 ( 37.8366 )         3330.54 ( 37.7984 )
 3327.03 ( 37.7585 )         3323.38 ( 37.7171 )
 3319.58 ( 37.674 )          3315.64 ( 37.6293 )
 3311.55 ( 37.5829 )         3307.31 ( 37.5348 )
 3302.92 ( 37.4849 )         3298.37 ( 37.4333 )
 3293.67 ( 37.3799 )         3288.8 ( 37.3247 )
 3283.78 ( 37.2677 )         3278.59 ( 37.2088 )
 3273.24 ( 37.1481 )         3267.73 ( 37.0855 )
 3262.05 ( 37.021 )
MONTHLY DAILY AVERAGE 3325.06 ( 37.7361 )
READY
```

Table 1-2 (Cont.)

```
>RUN
LATITUDE? 17.5
MONTH? SEPTEMBER

DAILY RATES:  BTU/SQ FT, (MJ/SQ M)

3256.2 ( 36.9547 )          3250.19 ( 36.8864 )
3244.01 ( 36.8163 )         3237.66 ( 36.7442 )
3231.14 ( 36.6702 )         3224.45 ( 36.5943 )
3217.57 ( 36.5165 )         3210.57 ( 36.4368 )
3203.37 ( 36.3552 )         3196.01 ( 36.2716 )
3188.49 ( 36.1862 )         3180.8 ( 36.099 )
3172.94 ( 36.0098 )         3164.93 ( 35.9188 )
3156.75 ( 35.826 )          3148.41 ( 35.7314 )
3139.92 ( 35.635 )          3131.27 ( 35.5368 )
3122.46 ( 35.4369 )         3113.51 ( 35.3353 )
3104.41 ( 35.232 )          3095.17 ( 35.1271 )
3085.78 ( 35.0206 )         3076.26 ( 34.9125 )
3066.6 ( 34.8029 )          3056.82 ( 34.6919 )
3046.9 ( 34.5793 )          3036.86 ( 34.4654 )
3026.71 ( 34:3502 )         3016.44 ( 34.2336 )

MONTHLY DAILY AVERAGE 3146.75 ( 35.7126 )
READY
```

```
>RUN
LATITUDE? 17.5
MONTH? OCTOBER

DAILY RATES:  BTU/SQ FT, (MJ/SQ M)

3006.06 ( 34.1158 )         2995.57 ( 33.9968 )
2984.99 ( 33.8767 )         2974.31 ( 33.7554 )
2963.53 ( 33.6332 )         2952.68 ( 33.51 )
2941.74 ( 33.3859 )         2930.74 ( 33.261 )
2919.66 ( 33.1353 )         2908.52 ( 33.0089 )
2897.32 ( 32.8818 )         2886.08 ( 32.7542 )
2874.79 ( 32.626 )          2863.46 ( 32.4975 )
2852.1 ( 32.3685 )          2840.71 ( 32.2393 )
2829.31 ( 32.1099 )         2817.89 ( 31.9803 )
2806.47 ( 31.8507 )         2795.05 ( 31.7211 )
2783.64 ( 31.5916 )         2772.24 ( 31.4622 )
2760.86 ( 31.3331 )         2749.52 ( 31.2043 )
2738.2 ( 31.0759 )          2726.93 ( 30.948 )
2715.71 ( 30.8206 )         2704.54 ( 30.6939 )
2693.44 ( 30.5679 )         2682.41 ( 30.4427 )
2671.45 ( 30.3184 )
MONTHLY DAILY AVERAGE 2840 ( 32.2312 )
READY
```

```
>RUN
LATITUDE? 17.5
MONTH? NOVEMBER

DAILY RATES:  BTU/SQ FT, (MJ/SQ M)

2660.58 ( 30.195 )          2649.8 ( 30.0726 )
2639.11 ( 29.9513 )         2628.53 ( 29.8313 )
2618.06 ( 29.7125 )         2607.71 ( 29.595 )
2597.48 ( 29.4789 )         2587.39 ( 29.3643 )
2577.43 ( 29.2513 )         2567.62 ( 29.1399 )
2557.95 ( 29.0303 )         2548.45 ( 28.9224 )
2539.1 ( 28.8163 )          2529.93 ( 28.7122 )
2520.93 ( 28.61 )           2512.11 ( 28.51 )
2503.48 ( 28.412 )          2495.04 ( 28.3162 )
2486.6 ( 28.2227 )          2478.76 ( 28.1315 )
2470.93 ( 28.0426 )         2463.31 ( 27.9562 )
2455.92 ( 27.8723 )         2448.75 ( 27.7909 )
2441.8 ( 27.7121 )          2435.09 ( 27.6359 )
2428.62 ( 27.5625 )         2422.39 ( 27.4918 )
2416.41 ( 27.4239 )         2410.68 ( 27.3588 )

MONTHLY DAILY AVERAGE 2523.34 ( 28.6374 )
READY
```

```
>RUN
LATITUDE? 17.5
MONTH? DECEMBER

DAILY RATES:  BTU/SQ FT, (MJ/SQ M)

2405.2 ( 27.2967 )          2399.98 ( 27.2374 )
2395.02 ( 27.1811 )         2390.33 ( 27.1279 )
2385.9 ( 27.0777 )          2381.75 ( 27.0305 )
2377.87 ( 26.9865 )         2374.27 ( 26.9456 )
2370.94 ( 26.9079 )         2367.9 ( 26.8733 )
2365.14 ( 26.842 )          2362.67 ( 26.814 )
2360.48 ( 26.7891 )         2358.58 ( 26.7676 )
2356.98 ( 26.7494 )         2355.66 ( 26.7344 )
2354.64 ( 26.7229 )         2353.91 ( 26.7146 )
2353.47 ( 26.7096 )         2353.33 ( 26.708 )
2353.48 ( 26.7097 )         2353.93 ( 26.7148 )
2354.68 ( 26.7233 )         2355.71 ( 26.735 )
2357.04 ( 26.7501 )         2358.67 ( 26.7686 )
2360.59 ( 26.7903 )         2362.79 ( 26.8154 )
2365.29 ( 26.8437 )         2368.08 ( 26.8754 )
2371.15 ( 26.9102 )
MONTHLY DAILY AVERAGE 2367.27 ( 26.8662 )
READY
```

Table 1-3

Annual daily average 2991.92 Btu/ft^2

```
READY
 RUN
LATITUDE? 18.0
MONTH? JANUARY

DAILY RATES:  BTU/SQ FT, (MJ/SQ M)

 2350.51 ( 26.676 )          2354.19 ( 26.7178 )
 2358.16 ( 26.7628 )         2362.41 ( 26.811 )
 2366.94 ( 26.8624 )         2371.74 ( 26.917 )
 2376.82 ( 26.9746 )         2382.18 ( 27.0354 )
 2387.8 ( 27.0991 )          2393.68 ( 27.1659 )
 2399.82 ( 27.2356 )         2406.22 ( 27.3083 )
 2412.88 ( 27.3838 )         2419.78 ( 27.4621 )
 2426.93 ( 27.5433 )         2434.32 ( 27.6271 )
 2441.94 ( 27.7136 )         2449.79 ( 27.8027 )
 2457.67 ( 27.8944 )         2466.17 ( 27.9887 )
 2474.69 ( 28.0853 )         2483.42 ( 28.1843 )
 2492.35 ( 28.2857 )         2501.48 ( 29.3893 )
 2510.8 ( 29.4951 )          2520.31 ( 28.6031 )
 2530.01 ( 28.7131 )         2539.88 ( 28.8251 )
 2549.91 ( 28.939 )          2560.12 ( 29.0548 )
 2570.47 ( 29.1724 )
MONTHLY DAILY AVERAGE 2443.66 ( 27.7332 )
READY
```

```
>RUN
LATITUDE? 18.0
MONTH? FEBRUARY

DAILY RATES:  BTU/SQ FT, (MJ/SQ M)

 2580.98 ( 29.2916 )         2591.63 ( 29.4125 )
 2602.42 ( 29.5349 )         2613.34 ( 29.6589 )
 2624.38 ( 29.7842 )         2635.54 ( 29.9109 )
 2646.81 ( 30.0387 )         2658.19 ( 30.1677 )
 2669.65 ( 30.2979 )         2681.2 ( 30.429 )
 2692.84 ( 30.5611 )         2704.55 ( 30.694 )
 2716.32 ( 30.8276 )         2728.16 ( 30.9619 )
 2740.05 ( 31.0969 )         2751.98 ( 31.2323 )
 2763.95 ( 31.3682 )         2775.96 ( 31.5044 )
 2787.96 ( 31.6409 )         2800.02 ( 31.7775 )
 2812.08 ( 31.9143 )         2824.13 ( 32.0511 )
 2836.18 ( 32.1879 )         2848.22 ( 32.3245 )
 2860.24 ( 32.4609 )         2872.23 ( 32.597 )
 2884.19 ( 32.7327 )         2896.11 ( 32.868 )

MONTHLY DAILY AVERAGE 2735.69 ( 31.0474 )
READY
```

```
>RUN
LATITUDE? 18.0
MONTH? MARCH

DAILY RATES:  BTU/SQ FT, (MJ/SQ M)

 2907.99 ( 33.0029 )         2919.82 ( 33.1371 )
 2931.58 ( 33.2706 )         2943.28 ( 33.4034 )
 2954.91 ( 33.5354 )         2966.47 ( 33.6665 )
 2977.94 ( 33.7967 )         2989.32 ( 33.9259 )
 3000.61 ( 34.0539 )         3011.79 ( 34.1809 )
 3022.88 ( 34.3067 )         3033.85 ( 34.4312 )
 3044.7 ( 34.5544 )          3055.44 ( 34.6762 )
 3066.05 ( 34.7966 )         3076.52 ( 34.9155 )
 3086.87 ( 35.0329 )         3097.08 ( 35.1488 )
 3107.14 ( 35.263 )          3117.05 ( 35.3755 )
 3126.82 ( 35.4863 )         3136.43 ( 35.5954 )
 3145.89 ( 35.7027 )         3155.18 ( 35.8082 )
 3164.31 ( 35.9119 )         3173.28 ( 36.0136 )
 3182.08 ( 36.1135 )         3190.7 ( 36.2114 )
 3199.16 ( 36.3073 )         3207.44 ( 36.4013 )
 3215.54 ( 36.4932 )
MONTHLY DAILY AVERAGE 3071.23 ( 34.8555 )
READY
```

```
>RUN
LATITUDE? 18.0
MONTH? APRIL

DAILY RATES:  BTU/SQ FT, (MJ/SQ M)

 3223.46 ( 36.5832 )         3231.21 ( 36.6711 )
 3238.77 ( 36.7569 )         3246.16 ( 36.8407 )
 3253.36 ( 36.9224 )         3260.38 ( 37.0021 )
 3267.21 ( 37.0797 )         3273.87 ( 37.1552 )
 3280.33 ( 37.2286 )         3286.62 ( 37.2999 )
 3292.72 ( 37.3692 )         3298.65 ( 37.4364 )
 3304.39 ( 37.5015 )         3309.95 ( 37.5646 )
 3315.33 ( 37.6257 )         3320.53 ( 37.6848 )
 3325.56 ( 37.7418 )         3330.41 ( 37.7969 )
 3335.08 ( 37.8499 )         3339.59 ( 37.9011 )
 3343.93 ( 37.9503 )         3348.1 ( 37.9976 )
 3352.1 ( 38.0431 )          3355.95 ( 38.0867 )
 3359.63 ( 38.1285 )         3363.15 ( 38.1685 )
 3366.52 ( 38.2067 )         3369.74 ( 38.2432 )
 3372.31 ( 38.2781 )         3375.73 ( 38.3112 )

MONTHLY DAILY AVERAGE 3311.37 ( 37.5809 )
READY
```


20

Table 1-3 (Cont.)

```
>RUN
LATITUDE? 18.0
MONTH? MAY

DAILY RATES:  BTU/SQ FT, (MJ/SQ M)

 3378.51 ( 38.3429 )          3381.15 ( 38.3727 )
 3383.65 ( 38.4012 )          3386.02 ( 38.428 )
 3388.26 ( 38.4535 )          3390.38 ( 38.4775 )
 3392.37 ( 38.5001 )          3394.24 ( 38.5213 )
 3396 ( 38.5412 )             3397.64 ( 38.5599 )
 3399.17 ( 38.5773 )          3400.6 ( 38.5935 )
 3401.93 ( 38.6085 )          3403.16 ( 38.6225 )
 3404.29 ( 38.6354 )          3405.34 ( 38.6472 )
 3406.29 ( 38.6581 )          3407.16 ( 38.668 )
 3407.96 ( 38.677 )           3408.67 ( 38.6851 )
 3409.31 ( 38.6923 )          3409.88 ( 38.6988 )
 3410.39 ( 38.7046 )          3410.83 ( 38.7096 )
 3411.21 ( 38.7139 )          3411.54 ( 38.7176 )
 3411.81 ( 38.7207 )          3412.03 ( 38.7232 )
 3412.2 ( 38.7251 )           3412.33 ( 38.7266 )
 3412.41 ( 38.7275 )
MONTHLY DAILY AVERAGE 3401.83 ( 38.6074 )
READY
```

```
>RUN
LATITUDE? 18.0
MONTH? JUNE

DAILY RATES:  BTU/SQ FT, (MJ/SQ M)

 3412.46 ( 38.7281 )          3412.47 ( 38.7281 )
 3412.44 ( 38.7278 )          3412.38 ( 38.7272 )
 3412.29 ( 38.7262 )          3412.18 ( 38.7249 )
 3412.04 ( 38.7233 )          3411.87 ( 38.7214 )
 3411.69 ( 38.7193 )          3411.48 ( 38.717 )
 3411.26 ( 38.7144 )          3411.02 ( 38.7117 )
 3410.76 ( 38.7088 )          3410.49 ( 38.7057 )
 3410.21 ( 38.7025 )          3409.91 ( 38.6992 )
 3409.61 ( 38.6957 )          3409.29 ( 38.6921 )
 3408.96 ( 38.6884 )          3408.63 ( 38.6846 )
 3408.29 ( 38.6807 )          3407.93 ( 38.6767 )
 3407.57 ( 38.6726 )          3407.2 ( 38.6683 )
 3406.82 ( 38.664 )           3406.43 ( 38.6596 )
 3406.03 ( 38.6551 )          3405.62 ( 38.6505 )
 3405.2 ( 38.6457 )           3404.77 ( 38.6408 )

MONTHLY DAILY AVERAGE 3409.59 ( 38.6954 )
READY
```

```
>RUN
LATITUDE? 18.0
MONTH? JULY

DAILY RATES:  BTU/SQ FT, (MJ/SQ M)

 3404.33 ( 38.6359 )          3403.87 ( 38.6306 )
 3403.4 ( 38.6252 )           3402.91 ( 38.6197 )
 3402.4 ( 38.6139 )           3401.87 ( 38.608 )
 3401.33 ( 38.6017 )          3400.76 ( 38.5953 )
 3400.16 ( 38.5885 )          3399.54 ( 38.5815 )
 3398.89 ( 38.5741 )          3398.21 ( 38.5664 )
 3397.5 ( 38.5583 )           3396.75 ( 38.5498 )
 3395.96 ( 38.5408 )          3395.13 ( 38.5314 )
 3394.26 ( 38.5215 )          3393.34 ( 38.5111 )
 3392.37 ( 38.5001 )          3391.35 ( 38.4886 )
 3390.28 ( 38.4764 )          3389.15 ( 38.4635 )
 3387.95 ( 38.45 )            3386.7 ( 38.4357 )
 3385.37 ( 38.4206 )          3383.98 ( 38.4048 )
 3382.51 ( 38.3881 )          3380.96 ( 38.3706 )
 3379.33 ( 38.3521 )          3377.62 ( 38.3327 )
 3375.82 ( 38.3123 )
MONTHLY DAILY AVERAGE 3393.36 ( 38.5113 )
READY
```

```
>RUN
LATITUDE? 18.0
MONTH? AUGUST

DAILY RATES:  BTU/SQ FT, (MJ/SQ M)

 3373.93 ( 38.2908 )          3371.95 ( 38.2683 )
 3369.87 ( 38.2447 )          3367.69 ( 38.22 )
 3365.41 ( 38.1941 )          3363.01 ( 38.1669 )
 3360.51 ( 38.1385 )          3357.89 ( 38.1088 )
 3355.16 ( 38.0778 )          3352.31 ( 38.0454 )
 3349.33 ( 38.0116 )          3346.22 ( 37.9764 )
 3342.91 ( 37.9397 )          3339.62 ( 37.9014 )
 3336.12 ( 37.8617 )          3332.48 ( 37.8204 )
 3328.7 ( 37.7775 )           3324.77 ( 37.7329 )
 3320.7 ( 37.6867 )           3316.48 ( 37.6388 )
 3312.11 ( 37.5892 )          3307.59 ( 37.5379 )
 3302.91 ( 37.4847 )          3298.07 ( 37.4299 )
 3293.07 ( 37.3732 )          3287.92 ( 37.3146 )
 3282.6 ( 37.2543 )           3277.11 ( 37.192 )
 3271.47 ( 37.1279 )          3265.65 ( 37.062 )
 3259.67 ( 36.9941 )
MONTHLY DAILY AVERAGE 3326.98 ( 37.7568 )
READY
```

Table 1-3 (Cont.)

```
>RUN
LATITUDE? 18.0
MONTH? SEPTEMBER

DAILY RATES:  BTU/SQ FT, (MJ/SQ M)

3253.52 ( 36.9243 )          3247.21 ( 36.8526 )
3240.72 ( 36.779 )           3234.06 ( 36.7034 )
3227.24 ( 36.626 )           3220.24 ( 36.5466 )
3213.08 ( 36.4653 )          3205.75 ( 36.3821 )
3198.24 ( 36.2969 )          3190.58 ( 36.2099 )
3182.74 ( 36.121 )           3174.74 ( 36.0302 )
3166.58 ( 35.9375 )          3158.25 ( 35.8431 )
3149.76 ( 35.7467 )          3141.12 ( 35.6486 )
3132.31 ( 35.5497 )          3123.36 ( 35.4471 )
3114.25 ( 35.3437 )          3104.99 ( 35.2386 )
3095.59 ( 35.1319 )          3086.04 ( 35.0235 )
3076.35 ( 34.9126 )          3066.53 ( 34.8021 )
3056.57 ( 34.6891 )          3046.48 ( 34.5746 )
3036.27 ( 34.4587 )          3025.94 ( 34.3415 )
3015.49 ( 34.2229 )          3004.93 ( 34.103 )

MONTHLY DAILY AVERAGE 3139.63 ( 35.6313 )
READY
```

```
>RUN
LATITUDE? 18.0
MONTH? OCTOBER

DAILY RATES:  BTU/SQ FT, (MJ/SQ M)

2994.26 ( 33.9819 )          2983.48 ( 33.8596 )
2972.61 ( 33.7363 )          2961.65 ( 33.6119 )
2950.6 ( 33.4864 )           2939.46 ( 33.36 )
2928.25 ( 33.2328 )          2916.97 ( 33.1048 )
2905.62 ( 32.976 )           2894.22 ( 32.8465 )
2882.75 ( 32.7164 )          2871.24 ( 32.5858 )
2859.69 ( 32.4547 )          2848.11 ( 32.3232 )
2836.5 ( 32.1915 )           2824.86 ( 32.0594 )
2813.21 ( 31.9272 )          2801.55 ( 31.7948 )
2789.88 ( 31.6624 )          2778.23 ( 31.5301 )
2766.58 ( 31.3979 )          2754.95 ( 31.266 )
2743.34 ( 31.1343 )          2731.77 ( 31.0029 )
2720.24 ( 30.872 )           2708.75 ( 30.7417 )
2697.31 ( 30.6119 )          2685.94 ( 30.4828 )
2674.63 ( 30.3544 )          2663.39 ( 30.2269 )
2652.24 ( 30.1003 )
MONTHLY DAILY AVERAGE 2824.27 ( 32.0527 )
READY
```

```
>RUN
LATITUDE? 18.0
MONTH? NOVEMBER

DAILY RATES:  BTU/SQ FT, (MJ/SQ M)

2641.17 ( 29.9747 )          2630.2 ( 29.8502 )
2619.33 ( 29.7268 )          2608.56 ( 29.6047 )
2597.92 ( 29.4838 )          2587.39 ( 29.3643 )
2576.99 ( 29.2463 )          2566.73 ( 29.1299 )
2556.6 ( 29.015 )            2546.63 ( 28.9018 )
2536.81 ( 28.7903 )          2527.15 ( 28.6807 )
2517.66 ( 28.573 )           2508.34 ( 28.4672 )
2499.2 ( 28.3635 )           2490.25 ( 28.2619 )
2481.48 ( 28.1624 )          2472.91 ( 28.0651 )
2464.55 ( 27.9702 )          2456.39 ( 27.8776 )
2448.44 ( 27.7874 )          2440.71 ( 27.6997 )
2433.21 ( 27.6146 )          2425.93 ( 27.532 )
2418.69 ( 27.452 )           2412.08 ( 27.3748 )
2405.52 ( 27.3003 )          2399.2 ( 27.2286 )
2393.13 ( 27.1597 )          2387.32 ( 27.0937 )

MONTHLY DAILY AVERAGE 2501.69 ( 28.3917 )
READY
```

```
>RUN
LATITUDE? 18.0
MONTH? DECEMBER

DAILY RATES:  BTU/SQ FT, (MJ/SQ M)

2381.76 ( 27.0306 )          2376.47 ( 26.9706 )
2371.44 ( 26.9135 )          2366.68 ( 26.8595 )
2362.19 ( 26.8085 )          2357.98 ( 26.7607 )
2354.04 ( 26.7161 )          2350.39 ( 26.6746 )
2347.01 ( 26.6363 )          2343.93 ( 26.6013 )
2341.13 ( 26.5695 )          2338.62 ( 26.541 )
2336.4 ( 26.5158 )           2334.47 ( 26.494 )
2332.84 ( 26.4754 )          2331.5 ( 26.4603 )
2330.46 ( 26.4485 )          2329.72 ( 26.44 )
2329.27 ( 26.435 )           2329.12 ( 26.4333 )
2329.27 ( 26.435 )           2329.72 ( 26.4401 )
2330.47 ( 26.4485 )          2331.51 ( 26.4604 )
2332.86 ( 26.4756 )          2334.5 ( 26.4943 )
2336.43 ( 26.5162 )          2338.66 ( 26.5415 )
2341.19 ( 26.5702 )          2344 ( 26.6022 )
2347.11 ( 26.6374 )
MONTHLY DAILY AVERAGE 2343.26 ( 26.5937 )
READY
```

Table 1-4

HISTORICAL SOLAR RADIATION* AND TEMPERATURE DATA
NORMAN MANLEY AIRPORT, KINGS' N, JAMAICA

Month	Surface Tilt 0°	10°	18°	25°	Ambient Temperature (°F)
JAN.	1825[1]	2081[2]	2248[2]	2365[2]	74.6
FEB.	2016	2204	2314	2380	77.4
MAR.	1969	2045	2071	2068	73.2
APR.	2161	2149	2105	2041	78.6
MAY	2223	2139	2040	1932	80.9
JUN	2238	2120	1997	1869	81.9
JUL.	2164	2067	1959	1845	84.5
AUG.	2197	2156	2088	2005	84.4
SEP.	1921	1961	1960	1936	81.9
OCT.	1851	1981	2051	2086	80.9
NOV.	1729	1937	2070	2159	79.1
DEC.	1759	2032	2214	2344	78.6
Annual Average	2004.4				

* Units are Btu/(day)(ft^2)

[1] Historical data (1974-75)

[2] Calculated from historical data by methods in Solar Energy for Heating and Cooling of Buildings, ASHRAE, 1977. Foreground reflection of 20% assumed.

21

Table 1-5

HISTORICAL SOLAR RADIATION* AND TEMPERATURE DATA
BODLES, ST. CATHERINE, JAMAICA

Month	Surface Tilt 0°	10°	18°	25°	Ambient Temperature (°F)
JAN.	1895[1]	2171[2]	2352[2]	2479[2]	73.1
FEB.	2068	2265	2381	2451	72.1
MAR.	2201	2294	2328	2328	73.8
APR.	2256	2245	2198	2131	75.7
MAY	2220	2136	2037	1929	76.8
JUN.	2279	2158	2031	1899	78.1
JUL.	2186	2087	1978	1862	79.1
AUG.	2039	2002	1940	1865	79.0
SEP.	1888	1926	1925	1901	77.7
OCT.	1987	2134	2215	2257	76.6
NOV.	1748	1960	2095	2186	76.6
DEC.	1737	2014	2206	2333	75.5
Annual Average	2042				

*Units are Btu/(day)(ft^2)

[1]Historical data (1974-75)

[2]Calculated from historical data by methods in Solar Energy for Heating and Cooling of Buildings, ASHRAE, 1977. Foreground reflection of 20% assumed.

30

Table 1-6

HISTORICAL SOLAR RADIATION* AND TEMPERATURE DATA
SMITHFIELD, HANOVER, JAMAICA

Month	Surface Tilt 0°	10°	18°	25°	Ambient Temperature (°F)
JAN.	1313[1]	1460[2]	1553[2]	1616[2]	74.4[3]
FEB.	1397	1498	1555	1586	74.5
MAR.	1478	1525	1539	1533	75.1
APR.	1633	1625	1593	1548	76.9
MAY	1600	1549	1486	1417	78.1
JUN.	1604	1533	1457	1376	79.5
JUL.	1644	1580	1507	1429	80.1
AUG.	1486	1462	1422	1372	80.1
SEP.	1375	1397	1393	1374	79.9
OCT.	1361	1439	1479	1496	79.5
NOV.	1257	1381	1457	1507	78.5
DEC.	1302	1466	1573	1647	77.0
Annual Average	1454				

*Units are Btu/(day)(ft^2)

[1]Historical data (1974-75)

[2]Calculated from historical data by methods in Solar Energy for Heating and cooling of Buildings, ASHRAE, 1977. Foreground reflection of 20% assumed.

[3]Data for Montego Bay

Table 1-7

TILT FACTORS* FOR 18° NORTH LATITUDE (R_D)

Month	Surface Tilt (Deg) 10°	18°	25°
JAN.	1.17	1.28	1.36
FEB.	1.12	1.18	1.22
MAR.	1.05	1.07	1.07
APR.	0.99	0.97	0.93
MAY	0.95	0.89	0.83
JUN.	0.93	0.86	0.78
JUL.	0.94	0.87	0.80
AUG.	0.98	0.94	0.89
SEP.	1.03	1.03	1.02
OCT.	1.10	1.15	1.18
NOV.	1.16	1.26	1.33
DEC.	1.19	1.32	1.40

* The tilt factor is the ratio of beam radiation on a tilted surface to that on a horizontal surface. (See Chapter 2.)

Figure 1-1

```
10 REM "THIS PROGRAM PROVIDES A MONTHLY AVERAGE EXTRATARRESTRIAL
20 REM DAILY INSOLATION LEVEL AS DEFINED BY KLEIN, DUFFIE, AND  BECKMAN.
22 REM ************** BY C.J. CROMER, NOV. 1982 ***************
25 G=0:E=0:DK=0:ST=0:N=0
45 CLS
50 PRINT"LATITUDE";:INPUT LAT
100 PRINT"MONTH";:INPUT MO$
1000 IF MO$="JANUARY" THEN G=1:E=31
1010 IF MO$="FEBRUARY" THEN G=32:E=59
1020 IF MO$="MARCH" THEN G=60:E=90
1030 IF MO$="APRIL" THEN G=91:E=120
1040 IF MO$="MAY" THEN G=121:E=151
1050 IF MO$="JUNE"THEN G=152:E=181
1060 IF MO$="JULY"THEN G=182:E=212
1070 IF MO$="AUGUST"THEN G=213:E=243
1080 IF MO$="SEPTEMBER"THEN G=244:E=273
1090 IF MO$="OCTOBER"THEN G=274:E=304
1100 IF MO$="NOVEMBER"THEN G=305:E=334
1110 IF MO$="DECEMBER"THEN G=335:E=365
1120 IF G=0 THEN PRINT"PLEASE SPELL THE FULL MONTH CORRECTLY":GOTO 100
1150 PRINT:PRINT"DAILY RATES:  BTU/SQ FT, (MJ/SQ M)":PRINT
1200 FOR N=G TO E
1210 FOR J=1 TO 2
1500 IF J=1 THEN SOLCST=429.2 ELSE SOLCST=4.371
2000 DK=23.45*SIN(360*(284+N)/365*.01745329)
2010 X=-TAN(LAT*.01745329)*TAN(DK*.01745329)
2020 SE=ATN(X/SQR(-(*X-1))+1.5708)*57.295779
2030 H1=7.6944*SOLCST*(1+.033*COS(N*6.2832/365))
2040 H2=COS(LAT*.01745329)*COS(DK*.01745329)*SIN(SE*.01745329)
2050 H3=SE*.01745329*SIN(LAT*.01745329)*SIN(DK*.01745329)
2060 H0=H1*(H2+H3)
2070 IF J=1 THEN PRINT H0;ELSE PRINT"("H0")",
2080 IF J=1 THEN Q=Q+H0 ELSE Q1=Q1+H0
2085 NEXT J,N
2090 PRINT:PRINT"MONTHLY DAILY AVERAGE" Q/(E-G+1)"("Q1/(E-G+1)")"
```

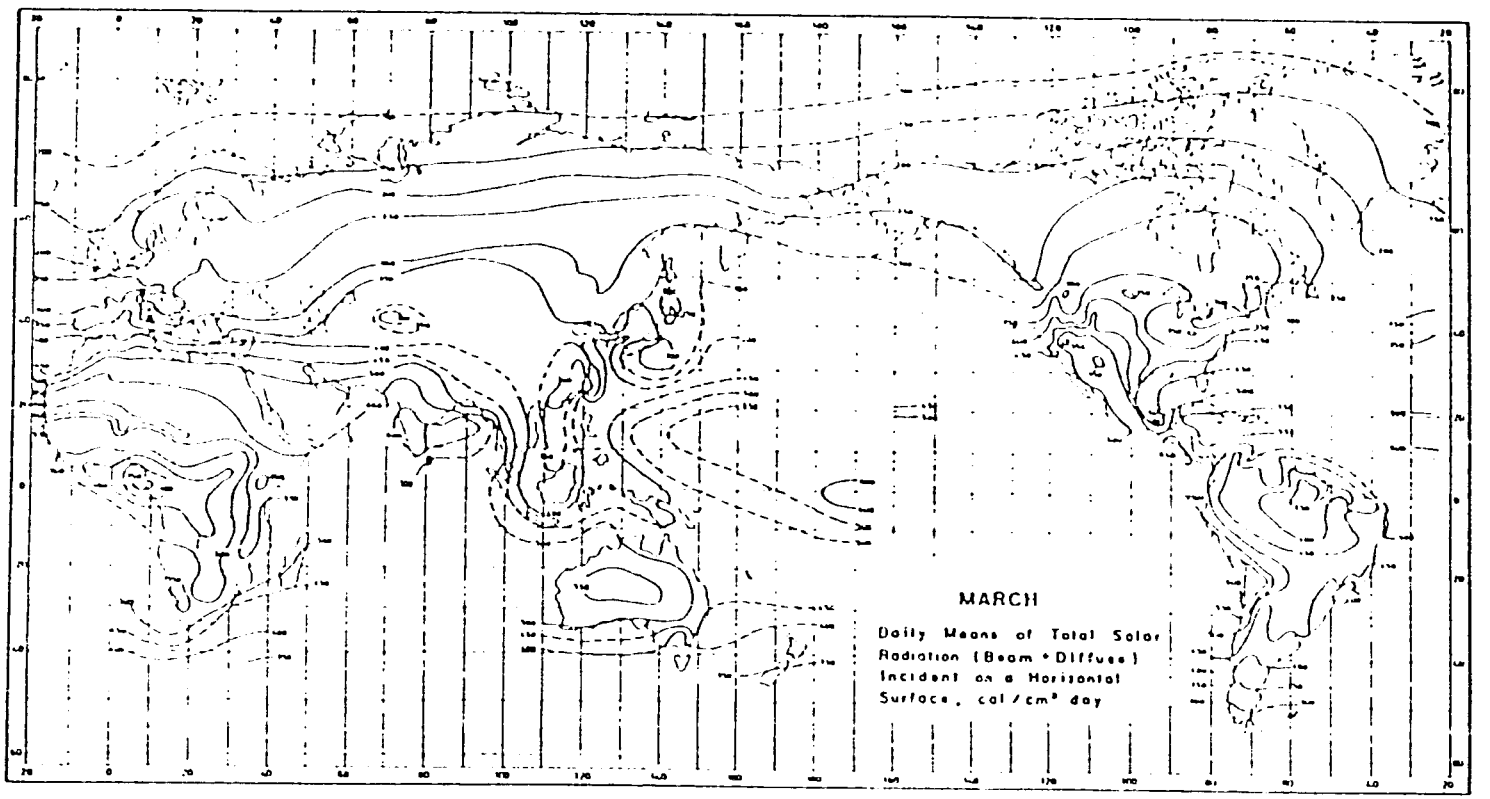

Figure 1-2 Daily radiation for March.

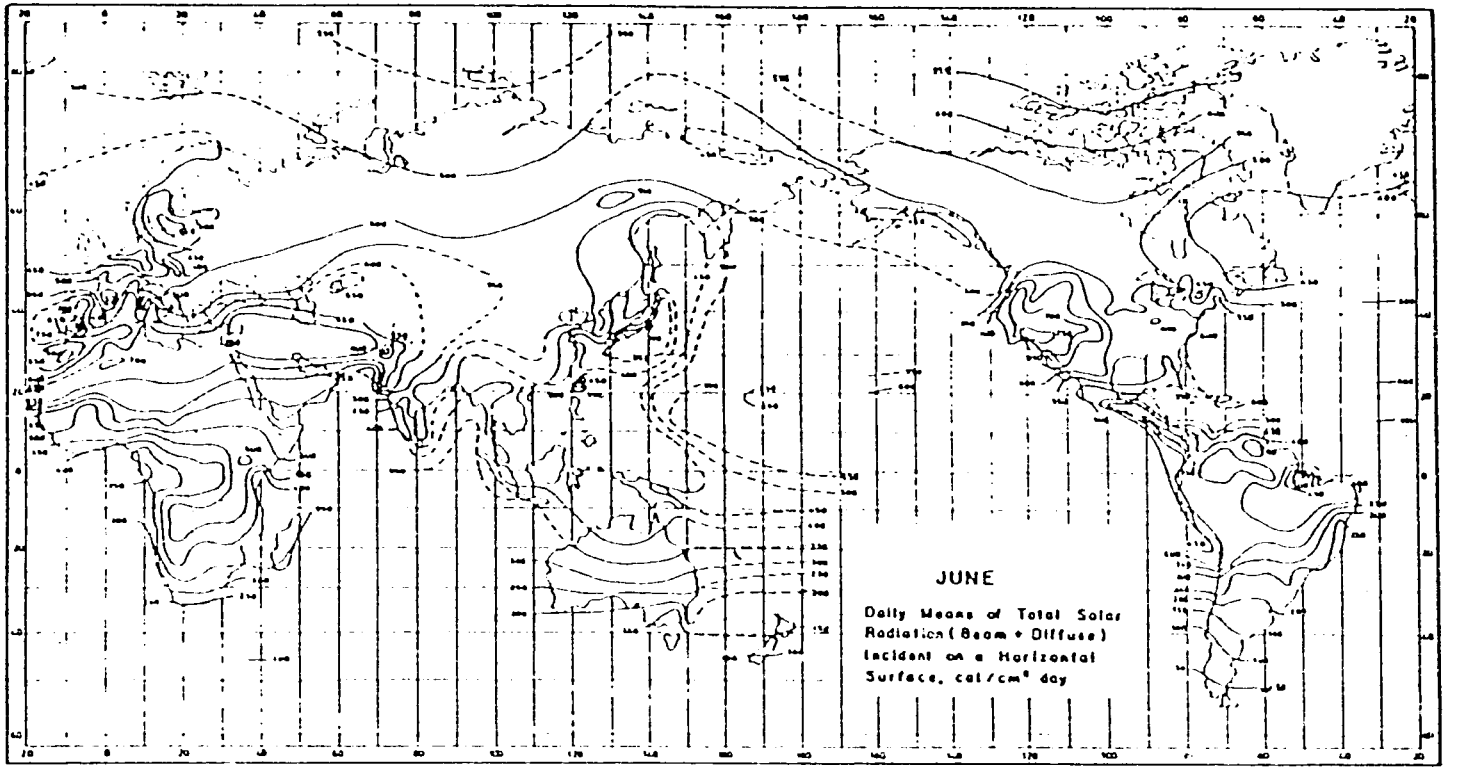

Figure 1-3. Daily radiation for June.

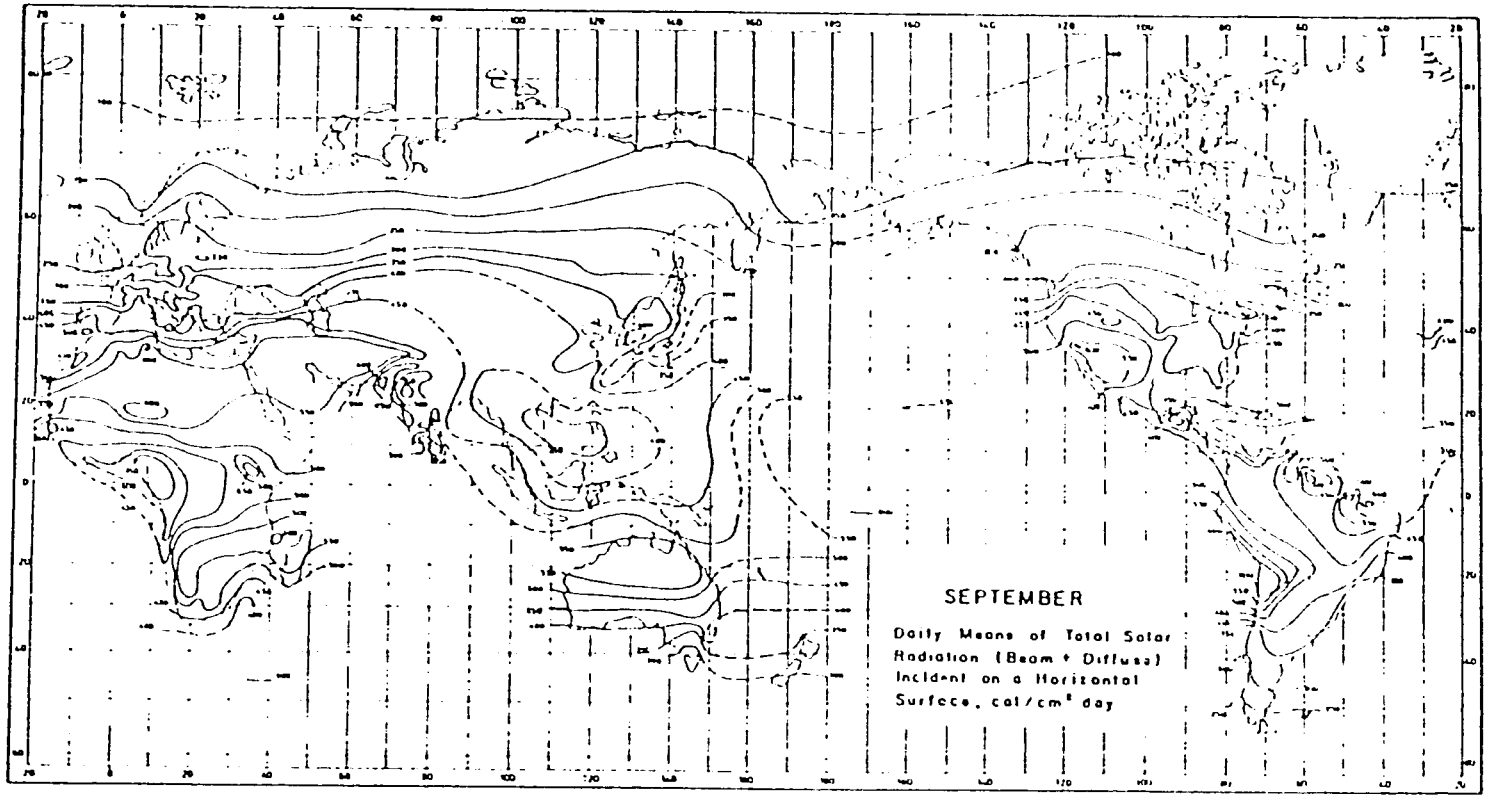

Figure 1-4 Daily radiation for September.

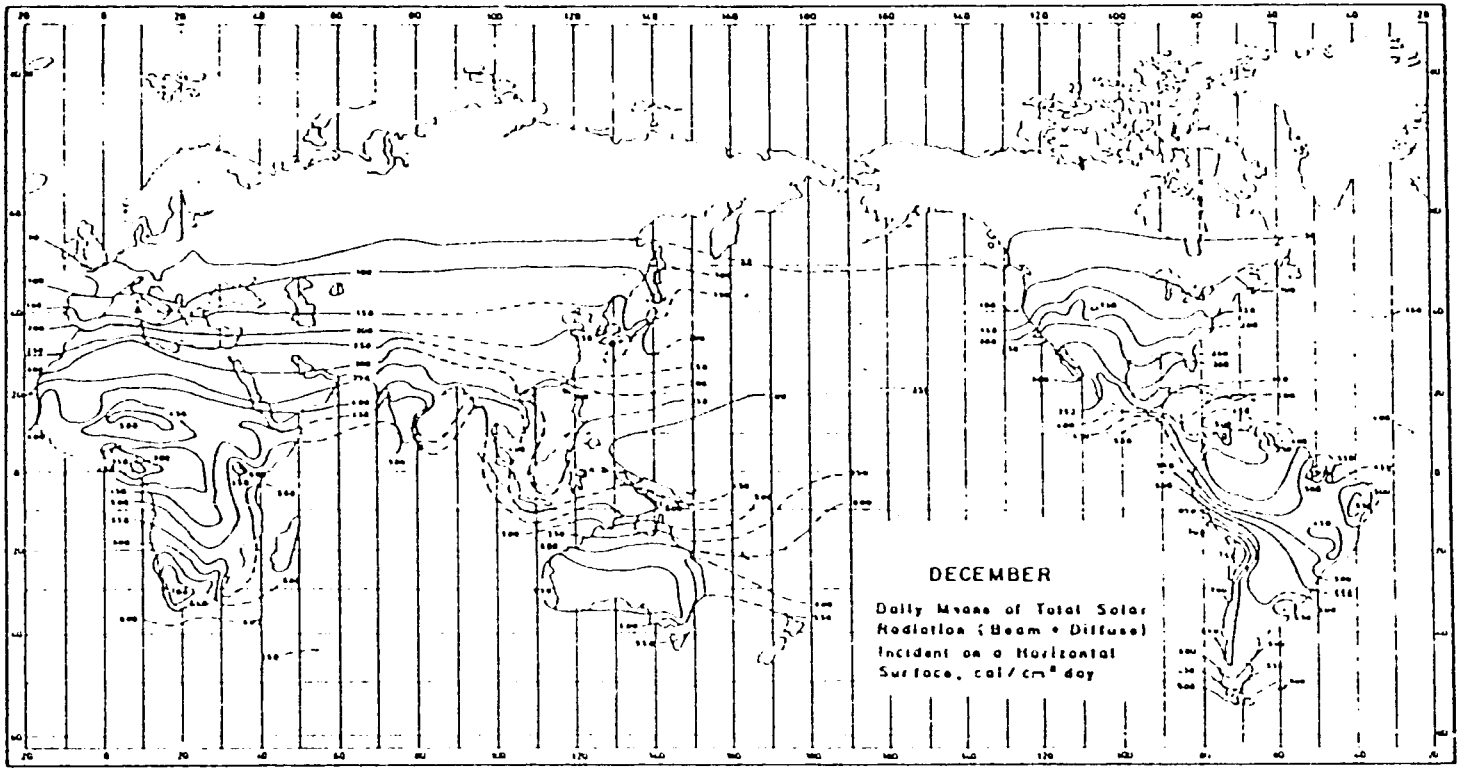

Figure 1-5 Daily radiation for December.

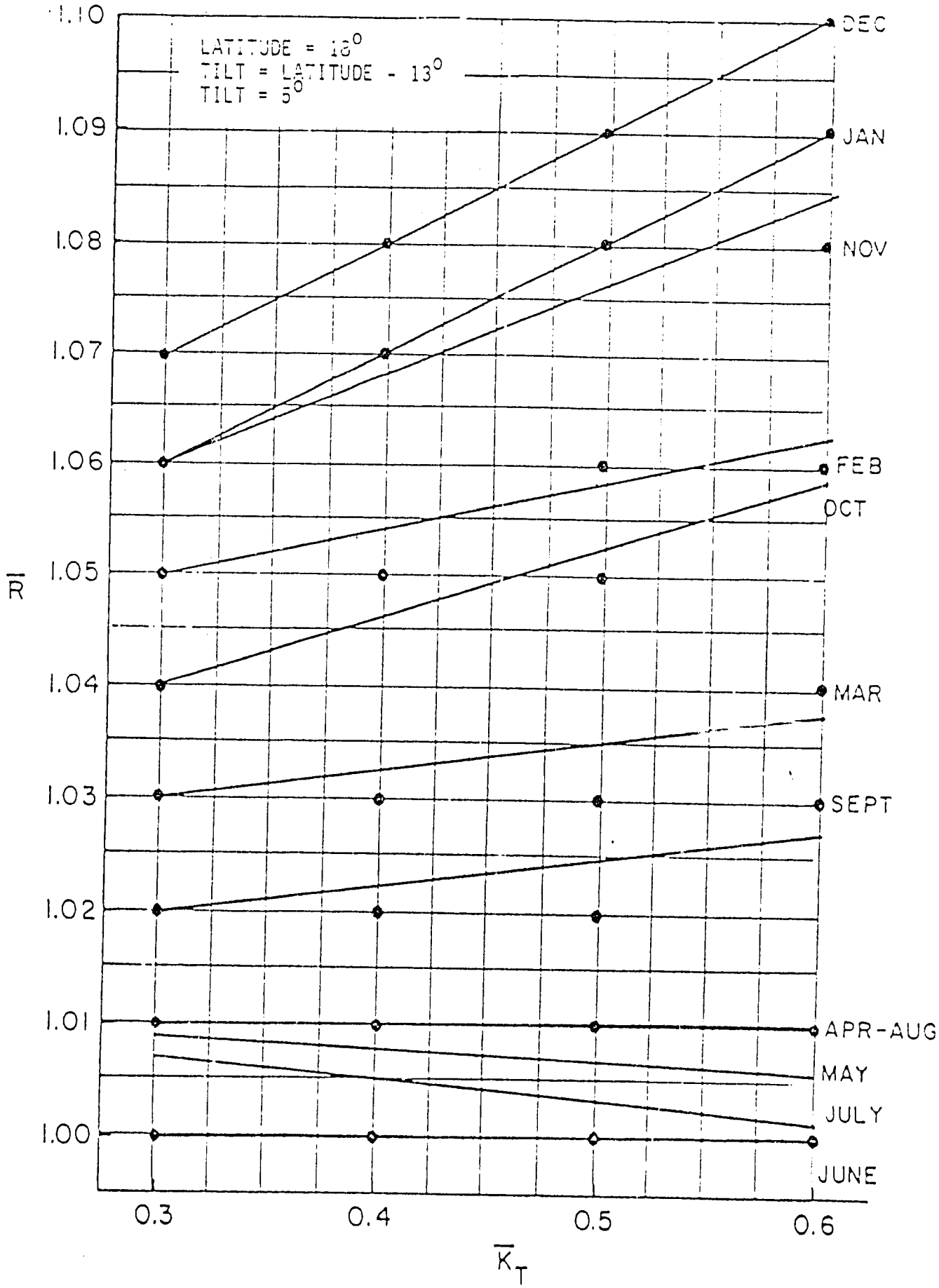

Figure 1-6

$\overline{R}$ versus $\overline{K}_T$

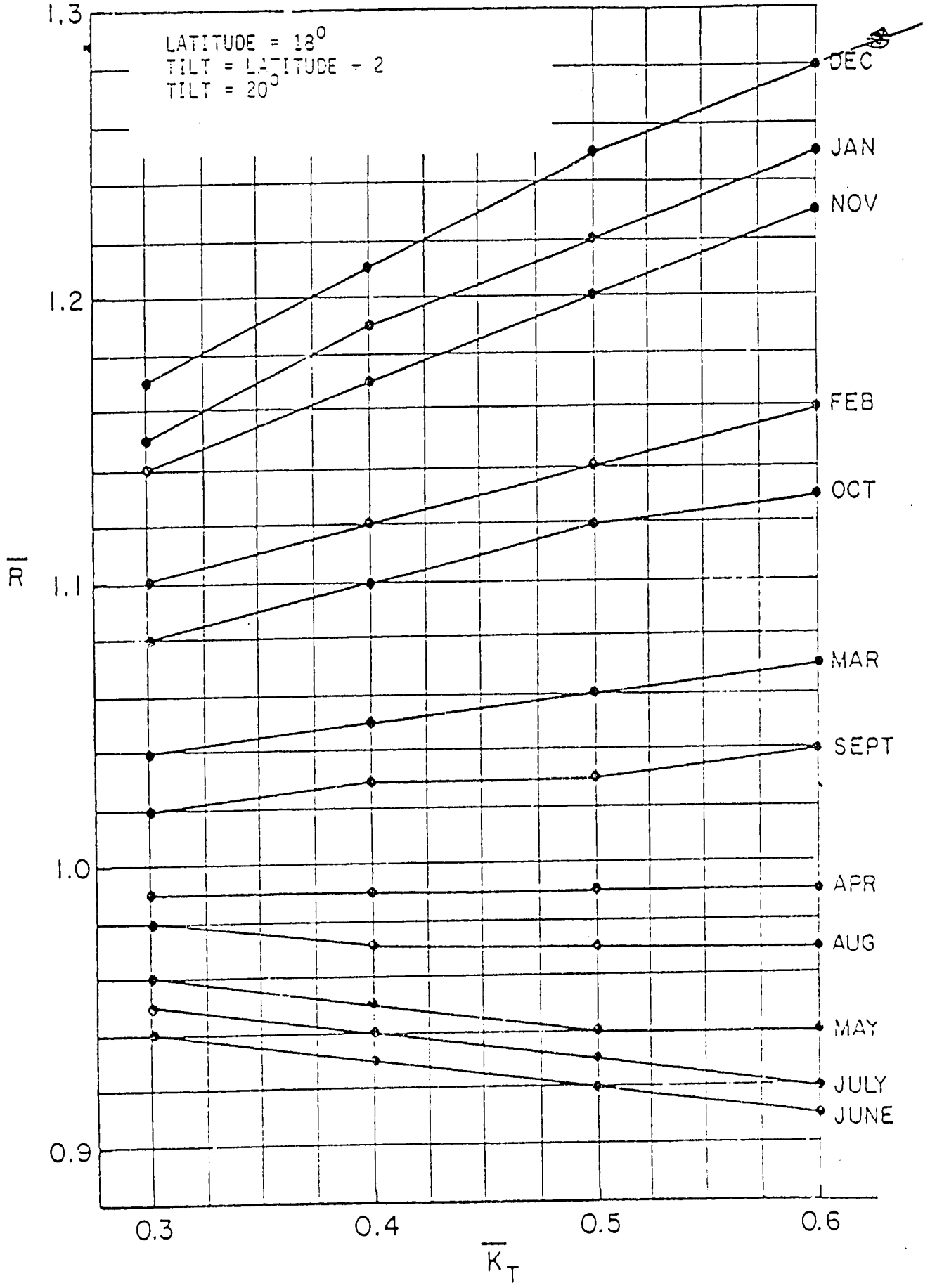

Figure 1-7

$\overline{R}$ versus $\overline{K}_T$

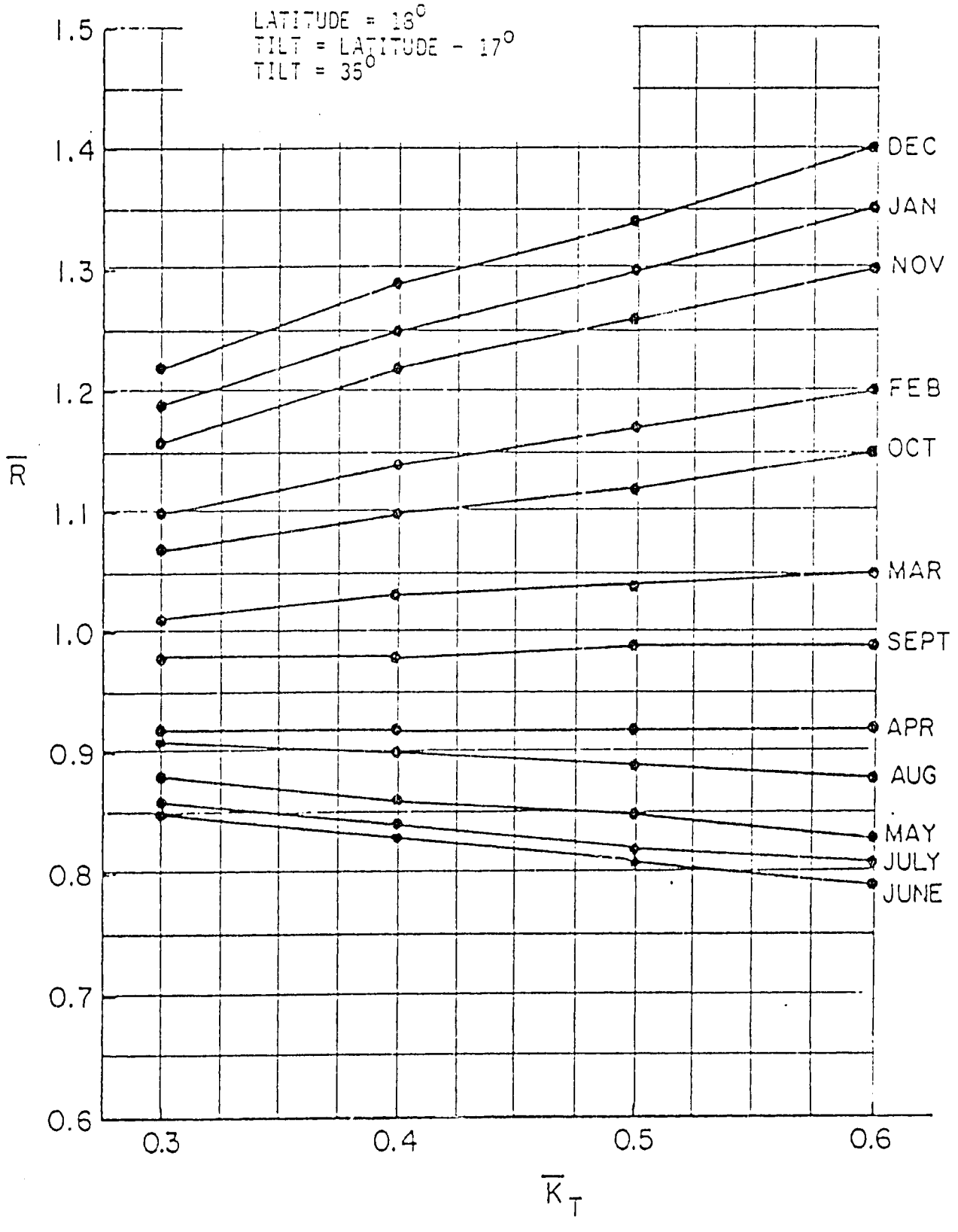

Figure 1-8

$\bar{R}$ versus $\bar{K}_T$

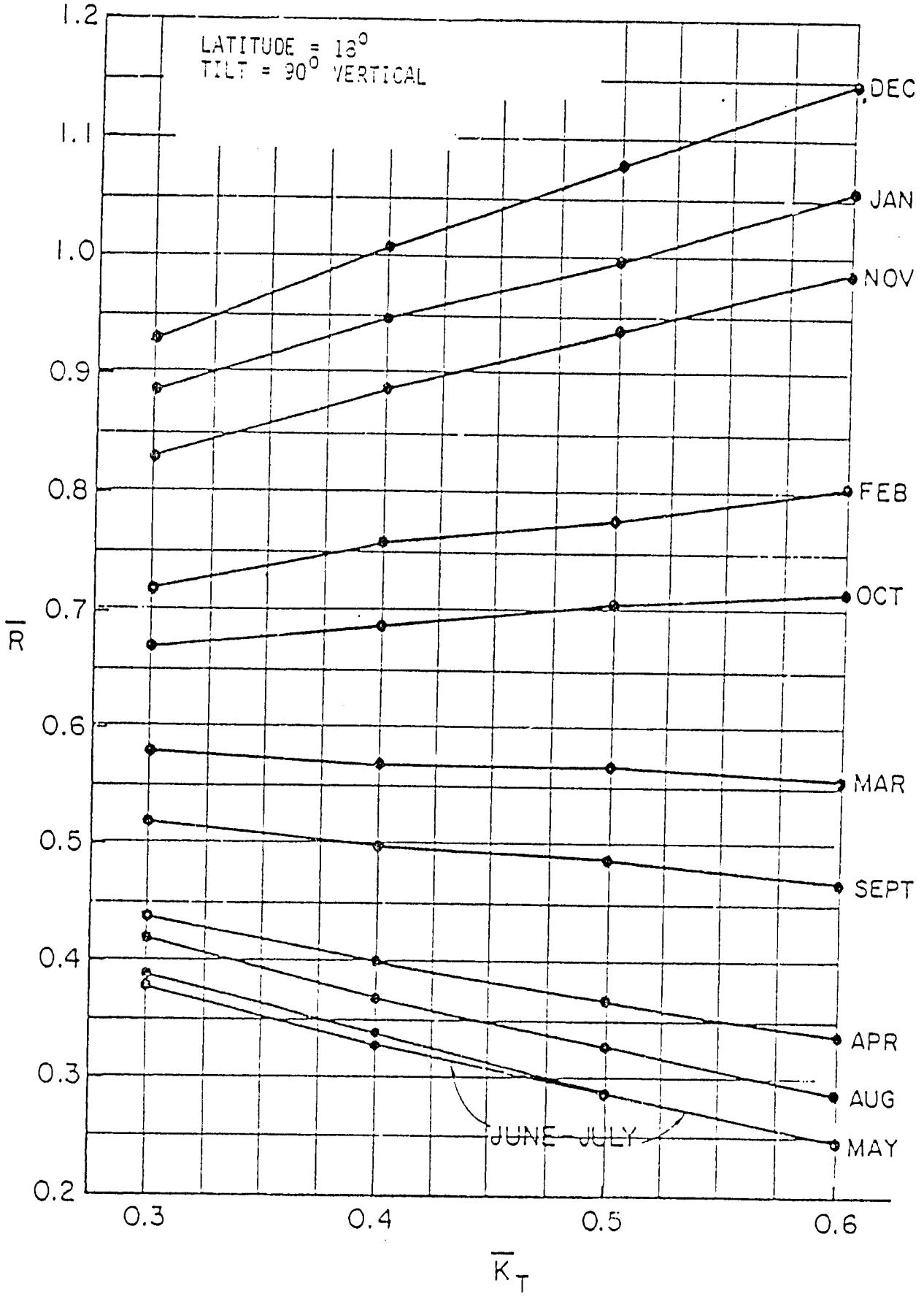

Figure 1-9

$\overline{R}$ versus $\overline{K}_T$

Figure 1-10

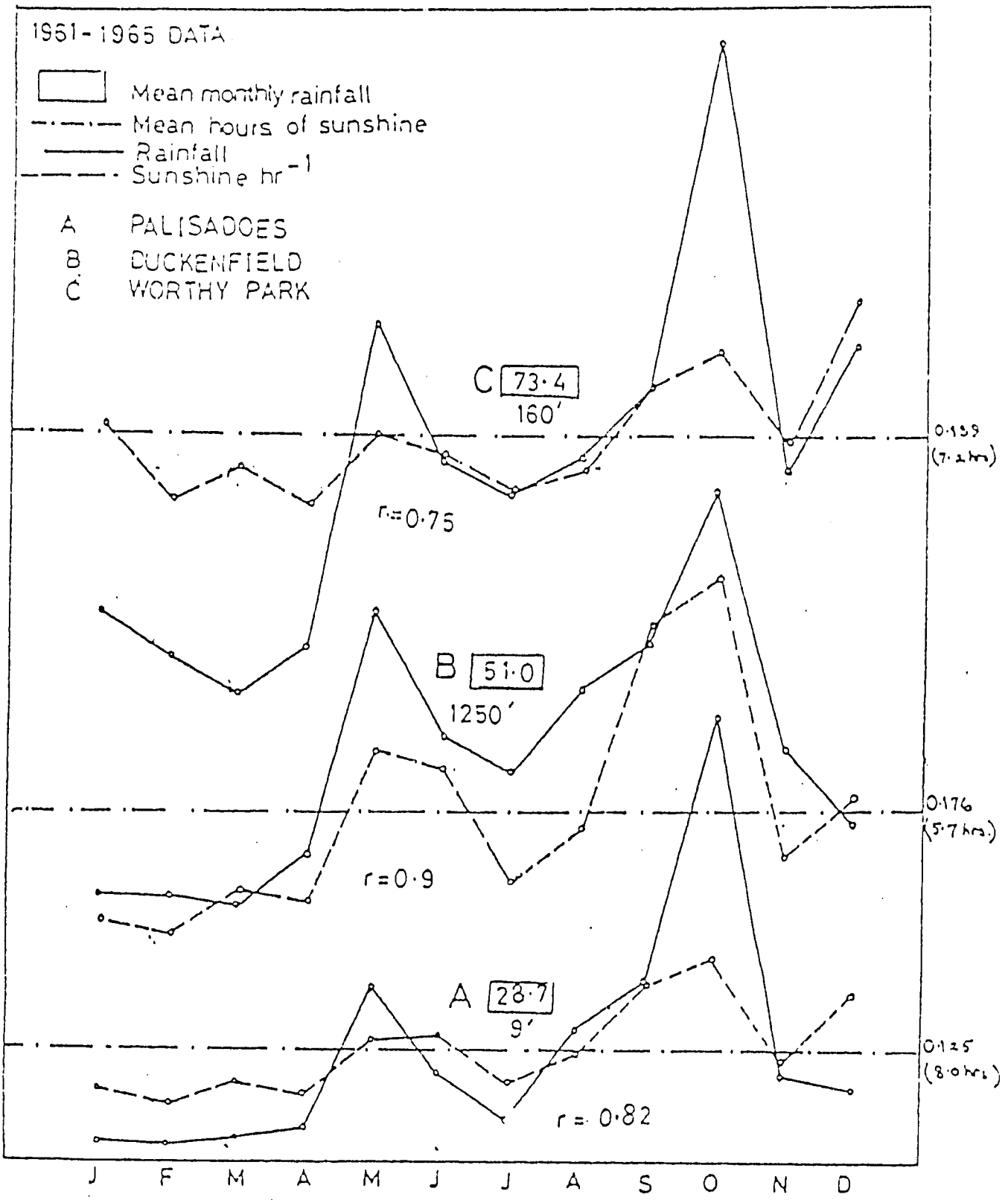
1961-1965 DATA
Mean monthly rainfall
Mean hours of sunshine
Rainfall
Sunshine hr^{-1}
A PALISADOES
B DUCKENFIELD
C WORTHY PARK
C 73·4
160′
r=0·75
0·159
(7·2 hrs)
B 51·0
1250′
r=0·9
0·176
(5·7 hrs)
A 28·7
9′
r=0·82
0·125
(8·0 hrs)
J F M A M J J A S O N D

inch cm $K_T \times \bar{H}_0 = \bar{H}$

inches	cm	K_T	x	$\bar{H}_0$	=	$\bar{H}$
40	101.6	.569		2991.92		1702
60	152.4	.524		2991.92		1568
80	203.2	.479		2991.92		1433
100	254.0	.439		2991.92		1298
150	381.0	.321		2991.92		960
200	508.0	.209		2991.92		625
250	635.0	.096		2991.92		287

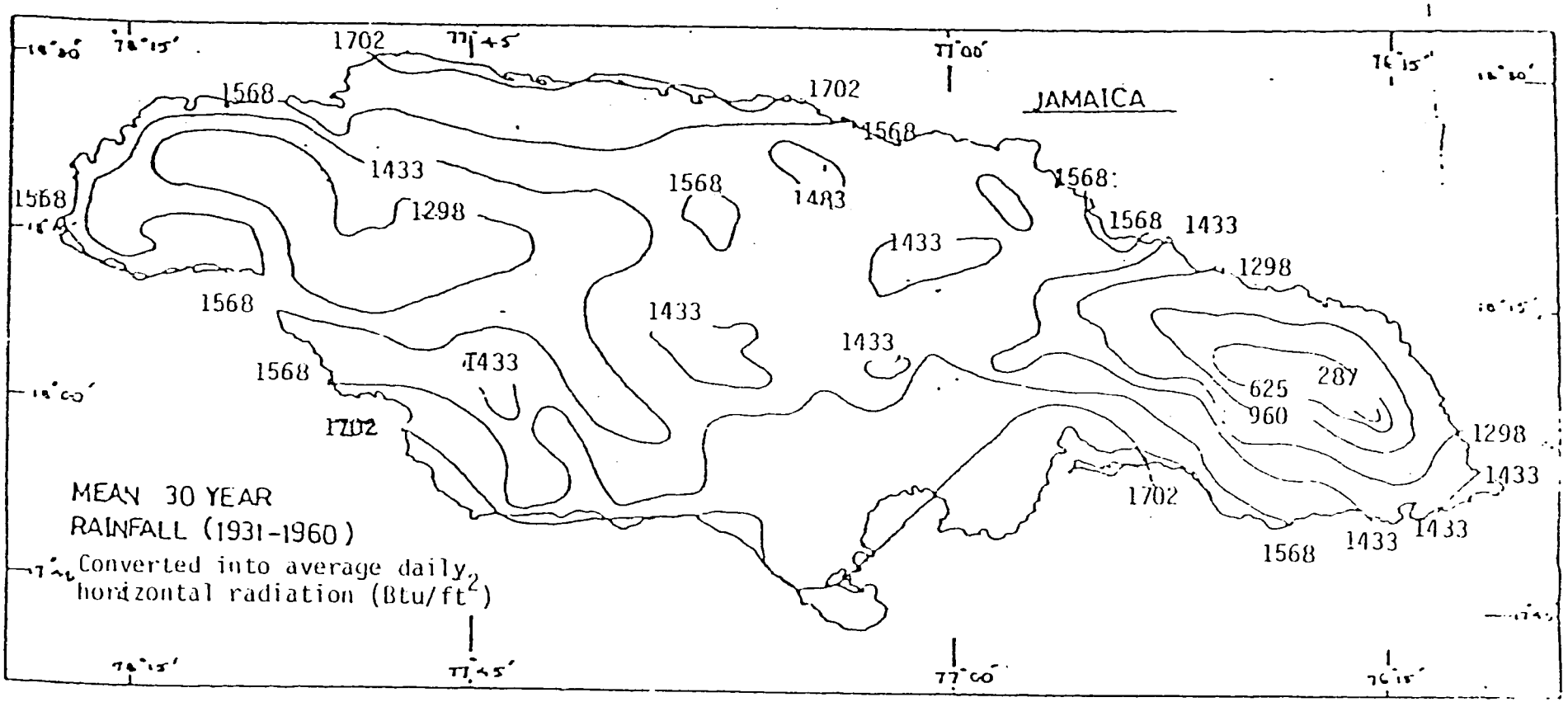

Figure 1-11

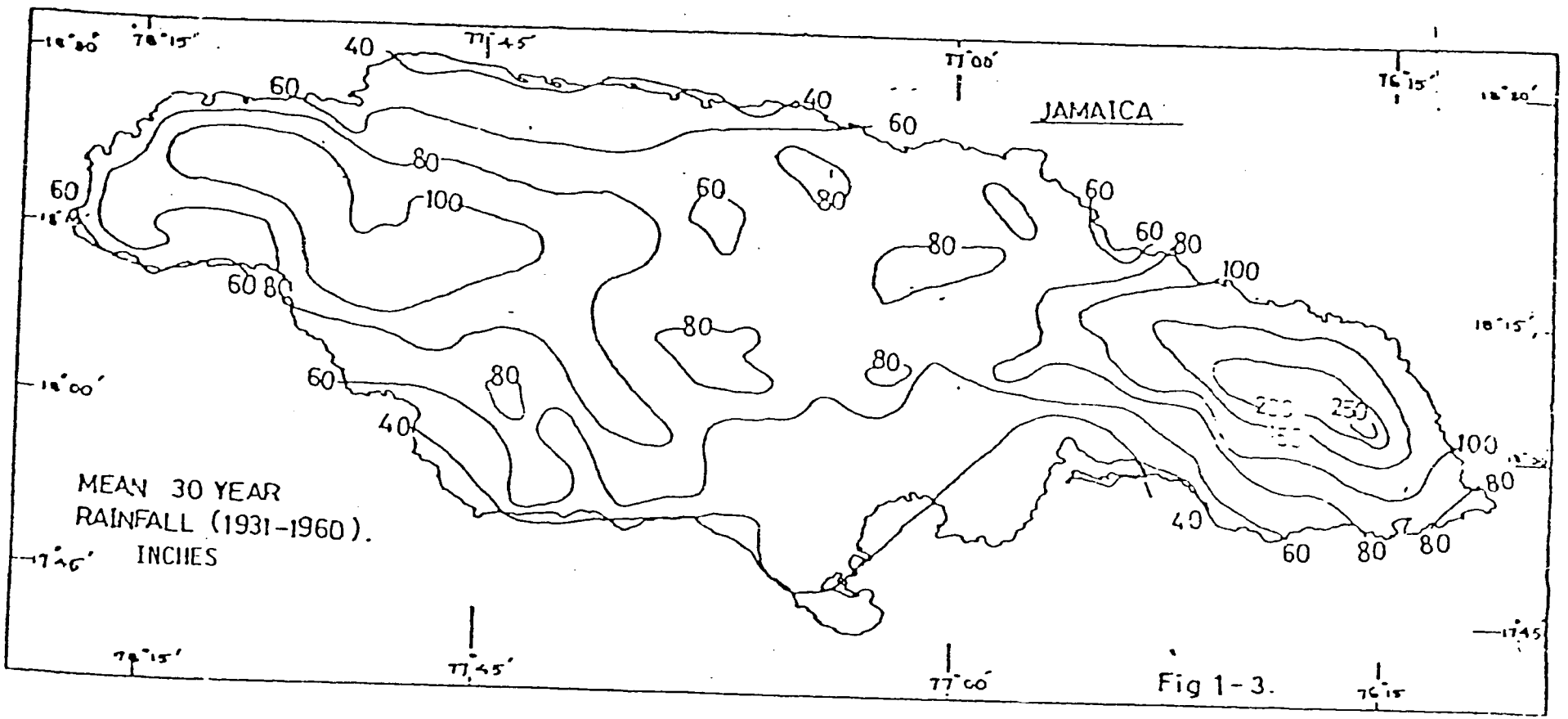

Figure 1-12

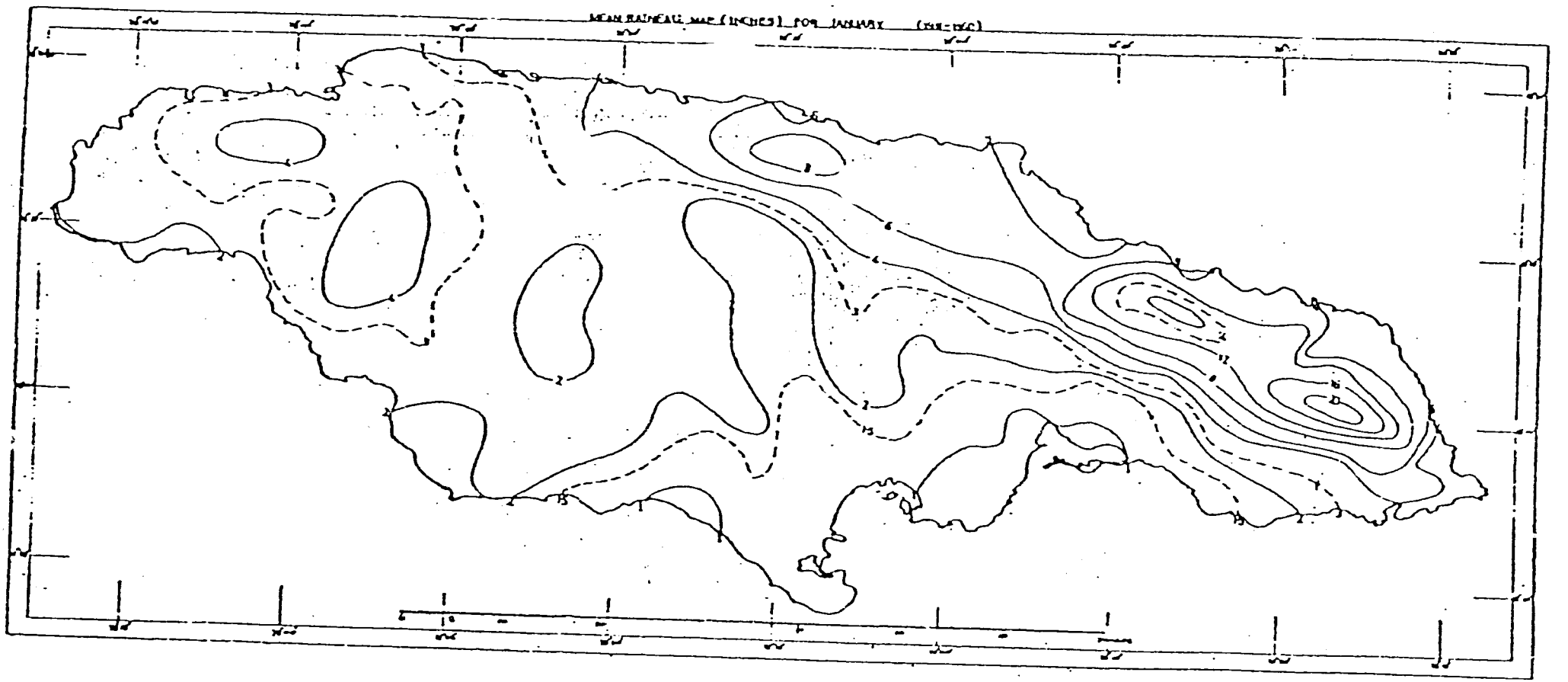

Figure 1-13

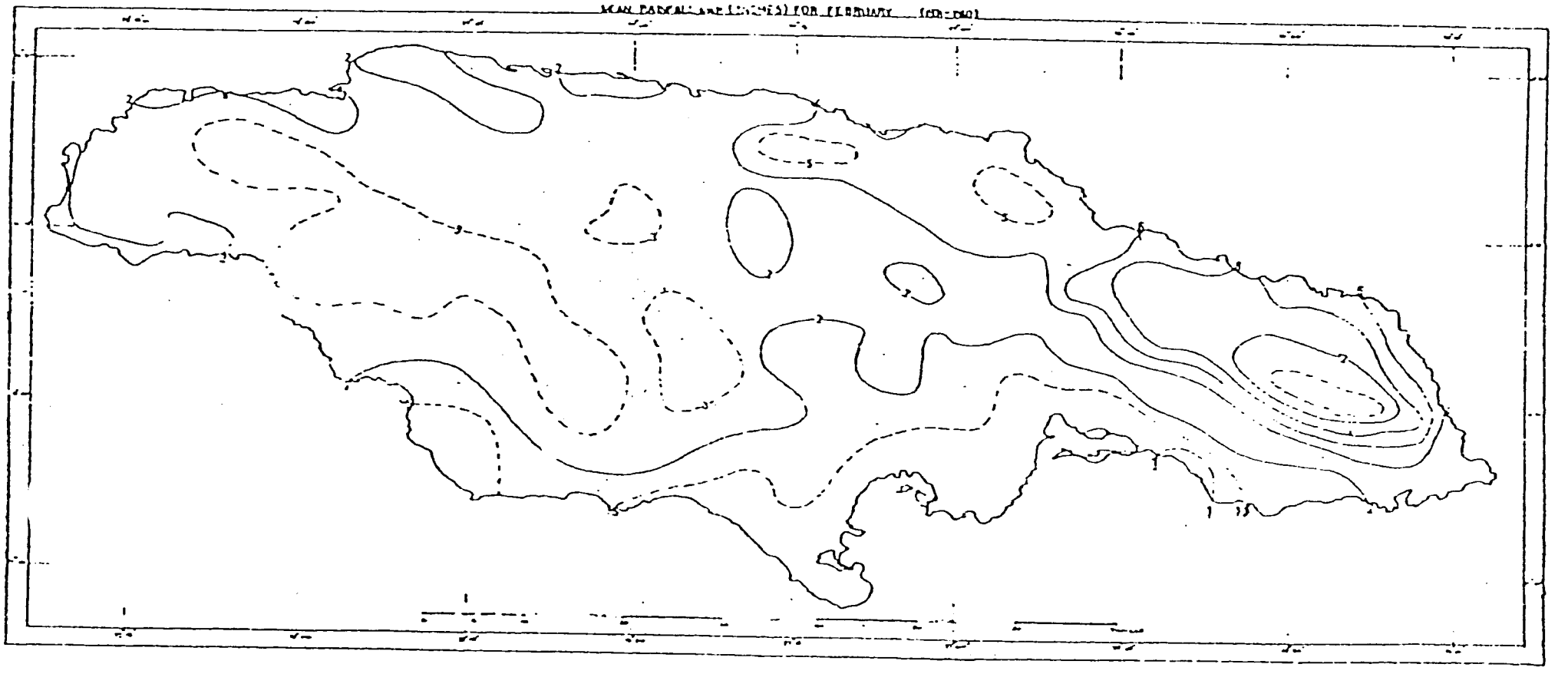

Figure 1-14

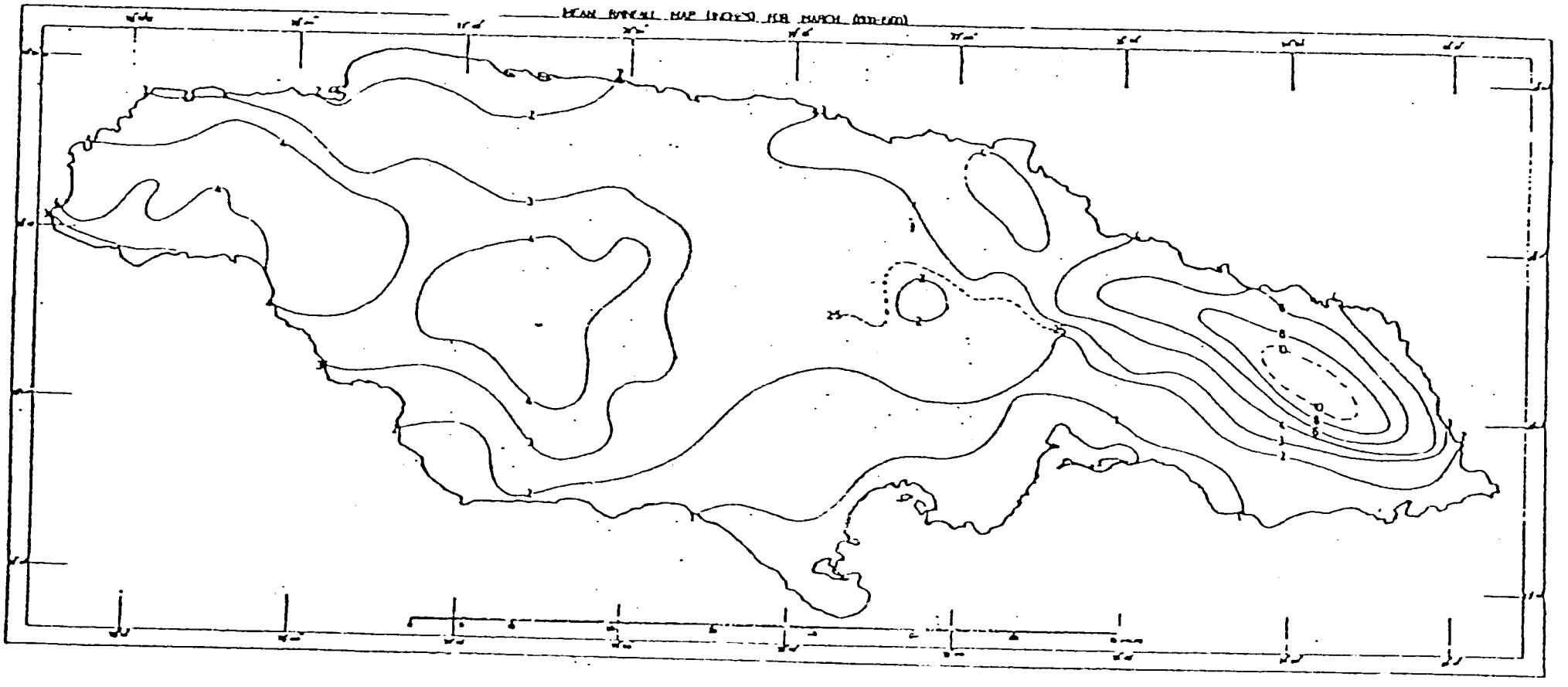

Figure 1-15

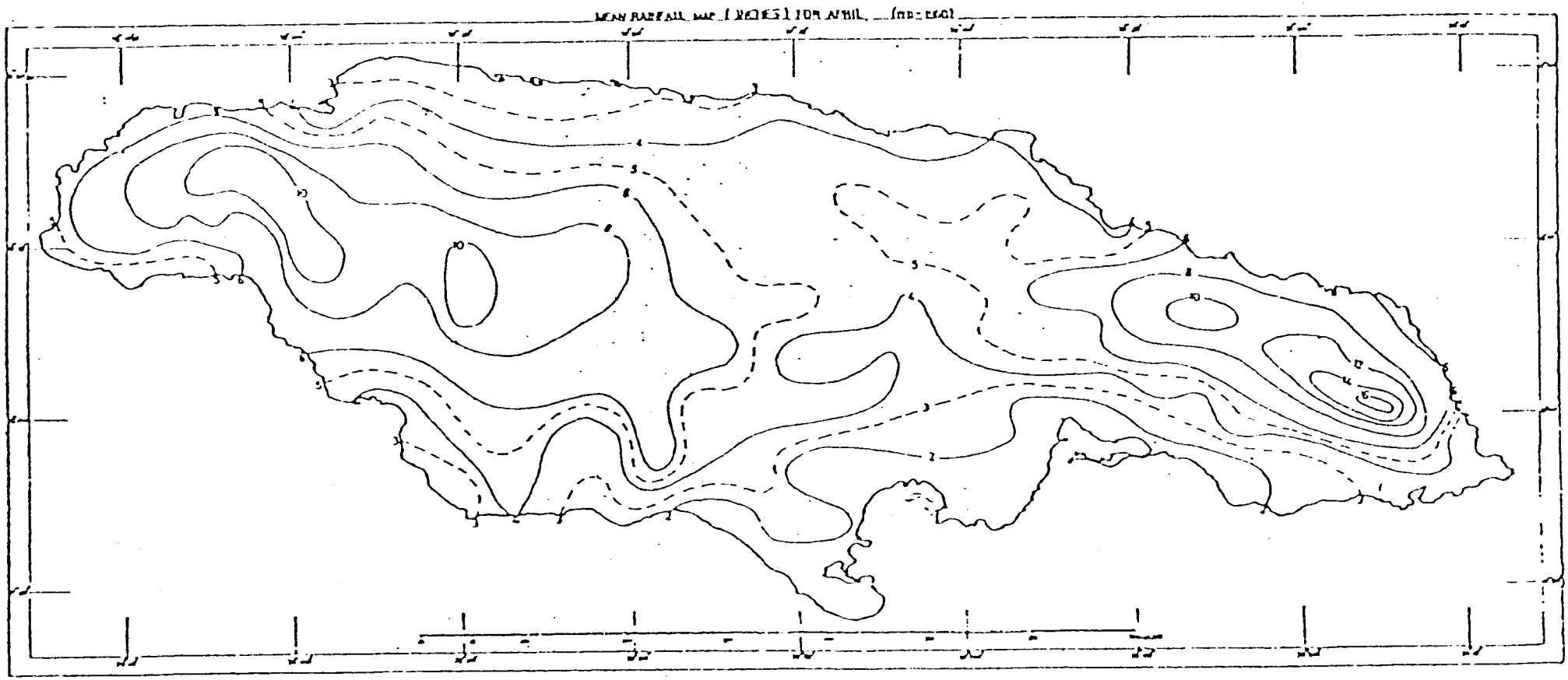

Figure 1-16

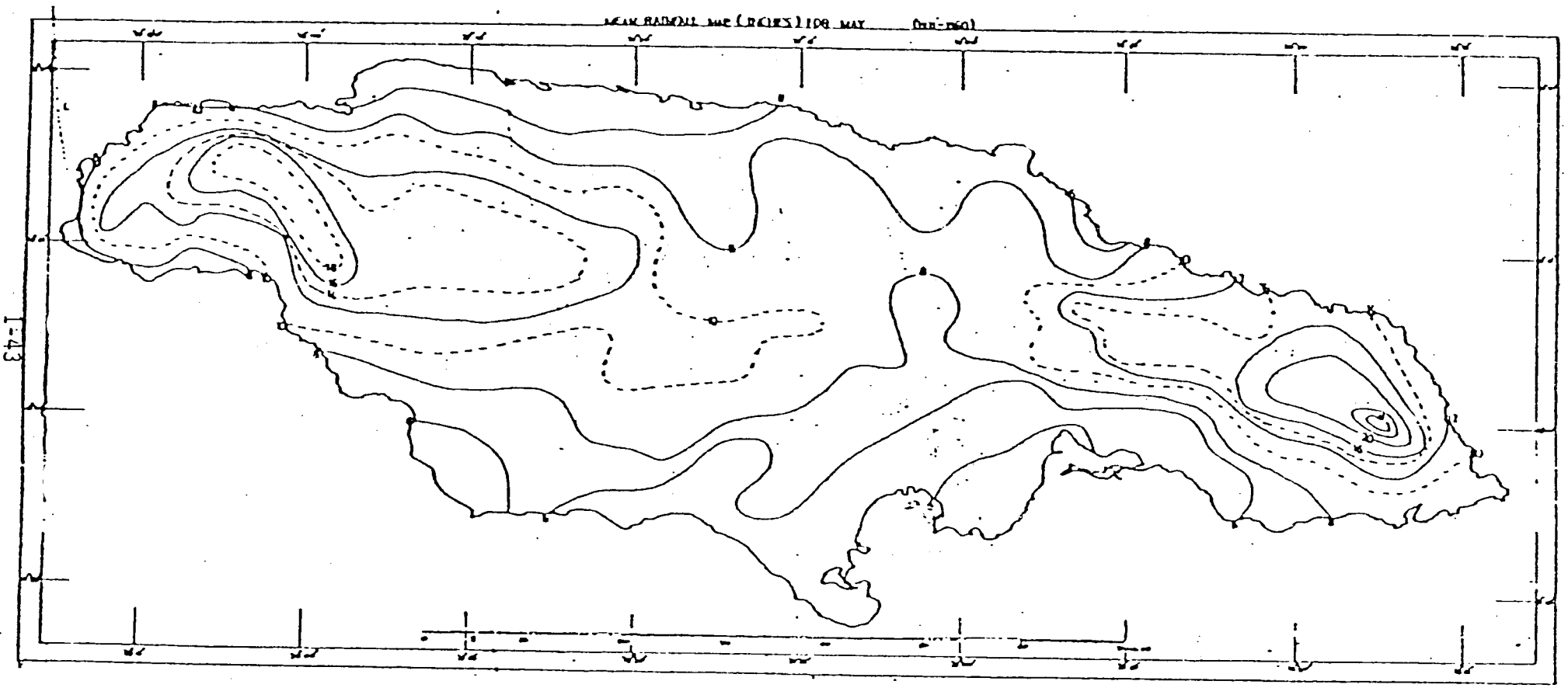

Figure 1-17

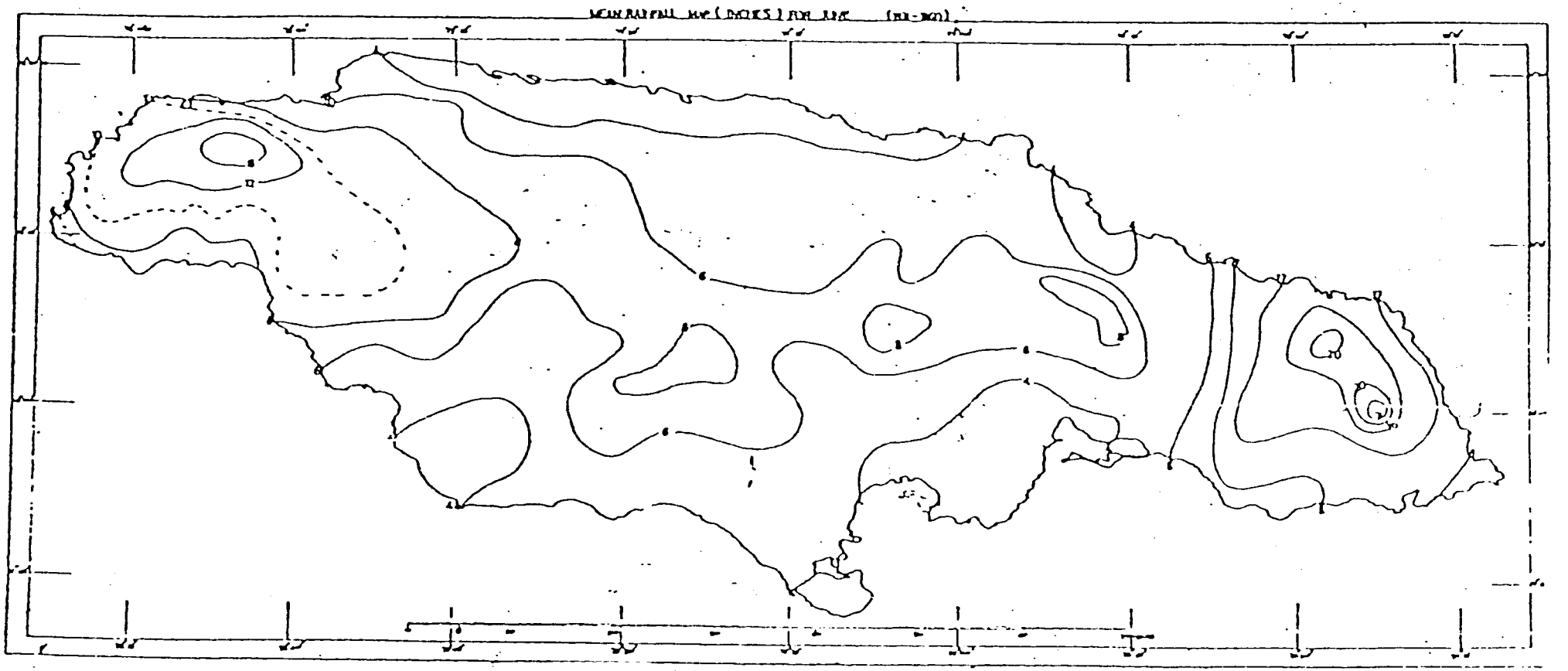

Figure 1-18

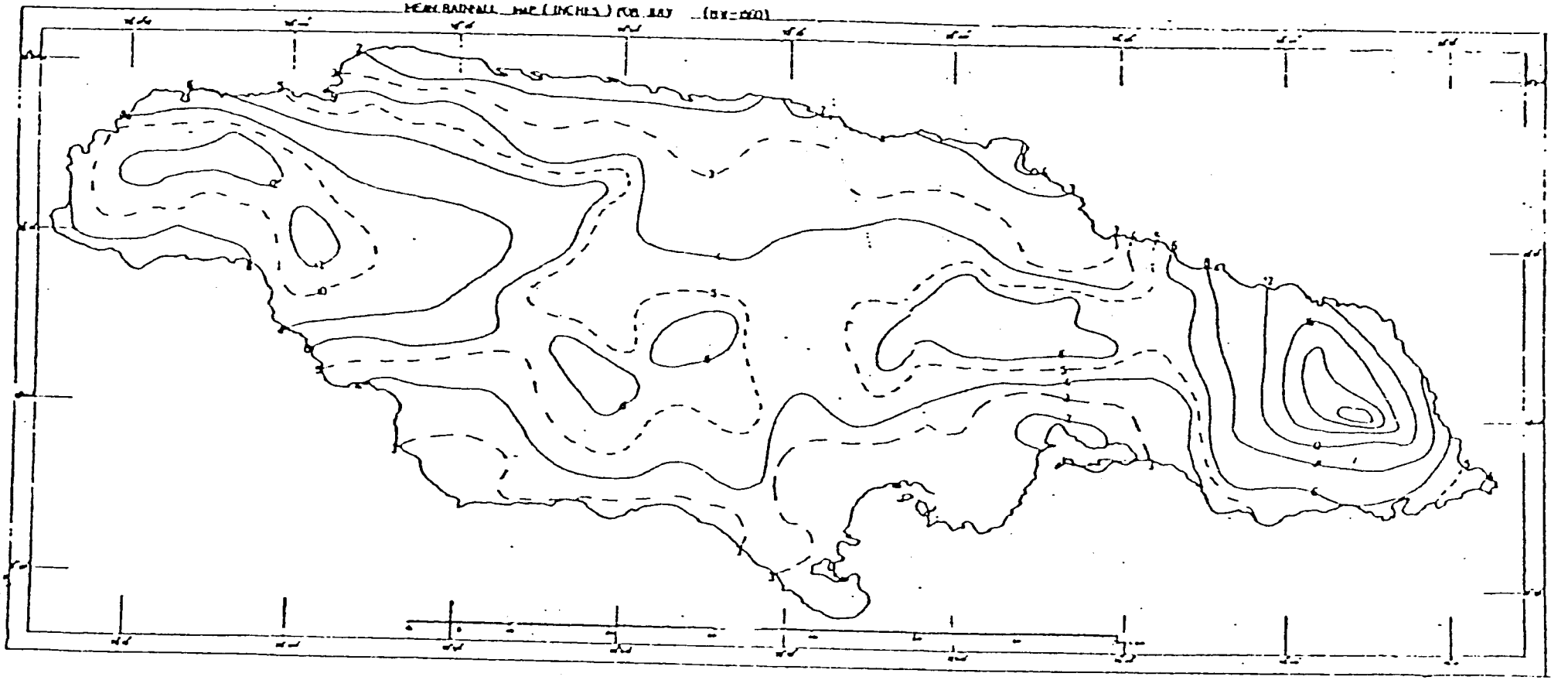

Figure 1-19

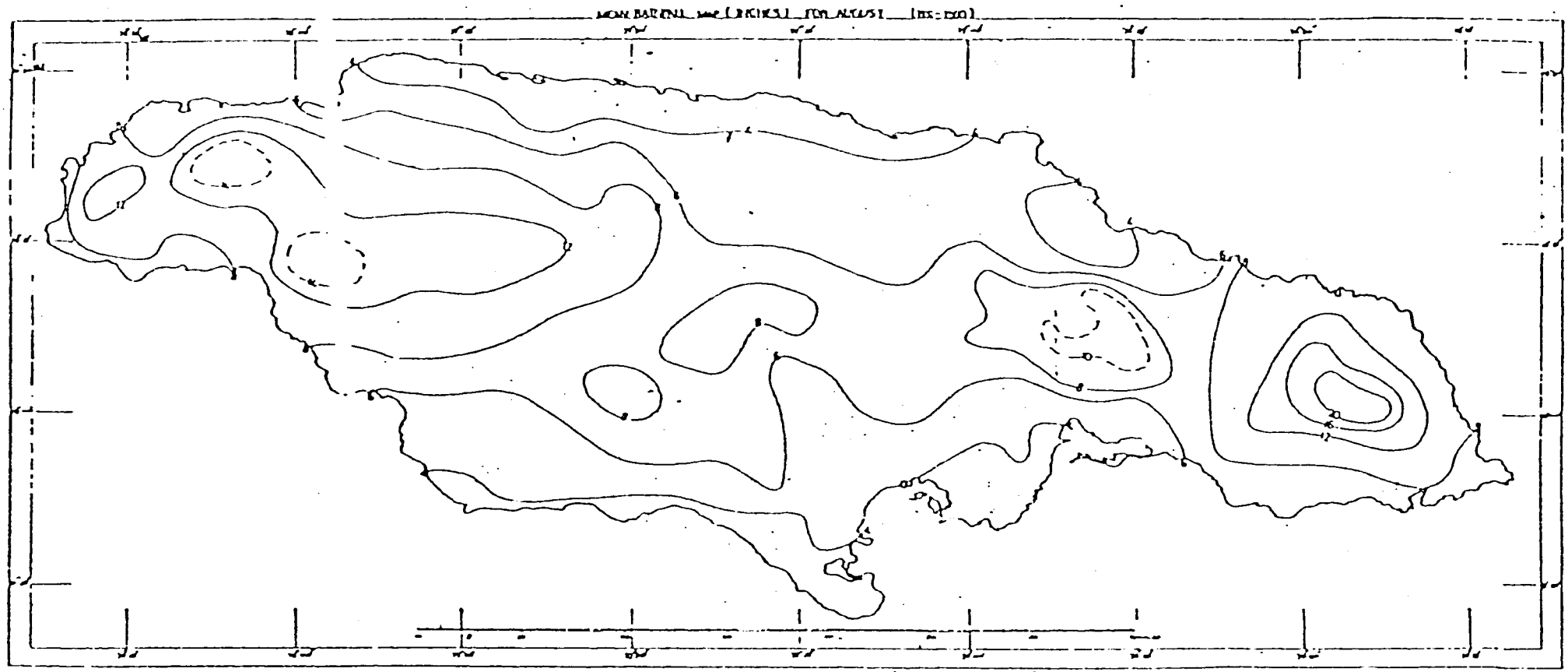

Figure 1-20

51

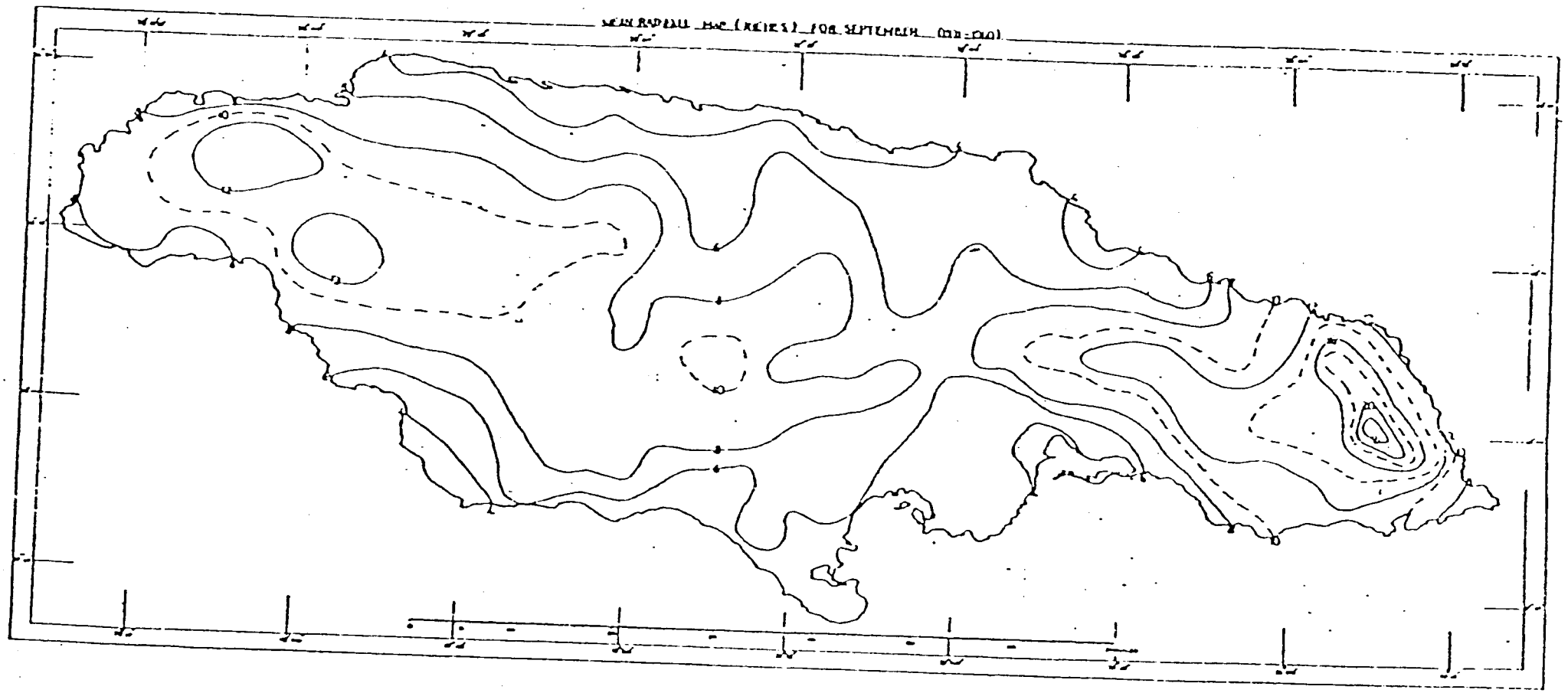

Figure 1-21

53

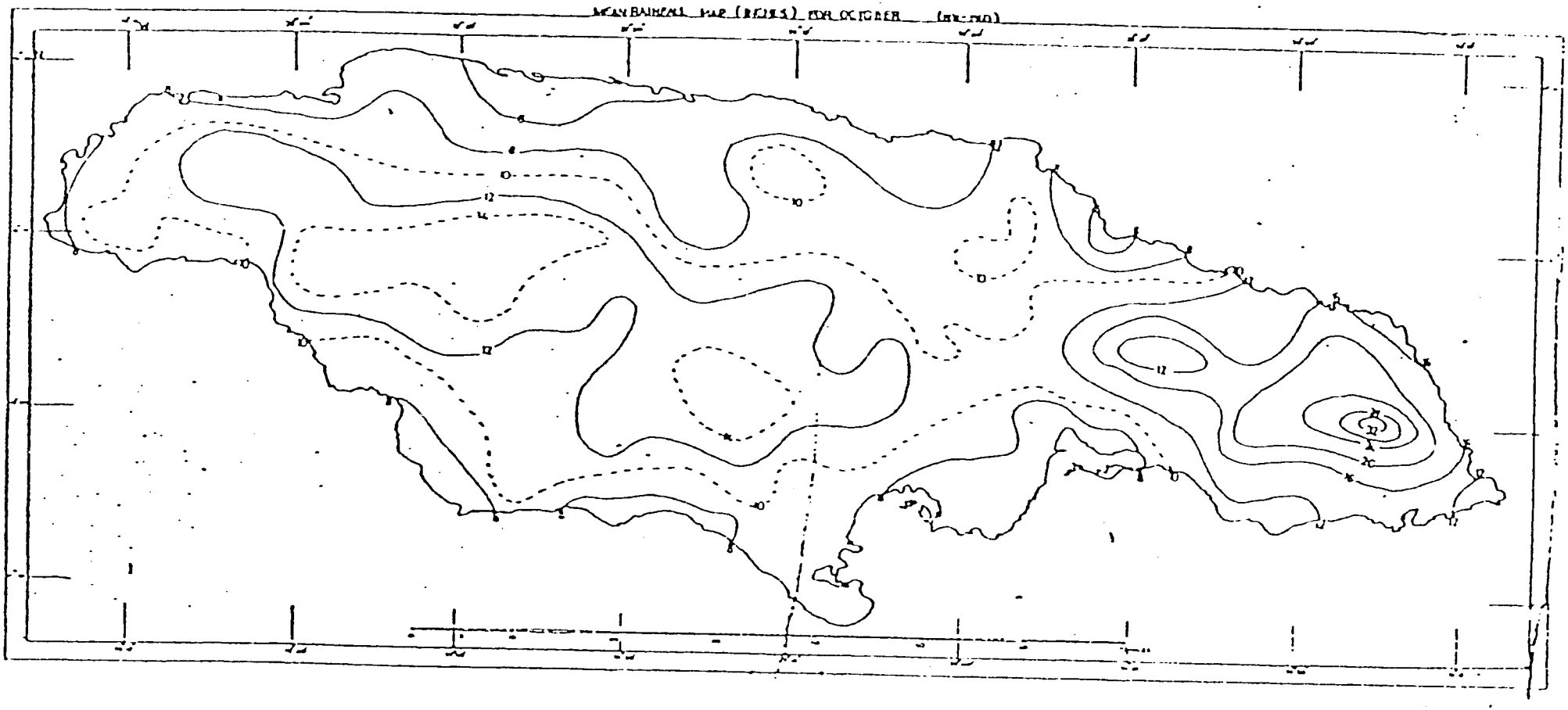

Figure 1-22

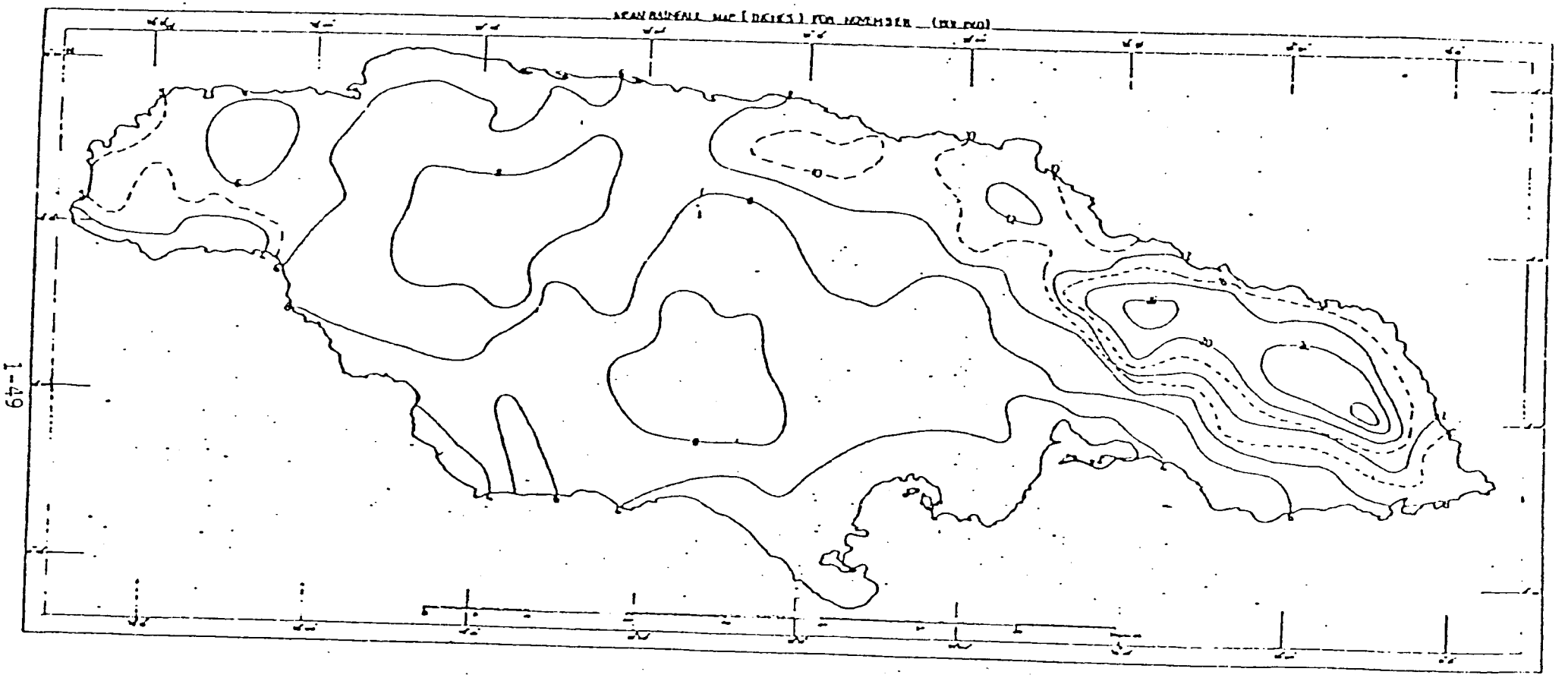

Figure 1-23

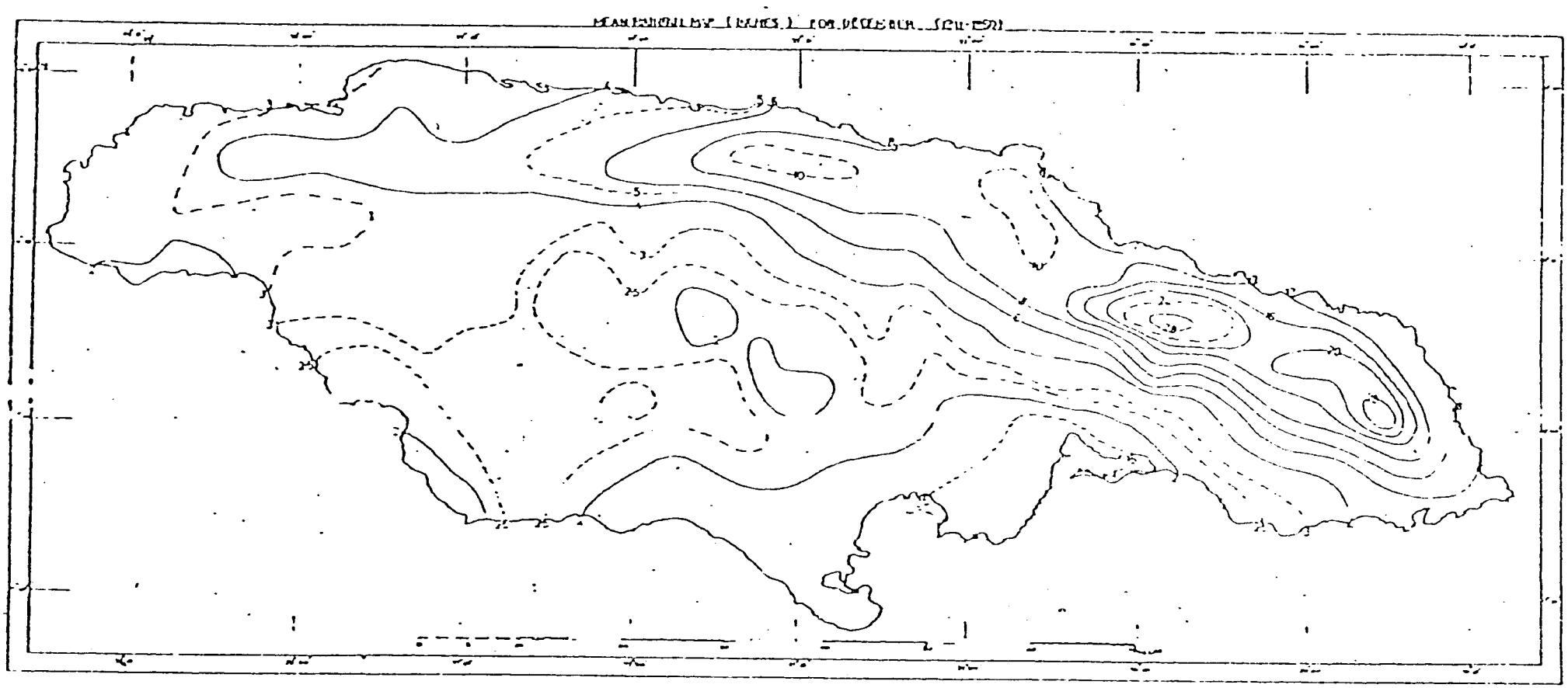

Figure 1-24

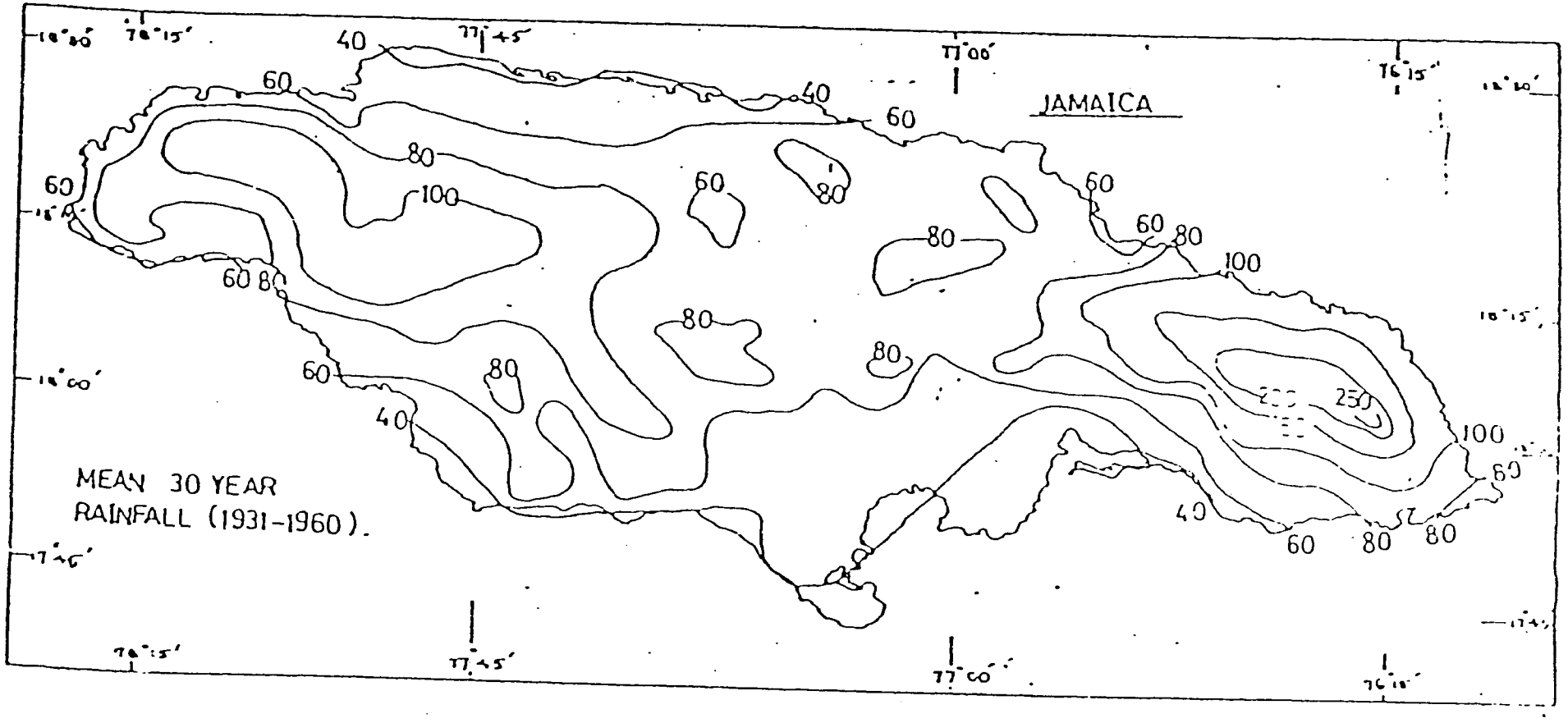
JAMAICA
MEAN 30 YEAR
RAINFALL (1931-1960).
40
60
80
100
250
77°45'
77°00'
76°15'
18°00'
17°45'

PAPER 1-1, From SOLAR ENGINEERING-1983

Proceedings of the ASME Solar Energy Division
Fifth Annual Conference, Orlando, Florida USA

ISOLATION IN PUERTO RICO

A. M. López and K. G. Soderstrom
Center for Energy and Environment Research
University of Puerto Rico
Mayaguez Puerto Rico

ABSTRACT

The geographical and temporal distribution of insolation in the Caribbean island of Puerto Rico has been studied through the analysis of precise measurements at six sites. Significant differences among the sites have been found. A relatively uniform distribution of horizontal insolation during the year is a common feature not found at temperate latitudes. A simple correlation between annual insolation and precipitation was determined. Significant differences in the correlation between daily diffuse and global insolation at the different sites were found. These correlations also differ from those reported at most continental sites.

INTRODUCTION

The Center for Energy and Environment Research (CEER) of the University of Puerto Rico has been measuring insolation at different locations on this Caribbean island for several years. The magnitude as well as the geographical, temporal and statistical distribution of insolation in Puerto Rico should be typical of other Caribbean islands and other tropical sites.

Geography of Puerto Rico

Puerto Rico is the smallest and most eastward member of the Greater Antilles. It has an area of 8800 sq km located approximately from 18° to 18.5°N latitude and from 66° to 67°W longitude (Fig. 1). The island has a roughly rectangular shape with a range of small mountains (typical peak elevation 1000 m) running east-west along its center.

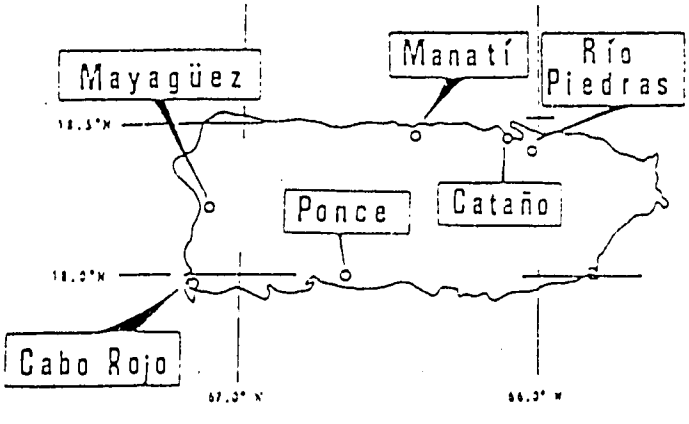

Fig. 1 Location of measurement sites

The meteorology of Puerto Rico is rather complex when compared with other areas of similar size. This is particularly true with regards to precipitation. Six distinct ecological life zones can be found within its area (1) ranging from a tropical rain forest (annual rainfall 400 cm) to a semi-desert (annual rainfall 80 cm). The main reasons for the geographical variation in precipitation are the constancy of the trade winds from the east and northeast and the presence of the mountain ranges. The trade winds bring warm, moisture laden air from the ocean. The mountains force the mixture of this air with colder, drier air at the higher elevations and the resultant precipitation occurs there. The air reaching the southwestern part of the island has lost its precipitation in the mountains and there is little rainfall in this region.

The large variations in rainfall are typical of the Caribbean islands and should be taken into consideration in the estimation of insolation at particular sites in this region.

Data Acquisition Methodology

The instrumentation used by CEER in its measurements has consisted of PSP precision pyranometers, electronic integrators, digital printers and shadow bands manufactured by Eppley Laboratories. Integrated insolation values are printed hourly. All measurements are made on a horizontal plane.

Pyranometer calibration is checked every two years by bringing all the instruments to the same location and testing them side by side on an outdoor stand. Integrator calibration is checked yearly using a reference voltage source.

The locations of the measurement stations are shown in Fig. 1. Global insolation is measured at all stations and diffuse at three sites. The measurement dates are presented in Table 1.

Electric power outages cause gaps in the data acquisition process. The integrators must be reset manually before data acquisition can resume. Longer gaps are caused by integrator malfunctions which require repair service in the United States.

Data Analysis Methodology

The results presented here are based only on recorded values of insolation. The gaps in the record were not filled in. In calculating average daily insolation, the average hourly values for each month were calculated first. This makes use of all the hourly data available including those days which had a partial record. Average insolation values for each location were found by averaging the twelve monthly values. Only days with complete records were used in calculating the standard deviations of the daily insolation distributions.

SURFACE INSOLATION

Geographical Distribution

Table 1 presents the values of average daily insolation measured at each location.

Table 1. Measurement Dates and Average Daily Insolation on a Horizontal Plane

Station	Component	Dates	Daily Insolation (MJ/m^2)
Mayagüez	Global	Jan 76-Dec 81	16.0
	Diffuse	Jun 77-Dec 81	6.9
Río Piedras	Global	Jun 78-Dec 81	16.6
	Diffuse	Jul 78-Dec 81	7.7
Ponce	Global	Mar 78-Dec 81	19.3
Cataño	Global	Jul 78-Jun 79	18.1
	Diffuse	Jul 78-Jun 79	7.9
Manatí	Global	Sep 79-Feb 81	18.6
Cabo Rojo	Global	Apr 80-Dec 81	19.9

The cities of Ponce and Cabo Rojo on the southwestern part of the island have the highest average global insolation. They are followed by Manatí and Cataño, which are on the northern coast. The city of Río Piedras, although only ten kilometers from the coast, is on the edge of the hills and receives approximately 10% less global insolation than the coastal areas.

The city of Mayagüez is on the western coast of the island. The weather in Mayagüez exhibits a particular daily pattern with few variations. Mornings are usually sunny, afternoons are cloudy and the nights are clear. Obviously, the weather here is strongly influenced by the mountains which lie close to the coast in this region and which surround Mayagüez on three sides. The overall effect is that Mayagüez receives less global insolation than any other station. The value measured at Mayagüez is 22% less than that at Cabo Rojo, the station with the highest daily average. These stations are within 30 km of each other. One conclusion of this study is that it is important to consider the small-scale geography of Caribbean islands in order to determine the applicability of insolation measurements at nearby sites.

Temporal Distribution

The temporal distribution of global insolation during the year is presented in Table 2. The results for Río Piedras, Ponce and Mayagüez (the cities for which the greatest amount of data exists) have been graphed in Fig. 2.

An interesting feature of all the graphs is the fact that the global insolation on a horizontal plane is rather uniformly distributed during the year. One of the reasons for this is the relative uniformity of the distribution of extraterrestrial horizontal insolation at tropical latitudes. This effect is shown in Fig. 3 where the distribution at 18° latitude is compared with that at 40° latitude. Although there is only a 20% difference in the annual averages of the two distributions, the extraterrestrial insolation on a horizontal surface at 18° latitude varies only by ±19% during the year while that at 40° latitude varies by ±50%.

Another effect which enhances the uniformity of the horizontal insolation in Puerto Rico is the existence of a rainy season which coincides roughly with the periods of highest extraterrestrial insolation. The rainy season in Puerto Rico extends generally from April to September. Although it is not as pronounced as in other parts of the world, it does influence the

Table 2. Average and Standard Deviation of Daily Global Insolation on a Horizontal Plane (MJ/m^2)

Month	Station					
	Mayagüez	Río Piedras	Ponce	Cabo Rojo	Cataño	Manatí
JAN	14.2 ± 3.0	14.8 ± 3.1	16.5 ± 2.8	16.5 ± 2.0	16.0 ± 2.0	15.2 ± 2.6
FEB	15.5 ± 3.6	16.2 ± 3.7	18.9 ± 2.8	19.1 ± 2.2	22.2 ± 2.5	16.5 ± 5.5
MAR	17.1 ± 3.8	18.0 ± 4.4	21.5 ± 3.4	22.2 ± 2.5	19.0 ± 5.9	21.7 ± 5.2
APR	18.0 ± 4.6	17.5 ± 5.3	21.7 ± 4.2	19.4 ± 3.2	20.3 ± 3.4	22.0 ± 5.6
MAY	17.1 ± 4.9	15.3 ± 5.8	19.2 ± 5.2	20.1 ± 1.2	16.6 ± 6.8	19.1 ± 5.8
JUN	17.6 ± 3.5	18.4 ± 5.2	20.0 ± 4.8	23.6 ± 2.9	16.8 ± 6.1	23.5 ± 6.4
JUL	16.5 ± 3.4	20.3 ± 5.0	22.4 ± 3.3	22.3 ± 2.7	24.6 ± 3.0	20.8 ± 3.0
AUG	17.2 ± 3.5	18.9 ± 5.7	22.0 ± 4.1	20.5 ± 3.8	21.0 ± 6.1	19.0 ± 4.4
SEP	16.3 ± 3.4	16.4 ± 4.0	20.4 ± 3.7	21.7 ± 2.4	17.9 ± 4.6	17.7 ± 6.4
OCT	15.2 ± 3.9	16.0 ± 4.5	18.3 ± 3.9	18.9 ± 2.9	17.0 ± 5.9	17.4 ± 5.6
NOV	14.7 ± 2.8	14.6 ± 3.3	16.4 ± 3.0	17.7 ± 1.8	16.1 ± 2.5	16.3 ± 6.0
DEC	13.1 ± 2.6	13.0 ± 3.5	14.8 ± 3.3	14.2 ± 2.8	14.8 ± 1.9	13.6 ± 3.5

59

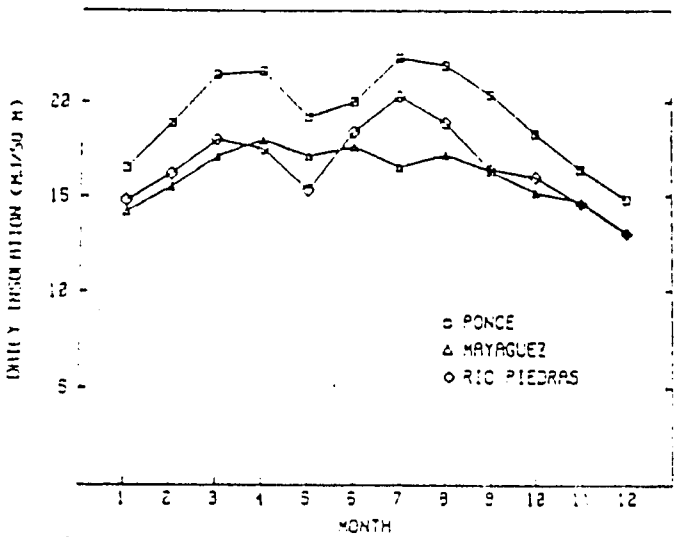

Fig. 2 Average daily insolation on a horizontal plane vs. month of the year

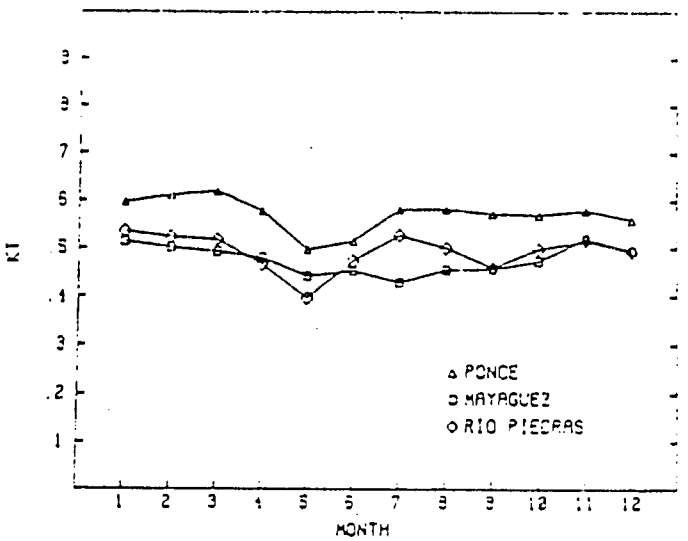

Fig. 4 Average daily K_T vs. month of the year

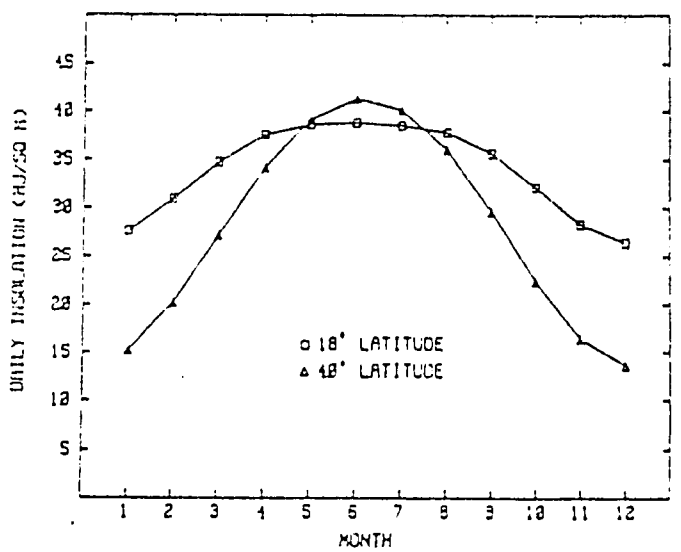

Fig. 3 Daily extraterrestrial insolation on a horizontal plane vs. month of the year

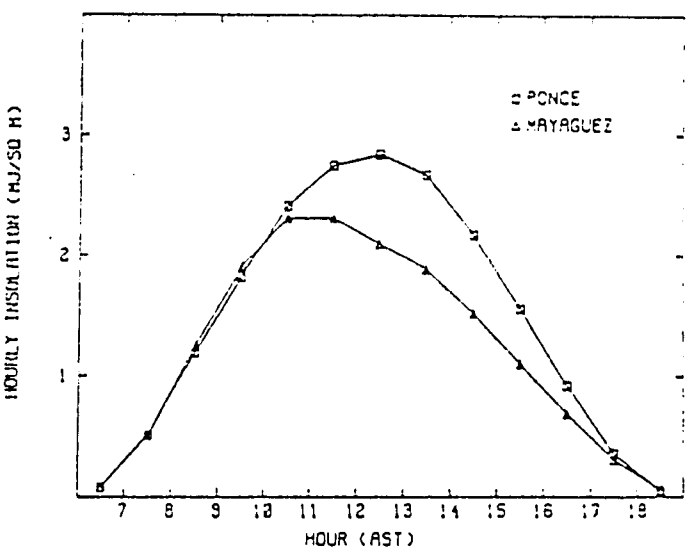

Fig. 5 Average hourly insolation on a horizontal plane vs. hour of the day

distribution of insolation. This is best demonstrated by Fig. 4 which is a plot of average daily K_T (ratio of global insolation on a horizontal plane to extraterrestrial insolation on a horizontal plane) vs. months of the year.

The yearly distribution of horizontal insolation has important implications in the design of optimized solar energy collectors. One striking example of this is a solar pond for an industrial application where a horizontal collector is to be matched to a year-round uniform load. The size of the storage layer for such a pond located in Puerto Rico can be made much smaller than for a similar system at a higher latitude. Even for solar collectors which can be tilted there are often esthetic and cost advantages to a horizontal mount.

The distribution of insolation during the day can also be important. Fig. 5 compares this distribution for the cities of Ponce and Mayagüez. It is clear that the difference in daily insolation for these two sites occurs during the noon to afternoon hours, but Mayagüez seems to be a very special case in this regard. All of the other locations studied had roughly symmetrical hourly distributions.

Statistical Distribution

The standard deviations of the statistical distributions of daily global insolation have been calculated (Table 2). Although for some stations the results are based on one year's record, some general trends are apparent. The higher insolation stations (Ponce and Cabo Rojo) tend to have lower standard deviations. (The low deviation values at Mayagüez are apparently due to the consistent weather pattern experienced there. See discussion above.) At all stations the deviations during the summer months are larger than during the winter months.

CORRELATION BETWEEN INSOLATION AND PRECIPITATION

Measurements of insolation levels are scarce in many parts of the world, particularly in the underdeveloped nations. Many countries in the Caribbean fall in this category. In addition, as has been shown above, insolation levels can vary appreciably within the small areas of tropical islands so that, even if measurements are available at some sites, they may not be applicable to other regions within the same country.

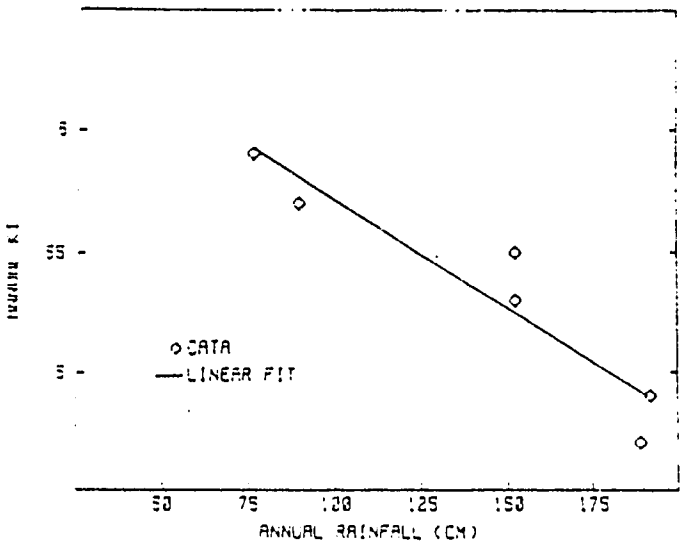

Fig. 6 Annual rainfall vs. annual K_T

Many ways have been proposed to estimate insolation levels at a given location. These are based on the statistical correlation of insolation to other more commonly measured meteorological variables such as cloud cover. Precipitation is an interesting possibility in this regard since accurate measurements of this variable are quite common worldwide.

This section presents the results of a study of the relationship between average annual insolation and average annual rainfall in Puerto Rico. (Rainfall is the only form of precipitation in Puerto Rico.) The data points shown in Fig. 6 correspond to the insolation measured at the CEER stations vs. the rainfall measured at nearby sites. Annual rainfall data has been provided by the U.S. National Weather Service. Rainfall measurements were available at sites within 4 km of all of the stations except Cabo Rojo. Rainfall data for a station at Ensenada, 25 km to the east of Cabo Rojo, was used for this point. (Ensenada is on the southern coast and has weather very similar to Cabo Rojo.) Insolation values are presented in the form of annual K_T in order to facilitate future comparison with sites outside Puerto Rico. A linear fit to the data points yielded a correlation coefficient of 94% with a standard error in K_T of 0.018. The equation for the straight line is:

$$K_T = 0.659 - 0.000886\ R$$

where R is average annual rainfall measured in cm.

Based on this linear fit and a rainfall map, an insolation map of Puerto Rico has been prepared (Fig. 7).

CORRELATION BETWEEN DIFFUSE AND GLOBAL INSOLATION

In order to be able to predict the performance of solar collectors accurately, it is necessary to know the partition of the global insolation into its diffuse and direct components. This is especially true of concentrating collectors (2). However, diffuse and direct insolation measurements require additional equipment which must be adjusted almost daily. These types of measurements are much rarer than global insolation measurements. In the underdeveloped nations they are almost non-existent. Thus, a method must be found to predict accurately the amount of diffuse radiation from the values of other more commonly measured variables.

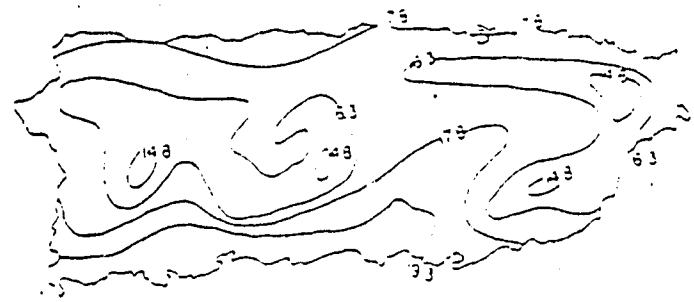

Fig. 7 Insolation map of Puerto Rico. Average daily insolation on a horizontal plane in MJ/m^2.

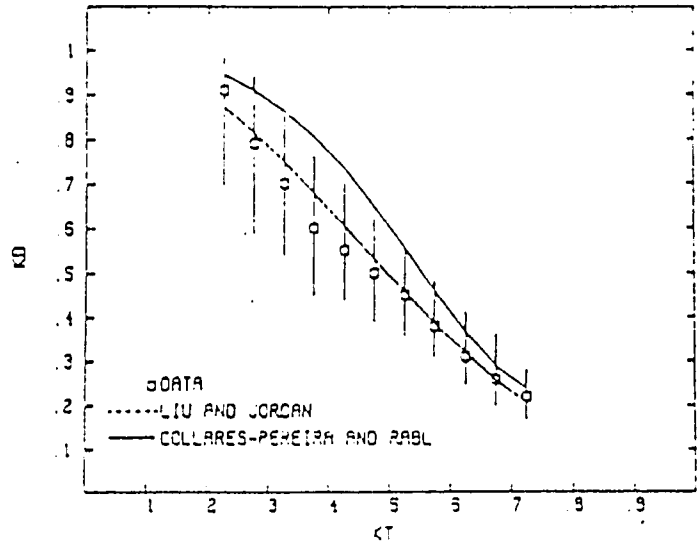

Fig. 8 Daily K_T vs. daily K_D. Data set includes three cities.

Although many different predictive correlations have been suggested for calculating the diffuse component, most include K_T as a correlation variable. Many take this to be the only variable. The diffuse component is predicted from the measurement or estimation of the global insolation and from the correlation of K_T vs. K_D (ratio of diffuse insolation on a horizontal plane to global insolation on a horizontal plane). This correlation is known to be far from perfect. There is usually a large scatter in the data. However, it has been suggested that the long term performance of solar collectors is sensitive only to the average correlation between these variables (3).

Fig. 8 presents the results of the measurements of daily K_T and K_D at Mayagüez, Río Piedras and Cataño. Only days for which there were data during all hours of the day were included in this analysis. A shadow band correction factor was applied to the K_D values. This factor depends on the month of the year and the values used were based on the manufacturer's recommendations (4). The range of correction factors is 1.12 to 1.23.

The individual days have been segregated into classes according to their value of K_T. (Each class corresponds to a K_T interval of 0.05) The data points represent the average K_D for each class vs. the K_T midpoint. Since the distribution of individual daily K_Ds around the average is not necessarily symmetrical, the error bars (one standard deviation) have been calculated independently for the daily K_Ds which are above the average and for those that are below the average in each class. Those classes which contain less than 30 days of data have not been plotted.

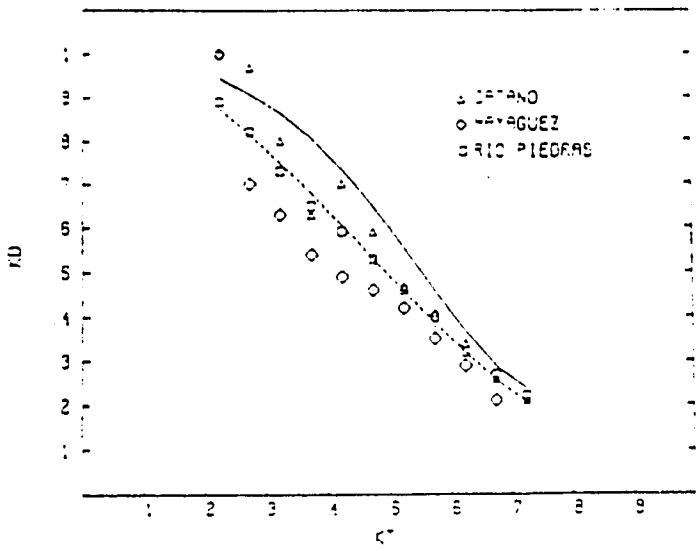

Fig. 9 Daily K_T vs. daily K_D. Data for individual sites are plotted separately.

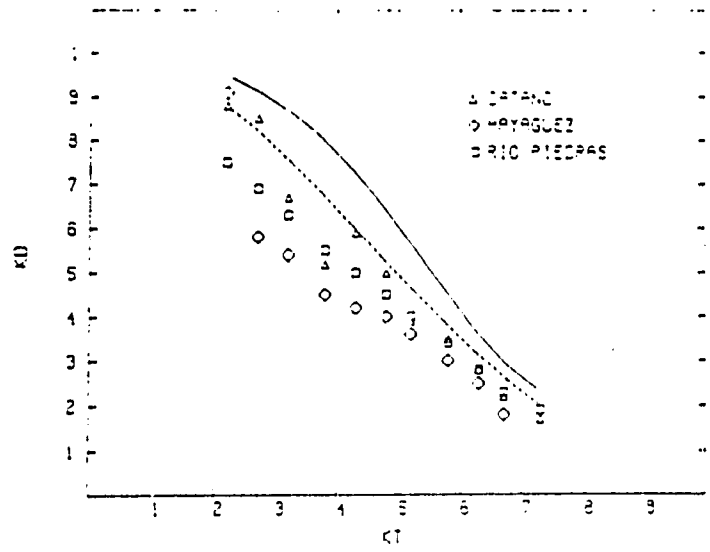

Fig. 10 Daily K_T vs. daily K_D. No shadow band correction has been applied to the data.

The lines in Fig. 9 are relationships commonly used in collector performance calculations. The solid line is the relationship determined by Collares-Pereira and Rabl from measurements at five sites in the continental United States all above 30° latitude (3). This relationship is quite similar to that found by Ruth and Chant in Canada (5). The dashed line is the relationship determined by Liu and Jordan from measurements at Blue Hill, Massachusetts (6). (The original Liu and Jordan relationship has been changed slightly to reflect the change in the accepted value of the solar constant since 1963.)

The differences between the Puerto Rico data and the results of other researchers depicted in Fig. 9 are statistically significant. The large standard deviations are due to the large scatter of the data from individual days. The statistical error in the determination of the average K_Ds, however, is much smaller (by at least a factor of 5) than the standard deviations.

The Collares-Pereira and Rabl relationship overestimates the diffuse component measured in Puerto Rico while the Liu and Jordan relationship provides a better estimate. However, it also overestimates the diffuse for K_T values between 0.3 and 0.5. The standard error for the comparison of the Collares-Pereira and Rabl relationship to the Puerto Rico results is 0.12 while for the Liu and Jordan relationship it is 0.05. (In calculating these errors the contribution of each class has been weighted by the number of days in it.)

In order to study the reasons for the differences between the Puerto Rico results and the Collares-Pereira and Rabl relationship, the Puerto Rico data have been analyzed for site dependence (Fig. 9). Significant differences have been found among the three sites. The points for Río Piedras fall between those at Mayagüez (low) and those at Cataño (high). Although none of the stations reaches the Collares-Pereira and Rabl curve, Cataño approaches it and the data there lies above the Liu and Jordan curve.

The discrepancy between the Collares-Pereira and Rabl correlation and the Liu and Jordan correlation may not be real (3). The first is based on pyrheliometer measurements and the second on measurements made with a pyranometer and shadow band. Liu and Jordan did not apply a shadow band correction to their measurements. Thus, the diffuse insolation at Blue Hill is actually larger than reported. In order to make a realistic comparison to the Liu and Jordan results, Fig. 10 has been prepared with data to which no shadow band correction factors have been applied. The conclusion can be made that the results from Mayagüez and Ponce are, in fact, significantly different from those at Blue Hill and different from those at the U.S. sites studied by Collares-Pereira and Rabl and the Canadian sites studied by Ruth and Chant. The relationship at Cataño, however, is closer to the relationships found at the continental sites.

The results at Cataño suggest that the difference in the relationships for Mayagüez and Río Piedras vs. those in the United States and Canada are not due completely to a "latitude effect" although some latitude effect can not be ruled out. This is also supported by Straub, Baylon and Smith's analysis of the Typical Metereological Year weather file and nine months of data from Seattle, Washington (7). These authors found the Collares-Pereira and Rabl relationship to overpredict K_D by approximately 0.07 in Seattle.

A possible explanation for the differences in the results obtained at the different sites is a dependence of the shadow band blocking factor on the cloudiness conditions. Such an effect has been reported by Spencer and Near (8). These authors also point out some disadvantages in the use of integrated pyrheliometer measurements to determine the diffuse component. More accurate measurements, perhaps requiring a pyranometer with a shadow disc, are necessary to determine the magnitude of a latitude effect, if any, on the K_T,K_D correlation.

CONCLUSIONS

It is important to consider the small-scale geography of Caribbean islands in order to determine the applicability of insolation measurements at nearby sites. Average annual precipitation can be correlated to average annual insolation in Puerto Rico fairly well. This provides a way of estimating insolation at sites where precipitation data are available. More accurate measurements of diffuse radiation are needed to determine the magnitude of a latitude effect on the daily K_T, K_D correlation.

62

ACKNOWLEDGEMENTS

Many students from the University of Puerto Rico have participated in the tedious labor of data processing and in the development of computer analysis programs whose results have been presented here. In particular the authors would like to acknowledge the efforts of Messrs. Luis Ciappi, Eddie Marrero and Humberto Vega. Dr. José Colón of the National Weather Service in San Juan provided the rainfall data and maps used in the analysis. Several institutions have cooperated in this work by maintaining measurement stations. These are the Catholic University of Puerto Rico, the Bacardi Corporation, Roche Products, Inc., the Nestle-Libby Co. and the U.S. National Wildlife Service. This work has been supported in part by the U.S. Department of Energy.

REFERENCES

1. Ewel, J.J., and Whitmore, J.L., "The Ecological Life Zones of Puerto Rico and the U.S. Virgin Islands," Forest Service Research Paper ITF-18, Dec. 1973, Institute of Tropical Forestry, U.S. Department of Agriculture, Río Piedras, Puerto Rico.

2. Erbs, D.G., Stauter, R.C., and Duffie, J.A., "The Basis and Effects of Inaccuracies in Diffuse Radiation Correlations," Proceedings of the 1980 Annual Meeting of AS/ISES, Vol. 3.2, 1980, pp. 1429-1433.

3. Collares-Pereira, M., and Rabl, A., "The Average Distribution of Solar Radiation - Correlations Between Diffuse and Hemispherical and Between Daily and Hourly Insolation Values," Solar Energy, Vol. 22, No.2, 1979, pp. 155-164.

4. "Instructions for the Operation and Maintenance of the Eppley Shadow Band Stand," 1976, Manual by The Eppley Laboratory, Inc., Newport, Rhode Island.

5. Ruth, D.W., and Chant, R.E., "The Relationship of Diffuse Radiation to Total Radiation in Canada," Solar Energy, Vol. 18, No.2, 1976, pp. 153-154.

6. Liu, B.Y.H., and Jordan, R.C., "The Interrelationship and Characteristic Distribution of Direct, Diffuse, and Total Solar Radiation," Solar Energy, Vol. 4, No.1, 1960, pp. 1-9.

7. Straub, D., Baylon D., and Smith, O. "Comparison of Modeled and Typical Meteorological Year Diffuse, Direct, and Tilted Solar Radiation Values with Measured Data in a Cloudy Climate: Seattle-Tacoma Data," Proceedings of the 1980 Annual Meeting of AS/ISES, Vol. 3.2, 1980, pp. 1420-1424.

8. Spencer, D.W., and Near, R.J., "Comparison of Theoretical Diffuse Shadow Band Corrections with Minute by Minute Data," Proceedings of the 1981 Annual Meeting of AS/ISES, Vol. 4.2, 1981, pp. 1511-1515.

61

MODULE 2: SITING THE COLLECTOR ARRAY

OBJECTIVE

The objective of this module is for the trainee to be able to determine from a particular site, any affects of shading or orientation on a collector array.

MODULE 2:

SITING THE COLLECTOR ARRAY:

The Solar Window:

If we were to spend all year standing at a site and recording the sun's path, we could chart its position on a sun path diagram. The path of the sun could be painted (projected) onto a dome, as could the outline of surrounding houses and trees. The morning and afternoon limits of useful solar collection, as determined by the three hours before solar noon and the three hours after solar noon define the "solar window".

Almost all of the useful sun that reaches the collector must come through this window except for diffused radiation. If any of the surrounding houses, trees, etc. intrude into this "solar window", the intrusion will cause a shadow on the collector. The isometric drawing below illustrates the solar window for a latitude of 28°N. The solar window changes for different latitudes.

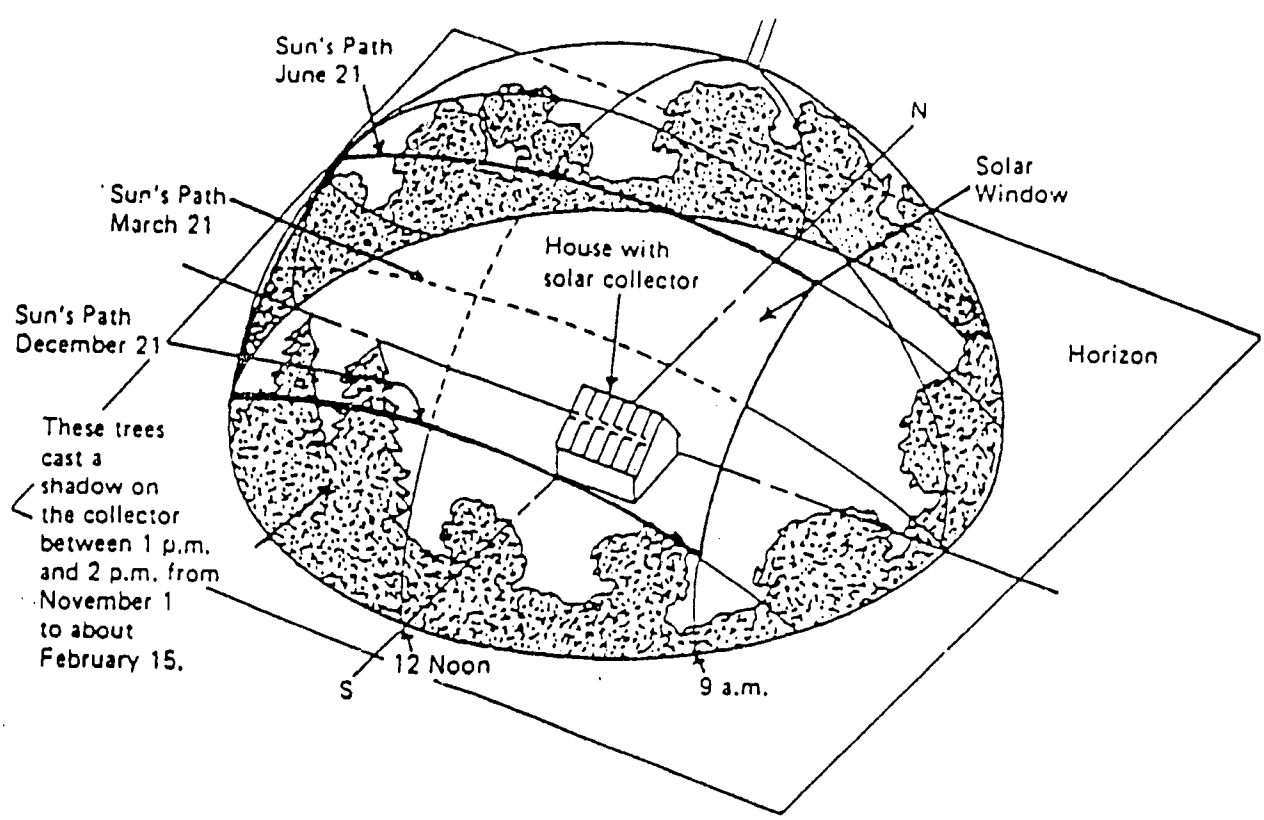

Figure 2-1
Solar Window

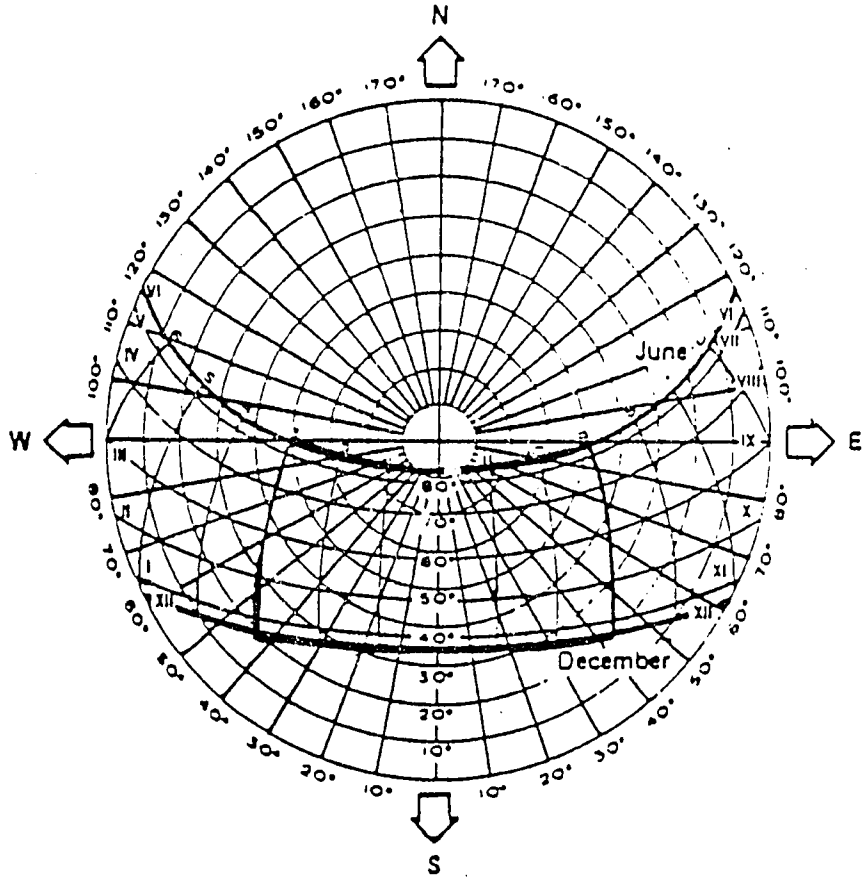

32° Latitude

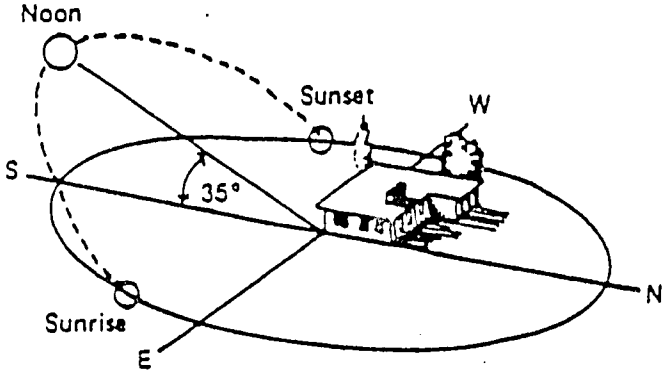

Winter Altitude

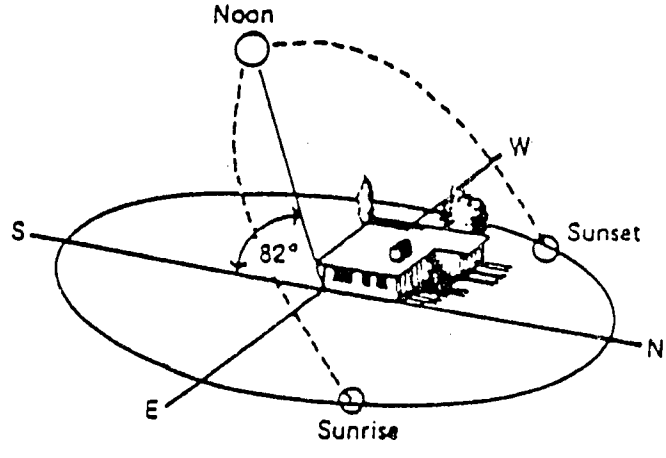

Summer Altitude

Figure 2-3

Sun Path Diagrams

66

BENNETT SUN ANGLE CHART:

This chart provides a means by which we can determine the position of the sun for any time of the year and time of day.

The curved lines with dates on them show the position of the sun in the sky for that date. The dotted lines give the position for the time of day. For example, on February 23rd, at 10:12 A.M., the sun is 52° high in the sky (solar altitude) and its compass heading (solar azimuth) is 135 degrees, or directly S.E. (see Figure 3-8).

A Bennett Sun Chart for your latitude (18°N) is valuable. If an obstruction is near your collector location, you can determine the altitude of its top and the azimuth of its two sides. By plotting these on the Bennett Sun Chart, you can determine the amount of shading the obstruction will produce during the year.

For example, if we have a building south of the proposed collector location and we measure its azimuth to start at 120° and end at 200°, and we estimate its height to be about 40° from the proposed site, then its shadow pattern is represented by the shaded part of Figure 3-9. We see that it would shade the collector solar window from 9:00 to 10:10 on December 22nd; 9:00 to 9:50 on November 22nd and January 21st; 9:00 to 9:30 on November 3rd and February 8th; and 9:00 to 9:15 on October 19th and February 23rd. Notice this shading is worse during the winter months, just when we need solar the most. We would lose about an hour of sunlight out of the 6-hour solar window during the two coldest winter months from this obstruction. As a result, if a better location could not be found, the collector array should be sized up by about 1/6th.

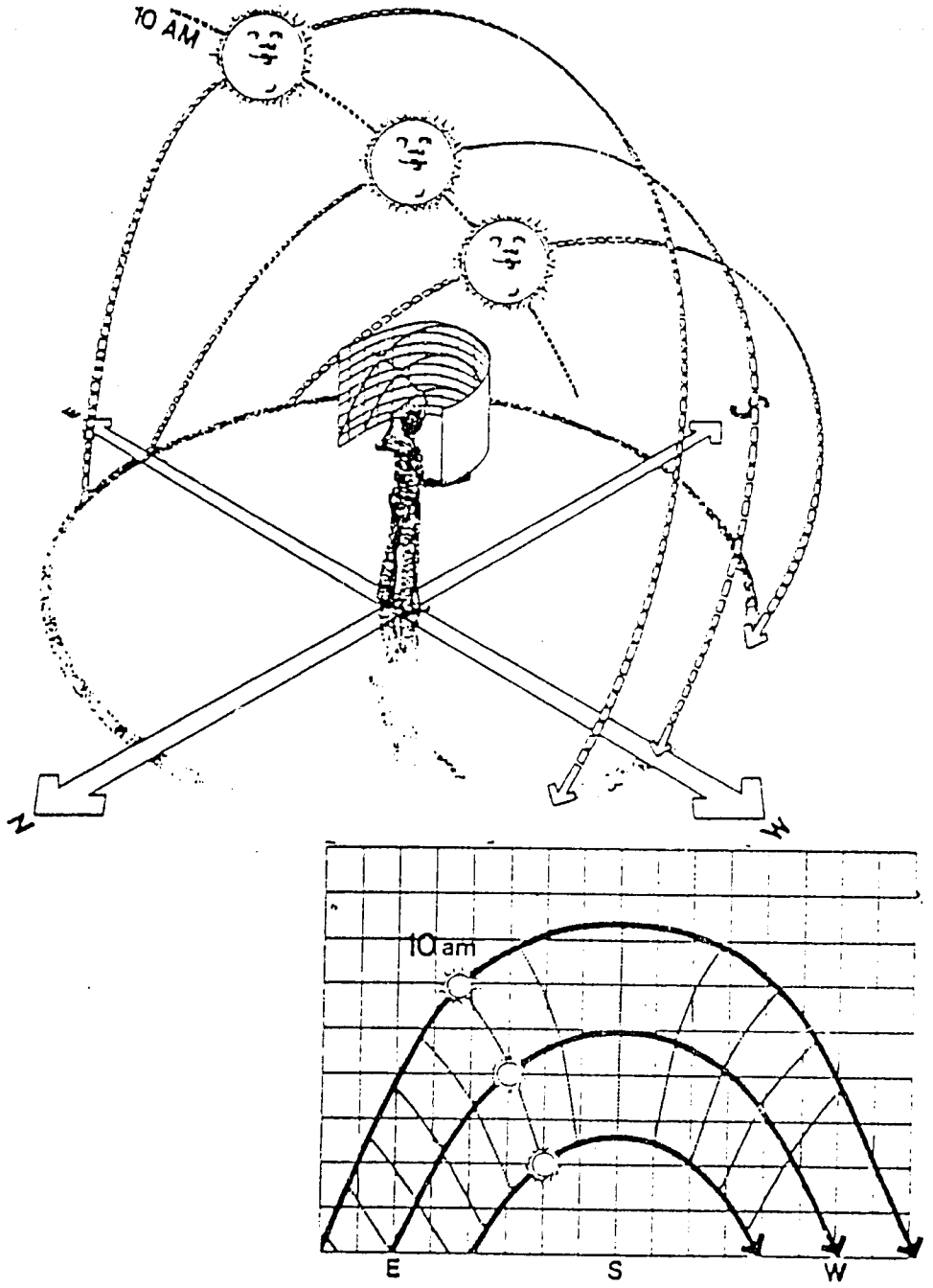

THE BENNETT SUN ANGLE CHART IS SIMPLY A PROJECTION OF THE SKY DOME SUN PATHS ONTO A FLAT SHEET.

Figure 2-4

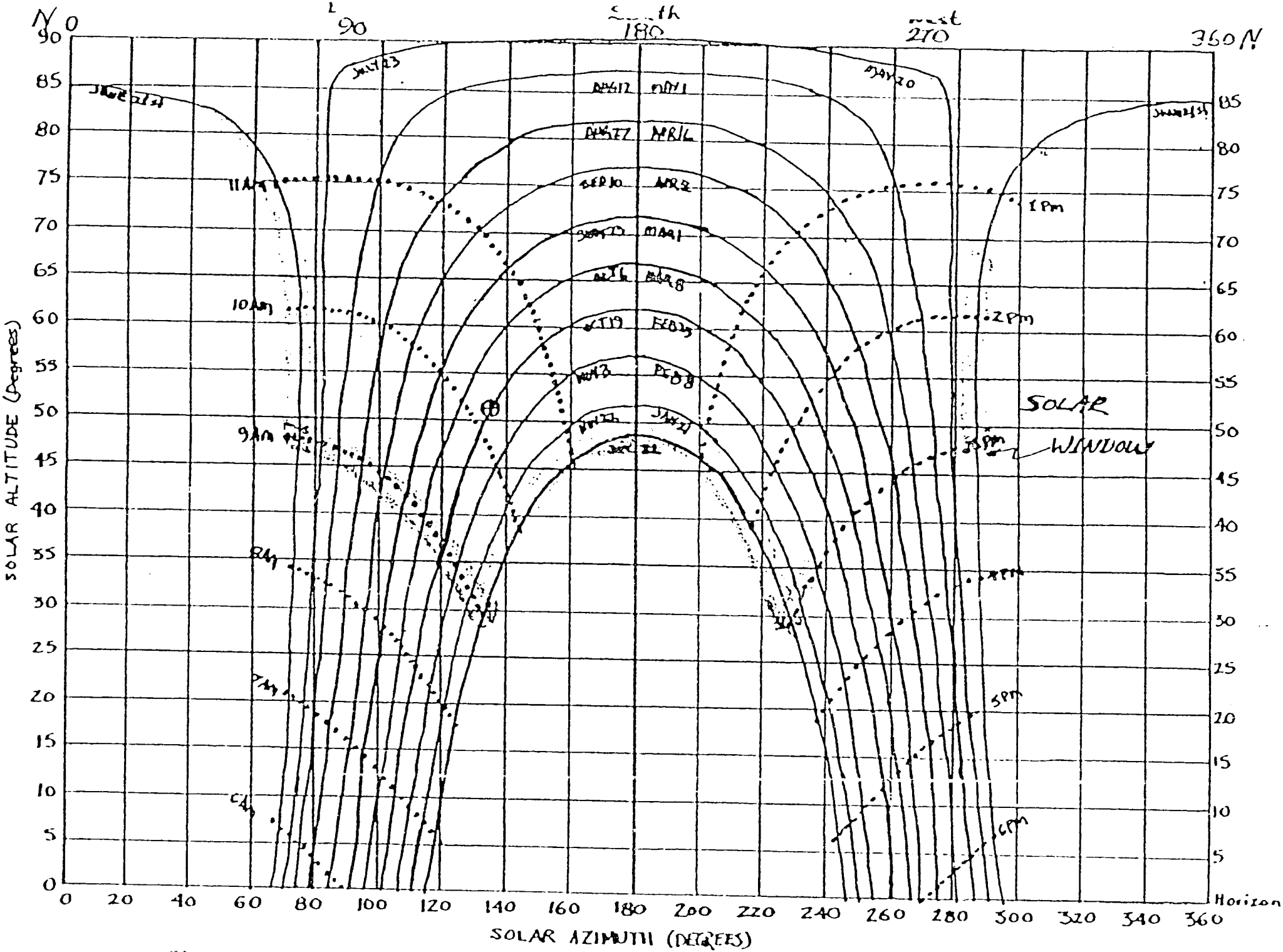

Figure 2-5

18° NORTH LATITUDE

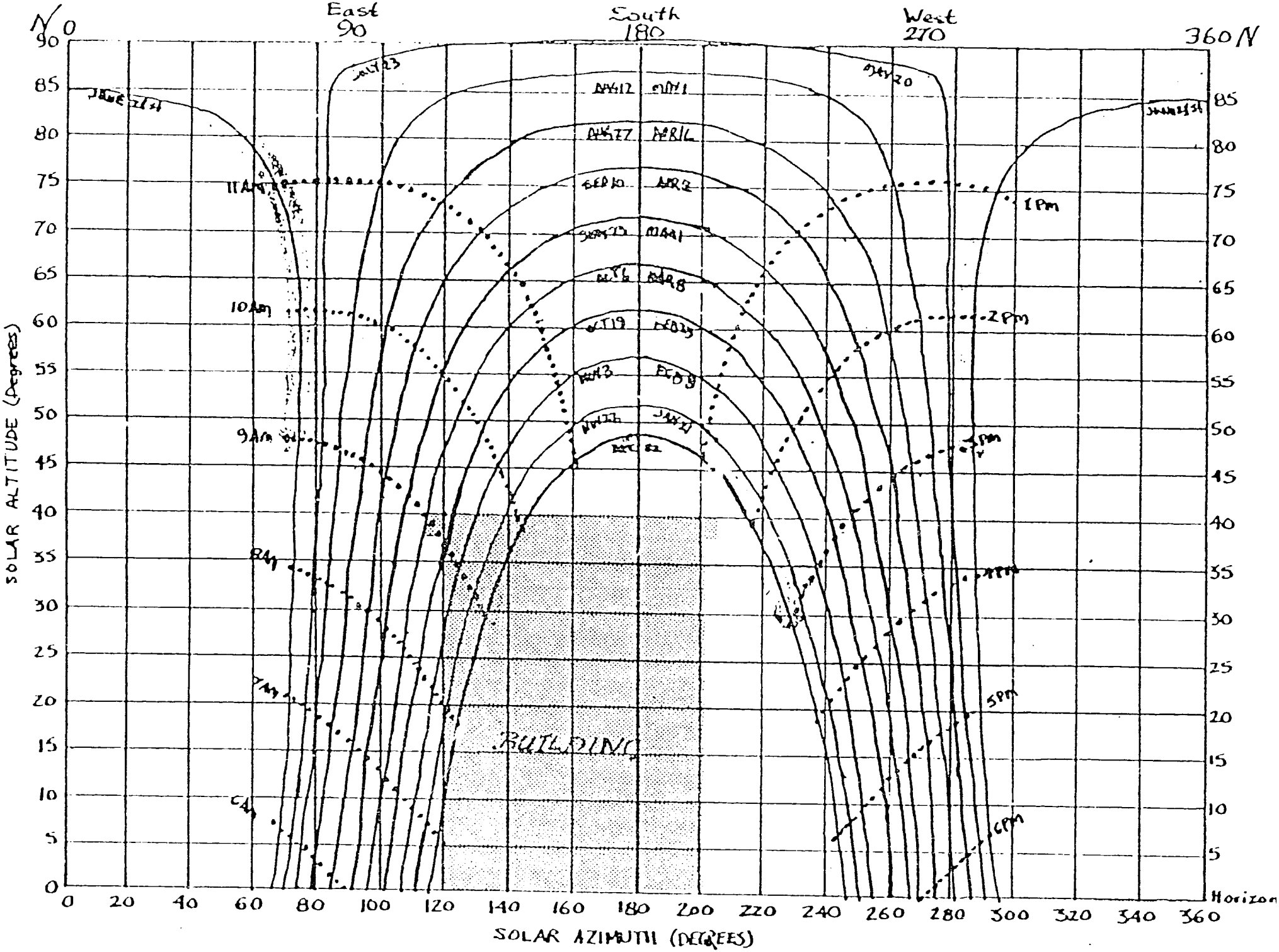

Figure 2-6

18° NORTH LATITUDE

Collector Orientation. All collectors work best when facing due south. If roof lines or other factors dictate different orientations, a penalty will be paid, as shown in Figure 2-7. For example, for 20° east or west of due south we must increase the collector area to 1.06 times the size needed with due south orientation (dashed lines on Figure 2-7 for the same energy output.

We have assumed that nothing shades the collector during any part of the day. If tall trees, for example, shade a collector until 10 a.m., an orientation west of south would be optimum, since the afternoon sun will provide the bulk of the energy collected each day. So the site must be studied to be sure that specific solar insolation factors are known in each installation.

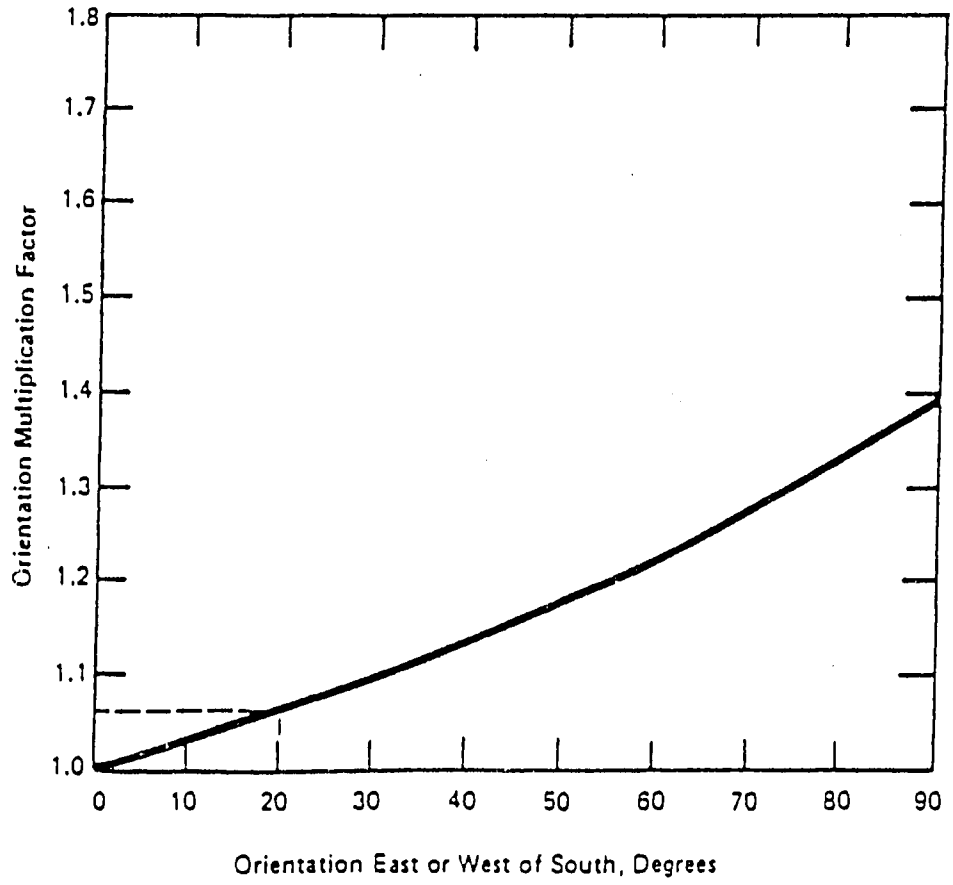

Figure 2-7

Effect Of Facing Collector in a Direction Other than Due South

MODULE 3: Collector Types and Construction

Objective

The Objective of this Module is for the trainee to become familiar with the different types of solar collectors, and to gain an understanding of the basic heat balance equation governing collector operation.

1V

TYPES OF COLLECTORS: Solar collectors are often grouped according to their thermal operating ranges: low- medium- or high-temperature.

Low-temperature collectors are used for heating swimming pools and similar tasks (below 100°F). Medium-temperature collectors are used for tasks like heating buildings and heating water (up to 200°F). High-temperature collectors are used to drive absorption air conditioners, produce steam, and melt materials without the danger of contamination (200°F to 5,000°F). Figure 3-1 shows several types of collectors in high-temperature categories.

The purpose of a solar collector is to gather radiant energy from the sun and transfer it in the form of heat to a fluid, usually water. The type of collector used depends upon the fluid temperatures required--for very high temperatures, a focusing-type (concentrating) collector is employed, which focuses the sun's rays onto a target or a receiver (see Figure 3-1). Burning paper with a magnifying lens is an example of this concept. The concentrating collector uses only the direct (beam) radiation and thus must follow the sun across the sky by means of complicated tracking equipment that must be relatively free of maintenance and able to withstand hurricane-force winds. Tracking equipment substantially increases the price of a system; also, in many areas, sunshine is diffuse and cannot be used by a concentrator. However, this diffuse radiation can be absorbed effectively by a flat-plate collector. On a daily basis, in Jamaica, a flat-plate collector will collect more heat than a concentrating type, so the overall efficiency of the flat-plate is higher. Because of lower efficiencies and higher cost, concentrators are used only when temperatures beyond the reach of a flat-plate collector are needed.

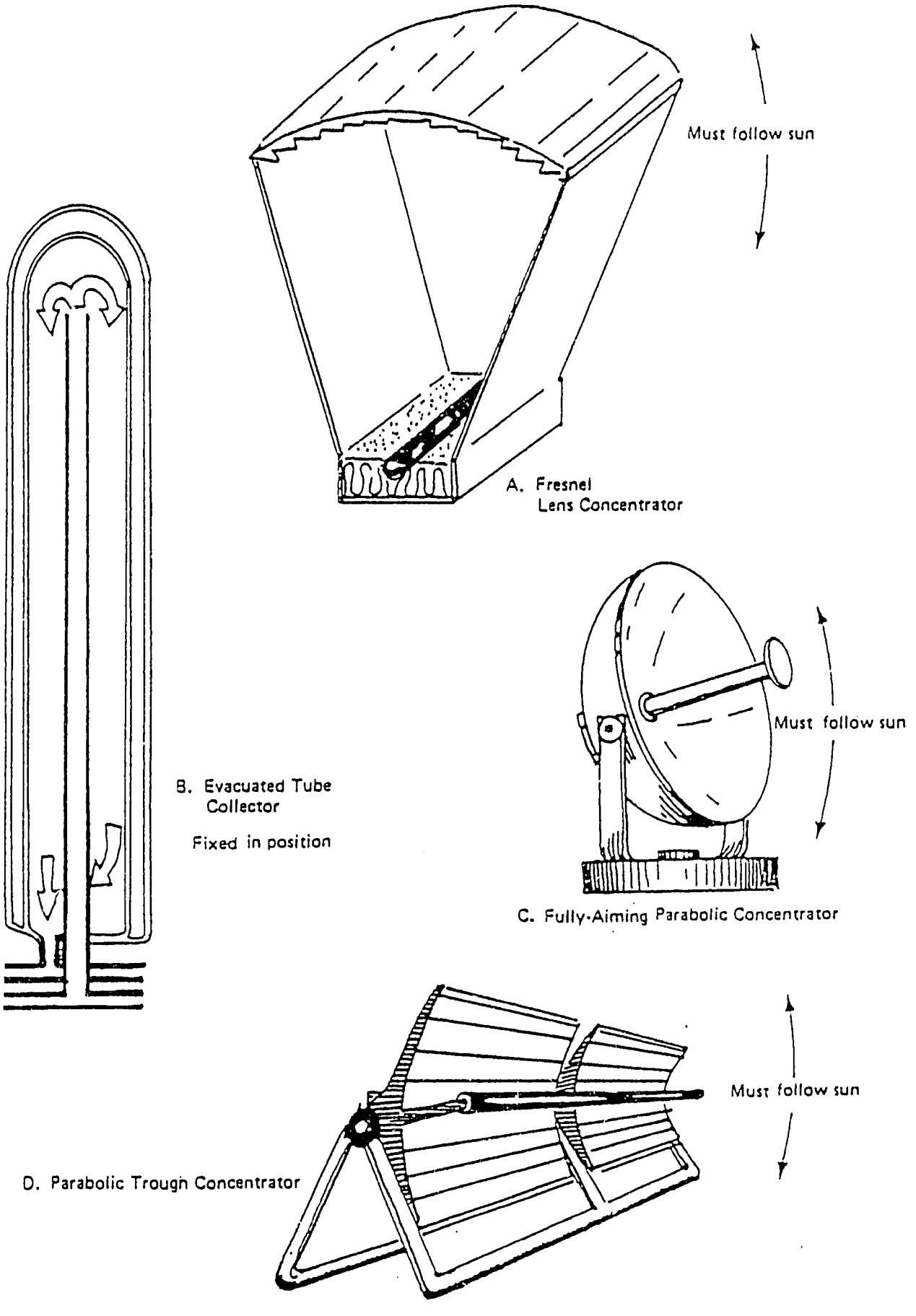

FIGURE 3-1
High-Temperature Collectors

Flat - Plate Collectors: The most basic flat - plate collector, used for low temperature heating, consists of a black metal or plastic deck with flow passages to remove the absorbed heat (see Figure 3-2) The amount of heat collected depends on the temperature of the fluid with respect to the ambient air temperature--the hotter the fluid the more difficult it is to add heat. The maximum temperature available from this type of collector is about 110°F; however, the fluid flow rate usually is very high, and the collector remains at about ambient temperature, where it operates at highest efficiency.

In domestic water heating, the final desired temperature is between 120°F and 160°F. Since the bare deck cannot deliver this temperature, a necessary alternative is to build a metal deck into a well-insulated box with a transparent cover (glazing), which not only allows solar radiation in but keeps the wind from removing heat and thus cooling the plate. The addition of glazing to the collector also causes what is known as the greenhouse effect--an example is the almost unbearable heat felt when getting into a closed car that has been sitting in the sun. The greenhouse effect works in the following manner: First, radiation enters through the transparent glazing, where most of it is absorbed as heat by the metal deck. Next, the deck gives off much of the heat as long-wavelength radiation, called infrared radiation, which is trapped inside because the glazing material is opaque to such wavelengths.(See Figure 3-3)

Flat-plate collectors have many uses today, depending on the temperature requirement. Unglazed collectors heat pools and operate well at up to 30°F above ambient temperature. By glazing and insulating the plate, the maximum temperature is increased to the range

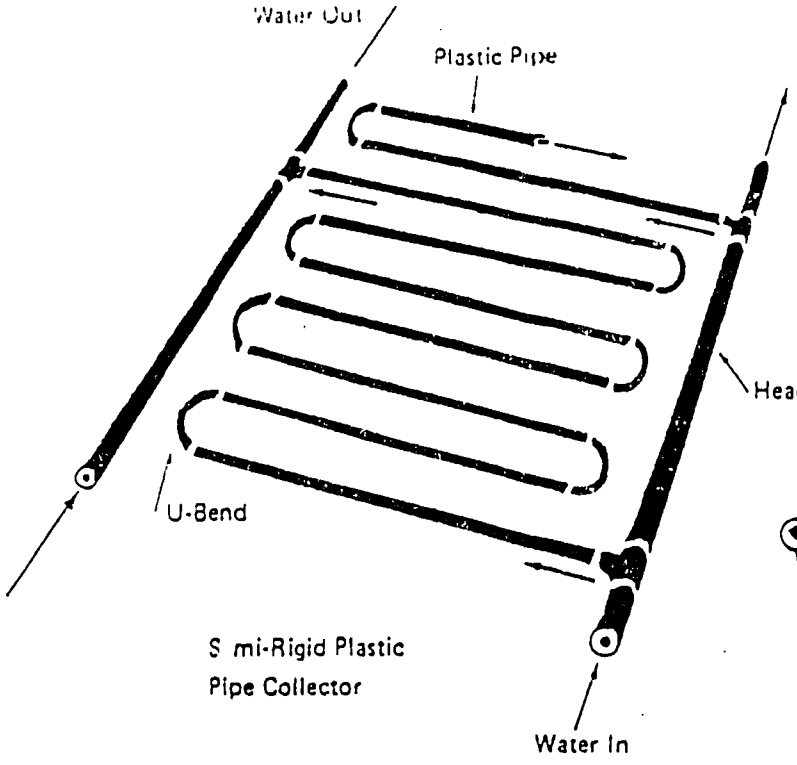

S mi-Rigid Plastic
Pipe Collector

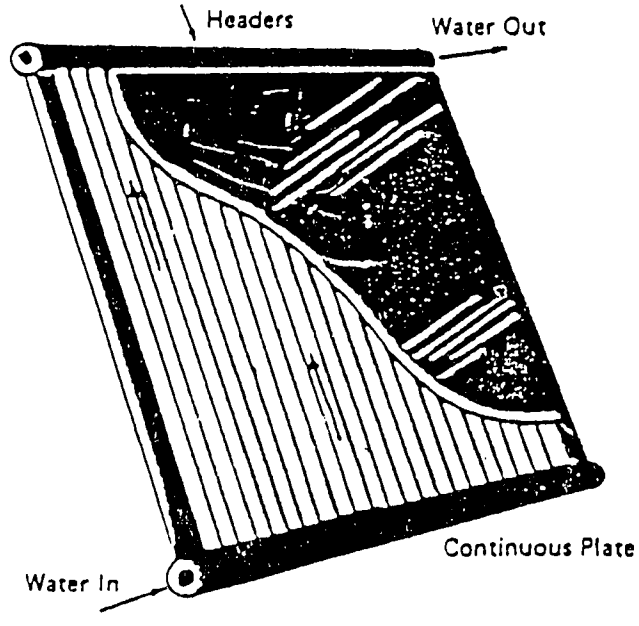

Flat Plastic Sheet Collector

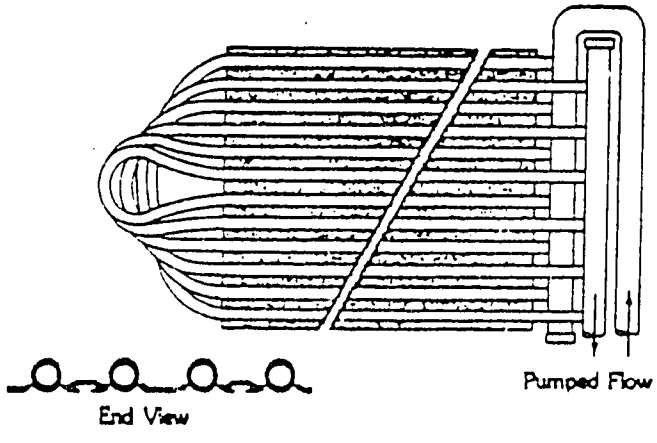

Rubber Mat Collector.

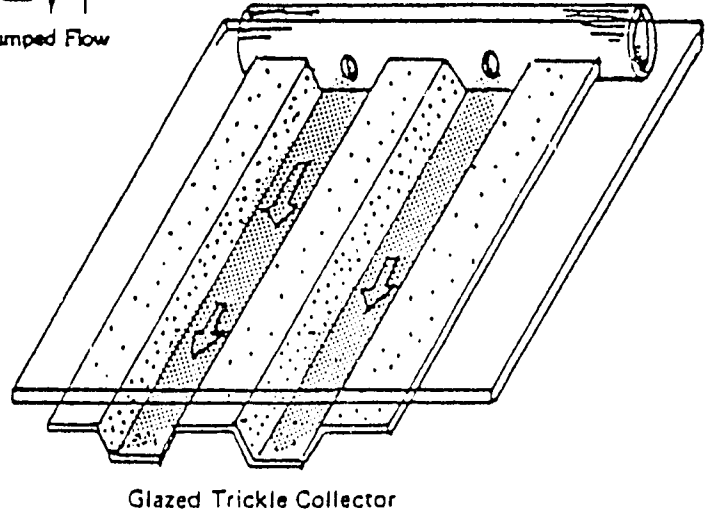

Glazed Trickle Collector

FIGURE 3-2

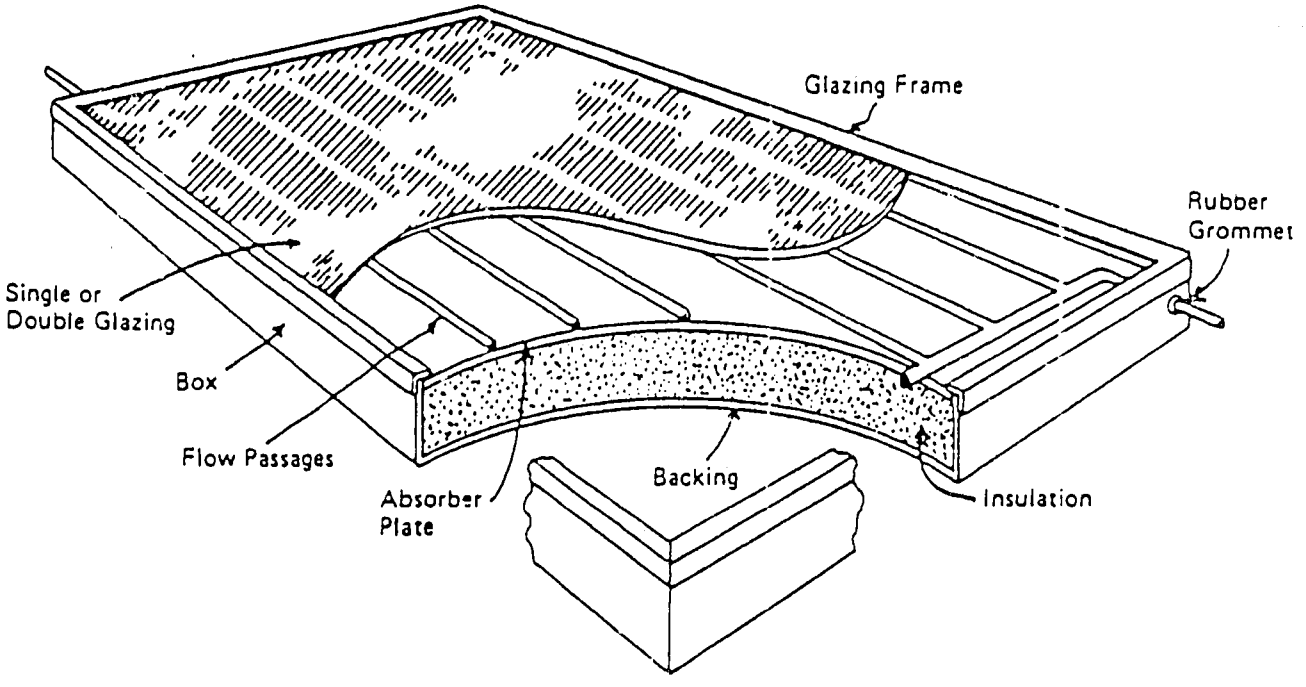

FIGURE 3-3
Collector Anatomy

of domestic water heating (120°-160°F). By using more expensive materials and double glazing, the temperature can be pushed as high as 200°F, useful for solar-powered air conditioning applications. The collector cost generally rises with higher output temperature requirements.

A collector's operating efficiency is dependent on insolation and the temperature of its fluid. As the fluid becomes hotter, adding heat to it becomes difficult, and the heat losses through the collector box increase.

On a flat plate collector, the inlet should be at the bottom and the outlet at the top so that the natural internal convection of the heated water tends to assist fluid movement.

Plastic collectors should be made of materials compounded with ultraviolet light inhibitors to retard degradation by constant exposure to sunlight. Fortunately, carbon black accomplishes this to a major degree and, at the same time, darkens the plastic and maximizes its effectiveness as a solar collector.

Transparent plastic films used to cover trickle collectors cannot, of course, contain carbon black. Mylar, tedlar, some teflon films, and other specifically-compounded transparent plastics are available for solar applications. Some are guaranteed for many years.

FLAT-PLATE COLLECTOR MATERIALS. The protective housing for a flat-plate collector may be made of metal, heat-tolerant plastic, treated wood, or even concrete formulated with vermiculite.

Metal housings should be isolated from thermal contact with the heat absorber plate. They are durable, attractive, strong, and may be built by well-established fabrication methods.

Plastic housings may be made in any shape or color. They are relatively light and offer some insulation to the heat collector. However, care must be taken in the selection of the plastic resin itself lest it

outgas at the stagnation temperatures which may develop in sunny weather if fluid flow through the collector is interrupted. The plastic must not soften at high temperatures.

In warm, moist climates only treated or rot-resistant lumber (cedar, cypress) should be used for wood housing, and even then, the long-term integrity of the structure may be subject to question. Wood is attractive from the standpoint of ease of fabrication and appearance.

Cast concrete collector housings have been used extensively in Australia. They are inexpensive, easy to cast on a mass production basis, durable, but very difficult to ship and install because of their weight.

Insulating materials should possess high thermal resistance, be tolerant of temperatures up to 350°F to 400°F, and be as water-resistant as possible. Fiberglass should not be used as insulation since wet weather causes it to absorb moisture and lose its insulation value.

Many manufacturers design their housings with screened 3/8-inch holes along the lower edges to drain any water which enters the box to escape. Isocyanurate and CO_2-blown urethane sheets about 1-inch thick are often used for insulating flat-plate collectors.

Transparent covers may be made of glass (preferably of low iron content), cast plastic sheets or flexible plastic films. Glass is heavy and hard to keep watertight at the edges, and it is very subject to breakage unless tempered is used. However, glass is optically transparent to sunlight and opaque to heat reradiated by the absorber plate, and it weathers better than the transparent plastics.

Several plastics have been specially formulated for use in solar applications. They are lightweight, easy to install, nearly as good as

glass optically, and cost about the same. For performance and durability, glass is better than the plastics.

Either glass or transparent plastic covers should be installed in such a way as to withstand severe wind loads as prescribed in local regulations.

Figure 3-4 shows several configurations used for absorber plates. Because tubes are expensive and sheet metal is relatively inexpensive, as little tubing as possible is used. It is very important to have a good thermal bond between the sheet metal absorber plate and the fluid transport passages. This may be accomplished by incorporating the tube in the sheet (Roll-Bond is an example); by soldering or brazing the tube to the sheet; or by clamping the tube to a grooved sheet and applying thermally-conductive adhesive to the area of contact.

The following tables give the thermal conductivity of commonly used absorber plate materials and the yield strengths of two types of solder:

	Material	Thermal Conductivity in Btu/hr-ft^2°F-ft
ABSORBER PLATE	Copper	217
	Aluminum	117
	Steel	26
COMPONENTS OF SOLDER	Tin	36
	Lead	20
	Antimony	10

SHEAR YIELD STRENGTHS OF SOLDER	50% Tin-50% Lead:	80	psi (at 250°F)
	95% Tin-5% Antimony:	250	psi (at 350°F)

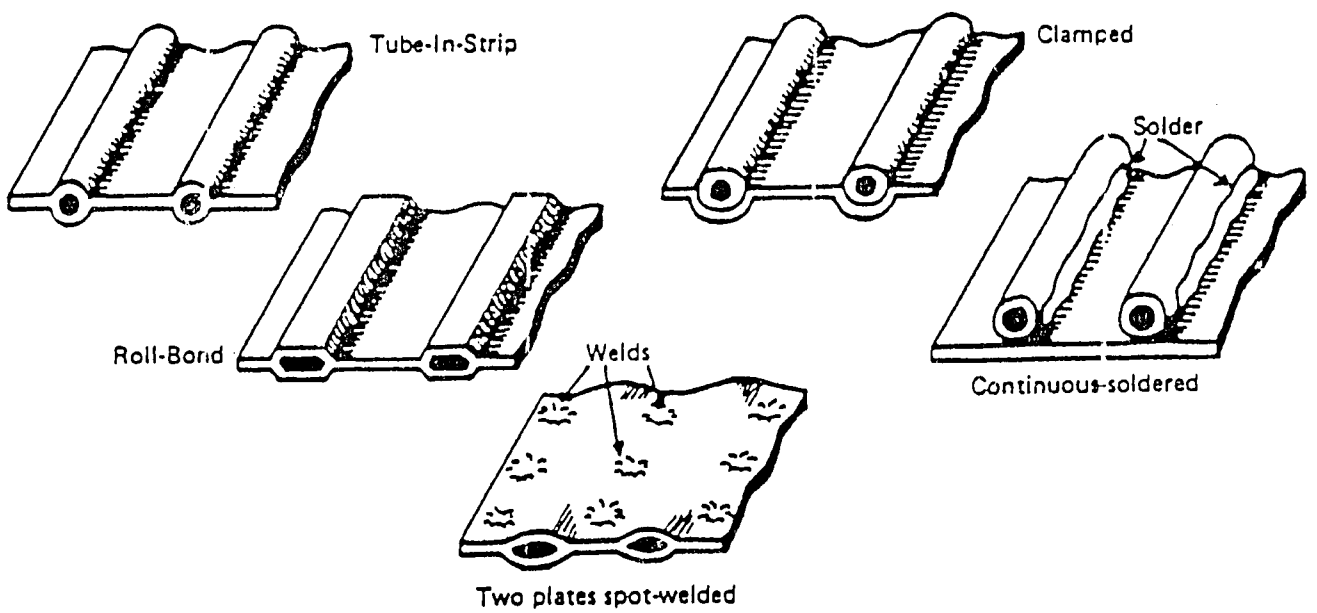

FIGURE 3-4
Absorber Plate Configurations

81

Copper, aluminum or steel may be used for heat absorbers, but both aluminum and steel passages must be protected from corrosion. Closed collector loops which contain corrosion-inhibited heat collector fluids can be used to protect aluminum and steel passages.

When dissimilar metals are used in tube and deck combinations, they must be studied for galvanic corrosion and thermal incompatibility problems.

Black coatings for heat decks may be classified according to how they are applied or according to whether they are optically selective or nonselective. Most coatings are applied as organic paints by spraying, brushing, rolling, or as metallic compounds by electrolytic deposition.

Nonselective coatings absorb more than 90 percent of the solar energy they receive, and they reradiate the same amount, but at longer wavelengths. In contrast, selective coatings also absorb about 90 percent of the solar radiation, but reradiate as little as 5 percent. Selective coatings are considerably the more expensive. Either may be applied to copper, steel or aluminum decks.

HIGH-TEMPERATURE COLLECTORS. The five broad categories into which high-temperature collectors fall are: parabolic or cylindrical troughs; compound parabolic concentrators; evacuated tubes; lenses; and paraboloids.

High-temperature collectors are less cost-effective for building heating, water heating and pool heating than are medium- and low-temperature collectors. They are used for solar air conditioning and for the production of steam. As mentioned previously, most concentrating collectors track the sun on a daily or seasonal basis (or

82

both), but they capture almost no diffuse energy. Compound parabolic concentrators and evacuated tube collectors need not track the sun, and they do capture both direct and diffuse energy. At the present time, high-temperature collectors are quite expensive.

Heat Flow

There are many ways to harness the sun's energy, but most examined in this manual fall in the solar-thermal category. "Solar-thermal" implies that the sun's energy is first converted to thermal, or heat, energy. What becomes of that heat depends on how well the system is designed. We would like to transfer most of the collected heat energy to water in a solar water heater, but some energy will inevitably be lost, and here we look into the various fates that can befall thermal energy.

Conduction: Heat conduction is a lot like electrical conduction; it requires a temperature difference and a path through some material. The heat and electrical conduction properties of materials are usually similar--metals conduct both well; most plastics do not. Short, wide paths conduct more heat than long, narrow paths. The rate of heat flow depends upon the difference in temperature from one end of the path to the other.

The similarity to electrical conduction is striking (if not electrifying!). We define resistance as a measure of the difficulty of conduction and speak of thermal resistance, R, as a property of materials, of conductors and insulators, of thermal paths in series and in parallel. See Figure 3-5 for illustrations of thermal conduction and equations for resistance of compound paths.

Convection: While conduction can and does take place through a fluid (a liquid or a gas), the flow of heat in fluids usually occurs through convection. In this process the fluid moves from one

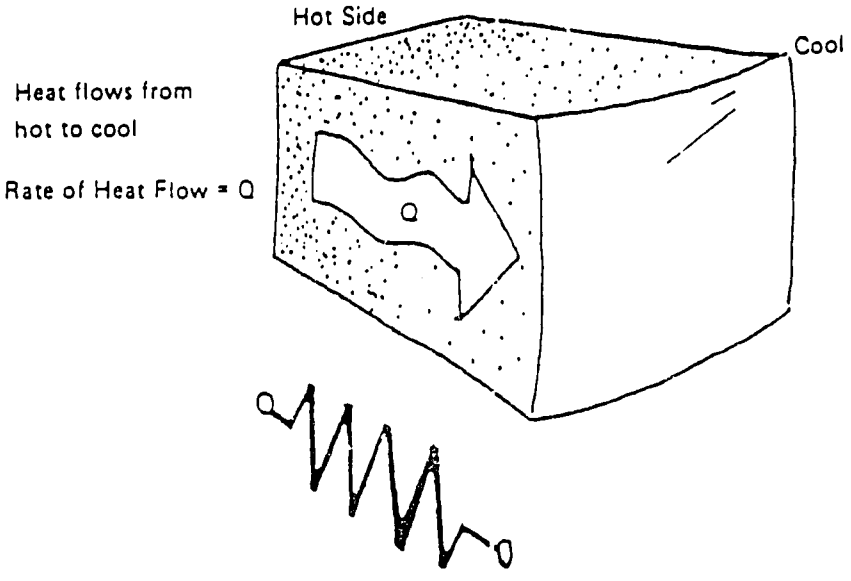

$$Q = \frac{T_{hot} - T_{cool}}{\text{Thermal Resistance}, R}$$

$$R = \frac{\text{Thickness}}{\text{Conductivity X Area}}$$

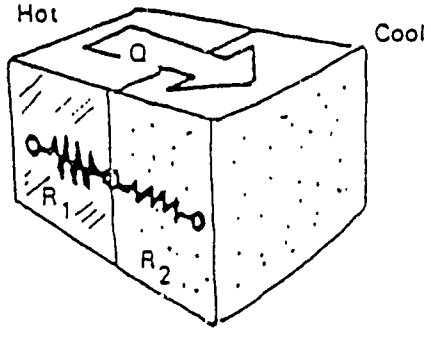

Material Resistance in Series

$$Q = (T_{hot} - T_{cool}) \left(\frac{1}{R_1 + R_2}\right)$$

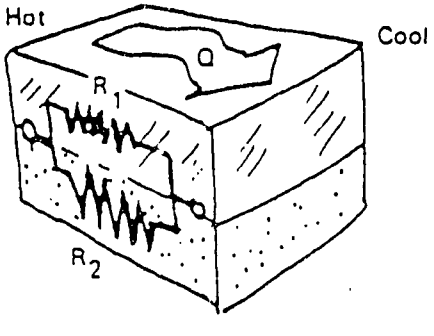

Material Resistance in Parallel

$$Q = (T_{hot} - T_{cool}) \left(\frac{1}{R_1} + \frac{1}{R_2}\right)$$

FIGURE 3-5
Thermal Conduction in Plain and Composite Solids

point to another, picking up heat and carrying it along. The gas or liquid also moves from warmer surfaces to cooler, serving as the medium of heat transfer. There is a thin film of conduction at the surface between the solid and the fluid, and from there on heat flow will depend strongly on the fluid and its speed of flow.

An air-cooled engine, for example, throws off most of its extra heat by convection. Heat from combustion travels by conduction to the surface of fins and from the fins out by convection in the air. The air moves past the fins by the motion of the vehicle in most motorcycles, or by a fan in many air-cooled car engines. Convection also occurs when heated air rises by its buoyancy--the heat itself causes the air movement.

Radiation Heat radiates outward from any hot body, just as radio waves radiate from an antenna. The heat flow depends on the temperature of surrounding surfaces, no matter how distant. A solar collector is normally warmer than its surroundings and will radiate heat away from its absorber plate. A fireplace in a still room will radiate heat to the person standing nearby. In solar systems, radiation must be considered, although its control is not as simple as control of conductive and convective flow.

GENERAL PRINCIPLES

A solar collector is a device for converting the energy in solar radiation to heat in a fluid. This conversion is accomplished by absorbing the solar radiation on a broad, thin metal surface which is in contact with a stream of liquid or gas. Absorption of solar energy causes the temperature of the metal surface to rise so that the temperature of the fluid increases as it moves past the surface.

Under steady conditions, the useful heat delivered by the solar collector is equal to the energy absorbed in the metal surface minus the heat losses from that surface directly and indirectly to the surroundings. This principle can be stated in the relationship:

$$Q_u = A_c \; [H_T \; \tau\alpha - U_L \; (\bar{T}_p - T_a)] \qquad 3.1$$

where

Q_u is useful energy delivered by collector, Btu/hour

A_c is total collector area, ft^2

H_T is the solar energy received on the upper surface of the sloping collector structure, Btu/hr·ft^2 of tilted surface

τ is fraction of the incoming solar radiation which reaches the absorbing surface, no dimensions

α is fraction of the solar energy reaching the surface which is absorbed, absorptivity, no dimensions

U_L is the overall heat loss coefficient, Btu, transferred to the surroundings per hour/ft^2 of exposed collector surface per degree difference between average collector surface temperature and the surrounding air temperature

T_p is average temperature of the upper surface of the absorber plate, ^oF

T_a is atmospheric temperature, ^oF.

A diagrammatic representation of the terms in this relationship is shown in Figure 3-6.

HEAT LOSSES FROM COLLECTOR

In order that the performance of the collector can be as high as economically practical, the design and operating factors which can maximize the value of $H_T \tau\alpha$ on the right hand side of the heat balance equation and can minimize the value of U_L are selected. In other words, the greater the energy absorption in the metal surface and the lower the heat loss from that surface, the higher will be the useful recovery. If a bare metal plate serves as the collector, and with typical values of 2 to 10 Btu/hr·ft^2·^oF for the coefficient of heat transfer to the atmosphere (U_L), the rates of heat loss will be large, so that an absorber plate temperature of 25 to 50 degrees above atmospheric temperature would be the maximum achievable under typical full solar radiation of 300 Btu/hr·ft^2. Under these conditions no useful heat would be delivered from the collector because the heat loss would be equal to the solar heat absorbed, leaving nothing for useful delivery.

To reduce the rate of heat loss occurring by radiation and convection, one or more transparent surfaces, such as glass, can be placed above the metal surface. The glass will transmit as much as 90 percent of the solar radiation striking it, and it will greatly reduce the heat loss coefficient, U_L. This reduction is due to the suppression of convection losses by the relatively stagnant air layer between the absorber plate and the glass, and by intercepting the long-wave, thermal radiation emitted by the hot metal

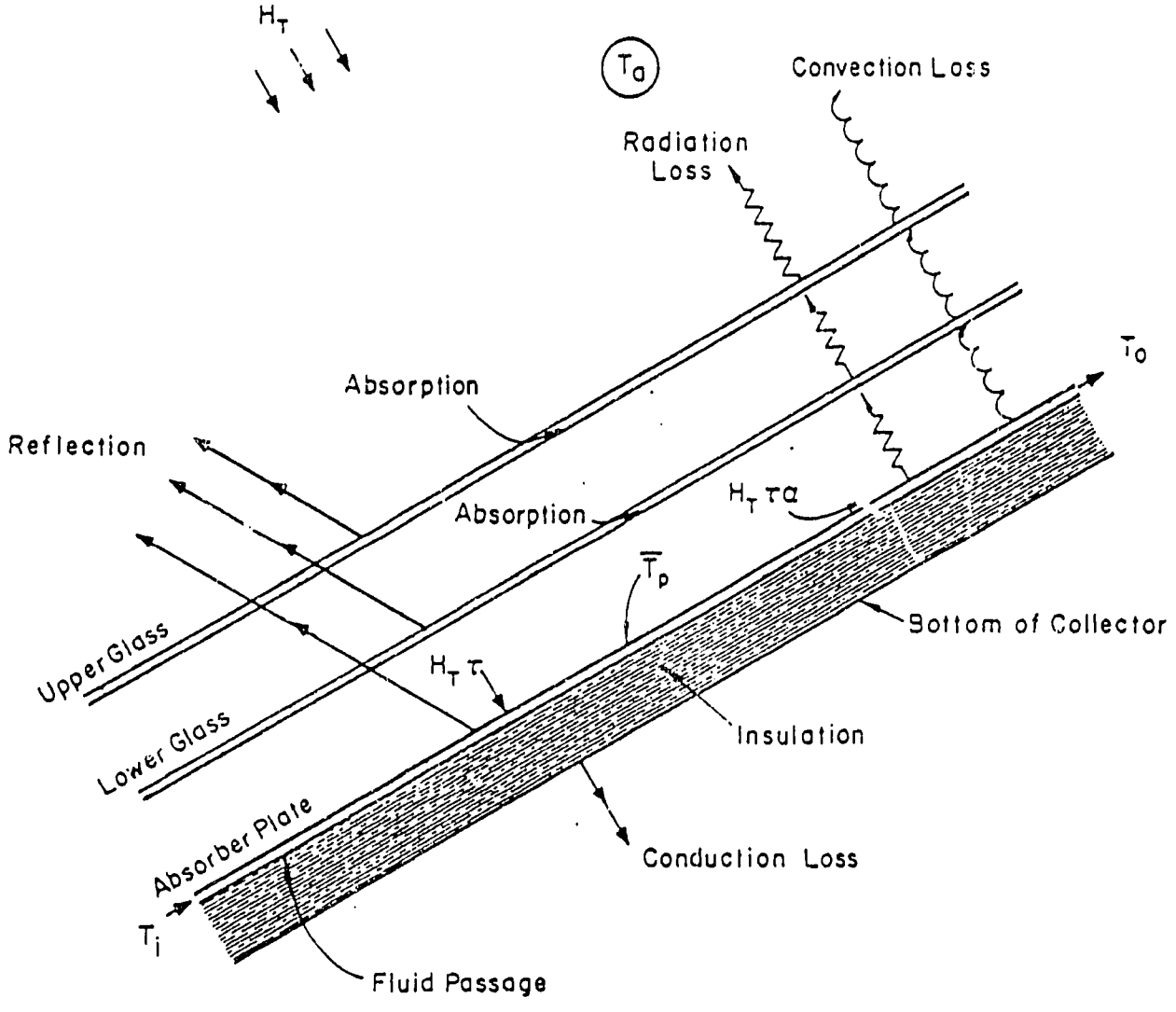

Absorbed Energy $= A_c H_T \tau \alpha$

Effective Heat Loss $= A_c U_L (\overline{T}_p - T_a)$

Figure 3-6 Definition Sketch for Collector Heat Balance Equation

49

surface because glass is opaque to the long-wave radiation. The heat loss coefficient can be reduced to 1 to 2 Btu/hr·ft^2·^{o}F by the use of one glass cover. Similar benefits can be realized by use of certain transparent plastic materials.

Further reduction in the heat-loss coefficient can be realized by using a second transparent surface with an air space between the two surfaces. Two relatively stagnant air barriers to convection loss are then present, as well as two surfaces impeding radiation loss. Coefficients in the range of 0.7 Btu/hr·ft^2·^{o}F are typically then obtained.

Radiation losses can be reduced by other techniques, such as by reducing the radiation-emitting characteristics of the heat-absorbing surface. This measure is discussed in the section pertaining to the solar radiation absorbing characteristics of the surface. Thermal radiation emitted by the absorber plate may also be reduced by reflecting it downward from the lower glass cover by employing an infrared-reflecting coating on the glass. An optically transparent, very thin layer of tin oxide or indium oxide deposited on the glass will reduce radiation loss by reflecting it back to the absorber plate. This coating absorbs a small fraction of the solar radiation, however, so the reduced thermal loss is largely offset by reduced solar energy input to the absorber plate and it is very expensive.

Significant losses can occur from the side and back of the collector unless insulation is used. It is advisable to use a high-temperature insulation adjacent to the back side of the absorber plate layered with a lower temperature insulation to provide the required resistance to heat flow. The total R value of the insulation should be at least 10 for medium-temperature flat-plate collectors.

A transparent layer of thin plastic film can also suppress radiation loss if interposed between the absorber plate and the glass cover. Convection loss suppression also can be achieved, leading to improvement of overall efficiency. Low- to moderate-priced plastic film does not appear to have sufficient resistance to damage by high collector plate temperatures so this technique has not been commercially utilized, but some of the newer films, like Dupont teflon may show promise.

The foregoing discussion has been concerned with methods for reducing U_L, the heat loss coefficient, to the lowest practical level. By so doing, the total heat loss is minimized and collector efficiency is increased. It is evident from Equation (3.1) that losses also decrease as the difference between plate temperature and air temperature decreases. The ambient (outside) air temperature is an uncontrollable factor, of course, but the fact that it varies with time and with geographic location means that collector efficiency will also be dependent upon these factors. It is clear, also, that a collector will be more efficient at lower plate temperatures than at high temperatures. But plate temperature is dependent largely on the way the collector is operated, that is, by the temperature of the fluid being circulated in contact with the plate, the rate of fluid circulation, and the type of fluid. Fluid temperature depends on conditions elsewhere in the system, whereas the other factors depend on the collector design and the operating conditions.

SOLAR ENERGY ABSORPTION

In Equation (3.1), the first term is the solar energy absorbed in the absorbing surface, which depends upon the solar energy incident on the tilted surface of the collector and is affected by collector orientation,

91

as outlined in Module 1. This climatic variable can be measured or derived from tables of averages, and if not already converted, can be calculated for the proper collector position.

The transmissivity of the glass, τ, is a function of the quality of the glass and the angle at which the solar radiation reaches the glass. At normal incidence (solar beam perpendicular to the glass surface), one sheet of ordinary window glass reflects about 8 percent of the solar radiation. Two sheets of glass with air space between reflect about 15 percent. Impurities in the glass, principally iron, result in some radiation absorption; typical glasses 1/8 inch in thickness absorb one to five percent per sheet. Glass with reasonably low iron content may absorb about 2 percent per sheet, so at normal incidence, the total transmission of 2 sheets of glass can be approximately 80 percent. The value of τ is, therefore, 0.8.

Because the beam radiation from the sun strikes the collector at an angle which varies throughout the day, as well as seasonally, a weighted mean transmissivity is somewhat lower than this normal-incidence value. Precise calculations can be made, but a satisfactory approximation for a single-glazed collector can be based on a 10-percent average reflection loss and a suitable absorption loss dependent on glass quality. Assuming 2-percent absorption, an average transmissivity, τ, could be about 0.88. In a double-glazed collector, an effective transmission coefficient of 0.78 could be used with good quality glass.

If plastics are used for the transparent surfaces, transmission coefficients could be appreciably different, depending upon the characteristics of the plastics. Some have transmissivities moderately higher than glass, whereas others show lower values.

92

Methods for reducing the reflectivity of glass surfaces have been developed. Metallic films formed by vapor deposition are commonly used as lens coatings in photographic equipment. These interference layers are too costly for use in solar collectors. Another process involves a delicate etching of the glass surface by acid treatment, producing essentially a slightly porous silica surface. Solar reflectivities as low as 1 to 2 percent can be obtained under carefully controlled conditions. Total transmissivity of a single-glazed collector can thereby be increased to values above 95 percent. The cost-effectiveness of this substantial improvement in performance has yet to be established.

The solar absorptivity of the radiation-receiving surface, α, is dependent on the optical property of the materials exposed to solar radiation. Surfaces which appear black to the eye have high absorptivity for the visible portion of the solar spectrum, and usually also are good absorbers for the infrared portion of the solar radiation. Carbon black, numerous metal oxides, and most black paints have absorptivities above 0.95, that is, they absorb 95 percent of the solar radiation reaching the surface. The remainder of the solar radiation is reflected upwards through the glazing. The overall efficiency of the collector is strongly dependent on the absorptivity of this surface.

The most common types of absorber surfaces are heat-resistant black paints, usually applied by spraying, followed by curing with heat to eliminate solvents and to secure permanence. These surfaces must be capable of prolonged exposure to temperatures of 300 to 400 ^{o}F in double-glazed collectors, without appreciable deterioration or outgassing. In a recently developed solar collector, sheet steel coated with black porcelain enamel (applied to the steel as a sprayed-on frit and fused to the surface in a furnace) is achieving successful application.

SELECTIVE SURFACES

Most surfaces that are good absorbers for solar radiation are also good radiators of heat. If, for example, a surface has an absorptivity of 0.95 for solar radiation, it will normally radiate heat at a rate about 95 percent of that of a "perfect" radiator. Certain combinations of surfaces, however, are capable of absorbing solar radiation effectively, while at the same time radiating heat at a low rate. These combinations are known as selective surfaces. Most selective surfaces are composed of a very thin black metallic oxide on a bright metal base. The black oxide coating is thick enough to act as a good solar absorber, with an absorptivity as high as 0.95, but it is essentially transparent to long-wave thermal radiation emitted by an object at a temperature of several hundred degrees F. Since bright metals have low emissivity for thermal radiation, that is, are poor heat radiators, and since the thin oxide coating is transparent to such radiation, the combination is a poor heat radiator. As a result, the radiation loss from this type of surface is considerably lower than from a conventional, non-selective surface. Thus, the overall heat loss coefficient, U_L, has a lower value when this type surface is used.

The most successful and stable selective surface developed to date is made by electroplating a layer of nickel on the absorber plate, then electrodepositing an extremely thin layer of chromium oxide on the nickel substrate. Such a technique is called "black chrome". Nickel oxide coatings have also been used, but they are less resistant to damage from moisture. Coatings of copper oxide on bright copper and nickel have similar properties, but temperature stability is limited. The most effective selective surfaces have solar absorptivities near 0.95 and thermal emmissivities near 0.1.

MODULE 4: TESTING OF COLLECTORS

OBJECTIVE

The objective of this module is to introduce the formulations behind the Ashrae 93-77 test of solar collectors and for the trainee to understand collector performance equations and the development of collector performance ratings.

MODULE 4: TESTING OF COLLECTORS:

ASHRAE Standard 93-77

Standards for determining the performance of, 1. major components of heating and air conditioning systems, 2. components for use in process and service water heating, and 3. swimming pool heati. , components have been in existence for many years. Prior to 1977 no such standards existed for the principal new component of solar systems, the solar collector. Its need was perceived, and since most HVAC standards for testing or rating the thermal performance of equipment have been developed by ASHRAE, that organization began in 1975 to develop a new standard for testing collectors. The standard was developed from a draft document then available from the National Bureau of Standards. The resulting standard is ASHRAE Standard 93-77, "Methods of Testing to Determine the Thermal Performance of Solar Collectors," (Ref. 2) which is also known as American National Standards Institute (ANSI) Standard 8198.1-77. Since it was issued, Standard 93-77 has become the basis for most performance testing of solar collectors in the United States, and many other countries as well.

In the early 1940's H. C. Hottell, Austin Whillier, and B. B. Woertz researched the performance of solar collectors. They showed that the plot of absorber temperature minus the ambient temperature in which the collector is located, divided by the rate of incoming solar irradiation, was a parameter which could be plotted against collector efficiency in converting the incoming solar energy to heat within the fluid passing through the collector.

We discussed this equation in Module 3:

$$Q_u = A_c \quad H_T \tau\alpha - U_L (\overline{T}_p - \overline{T}_a) \qquad (4.1)$$

We can see from the equation above, that if the numerical values of all the terms are known, the rate of useful heat recovery, Q_u, can be calculated. In addition to the design characteristics of the collector discussed above, the three operation conditions, solar radiation, average absorber-plate temperature, and ambient temperature, must be known. With the exception of plate temperature, these terms can readily be measured or obtained from tables or charts. Absorber-plate temperature, however, is seldom known, nor can it be easily determined. It is affected by the other collector operating conditions and, most critically, by the temperature of the fluid being supplied to the collector to be heated.

In an operating system comprised of collector, storage, and hot water load, the temperature of the fluid in storage can be measured. When a system is being designed for a building, storage temperature can be calculated or assumed until confirmed. This fluid is supplied to the collector and strongly controls the absorber-plate temperature in Equation (4.1). In a typical liquid collector, average plate temperatures usually are 10 to 20 degrees above inlet liquid temperature, and in air collectors, the temperature difference is 30 to 50 degrees. As a convenience, therefore, Equation (4.1) can be modified by substituting inlet fluid temperature for the

average plate temperature, if a correction factor is applied to the resulting useful heat determination. The resulting equation is

$$Q_u = F_R A_c \left[H_T \tau\alpha - U_L (T_i - T_a)\right] \tag{4.2}$$

where:

T_i is the temperature of the fluid entering the collector

F_R is a correction factor or "heat recovery factor", having a value between 0 and 1.0, such that the useful heat recovery calculated by Equation (4.1) is equal to that calculated by Equation (4.1).

Ashrae Standard 93-77 uses the modified heat balance equation of (4.2).

HEAT RECOVERY FACTOR

The heat recovery factor, F_R, can be interpreted as the ratio of the heat actually recovered to that which would be recovered if the collector plate were operating at a temperature equal to that of the entering fluid. This temperature equality would theoretically be possible if the fluid were circulated at such a high rate through the collector that there would be a negligible rise in the temperature of the fluid passing through the collector, and the heat transfer coefficient were so high that the temperature difference between the absorber surface and the fluid would be negligible.

In Equation (4.2), the temperature of the inlet fluid is dependent on the characteristics of the complete solar heating system and the hot water demand of the building. F_R, however, is affected only by the collector characteristics and the fluid flow rate through the collector. As indicated above, the numerical value of F_R would be 1.0 if the entering fluid temperature and the average plate temperature were the same.

COLLECTOR TEMPERATURE PATTERNS

The better the heat transfer coefficient between the metal plate and the fluid, the more nearly the fluid temperature will approach the plate temperature at any one position in the collector, hence the higher will be the value of F_R. Similarly, the greater the fluid circulation rate, the smaller will be the temperature change from inlet to outlet and the closer will be the inlet fluid temperature to the average plate temperature. Figure 4.1 shows a typical temperature pattern in a solar heater being supplied with liquid at 130 degrees. Liquid leaves the collector at about 150 degrees, the collector-plate temperature is about 10 degrees above the liquid temperature throughout the collector, and the average plate temperature is about 150 degrees. If typical values of the collector parameters are substituted in Equations (4.1) and (4.2), it will be found that using 130 ^{o}F as inlet fluid temperature in Equation (4.2) instead of 150 ^{o}F as the average plate temperature in Equation (4.1) would necessitate use of a heat recovery factor, F_R, of about 0.9 to obtain the correct value of Q_u. If the coefficient of heat transfer between the collector plate and the liquid is lower, or if a lower fluid circulation rate is used, the value of F_R would be slightly less.

99

Figure 4-1

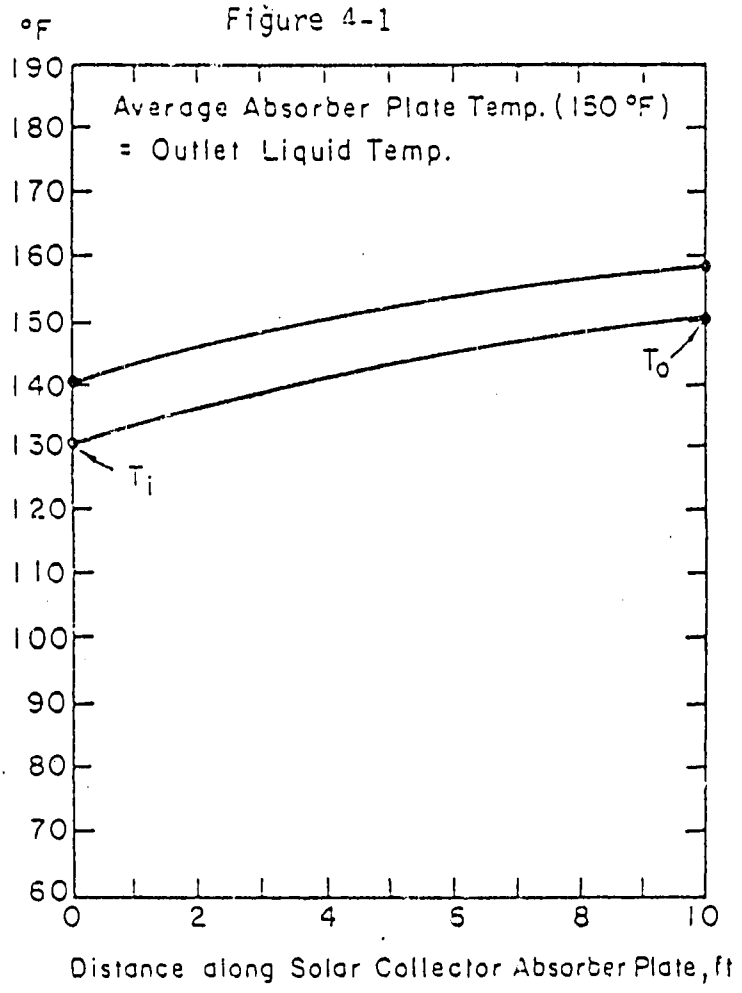

COLLECTOR EFFICIENCY

Equation (4.2) may be rewritten as an efficiency of solar collection, that is, the ratio of useful heat delivery divided by the total solar radiation, by dividing both sides of the equation by H_T and by A_c. Equation (4.3) is the result.

$$\frac{Q_u}{H_T A_c} = F_R \tau\alpha - F_R U_L \frac{(T_i - T_a)}{H_T} = \text{collector efficiency} \qquad (4.3)$$

For a given collector operating at a constant fluid circulation rate, A_c, F_R, τ, α, and U_L are nearly constant regardless of solar and temperature conditions. Assuming that they are constant, Equation (11.3) represents a straight line on a graph of efficiency versus $\frac{T_i - T_a}{H_T}$*. The characteristics

* note: $T_i - T_a / H_T$ is sometimes called the "fluid Parameter".

of this line are an intercept (the intersection of the line with the vertical efficiency axis) equal to the numerical value of $F_R \tau\alpha$ and a "slope" of the line, that is, the vertical scale change divided by the horizontal scale change, equal to $(-F_R U_L)$. So if experimental data on collector heat delivery at various temperatures and solar conditions are plotted on a graph, with efficiency as the vertical axis and $\frac{T_i - T_a}{H_T}$ as the horizontal axis, the best straight line through the data points is a complete representation of the collector performance over its entire operating range. Where the line intersects the vertical axis corresponds to the fluid inlet temperature being the same as the ambient temperature, and collector efficiency is at its maximum. Where the line intersects the horizontal axis, collection efficiency is zero. This situation corresponds to such a low radiation level or such a high temperature of the fluid supply to the collector that heat losses are equal to solar absorption and no useful heat is delivered from the collector.

Typical Collector Characteristics

Figure 4.2 shows efficiencies of several types of collectors correlated in this way. These lines are the results of actual measurements. Collectors 4 and 7 are seen to have the highest efficiencies, but final selection also depends on costs, durability, appearance, and so on. Collector 4 appears to have the best performance of all those compared in Figure 4.2 if normally operated at conditions represented by the left-hand side of the graph. Such conditions are low operating temperatures or high solar radiation. Near the right-hand side of the graph, however, collector 7 is more efficient than collector 4, where high inlet collector temperatures or low solar radiation prevail. It is evident that some collectors are better than others in some temperature and radiation ranges, whereas a reversal can occur at different conditions.

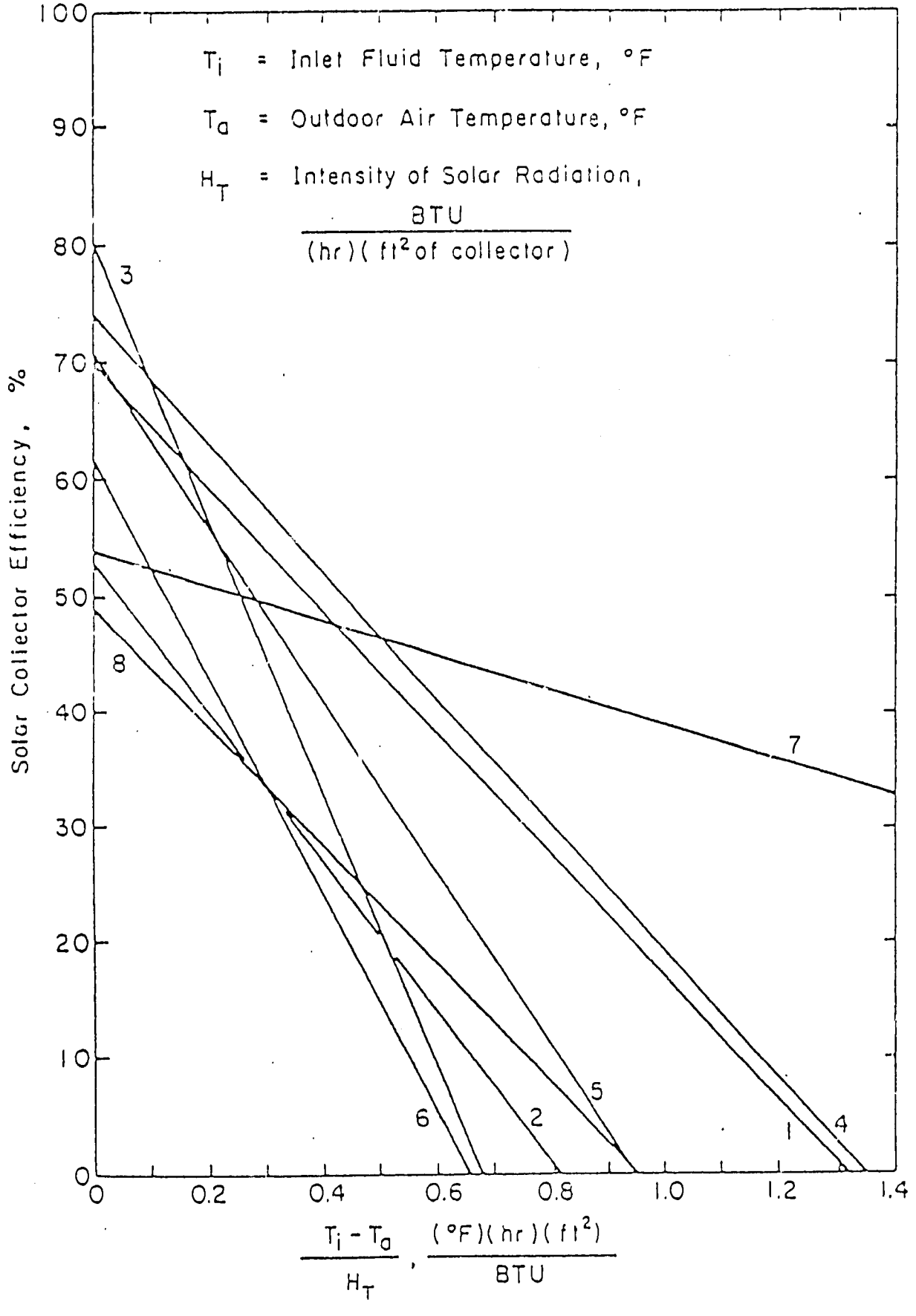

Figure 4-2 Solar Collector Efficiency

A graph such as that in Figure 4-2 for a particular collector, when compared with others of similar type, can be used for selecting suitable equipment. Collector manufacturers usually provide such data. Of equal value are dependable data on the quantities $F_R\tau\alpha$ and F_RU_L. Knowledge of those two factors is equivalent to having the grachical relationship. Table contains this information for the same collectors shown in Figure

Not all collectors show straight line relationships in their efficiency plots. The general characteristics of several varieties of collectors are shown in Fig. 4-3. Any collector shown can be used in applications in which the value of $(t_i - t_a)/I$ is less than the value shown by the x-axis intercept for that collector. It is obvious that at low values of the parameter some collectors will provide more thermal energy than will others, and that at high values of the parameter, some collectors will collect energy while others will collect none at all.

Values for the performance equation 4.3 can be calculated for various types of collectors and plotted as a performance curve. Such a group of graphs is shown as Figure 4-5.

Dr. Block and J. Huggins from the Florida Solar Energy Center have made such an analysis of generic collector types using actual collector test data (See Paper 4-1, attached). The data provided in their Table 5 are useful to a designer in doing general analysis of the potential performance of generic collector type.

103

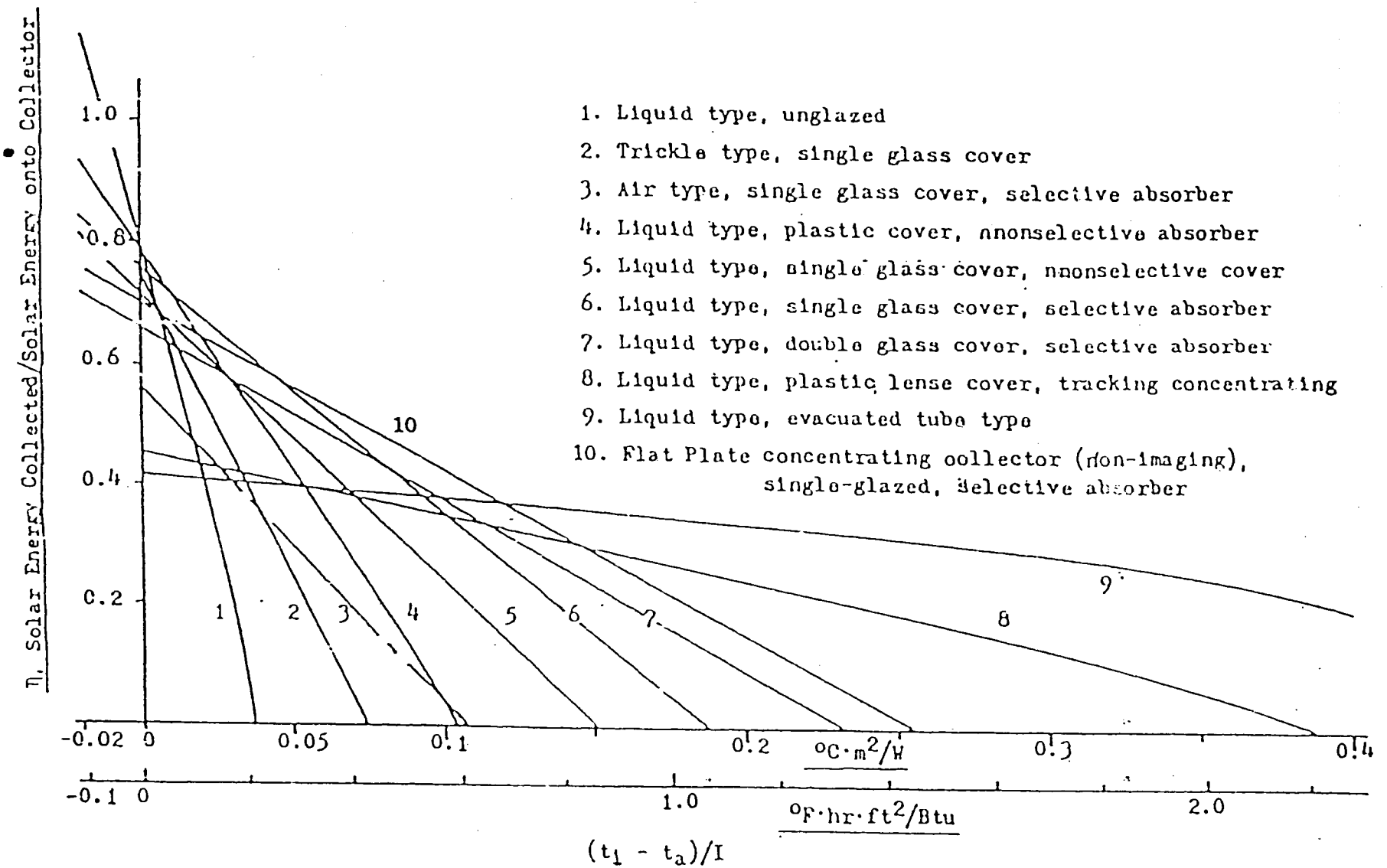

FIGURE 4-3
Performance of a Variety of Collectors.

Collector Performance Ratings

For Discussion, lets use a good flat plate performance curve:

$$\eta = 76.0 - 64.0 \times (T_i - T_a) / I$$

If we know the variables of the fluid parameter: Panel temperature (T_i), ambient temperature (T_a), and insolation (I), we can find the efficiency of the collector. From collector efficiency, we can find heat output.

For example, say our panel temperature is 122°F, ambient is 81°F, and insolation is 144 Btu per square foot for the hour of 2:30 to 3:30. We will get a panel efficiency of:

$$\eta = 76.0 - 64.0 \times \frac{122^{\circ} - 81^{\circ}}{144} = 76.0 - 18.22 = 57.78\%$$

Our collector converts 57.78% of the incoming sunlight into hot water. Since we know we have 144 Btu coming in, we know we get 144 x .5778 or 83.20 Btu's added to our hot water during that particular hour. If we specify conditions for every hour of the solar day, we can add up the hourly contributions to get the heat provided by the panel for that day. This is how thermal performance ratings are found. The Florida Solar Energy Center has developed a "Standard Day" for such ratings. The same "Standard Day" is used in rating all Florida's collectors. This day contains ten hours and totals to 1600 Btu/ft^2 as follows:

"FLORIDA STANDARD DAY"

Hour	I	T_a	Hour	I	T_a
7:31 - 8:30	16 Btu	75°F	12:31 - 1:30	272 Btu	84°F
8:31 - 9:30	80 Btu	77°F	1:31 - 2:30	208 Btu	82°F
9:31 - 10:30	176 Btu	81°F	2:31 - 3:30	144 Btu	81°F
10:31 - 11:30	240 Btu	84°F	3:31 - 4:30	112 Btu	79°F
11:31 - 12:30	304 Btu	86°F	4:31 - 5:30	48 Btu	77°F

You may want to verify that the above panel's equation gives the following ten hourly Btu outputs at a panel temperature of 122°F (domestic hot water): 0, 32.0, 107.52, 158.08, 208.00, 182.40, 132.48, 83.20, 57.60, 7.68. The sum of the ten hourly outputs is 968.96 Btu/ft^2 per day. This is its Dhw performance rating per square foot. Since this is a 4 x 8 panel or 32 square feet, its standard day output is 32 ft^2 x 968.96 Btu/ft^2 day = 31,000 Btu/day.

The standard day for Florida is calculated on a 1600 Btu/sq ft per day total. This is high for Florida as it represents a good clear solar day in Miami.

Figure 1-11 shows average annual insolation values ranging from 1433 to 1702 along most of the populated area of Jamaica. (Some values are much lower up into the mountains). These are horizontal values, however, values for tilted panels (20°) only improve annual performance by about 4%. This would indicate that the 1600 Btu/sq foot perday value may be a little low for Jamaica but is nevertheless a good starting point for engineering evaluation until good actual insolation data is obtained. Indeed, calculations done by S. Chandra of the Florida Solar Energy Center on several hospital systems in June of 1982 using the F-Chart simulation technique, showed a close relationship between the Florida rating and the F-Chart predicted panel performance in Jamaica.

The Incident Angle Modifier. As the sun position departs from the nearly right angle position directly in front of the collector, at which conditions the Ashrae 93-77 test is done, variations occur in the amount of energy transferred to the fluid in the collector. The frontal position of the sun on a line drawn at 90 ^{o}deg. outward from the plane of a flat collector or along the reflector axis of a tracking collector, is called the "normal incidence angle." Angles of incidence are measured as a departure from this normal incidence angle, usually referred to as simply "normal." For collectors in rigid or fixed mounts, there is usually only one time during any day when the sun is exactly normal to them. For those periods when the sun is not in the normal position, various things happen which are peculiar to the collector which change the amount of thermal energy accepted. For example, the cover or surface of the collector may reflect increasing amounts of solar energy away from the collector as the incident angle increases; some portions of the collector may shade the absorber from the sun; energy may be reflected away by the absorber plate itself; and in some cases more solar energy may be reflected onto the absorber as the incident angle increases.

The effect of these factors is to change the y-axis intercept of the performance curves by inserting the term K in Equ. 4.3

$$\eta = K(F_R\ T\alpha) - F_R\ U_L\ \frac{(T_i - T_a)}{H_T} \qquad (4.4)$$

Knowing the value of K, additional performance lines can be drawn on the basic plot as is shown in Fig.4-4. These added lines show the efficiency of the collector for different values of K inserted as a multiplier for the first term of the performance equation. The second term, which deals only with the overall thermal loss through conduction and radiation, is not changed by insertion of the incident angle modifier.

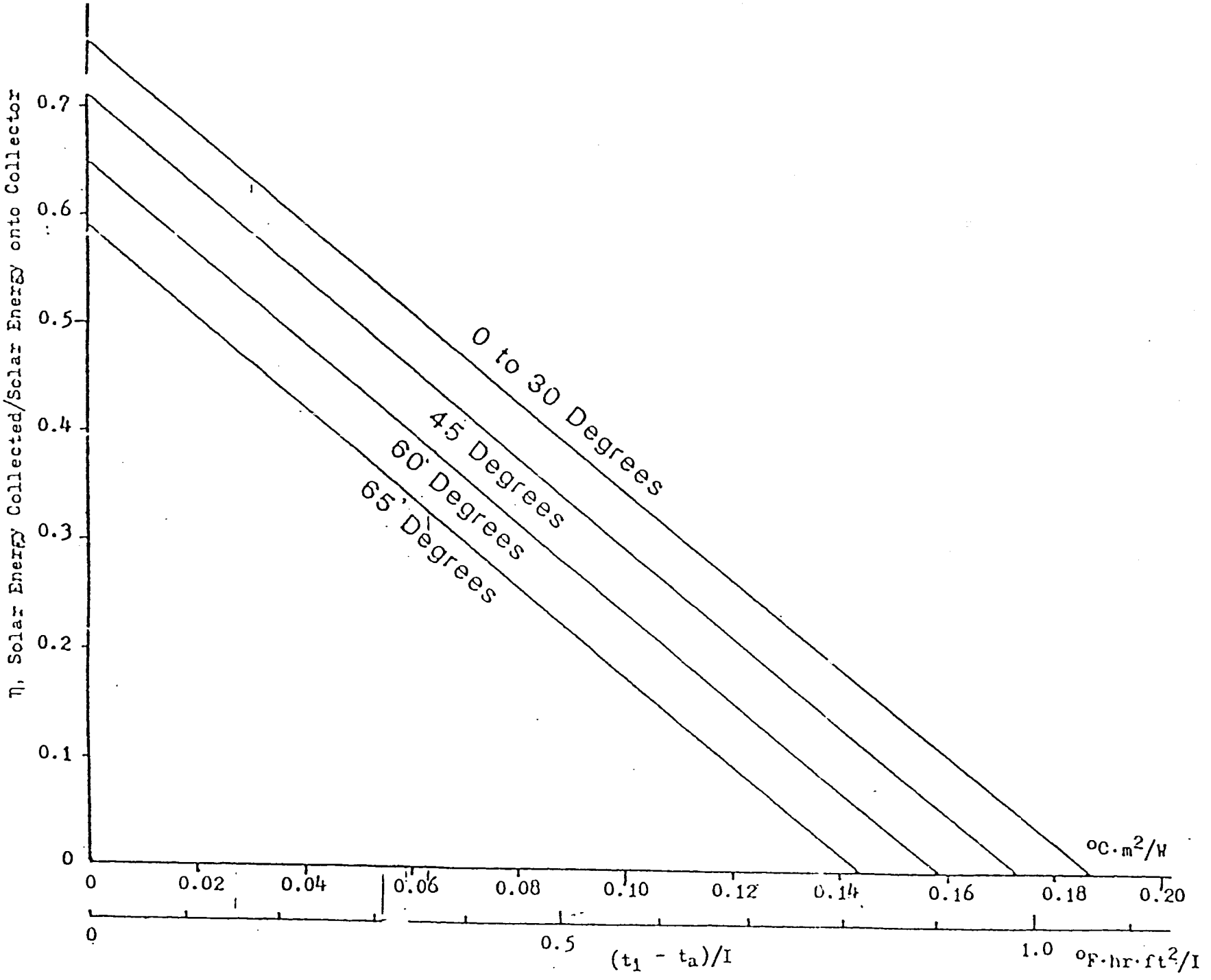

FIGURE 4-4 Collector Performance at Different Incident Angles.

The Cosine Effect: Figure 4-5 provides performance lines showing the collector performance as the incidence angles change with respect to the plane of the collector and its outward-drawn normal. Most flat plate collectors respond symmetrically, whatever the direction of change in the incidence angle. All collectors, except those in tracking mounts, experience a wide variety of incident angles in one or more planes. As the incident angle increases, the amount of the radiation intercepted, and hence its intensity, decreases in proportion to the cosine of the incident angle purely as a result of the geometric shape presented to the incoming radiation.

When panels are tested at other than normal tilt, the combined tilt effects of τ, α and cosine effect are measured and presented by the incident angle modifier equation:

$$K = 1.0 - b_o (1 / \cos\theta - 1)$$

where b_o = measured tilt factor

θ = angle of beam radiation off normal.

Notice that the maximum angle at which a collector can receive any energy is defined as:

$$\theta_{MAX} = \mathrm{Cos}^{-1} \frac{b_o}{1 + b_o}$$

This is also shown as the zero intercept on Figure 4-6.

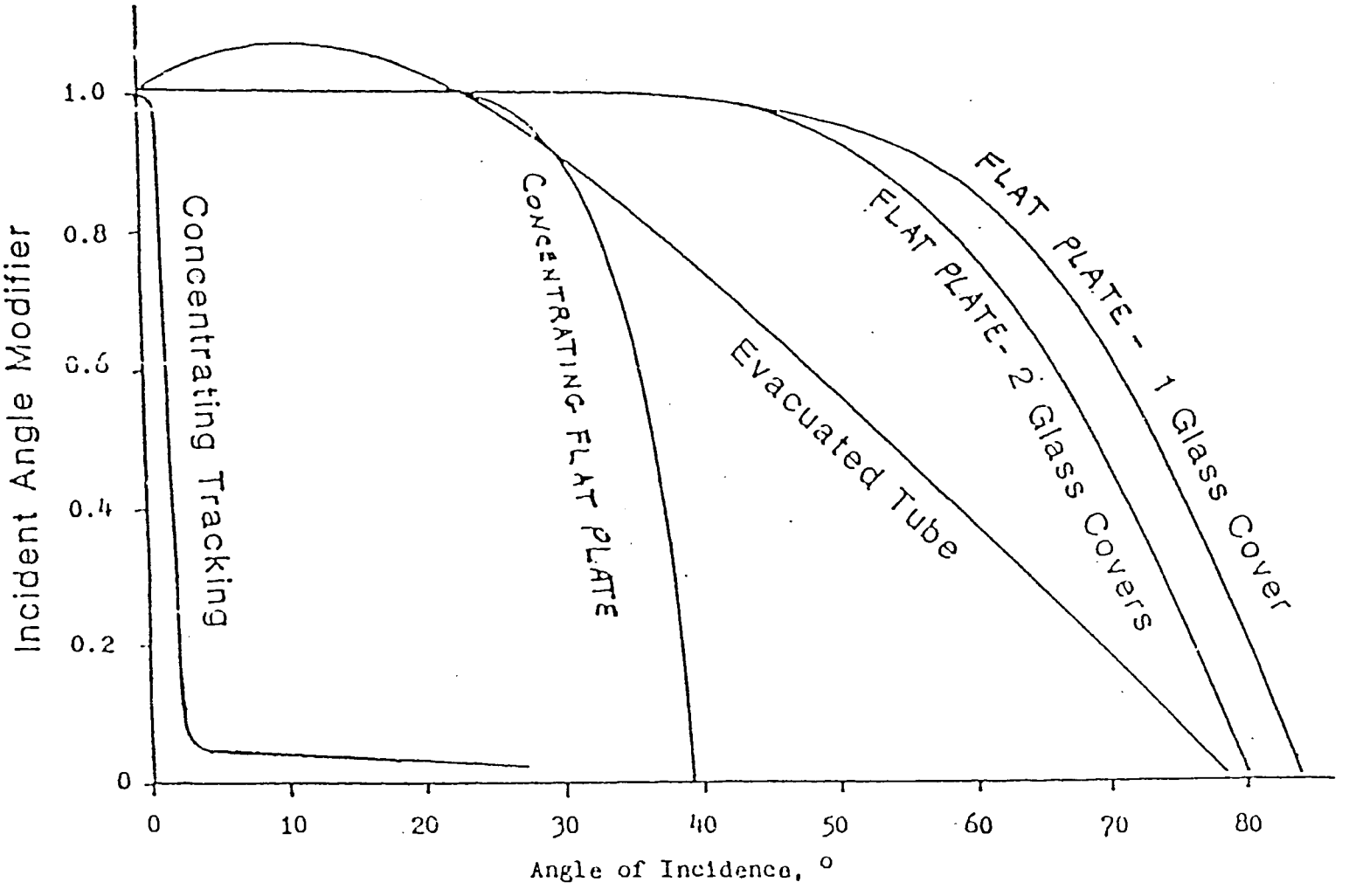

FIFURE 4-6 Incident Angle Modifiers for Various Collectors.

110

K for Various Collectors. Fig. 4-6 is a plot of the incident angle modifiers for examples of several types of collectors.

Most flat plate collectors show the general characteristics for their incident angle modifiers indicated by the curves in Fig. 4-6 labelled "1 Glass Cover" or "2 Glass Covers", but any deviations from flatness in either the absorber plate or the cover may result in a differently shaped curve. Other types of collectors may have quite different types of curves.

Reference to Fig. 4-6 shows that flat plate collectors with one or two cover glasses should receive most of this diffuse insolation, and indeed such collectors are usually considered to receive whatever diffuse insolation exists. Flat plate concentrating collectors will suffer very little loss in performance from diffuse components in the horizontal direction, since they have the same performance curve in Fig. 6 as the 2-glass cover collectors. However, they may be expected to lose the vertical portion of hemispheric diffuse insolation, since the incident angle modifier shown by the Concentrating Flat Plate (vertical) line is zero at angles of incidence above 38°. Concentrating tracking collectors will lose essentially all the diffuse insolation, since their angle of acceptance is but a few degrees wide in the plane of their focus. An evacuated tube collector with the incident angle modifier curve shown in Fig. 6 would have a modifier of 0.57 under hemispheric diffuse conditions, but would have a multiplier of 1.06 under optimum minimum diffuse angle conditions. Because of the effect of K on thermal performance, and because of the high diffuse to direct raitos $\overline{D} / \overline{H}$ found in Jamaica, the author suggests careful analysis be made before concentrating style collectors are utilized in design of thermal systems.

Block and Huggins (paper 4-1) also provide a measure of b_0 generic collectors. These range from .11 to .14 and represent a $\theta_{MAX} = 84.3^{\circ}$ to 82.9° respectively - not much difference.

Notice from Figure 4-6 that for flat plate collectors, K remains close to one until about 40° tilt. Since the available insolation at angles above 40° for a south facing collector tilted at latitude $\pm 15^{\circ}$ is small, the effect of incident angle modifiers for typical flat plate collectors on total daily performance can be ignored when comparisons are made. For this reason, and to keep things as simple as possible, K is not usually utilized in calculating standard day performance ratings for flat plate collectors.

Collector Time Constant

This is the time required for the outlet fluid temperature to attain 63.2 percent of its steady state value following a step change in the input. Most collectors will have relatively short time constants, such as one to three minutes, but in those collectors where the mass of the fluid is large compared to the area of the absorber surface such as a bread box heater time constants as long as 30 to 40 minutes may be experienced.

The time constant is used as the minimum time period over which temperature and irradiance data are taken to obtain the computed efficiency values for the thermal performance test.

The time constant can be useful information in defining a control system for a collector array which can avoid instability.

References:

1. ASHRAE, 1978 Applications Handbook, Chapter 58
2. ASHRAE Standard 93-77, "Method of Testing to Determine the Thermal Performance of Solar Collectors", 1982
3. ASHRAE, 1977 Handbook of Fundamentals, pp. 26.2 - 26.9
4. ASHRAE, GRP-170, "Application of Solar Energy for Heating and Cooling of Buildings"
5. Liu, B. Y. H., and Jordan, R. C., "The Interrelationship and Characteristic Distribution of Direct, Diffuse, and Total Solar Radiation", Solar Energy, Vol. 4, No. 5, pp 1 - 19, July 1960
6. NTIS, ALO/45356-2, Superior Heat Transfer Fluids for Solar Heating and Cooling Applications

PAPER 4-1

THERMAL PERFORMANCE OF FLAT PLATE SOLAR COLLECTORS BY GENERIC CLASSIFICATION*

David L. Block James C. Huggins

FSEC-PF-22-82

*This paper was prepared for presentation at the ASME Convention in Orlando, Florida, April 1983. Views and opinions expressed here represent those of the authors and not necessarily those of the Florida Solar Energy Center.

Thermal Performance of Flat Plate Solar Collectors By Generic Classification

By
James C. Huggins
David L. Block
Florida Solar Energy Center
300 State Road 401
Cape Canaveral, FL 32920

ABSTRACT

This paper presents thermal performance equations for glazed flat-plate solar collectors categorized by generic classification. The equations are derived from analyses of experimental test data collected for the past six years on tests of 270 solar collectors performed according to ASHRAE 93-77 procedures and leading to certification by the Florida Solar Energy Center (FSEC). Presented here are the straight line efficiency curves (intercept and slope values) for eight solar collector generic classifications based on the number of covers, the cover plate material, and the absorber plate coating used in their construction. The collector efficiency curves were developed from a computer search to establish a list by generic type and then from a statistical evaluation of each generic listing. Of the 270 test collectors, 170 were tested at FSEC and 100 were tested at other laboratories.

From the generic thermal performance equations presented, a solar designer is able to select a generic type of solar collector for a particular application and then to size and evaluate the performance of the selected system based on the developed generic thermal efficiency curve. This procedure allows the designer to make decisions on system performance and economics early in the design process and before selecting a specific collector manufacturer.

INTRODUCTION

The solar collector is the crucial component and critical design variable of a solar system -- it is the heart of the system. In designing solar systems, most designers first select a particular solar collector manufacturer and then structure the design around the selected manufacturer's collector. It would certainly be beneficial if, instead, the designer could base the solar system design upon the desired collector characteristics and then, when the design is complete, select the collector manufacturer on a competitive basis.

The purpose of this study was to provide discriminatory design criteria by determining the relationship between collector thermal performance and solar collector generic classifications. This relationship was established by analyzing ASHRAE 93-77 solar collector test results for 270 collectors in the solar collector certification program at FSEC.

COLLECTOR THERMAL PERFORMANCE

The thermal performance of a solar collector is evaluated by establishing the collector's thermal efficiency curve. The thermal efficiency curve is obtained experimentally by performing tests on a collector according to the test procedures described by ASHRAE Standard 93-77, "Methods of Testing to Determine the Thermal Performance of Solar Collectors" (1).

In the ASHRAE procedures, a collector is tested under a prescribed set of conditions. Measurements are made of the flow rate, the temperature rise across the collector, and the incident radiation. The flow rate and the inlet water temperature are kept constant. The measured flow rate multiplied by the fluid specific heat and the measured temperature rise across the collector is the instantaneous energy collected by the collector. This quantity divided by the measured incident radiation is the instantaneous collector efficiency. Performing the test at several inlet water temperatures supplies additional data points.

The efficiency curve is derived from the data points by a least squares fit of the data points assuming either a first or second order efficiency curve. In this study, the first order efficiency curve based on the Hottel-Whittier-Bliss analytical model is used. This efficiency curve is described as follows:

$$\eta = F_R\,(\tau\alpha)_e - F_R U_L\,\frac{(T_i - T_{amb})}{I}$$

where

η	=	collector instantaneous thermal efficiency
F_R	=	collector heat removal factor
$(\tau\alpha)_e$	=	effective transmittance-absorptance product
U_L	=	heat transfer loss coefficient [W/(m²·°C) or Btu/(hr·ft²·°F)]
$\frac{(T_i - T_{amb})}{I}$	=	efficiency fluid variable consisting of inlet fluid temperature minus ambient air temperature divided by incident radiation.

The coefficients $F_R(\tau\alpha)_e$ and $F_R U_L$ (intercept and slope of efficiency curve, respectively) are functions of the collector's generic characteristics -- the materials, components and/or configuration used in the manufacture of the collector. Each collector manufacturer constructs each collector model with a unique combination of generic characteristics. The ASHRAE 93-77 tests thus produce, for each collector test, a combination of distinct coefficients $F_R(\tau\alpha)_e$ and $F_R U_L$ (intercept and slope).

The intercept and slope coefficients for flat plate collectors are, in general, a function of seven generic characteristics which are briefly described as follows:

1. Number of cover plates. The majority of collectors certified in the FSEC program have one cover plate. Double glazed, two-cover plates, are more commonly used in colder climates.
2. Cover plate material. The transparent cover plate materials commonly used are:
   Glass, the most widely used glazing material with high transmittance and long-term durability.

Glass is fragile and heavy. Because iron in glass reflects the sun's radiation, a low iron content in glass is desirable. The iron content of glass was not considered in this study.

Fiber reinforced plastic (FRP), the second most widely used material. FRP is not as optically efficient or as durable as glass but it is lightweight and less costly.

Thin film plastics with the trade names of Tedlar, Mylar, Teflon and Lexan. These have high transmittance qualities and are inexpensive. However, they do not retain heat very well and have a tendency to deteriorate under ultra-violet exposure.

3. Absorber Plate Coating. Common coatings are: Selective surface coatings such as black chrome, black nickel and copper oxide which have high absorptance and low emmitance properties. Selective coatings are more expensive than paint. The infrared emissivity of these surfaces is below 0.2.

   Moderately selective surface coatings, special paints which have moderately selective surface properties. The emissivity of these surfaces range from 0.2 to 0.7.

   Flat black paints, non-selective, high heat resistant paints that are inexpensive but which do not possess the emittance qualities of a selective surface. The emissivity of these surfaces range from 0.7 to 0.98.

4. Absorber material Type. Absorber materials are copper, aluminum and stainless steel. These materials may be used in combinations of tubes and fins, or integral tubes in plates.

5. Absorber configuration. The absorber may be configured with parallel pipes, series or serpentine pipes, a parallel and series combination, or plate flow.

6. Enclosure type. The frame holding the collector components may be either metallic or non-metallic.

7. Insulation materials. The insulation materials used to keep heat from escaping from the back and sides of the collector are fiberglass, foam, or a combination of both.

Presented in this paper are statistical mean and standard deviation values of the coefficients $F_R(\tau\alpha)_e$ and F_RU, as a function of these collector characteristics within generic collector categories.

FSEC SOLAR COLLECTOR PROGRAM

The Florida Solar Energy Center (FSEC) has been setting standards for, testing, and certifying solar collectors since 1977 when the Florida Legislature passed a statute (Florida Statute 377.705) requiring these activities. In 1980 the certification program became mandatory for all collectors manufactured and/or sold in the state.

The present certification program uses ASHRAE 93-77 as the test method and follows the certification procedure developed by FSEC (2,3). This certification program is also equivalent to the procedures set by the Interstate Solar Coordination Council (ISCC). The current sequence of tests is as follows:

1. Receiving inspection.
2. Static pressure test.
3. Thirty-day exposure test.
4. Thermal shock/water spray tests.
5. Thermal shock/cold fill test.
6. Static pressure test.
7. Collector time constant determination test (ASHRAE 93-77)
8. Post exposure thermal performance test. (ASHRAE 93-77)
9. Incident angle modifier test. (ASHRAE 93-77)
10. Disassemoly and final inspection.

The results of an FSEC certification are published in several forms. A complete test report is issued by the testing laboratory for each test that is conducted. For each FSEC certification, a Summary Information Sheet is published to give the consumer a brief description of the collector, the thermal performance equations, and a thermal performance rating.

From the inception of the certification program, FSEC has certified 520 flat-plate collectors representing 145 manufacturers. Of the 520 collectors, 120 are no longer being manufactured, thus, there are 400 current certifications. Of the 400 current certifications, 364 are for glazed collectors and 36 are for unglazed collectors.

RESULTS

This study addresses six years of test results on glazed collectors for which ASHRAE 93-77 test results are available. Presented in Table 1 are the number of collectors tested during each of the six years.

TABLE 1. Number of Collectors Tested Per Year

Year	Number of Glazed Collectors
1977	15
1978	52
1979	37
1980	68
1981	55
1982	43
Total	270

Of the 270 tested collectors, 170 were tested at FSEC and 100 were tested by other testing laboratories. The apparent discrepancy between the 520 and 270 numbers can be accounted for by the fact that some collectors are certified under more than one manufacturer's name and many collector models of differing surface areas are certified through a single collector test. The 270 total represents a listing of only the collectors on which an ASHRAE 93-77 test was performed. All evacuated tubular, unglazed, and triple-glazed collectors were excluded from the list.

In presenting these collectors and tests, the following general comments are made:

- The weather conditions under which the ASHRAE tests were performed were variable by location (Florida, Arizona, California, etc.). Tests were done during all months and days of the year. All weather conditions did prescribe to the limits of ASHRAE standards.
- The collector tests represent performance measurements made before exposure testing and after exposure testing. Prior to March 1981, collector performance was determined by tests conducted only before exposure testing. After March 1981, collector performance was determined by tests conducted after 30 day exposure. Both conditions are used herein.
- The collectors represent those of manufacturing companies both active and defunct, from small backyard operations to large corporations.

It is believed that FSEC, because it is both a state agency and a research and development organization, is unique in having test results for such a large number of collectors. These unique qualifications made this study possible.

The study began approximately one and one-half years ago when FSEC started a project to place all

116

certified solar collector data on the FSEC computer. This project was then accomplished by analyzing the tested collectors by generic classifications. When a listing by generic type had been compiled, calculations were made to determine the mean and standard deviation of the collector efficiency curve (intercept and slope) and of the collector incident angle modifier.

Before considering the results of this study, a comment needs to be made concerning the accuracy of ASHRAE test procedures. The results presented here are based on the ASHRAE 93-77 test procedures. Consequently, errors in measurements built into the ASHRAE procedures will also appear in the results presented. The errors associated with ASHRAE test procedures have been thoroughly discussed by Streed and Waksman (4) and Lumsdaine (5). Streed and Waksman found an average error of approximately ±2.4% of the measured value in the intercept obtained by a number of test laboratories under a wide range of conditions. The variation in the slope of the performance equations was found to be ±3.4%. Reference is made to these publications for further discussion of measurement errors and the subsequent accuracy or inaccuracy of the test results.

The first analysis was to construct a listing of collectors according to the seven collector characteristics described in the Collector Thermal Performance section.

This produced a listing of 116 different collector characteristic combinations. The largest number of collectors in a separate list was 30, and the second largest number of collectors was 15. The analysis also produced 74 combinations with only one collector and 13 combinations with only two collectors. Because more than half the combinations had only a single collector, the results from using seven generic types were not statistically significant and were not used.

The seven generic types were then reduced to four -- the number of cover plates, the cover plate material, the absorber coating and the absorber type. Table 2 presents a listing of the number of collectors for each generic type as a result of this analysis.

TABLE 2. Number of Collectors per Generic Type for the Four Generic Classifications

Number of Collectors per Generic Type	Number of Generic Types	Total Collectors
1	37	37
2	9	18
3	5	15
4	3	12
5 or above	8	188
		270

The results of Table 2 show 46 generic types with only one or two collectors. However, it is important to observe that 188 of the 270 collectors (70 percent) are represented by eight generic types.

Presented in Table 3 is a list of the eight generic types in which there are five or more collectors. The first three columns specify the generic type, the fourth column shows the number of collectors in each category, and the final columns list the statistical values for intercept and slope. Under the intercept and slope columns, the values given are the mean, the standard deviation, and the maximum and minimum values. To show the scatter distribution of a particular generic type, the 26 collectors comprising the single cover, FRP, copper tube and fin, flat black paint classification were plotted and are presented in Figure 1. The dashed line represents the mean intercept and slope.

Table 3. Collector Intercept and Slope by Generic Type.

GLAZING & COVER MAT'L	ABSORBER MAT'L & TYPE	ABSORBER COATING	NUMBER OF COLLECTORS	INTERCEPT				SLOPE (Btu/hr °F ft²)			
				MEAN	STANDARD DEVIATION	MAX	MIN	MEAN	STANDARD DEVIATION	MAX	MIN
Single Glass	Copper Tubes and Fins	Flat Black Paint	47	67.2	5.0	75.6	56.2	-115	14	-72	-140
Single Glass	Copper Tubes and Fins	Moderately Selective	9	73.0	3.6	78.0	68.0	-112	11	-100	-130
Single Glass	Copper Tubes and Fins	Selective Surface	58	71.7	3.3	81.4	62.0	-83	11	-61	-124
Single Glass	Copper Tubes and Aluminum Fins	Flat Black Paint	22	69.1	6.0	84.6	58.8	-116	12	-96	-138
Single Glass	Copper Sheet Integral Tubes	Selective Surface	6	70.5	5.1	77.4	62.0	-89	17	-71	-120
Single FRP	Copper Tubes and Fins	Flat Black Paint	26	61.9	5.5	70.5	53.0	-117	15	-86	-147
Single FRP	Copper Tubes and Aluminum Fins	Flat Black Paint	11	57.1	6.2	65.5	48.1	-114	10	-102	-132
Double Glass	Copper Tubes and Fins	Flat Black Paint	9	59.7	6.7	66.1	44.4	-84	9	-69	-95

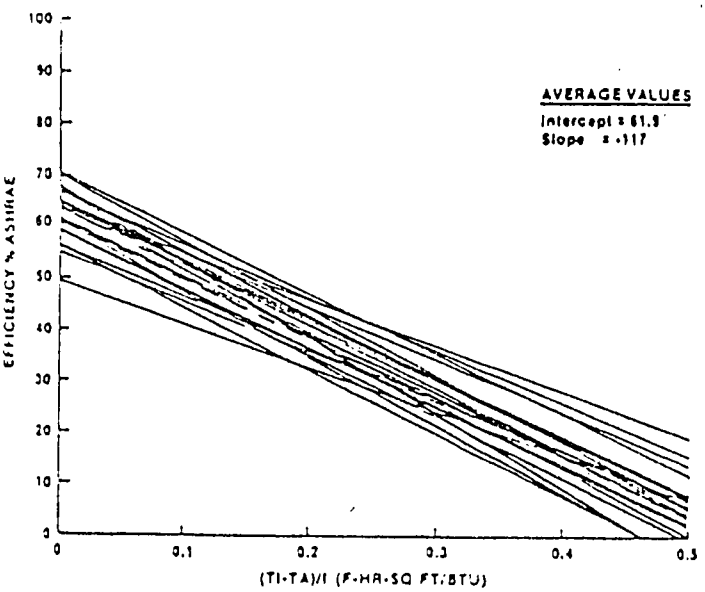

Figure 1. Plot of 25 Collector Efficiency Curves and the Average Efficiency Curve for the Generic Classification of FRP Cover, Flat Black Paint and Copper Tube and Fin Absorber.

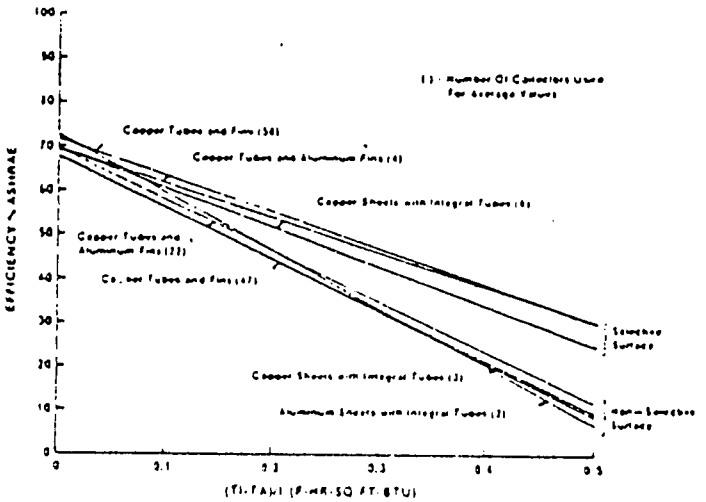

Figure 2. Comparison of Average Efficiency Curves for Absorber Type and for Selective and Non-Selective Surfaces and Glass Cover Plates.

Figure 2 presents a graphic comparison of the effects of different absorber types used in single-glazed, glass-covered collectors with selective and flat black paint surfaces. The comparison indicates that the absorber type is not a major factor in the generic classification. Thus, the absorber type was eliminated from the generic list which was then reduced to three characteristics -- the number of covers, the cover plate material and the absorber coating.

Table 4 presents the results of the analysis for these three generic types.

The three generic types represented by Table 4 are the minimum acceptable if the results are to be meaningful. Table 5 presents a listing of the results for the three generic types and for cases with five or more collectors per generic type. These results agreed well with those obtained by Kirkpatrick (6).

TABLE 4. Number of Collectors per Generic Type for the Three Generic Type Classifications

Number of Collectors per Generic Type	Number of Collectors	Total Number of Collectors
1	7	7
2	3	6
3	2	6
4	0	0
5	1	5
6 or above	6	246
		270

Note that the Kirkpatrick results are for 117 collectors tested as part of the DOE test program and do not separate the collectors by glazing materials as was done for this study: the Kirkpatrick results only consider the number of glazings and the absorber coating.

Table 5 presents the primary results of this study. These results allow a designer to select the thermal performance equation for a generic type of

Table 5. Collector Intercept, Slope Incident Angle Modifier by Generic Type.

GLAZING & COVER MAT'L	ABSORBER COATING	NUMBER OF COLLECTORS	INTERCEPT				SLOPE (Btu/hr °F ft²)				INCIDENT ANGLE MODIFIER			
			MEAN	STANDARD DEVIATION	MAX	MIN	MEAN	STANDARD DEVIATION	MAX	MIN	MEAN	STANDARD DEVIATION	MAX	MIN
Single Glass	Flat Black Paint	81	67.6	5.5	84.6	51.3	-116	13	-72	-140	-0.11	0.05	-0.02	-0.25
Single Glass	Moderately Selective	14	71.4	4.6	78.0	59.7	-112	14	-89	-141	-0.13	0.06	-0.05	-0.23
Single Glass	Selective	75	71.2	4.5	81.4	62.0	-82	13	-61	-124	-0.14	0.10	-0.04	-0.23
Single FRP	Flat Black Paint	44	60.0	6.2	70.5	48.1	-117	15	-86	-157	-0.12	0.07	-0.05	-0.20
Single FRP	Moderately Selective	6	59.6	6.6	66.4	51.6	-115	14	-100	-130	-0.12	0.01	-0.10	-0.14
Single FRP	Selective	5	63.2	1.7	64.9	61.4	-73	7	-66	-79	-0.14	0.01	-0.13	-0.15
Double Glass	Flat Black Paint	13	61.9	6.7	70.6	44.4	-84	9	-69	-95	-0.11	0.06	-0.05	-0.20

solar collector and to perform system sizing and analysis. With this information, system performance decisions can be made early in the design process, and the collector options can be evaluated before a specific manufacturer is selected.

Using the results of Table 5 the effects of different variables can be evaluated. Figure 3 shows a comparison of selective vs. moderately selective vs. flat black paint absorber surface for single glass cover plate collectors. As expected, the selective surface shows better performance. Figure 4 presents a comparison of glass vs. FRP cover plates and selective vs. non-selective surfaces. As expected, glass and selective surfaces perform better. Finally, Figure 5 shows a comparison of single vs. double glazings for glass covered collectors. This result is also as expected.

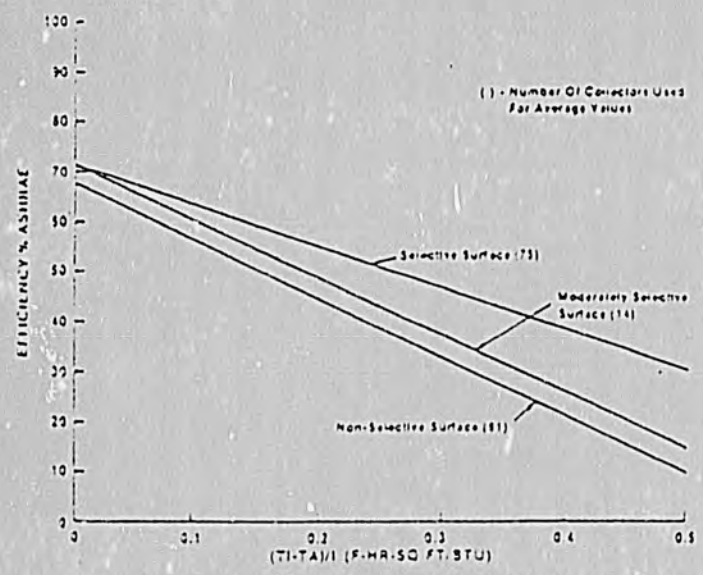

Figure 3. Comparison of Average Efficiency Curves for Absorber Coatings and Glass Cover Plates

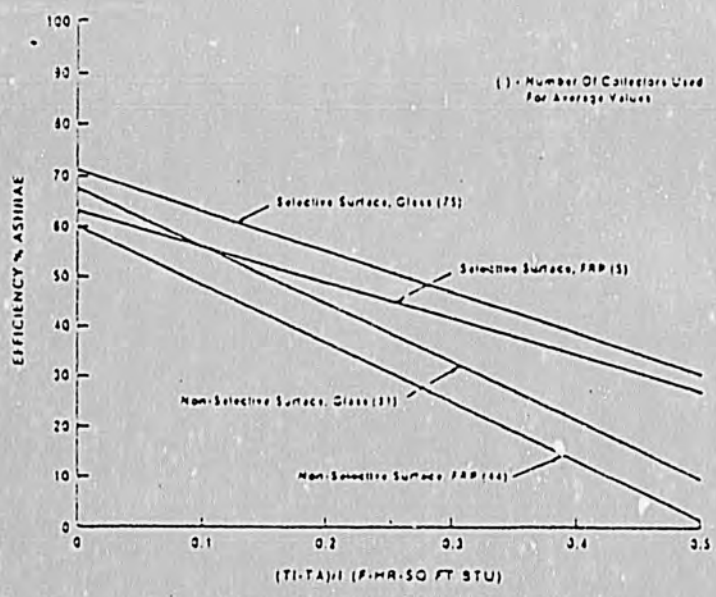

Figure 4. Comparison of Average Efficiency Curves for Selective vs Non-Selective Absorber Coatings and for Glass vs FRP Cover Plates

CONCLUDING REMARKS

Results have been presented which give thermal performance equations for flat-plate solar collectors by generic classification. The final classification considers the number of cover plates (either single or double), cover plate material (either glass or fiber reinforced plastic), and absorber coating (selective, moderately selective or flat black paint). From these results, the mean, standard deviation, maximum and minimum values of the intercept and slope of the linear collector performance curve and of the incident angle modifier are determined for each generic classification.

The results are based entirely upon the performance analysis of 270 solar collectors tested according to ASHRAE 93-77 procedures and certified by the Florida Solar Energy Center. The results represent six years of FSEC collector testing activities.

Using the generic thermal performance equations, designers can size and evaluate the performance of a solar system by generic collector type. This procedure should lead to more efficient system design and more competitive procurement of collectors. Also, these performance characteristics may be useful in comparing collectors within the generic type or determining if a particular collector is better than average for that generic type.

Figures based on the derived results are also presented which compare selective vs. non-selective surfaces, glass vs. fiber reinforced plastic cover plates, and single vs. double glazing.

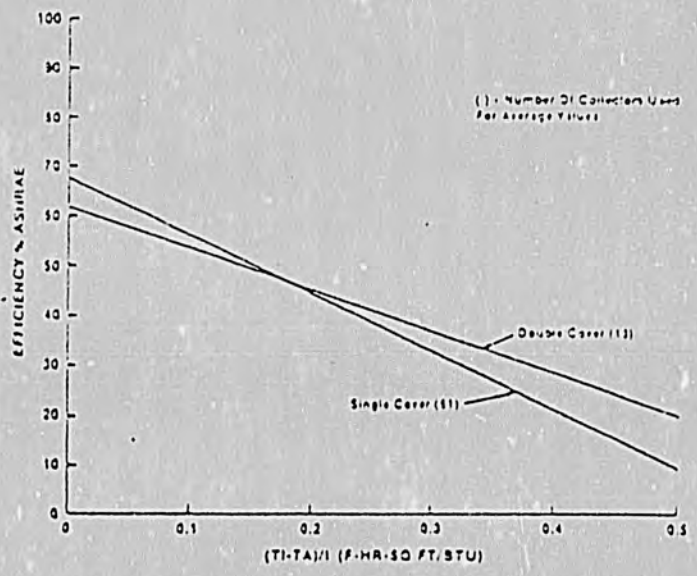

Figure 5. Comparison of Average Efficiency Curves for Single vs Double Glass Cover Plate Collectors with Flat Black Paint.

REFERENCES

1. "Methods for Testing to Determine the Thermal Performance of Solar Collectors, Standard 93-77," American Society of Heating, Refrigeration and Air Conditioning Engineers, Inc., 345 E. 47th St., New York, NY 10017.

2. "Test Methods and Minimum Standards for Solar Collectors," FSEC 77-5-R80 Cape Canaveral, FL 32920.

3. "Operation of the Collector Certification Program," FSEC 77-6-R80, Cape Canaveral, FL 32920.

4. Streed, Elmer and Waksman, David. "Uncertainty in Determining Thermal Performance of Liquid Heating Flat Plate Solar Collectors," National Bureau of Standards, Tech Note 1140, April 1981.

5. Lumsdaine, Edward. "On the Testing of Solar Collectors to Determine Thermal Performance," Proceedings of ISES Annual Conference, Denver, CO, June 1978.

6. Kirkpatrick, D.L. "Solar Collector Data Manual," Final report to the Solar Energy Research Institute, Golden, CO, July 1981.

Module 5: Sizing the Solar Array

Objective

The objective of this module is for the trainee to be able to size a solar system tank and array to meet a hot water load requirement.

121

Module 5: SIZING THE SOLAR ARRAY

The sizing procedure involves four steps:

1) Determine the hot water load or average daily demand.
2) Size the tank based on the daily load.
3) Determine heat needed for solar to meet demand.
4) Size solar to meet a designated fraction of demand.

The Hot Water Load: This is probably the hardest determination to make without actual data that has measured gallons per day usage.

For residential applications, J.J. Mutch (Ref. 1) determined that for a New York high rise apartment, approximately 20 U.S. gallons of hot water was used per day per person. Mutch has developed a profile of daily usage by hour - usually referred to as the "Rand" profile. Research at the Florida Solar Energy Center on 80 actual hot water systems, show hot water demand to be quite variable, ranging from 11.4 gallons to 18.5 gallons per day per person monthly average in the summer to 17.5 to 28.6 gallons per day per person in the winter. Hot water use is quite influenced by individual life style. In the U.S., 20 gallons/day per person is typically used as residential sizing load. For Florida, the figure is 17.5 gallons/day per person which would more nearly represent the load in Jamaica. Though the actual load is reduced in the summer months, the sizing load is typically closer to the winter demand load because that is when the desire for hot water is the greatest, and that is when it is harder to do without.

For commercial applications, such as schools and hospitals there are typical figures available for the U.S. but these are probably too high for usage in Jamaica. Table 5-1 (Ref. 2) gives such figures.

TABLE 5-1 Approximate Service Hot-Water Demand Rates (Ref. 2)

Usage Type	Demand per Person L/day	gal/day
Retail store	2.8	0.75
Elementary School	5.7	1.5
Multi-family Residence	76.	20.
Single-family Residence	76.	20.
Office Building	11.	3.

The recommended approach to the design engineer in determining load, is to talk with those who will be using the hot water. In a hospital for example, one can find out how many beds and showers are in the wards. Are all the patients required to take a daily shower? How many loads does the laundry do a day and what size? How many loads of dishes in the kitchen, how much for food preparation, etc? Such research on your own may be the only way a good estimate of load can be obtained without a previously established data base.

Once load L, in U.S. gallons per day is established, the heat requirement, Q_L, is:

$$Q_L = L\ 8.3453\ C_{pw}\ (T_d - T_s) \qquad (5.1)$$

where,

Q_L = service requirement in Btu/day
L = U.S. gallon/day use
C_{pw}= specific heat of water (usually assumed 1.0)
T_d = Water delivery temperature
T_s = water supply temperature

Sizing the Tank:

Tank sizes are usually available in nominal sizes and should be insulated to R13. The appropriate storage size in gallons for direct open loop solar systems is equal to the gallons of hot water used perday (gpd). Smaller tanks may be grouped to provide larger storage sizes if necessary.

Sometimes the figure of 2.0 U.S. gallons/ft^2 collector is used to estimate storage. This value is appropriate for high output flat plate collectors (800 Btu/ft perday) and may over size the tank for the less exotic collectors used in Jamaica. For this reason, the author prefers sizing the tank to the gpd demand.

Finding Solar Panel Requirement: The heat requirement of the solar panel, Q_s, is equal to the load devided by the system efficiency factor, μ_s.

$$Q_s = \frac{Q_L}{\mu_s} \qquad (5.2)$$

where μ_s is expressed as a decimal efficiency representing tank heat losses, pipe losses, etc.

For direct solar systems μ_s is typically around 65% for poorly insulated tanks (R8) and 80% for well insulated tanks (R20).

The solar load is then:

$$Q_s = L \quad \frac{8.3453}{\mu_s} \quad C_{pw} \, (T_d - T_s) \qquad (5.3)$$

124

Example: Assume $C_{pw} = 1.0$,

$T_d = 131^oF$

$T_s = 79^oF$

$\mu_s = .789$ (good system)

then $Q_s = 550$ L

where Q_s is the average solar panel load in Btu/day and L is the average hot water usage in U.S. gal./day.

for a family of 4, L = 70 gpd

$Q_s = 38{,}500$ Btu/day

Sizing to Solar Fraction:

It has been shown by earlier work done in 1977 (Ref. 2) that F-chart optimizes at very high solar fractions for Jamaica - close to 100%. The cost of power has continued to rise since that time, the author therefore recommends sizing at 100%, with a minimum of 85%. Remember that a solar system sized at 100% will only provide 100% of the load if the auxillary heat is turned off. The only places where this is not recommended is in hospital operating theaters or places where an occasional reduction in hot water temperature could not be tolerated.

To size at a solar fraction, f,

$$Q_s' = f \times Q_s \qquad (5.4)$$

for a solar fraction of 85% in our example,

$Q_s' = .85 \times 38{,}500$ Btu/day

$Q_s' = 32{,}725$ Btu/day

F-Chart

One of the most commonly used methods for calculating system performance is the F-Chart method. This method provides an overall annual solar fraction for a system, i.e. the fraction of the load

provided by solar, with the remainder provided by backup heat. F-chart is covered in much more detail in the appendix, however, there are some factors that need to be considered in its use for Jamaica.

Figure 5-1 shows the schematic used by F-chart. If one uses a heat exchanger efficiency of 1.0, then all the predicted panel output goes into the tank as represented by Figure 5-2. In the F-chart representation, a preheat system is simulated. Losses from the second tank, Q'_{LS}, are simulated by adding to the load Q_L. For a single tank system, this heat loss from the second tank should be made zero and $\dot{Q}_{LS}$ should be the heat loss coefficient of the single tank (or total of tanks if circulating through more than one tank).

This is how F-chart should be set up, however, there are two additional major problems in using it. One is the weather information needed. As already discussed in Module 1, this information would need to be developed for the Jamaica climate and perhaps, several weather profiles would be needed for the seperate areas of the island.

Secondly, F-chart predicts by solar fraction. Solar fraction has no meaning without a backup element. As mentioned earlier, solar fraction is the ratio of solar heat to the total heat load. Since Q'_{LS} (heat loss from second tank) is added to the load by the program then:

$$\text{Solar Fraction} = f = \frac{Q_s}{Q_L + Q'_{LS}}$$

but since there is no second tank, we assign:

$$Q'_{LS} = 0$$

then:

$$Q_S = f \cdot Q_L \qquad (5.6)$$

where Q_S is the heat provided by solar.

FSEC

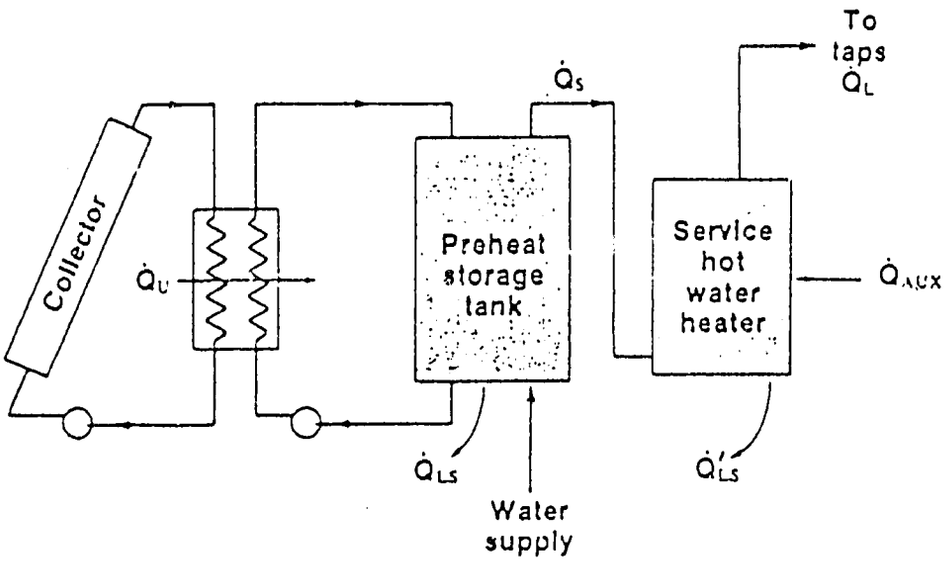

F-Chart Schematic of an Open-Loop DHW System

FIGURE 5-1

FSEC

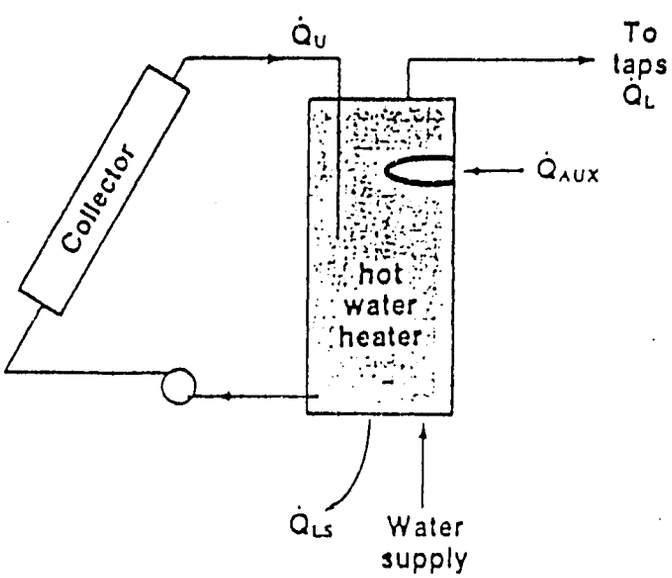

Schematic of an Open-Loop Single Tank System

FIGURE 5-2

The technique is to pick a fixed setting - say 100°F, it does not make much difference what low temperature is selected. F-chart provides the load, Q_L, and solar fraction, f. The heat provided by the total solar system as if the heater element were not turned on, can be calculated by equation (5.6).

Simplified Sizing Procedure

The sizing procedure presented in this document was developed by S. Chandra and modified by C. Cromer by analyzing direct pumped solar domestic hot water (DHW) systems with the TRNSYS and F-CHART computer programs. Although this procedure was developed for pumped systems with on-off differential temperature controllers, it is also applicable to proportional flow, photovoltaic, snap-switch, thermosiphon and timer-controlled DHW systems. While the method can be applied to indirect systems with heat exchangers, the results are less accurate.

The sizing procedure was developed primarily for single-family residential applications but may also be used for sizing commercial systems for condominiums and motels if the desired water temperature does not exceed 140°F.

We believe that systems sized according to this procedure will satisfy most consumers if quality system components are used and are installed correctly. The calculated savings should be achieved if the system is used year-round; however, it should be noted that variations in assumed water use patterns, component performance and reliability, and installation workmanship may significantly affect actual dollar savings.

SAMPLE PROBLEM

A FAMILY OF FOUR USES LPG AT J$2.50/GAL TO HEAT THEIR HOT WATER. YOU HAVE A SOUTH ROOF OF 4 IN 12 PITCH. YOUR PANELS ARE 3 FT. X 8 FT. AND DELIVER 680 BTU/SQ FT PER DAY.

SIZE THE SOLAR SYSTEM AND DETERMINE THE MONTHLY SAVINGS.

SIMPLIFIED SIZING PROCEDURE
FOR
SOLAR DOMESTIC HOT WATER SYSTEMS

HOT WATER DEMAND and TANK SIZE

Step 1. Using Table 1, estimate daily hot water use (GALLONS) and select a nominal tank size (TANK SIZE).

70 gal/day
GALLONS

80 gal
TANK SIZE

Step 2 Calculate how much energy is needed (BTUNEED) to heat the water to 131°F.

BTUNEED = 550 x GALLONS

BTUNEED = 550 x 70 (step 1)

38,500 Btu/day
BTUNEED

COLLECTOR SIZING

Step 3 Penalty factors that affect sizing must be determined.

a. Select the System Factor from Table 2. 1.2 System Factor

b. Select the proper Tilt Factor from Table 3. 1.0 Tilt Factor

c. Select the Orientation Factor from Table 4. 1.0 Orientation Factor

Calculate the overall penalty factor (PENALTY) for the combination of all three individual effects:

PENALTY = System Factor x Tilt Factor x Orientation Factor

PENALTY = 1.2 x 1.0 x 1.0

1.2
PENALTY

Step 4 Calculate the energy requirements of the solar system (BTUSOLAR) using the formula:

BTUSOLAR = BTUNEED x PENALTY

BTUSOLAR = 38,500 (Step 2) x 1.2 (Step 3) 46,200 Btu/day
BTUSOLAR

Step 5 For the collector selected, record the thermal performance rating at the intermediate temperature (BTURATING) in Btu/day and the gross collector area (GROSSAREA) in square feet from the required label.

Thermal Performance Rating at the Intermediate Temperature (Btu/day) 16,320 Btu/day
BTURATING

680 x 24 = 16,320

Gross Collector Area (ft^2) 24 ft^2
GROSSAREA

Estimate the number of collectors needed using:

$$NUMBER = \frac{BTUSOLAR}{BTURATING}$$

$$NUMBER = \frac{46,200 \text{ (Step 4)}}{16,320 \text{ (Step 5)}}$$

2.81
NUMBER

Step 6 Select the actual number of collectors to be used. This is the nearest whole number

3
NO.COLLECTORS

The total area of the collector array is:

TOTAL AREA = NO.COLLECTORS x GROSSAREA

TOTAL AREA = 3 (Step 6) x 24 (Step 5) 72 ft^2
TOTAL AREA

(3)

TABLE 2. SYSTEM FACTORS

System Configuration	System Factor
Direct system with no heat exchanger.	1.2
Indirect system with a heat exchanger between collector and storage tank.	1.3

TABLE 3. TILT FACTORS

COLLECTOR TILT			TILT FACTORS
Tilt Angle	Roof Pitch	Roof Tilt	
0° to 3°	0	0°	1.12
3° to 7°	1 in 12	4.8°	1.06
7° to 12°	2 in 12	9.5°	1.03
12° to 16°	3 in 12	14.0°	1.01
16° to 20°	4 in 12	18.4°	1.00
20° to 25°	5 in 12	22.6°	1.00
25° to 30°	6 in 12	26.6°	1.02
30° to 37°	8 in 12	33.7°	1.06
37° to 43°	10 in 12	39.8°	1.12
43° to 50°	12 in 12	45.0°	1.20

TABLE 4. ORIENTATION FACTORS

Collector Orientation	Orientation Factor
South or nearly south	1.00
Southeast or southwest	1.15
East or West	1.40

130

Step 7 Based upon the actual number of collectors to be used, compute the solar fraction (SOLAR FRACTION):

$$\text{SOLAR FRACTION} = \frac{1.0 \times \text{NO.COLLECTORS}}{\text{NUMBER}}$$

$$\text{SOLAR FRACTION} = \frac{1.0 \times \overset{3}{\overline{(\text{Step } 6)}}}{\underset{(\text{Step } 5)}{2.81}}$$

1.06

SOLAR FRACTION

If the solar fraction (Step 7) is less than .85 , the collector array is undersized. Consider either adding another collector or a different model/size collector.

TABLES AND FIGURES

TABLE 1. HOT WATER DEMAND and TANK SIZE

Average GALLONS and minimum TANK SIZE based upon number of people:

People	GALLONS	Minimum TANK SIZE (Gallons)
1	20	40
2	40	52
3	55	66
→ 4	70	80
5	85	80
6	100	100
7	115	120

(Add 15 gallons per person for each additional person.)

ENERGY AND COST SAVINGS

Step 8: Determining the backup factor:

The backup factor represents the furnace efficiency for the backup water heating system (powered by electricity, gas or oil). It has a value of one for electricity, and is less than one for gas and oil, which accounts for pilot light and flue losses. Select the appropriate value from Table 5:

TABLE 5 BACKUP FACTORS

Backup Power	Backup Factor
Electricity	1.00
Gas or oil (standard)	0.65
Gas or oil with electronic ignition or flue gas damper	0.75
Gas or oil with electronic ignition and flue gas damper	0.85

Step 9. Determining the average monthly savings, MONTHLY SAVINGS:

16,320 x 3 = 48,960

BTU Solar ÷ backup factor × 30 = energy saved/month in MMBtu

48,960 ÷ .65 × 30 = 2,259,692 = 2.26 MMBtu

Energy saved/month x conversion factor × cost/unit = monthly savings

2.26 MMBtu x 10.93 × $2.50 = $61.75

TABLE 9 FUEL COST CONVERSION FACTORS

Fuel Type and Conventional Cost Units	Conversion Factor
Electricity in $/kwh	293.00
Fuel oil in $/gal	7.14
Gas in $/therm	10.00
Propane or LPG in $/gal	10.93
Propane or LPG in $/LP-lb	46.34

It should be noted that the monthly costs of heating water without a solar system can easily be calculated by dividing the monthly savings (MONTHLY SAVINGS, Step 9) by the solar fraction (SOLAR FRACTION, Step 7).

Step 10. Calculating the SIMPLE PAYBACK PERIOD:

The simple payback period is a rough estimate of the time it takes for a solar system to pay for itself in energy cost savings. Although not as accurate an indicator as some prefer, it is often used and requested.

To find the simple payback, multiply the monthly savings found in Step 9 by 12 to get the annual savings.

Monthly Savings x 12 = annual savings

61.75 (step 9) x 12 = $741.00 (annual savings)

Divide the cost of the system by the annual savings to get the payback in years.

Cost of System ÷ annual savings = Simple payback

$3800 ÷ $741.00 (Step 10) = 5.1 yrs

References

1) Mutch, J.J.: Residential Water Heating, Maxwell Scientific International, Elmstod, New York, 1974.

2) K. George, J. Kreider, A. Nunez: Design, Construction and Installation Manual Solar Water Heating Systems in Jamaica and the West Indies. Ministry of Mining and Natural Resources, Kingston 5, Jamaica; 1977.

MODULE 6: Types of Solar Hot Water Systems

Objective

The objective of this module is for the trainee to become familiar with the types and attributes of Solar Hot Water Systems installed throughout the world and reviewed in the Solar literature.

Thermosiphon. Figure 6-1 is a schematic diagram of a thermosiphon system. Cold water from the bottom of the elevated storage tank flows to the lowest point in the system (which is the bottom of the solar heat collector).

As it is warmed it becomes less dense and flows back up to a side port near, but not at, the top of the storage tank. If the tank is about two feet above the top of the collector, the system will not back-siphon at night. If back-siphoning were to occur, the warm water would be cooled during its passage through the dormant collector. Thermosiphoning systems have no moving parts and are self-regulating in terms of flow rate.

The elevated tank presents problems if it is mounted on a roof or in an attic. First, a 100-gallon tank weighs about 1,000 pounds when full of water, so special bracing may be required for its support. Second, the large tank should be attractively housed, and it costs money to make an imitation chimney or a cupola for this purpose. Third, leaks in tanks mounted above living space can present serious problems; drip pans and drain lines offer only limited protection if the homeowner allows them to become clogged with debris during the 10 or 15 years of useful tank life.

Forced Circulation. Figure 6-2 shows the manner in which many modern solar water heaters are installed. The collectors are mounted on a south-facing roof and connected to a pump and storage tank through a series of pipes and control valves. A check valve

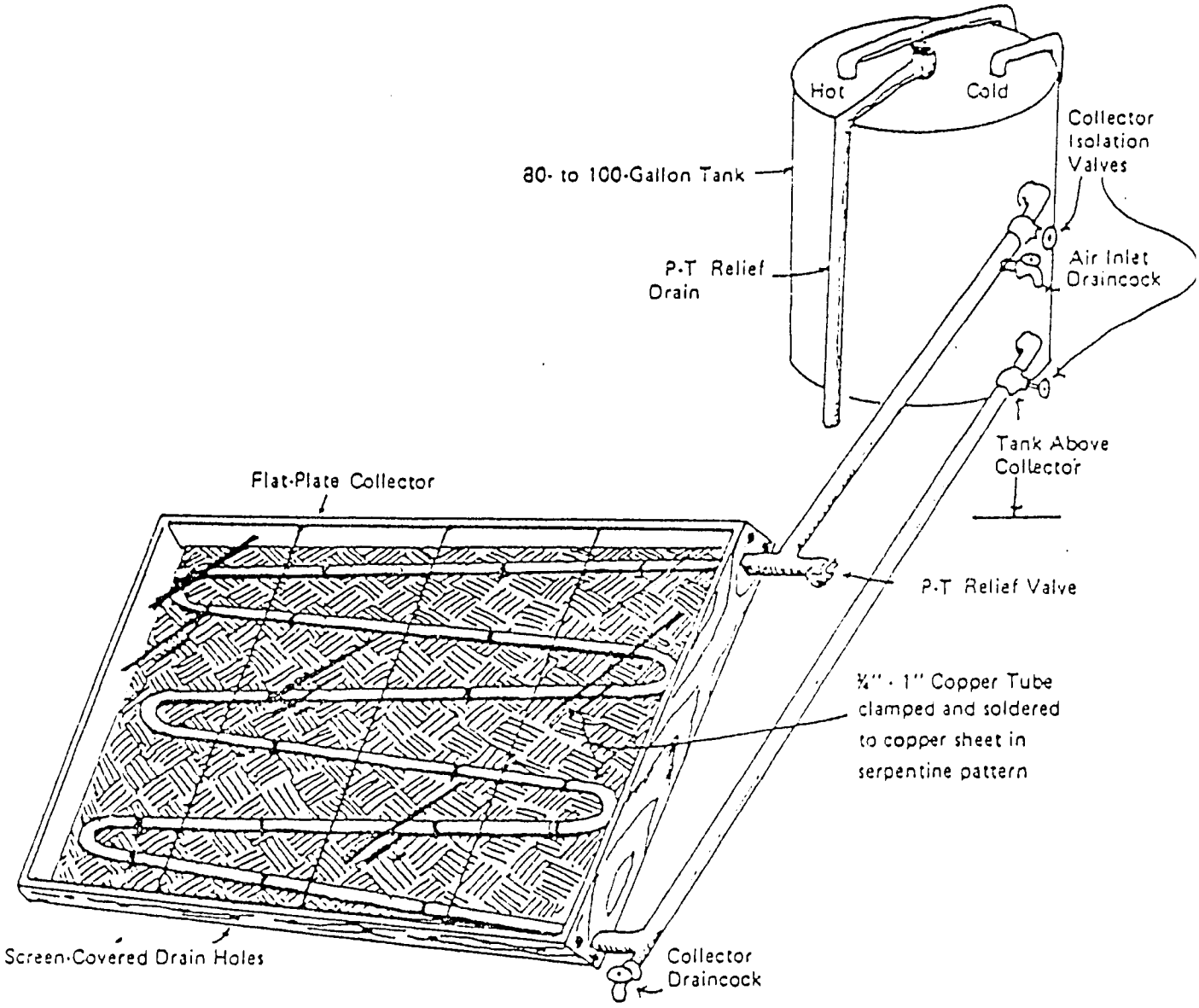

FIGURE 6-1
Conceptual Diagram of a Thermosiphon System

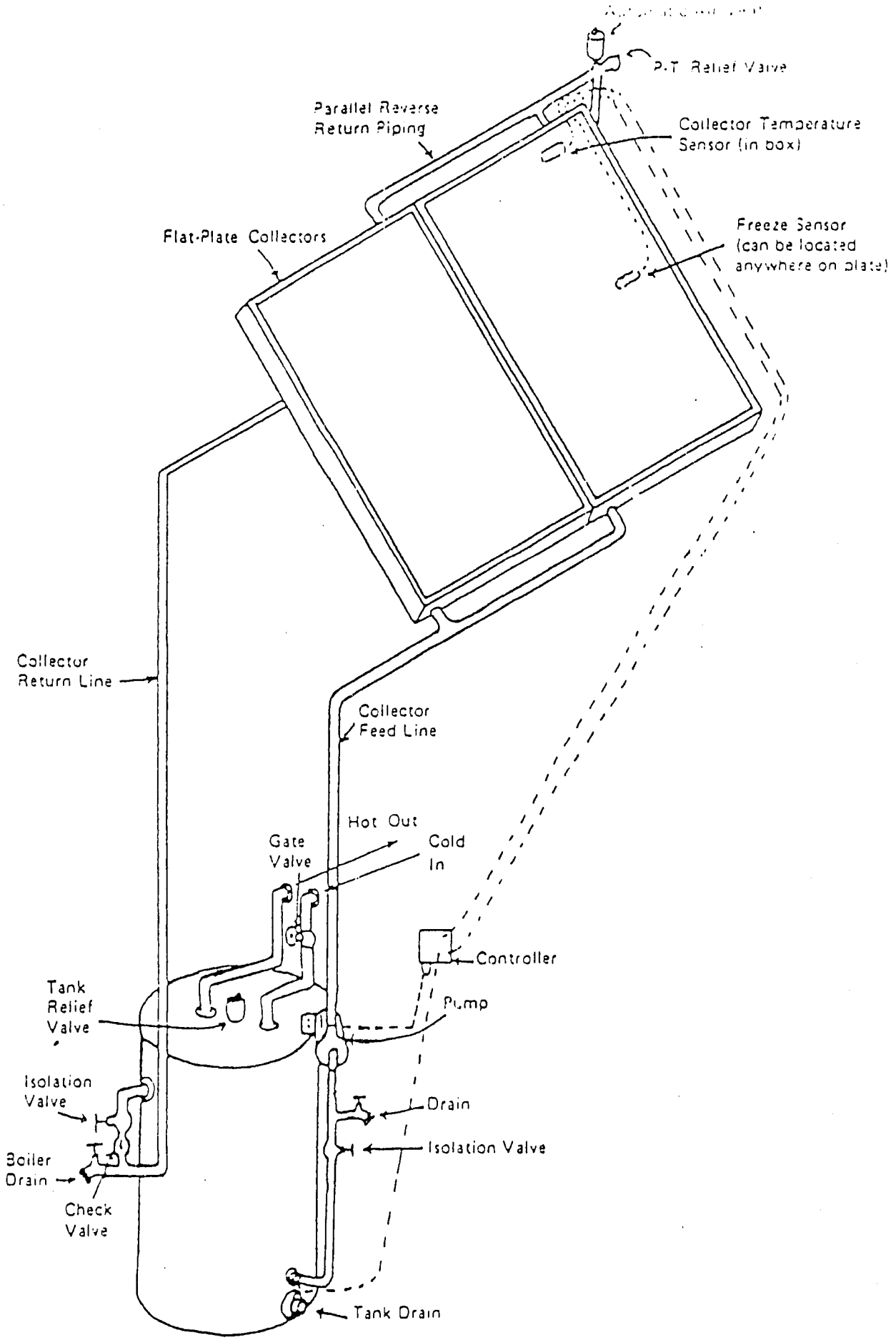

FIGURE 6-2
Conceptual Diagram of a Forced-Circulation System

(gravity-, spring-, solenoid- or motor-operated) prevents back-siphoning at night. A dual sensing thermostat, called a differential controller, turns the pump on when the water in the collector is warmer than that in the bottom of the storage tank. The electricity to operate the pump and controller costs about 50¢ a week for residential installations. Forced-circulation systems may use potable water as a heat collector liquid (open systems) or may use a non-freezing, non-corrosive liquid in a separate heat collector loop (closed system). (Thermosiphon systems which employ a closed collector loop are rarely encountered.)

INTEGRAL OR "BREADBOX" SYSTEMS

A breadbox system uses the hot water tank to function as the solar collector as well as a storage tank. The water tank is painted black or coated with a selective serface and placed in the sun. Since nightime losses are great, this type of system is very inefficient. They are usually used as a "preheat" to a standard hot water heater. Figure 6-3 shows a breadbox encased in an insulated box with glazing.

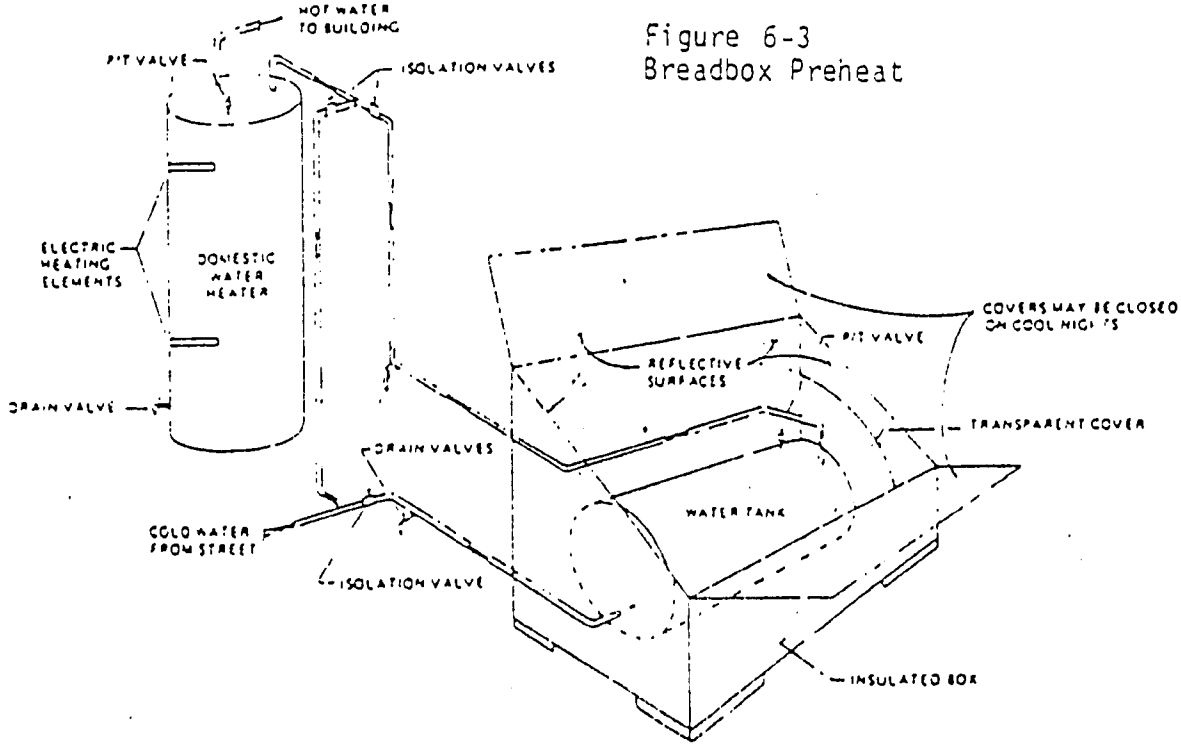

Figure 6-3
Breadbox Preheat

Photovoltaic Circulated Hot Water

Circulation pumps for solar domestic hot water systems require a reliable electrical switching mechanism (controller) and electrical power to utilize fully the available panel heat. The controller has long been termed the weakest mechanism in solar domestic hot water hardware. In some areas, electrical power is not available or the supply is not always reliable. Perhaps the best solution to these problems is the use of photovoltaic (PV) panels to convert sunlight to direct current which drives a DC circulating pump. With PV power output proportional to insolation intensity, a variable flow pumping output is produced which is proportional to absorber heat availability.

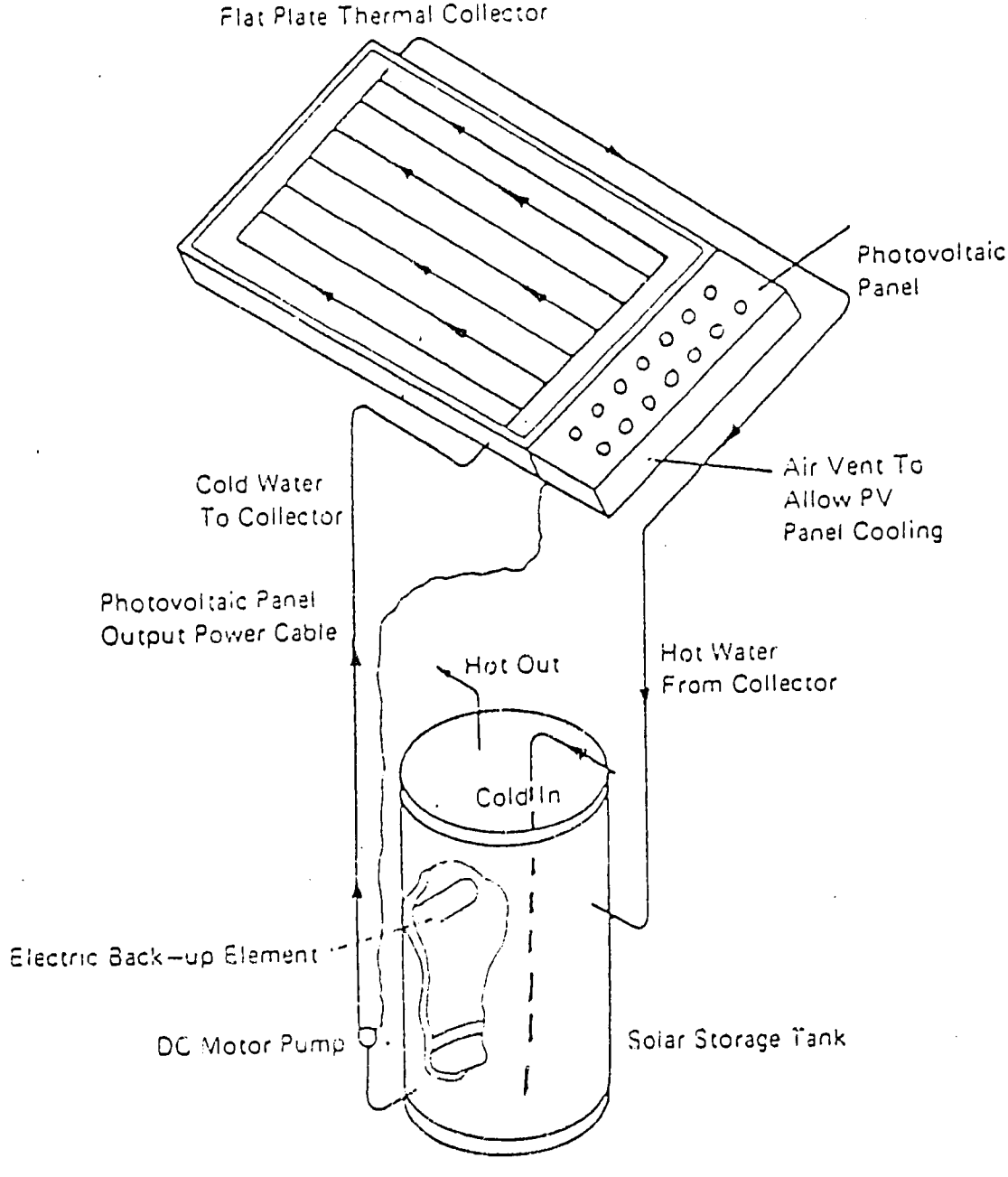

147

Pumped Circulation with Heat Exchanger--In the system depicted in Fig. 6-4 collector water is pumped through a closed pipe loop with a heat exchanger coil in the storage tank. Because collector water and domestic water do not mingle, antifreeze solution can be added to the collector water for low-temperature protection. Single-wall heat exchangers may be permitted when the antifreeze is of a largely non-toxic type such as propylene glycol. Safety regulations may call for use of a "double-wall" heat exchanger which provides a double barrier between antifreeze solution and potable water, when toxic antifreeze solutions are used. The closed collector pipe loop must have an expansion tank and a separate pressure relief valve in additon to the valve on the storage tank.

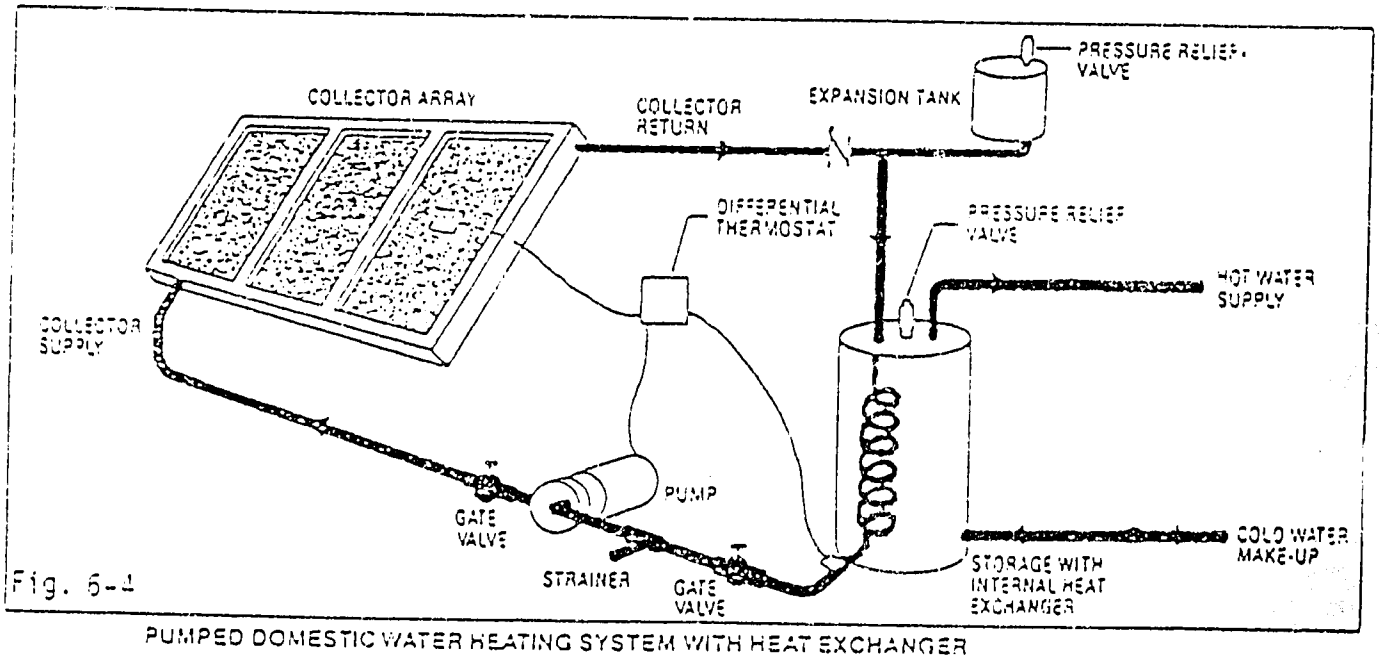

Fig. 6-4

PUMPED DOMESTIC WATER HEATING SYSTEM WITH HEAT EXCHANGER

Because collected heat must be transferred through the heat exchanger, the collection fluid must be hotter and thus this system is somewhat less efficient than one in which domestic water circulates through the collector directly. A check valve in the collector return prevents the migration of heat from tank to collector by thermosiphon action on cold nights.

Pumped Circulation with Drain-back--Fig. 6-6 (next page) shows a solar hot water system which provides domestic hot water during the day by means of solar energy or, at night, by means of an auxiliary heater.

The major portions of this solar energy system are: a closed water-filled solar loop for absorbing heat energy from the sun by means of roof-mounted solar collectors; and a separate domestic hot water loop to which this heat energy is transmitted. A solar coil immersed in a hot water tank, through which the solar loop water is made to circulate by means of a circulator pump, heats city water stored in the tank to a maximum temperature of 165 degrees Fahrenheit, and thus provides domestic hot water for distribution.

(For dwellings in which the circulating water is pumped 20 feet or more vertically from storage to the solar collectors, two circulator pumps are required.) The circulating water is stored in a 12-gallon reservoir when the solar loop is inactive.

If sufficient energy exists for heating the stored water, the solar controller starts the circulator pump and the solar loop water heated by the sun is forced through the solar coil in the hot water tank which, in turn, raises the temperature of the domestic hot water supply. When a reduction of heating capability from the roof-mounted solar collectors is sensed, the circulator pump is shut down by the solar controller, and the solar loop water drains back into the reservoir. This drainback feature permits the use of city water, thus eliminating the need for harsh chemicals in the solar loop.

Two swing check valves are mounted in the system. One check valve, mounted in the return piping of the solar loop above the reservoir allows one-way venting of air from the tank during the solar loop drainback stage. The second check valve, mounted in the city water supply line to the tempering valve prevents heat loss due to temperature differences between the top and

DRAINBACK SYSTEM

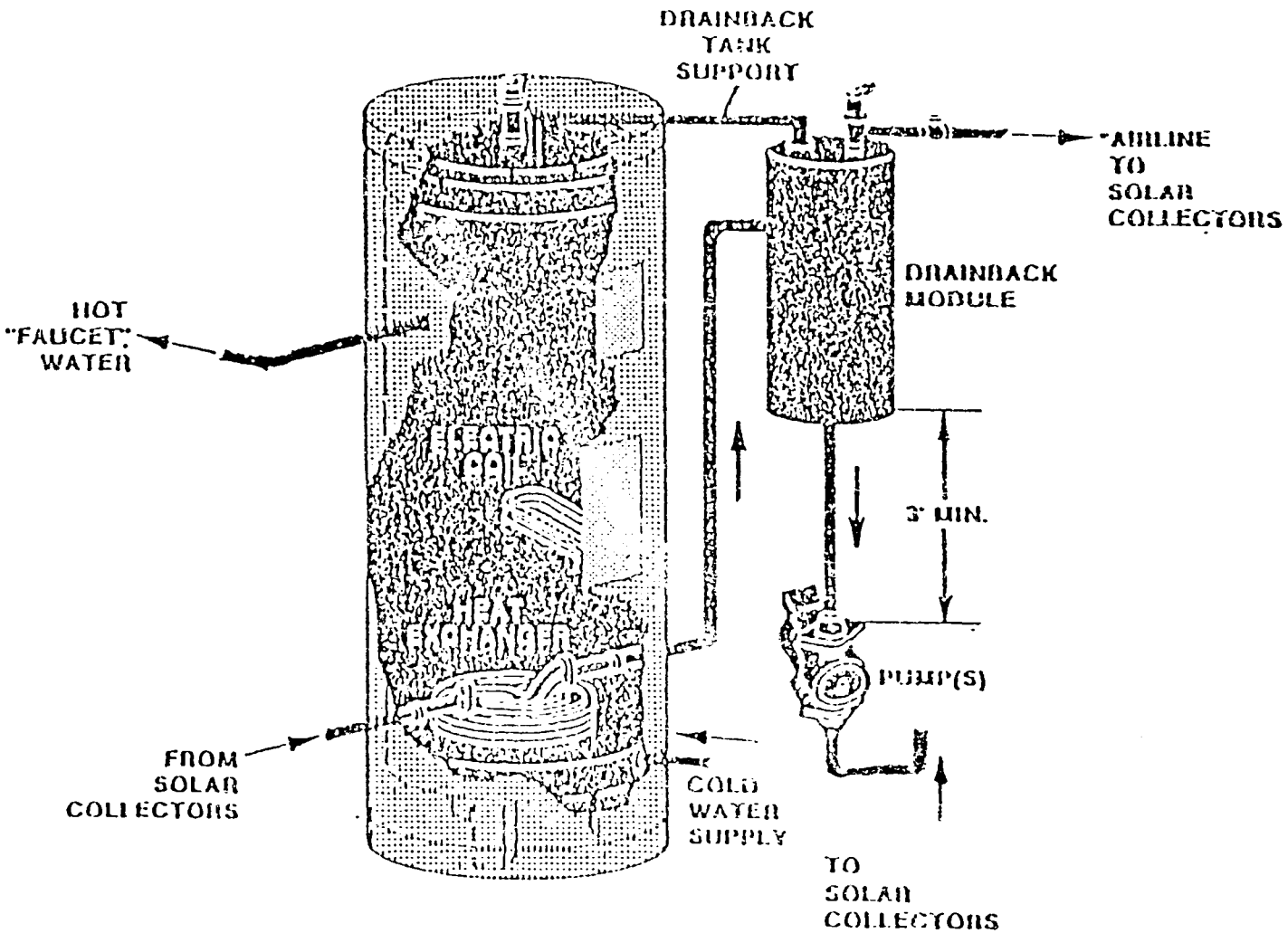

Figure 6-5

bottom of the hot water tank.

Each tank is protected by a safety valve. A temperature and pressure relief valve is mounted on the hot water tank and is designed to provide temperature and pressure relief at a temperature of 210 degrees Fahrenheit and pressure of 150 psi. A low-pressure (15 psi) pressure relief valve is provided on the reservoir.

A hot water thermometer with a temperature range of 40 degrees to 280 degrees Fahrenheit is mounted in the solar loop for monitoring output of the solar collectors.

Pumped Circulation with Drain-down--Fig. 6-6 shows another method for assembling components for solar water heating. This system, again, has a circulating pump for collector water, but does not have a heat exchanger. With this method, the collector circuit is drained of water.

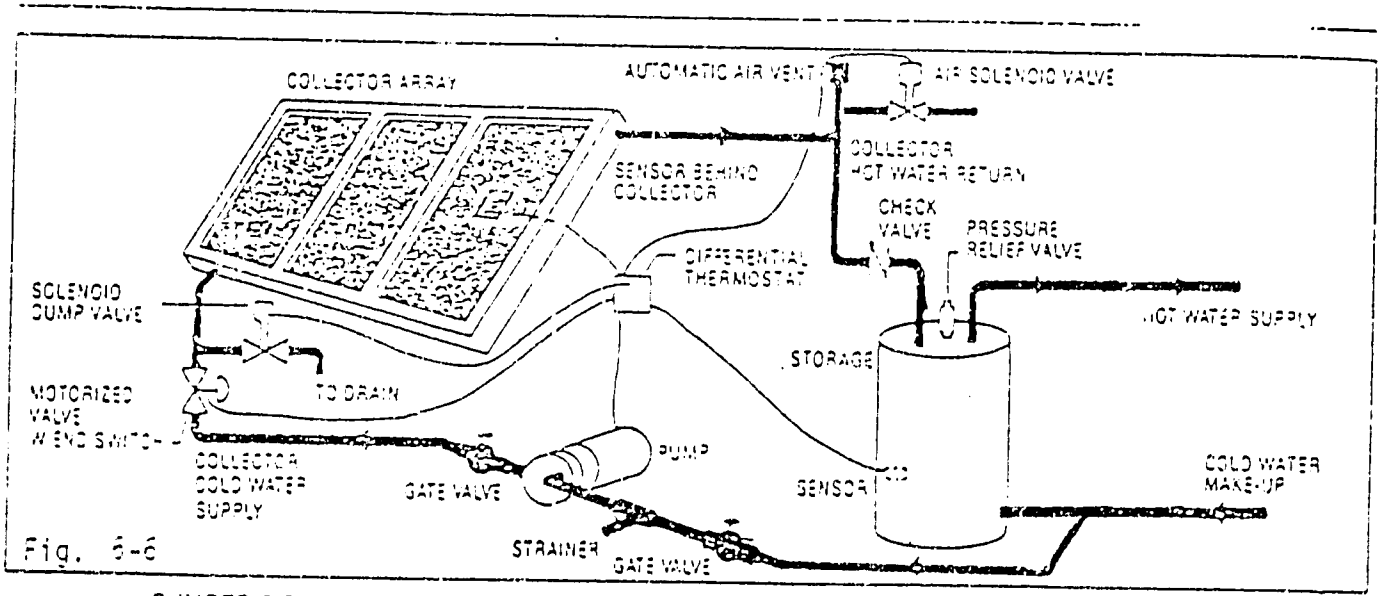

Fig. 6-6

PUMPED CIRCULATION DOMESTIC WATER HEATING SYSTEM WITH DRAINDOWN

When this system drains, the motorized valve closes in the collector supply. Reaching its fully closed position, the valve trips an end switch that trips the solenoids of both the dump valve and the air inlet valve. Water then drains freely from the collector circuit and out of the system. Typically, the amount of water drained is not more than two or three gallons including that in all piping.

The pressurized source water is prevented from flowing to the collector by means of the motorized valve in the supply line and the one-way check valve in the return.

Whenever the absorber plate temperature rises to a pre-set difference above storage, the motorized valve begins to open, the circulating pump restarts, and the dump valve and air inlet valve close. As the collector circuit refills, trapped air is relieved through the automatic vent and normal circulation of collector water is resumed.

Module 7: Plumbing Multiple Tanks

Objective

The objective of this module is for the trainee to understand the concepts behind multiple tank plumbing connections.

MODULE 7: PLUMBING MULTIPLE TANKS

Many installations may require several tanks to provide the needed hot water storage. This occurs often when the homeowner has a new standard hot water tank. He does not want to give up this tank to be replaced by a larger solar tank because it still has many years of useful service. He can be accommodated by adding a second smaller tank to bring the total volume up to the needed gallons.

There are three ways to connect multiple tanks: preheat, series, and parallel. The preheat mode must be used when the back-up tank burns gas or oil. In this mode, the solar loop circulates through the preheat tank only. The preheat tank will thus heat up during the day as the solar system adds heat. Such a system is shown on Figure 7-1(A). Notice that the solar heated water does not enter the back-up tank for use unless the user draws hot water. As a result, during low demand periods, the back-up element may have to come on to reheat the back-up tank because of stand-by heat losses, even when there is plenty of solar hot water available.

Figure 7-1(C) also shows a preheat mode. But in this case, the back-up tank is elevated and a thermosiphon loop (I) is connected to the lower solar tank. Now, if there is solar heated water that is hotter than the back-up tank, it will naturally rise and keep the back-up tank filled with ready hot water. This configuration is the preferred one to use if preheat must be installed.

A series connection is shown in Figure 7-1(B). Notice that the solar loop returns hot water to the back-up tank through a dip tube located about half-way down. The solar loop than draws from the bottom of the back-up tank

A. Cold Water In
B. Large Preheat Tank
C. Tank Sensors
D. To Collector
E. From Collector
F. Small Backup Tank
G. Backup Electric Heater Element
H. Hot Water Out
I. Thermosiphon Loop

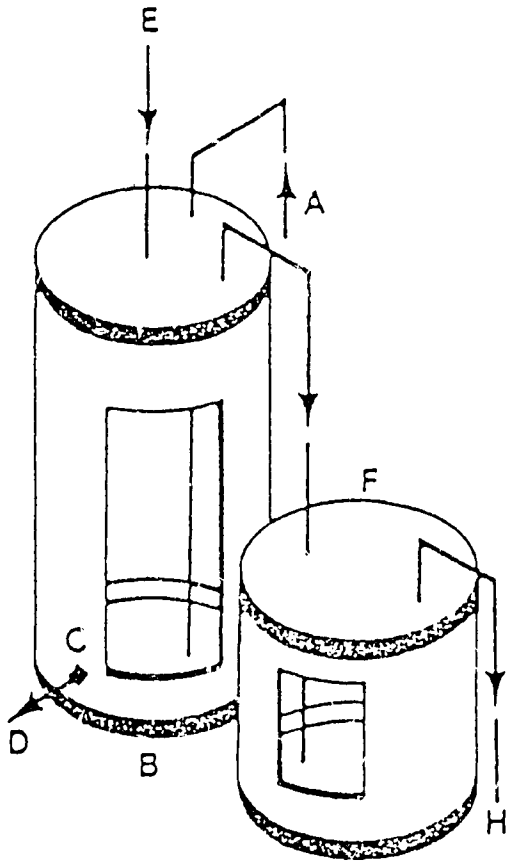

A) Plumbing for Two-Tank System With Large Preheat and Small Backup Tank

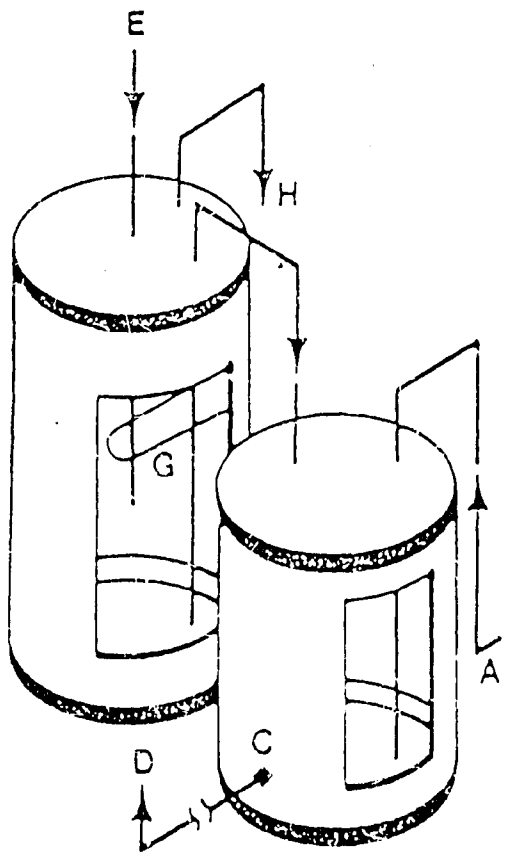

B) Plumbing To Fully Utilize the Volume of Both Tanks

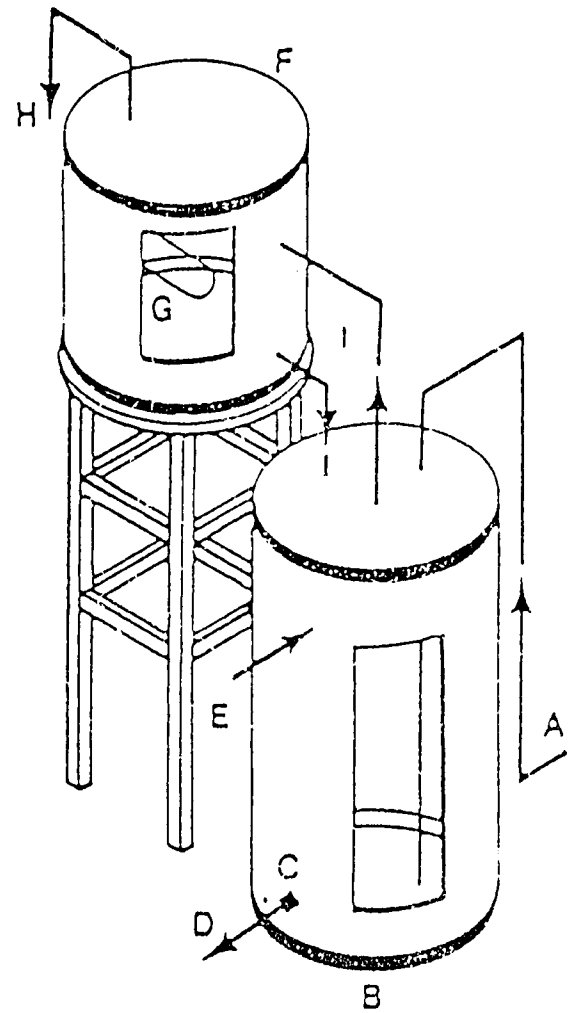

C) Two-Tank System Plumbing With an Elevated Backup Tank

FIGURE 7-1
Multiple Tank Connections

150

and enters the top of the second tank. Finally, the water exits the bottom of the second tank on its way to the collector. In a series configuration, the pumped water of the solar loop passes through all tanks, one after the other. This configuration is the preferred set-up for multiple tanks on a pumped system.

A parallel type connection system is shown in Figure 7-2. When connected in parallel , the water of the solar loop travels out of the bottom of all tanks and to the collectors and then returns to the top of all tanks. This system should only be used on thermosiphon systems using multiple tanks. For such a system, as each tank is closer to the water draw point, it should be elevated so that natural convection will cause the hottest water to be available for use at all times.

When using three or four tanks, combinations of these configurations might be used. For example, two pumped tanks may be in series providing preheat to an elevated thermosiphoning third back-up tank. Research has not been conducted to date to say which of these multible tank combinations is optimum.

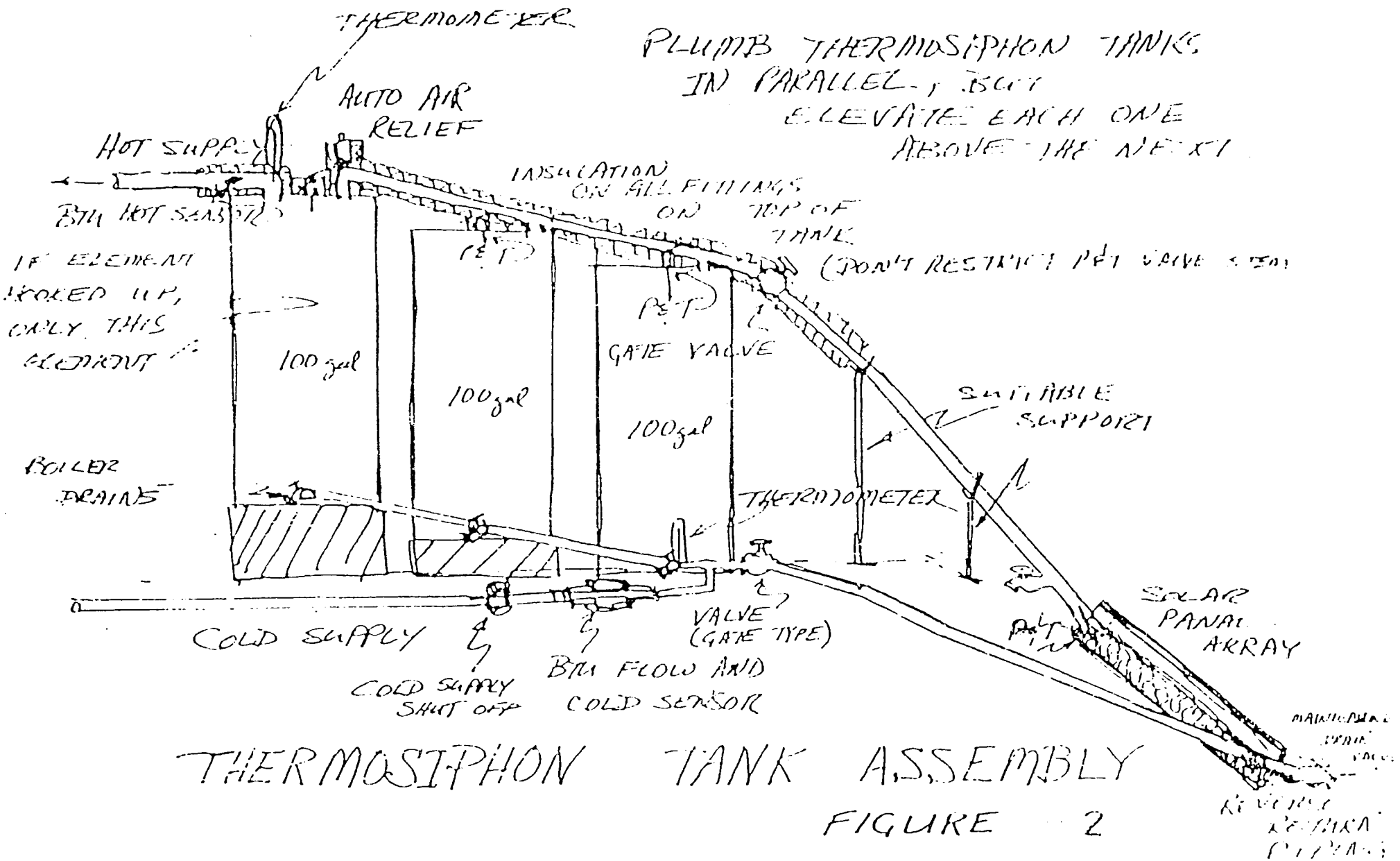

THERMOSIPHON TANK ASSEMBLY

FIGURE 2

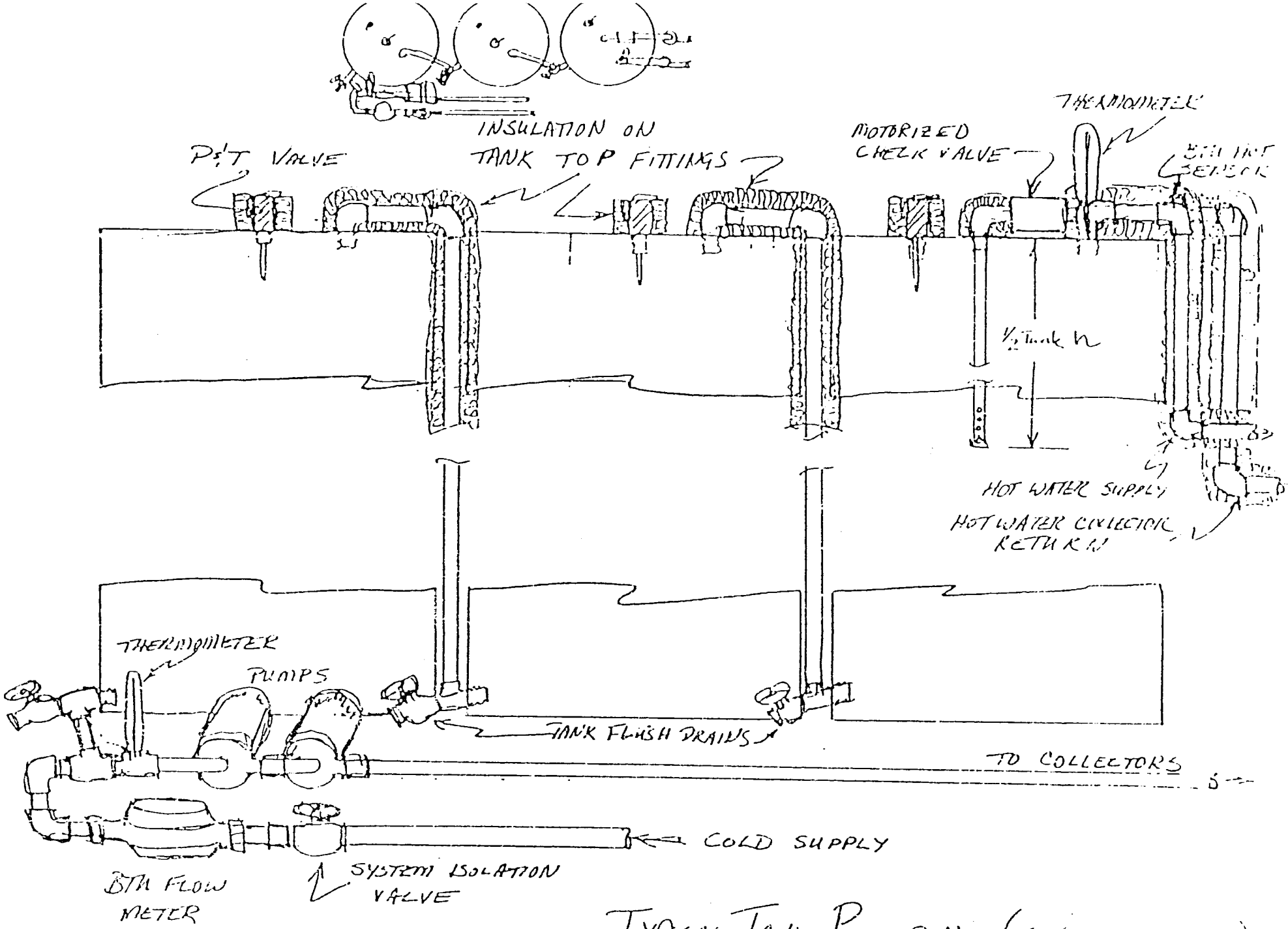

TYPICAL TANK PLUMBING (FOR PUMPED SYSTEM)
FIGURE 7-3

Module 8: Types of Controls and Controllers

Objectives

The objective of this module is for the trainee to understand the types of solar control systems and their operations, and to be able to properly design a PV pump circulation system to meet designated pumping requirements.

MODULE 8: TYPES OF CONTROLS AND CONTROLLERS

A control system usually refers to the mechanism by which a pump is turned on or off. A thermosiphon system uses the natural density difference between its heated and cooler fluid to induce circulation. Though this provides a natural thermal control of flow, it is not usually considered when the term "control" is used.

The following are control types--methods for controlling fluid flow in a pumped system:

1) manual on-off switch
2) time clock
3) flow thermostat
4) aquastat
5) snap-switch
6) differential
7) variable flow differential
8) photovoltaic

While one of the simplest methods of controlling pumps is to use an off-on switch, the problem is that the system is not automatic. People are simply an unreliable method for sensing when the panel is hot and when it is not. Never try to outguess a switching system without knowing the temperatures.

A more sophisticated method is the use of a preset thermostatic valve in the collector's exit line, which can be set to allow water no cooler than 120°F to exit the collector. A time clock may be used with such a system, but

the pump must not be subject to overload when the valve is closed. (A magnetically-coupled pump is less subject to overload than a mechanically-coupled pump.)

A time clock by itself can be used, but this method is far from optimum because it will lose heat during cloudy conditions.

An aquastat uses a bulb filled with some type of fluid. This bulb is placed at the hot water outlet of the panel or on the collector itself. As the bulb heats up, the liquid expands and throws a relay that turns on the pump. Usually this type of control requires running the pump's 110v line to the roof and back to the pump. Such a 110v line is hazardous and should be avoided if possible. Also, such bulbs usually have a slow response time and, as a result, aquastats are not the best choice. Aquastats also have a mechanical switch that may degrade with weathering after several years.

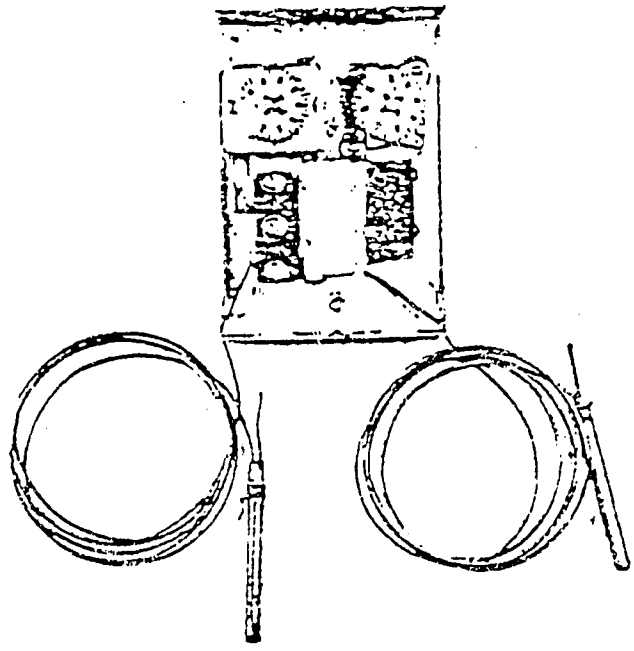

Aquastat

A snap-switch is similar to an aquastat in that it turns the pump on and

156

off at a fixed temperature. A small sensor switch is placed on the panel or on the panel outlet pipe. Low voltage (coming from a transformer) is switched by the sensor and throws a high-voltage relay that switches the pump. Snap-switches are sealed from the weather and have fast response time to temperature changes. Also, the relay and transformer can be located by the pump out of the weather.

Both aquastats and snap-switch controls have one efficiency drawback. Since they are set to switch at a fixed temperature, say 110-120 degrees F, if the solar system has filled the tank up during the day with water hotter than the switching temperature, they will continue to run the pump until the entire tank is cooled to the set-point temperature. Coupling a timer with an aquastat or snap-switch helps reduce this late afternoon loss of heat. Another alternative used on snap-switch systems is to run the voltage of the snap-switch through a light-sensitive resistor. If sunlight is available, the snap-switch operates normally. If no or low sunlight is present, there is high resistance through the light-sensitive resistor and the snap-switch cannot turn on the pump.

The differential thermostat receives signals from the sensors and uses this input to control the system. It is usually factory-set for high and low temperature differentials to maximize the amount of heat energy collected and stored and to minimize excessive cycling. This reduces wear on pumps and relays and minimizes the amount of power necessary to operate the solar DHW system. Most differential thermostats are of the on-off type; the pump is either full on or off. Typically, the system comes on when there is a 10 to 18 degree F positive temperature difference between collector and storage and shuts down when there is a 3 degree F temperature difference.

Proportional differential thermostats are available that can vary pump speeds as a function of the temperature differential between collector outlet and storage. Proportional controllers are not recommended for drain-back or draindown systems because pumps may not receive enough power initially to fill the system at a reasonable rate. Be sure to use the size and type of wire specified by the manufacturer.

Photovoltaic Circulation Control

Circulation pumps for solar domestic hot water systems require a reliable electrical switching mechanism (controller) and electrical power to utilize fully the available panel heat. The controller has long been termed the weakest mechanism in solar domestic hot water hardware. In some areas, electrical power is not available or the supply is not always reliable. Perhaps the best solution to these problems is the use of photovoltaic (PV) panels to convert sunlight to direct current which drives a DC circulating pump. With PV power output proportional to insolation intensity, a variable flow pumping output is produced which is proportional to absorber heat availability.

The use of photovoltaics for circulation of solar hot water systems is an ideal application for Jamaica. The system eliminates the use of sensors and controller. The sun itself is the controller. Hot water will continue to be collected even during power outage. The installation is much simpler than the differential controller or even snap switch type of control. The reliability of such a control system is much better than conventional differential controls which are somewhat suspectible to damage by transients or surges. Finally the cost of electrical power, is quite high in Jamaica and its production requires

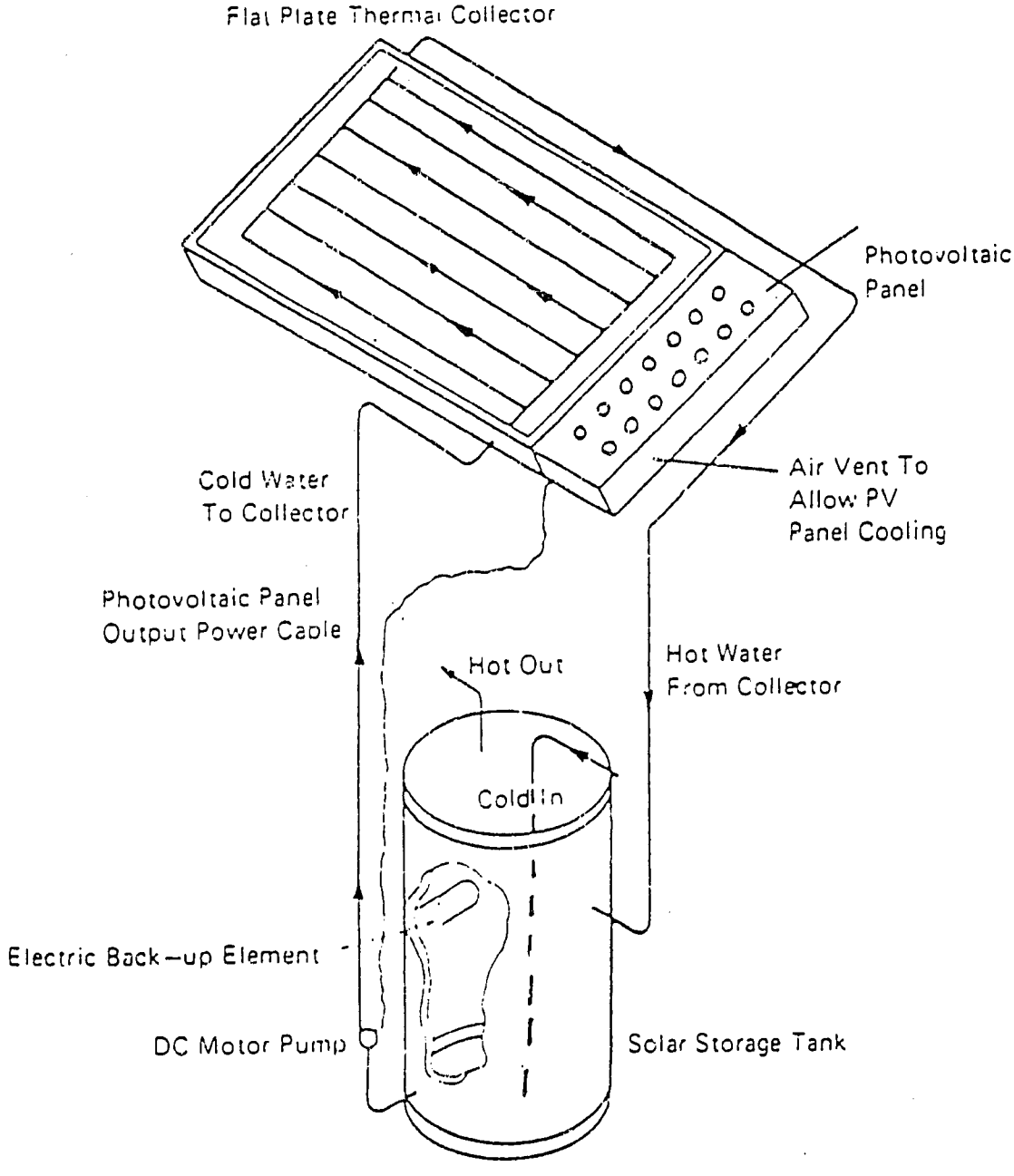

FIGURE 8-2

foreign currency, a balance of payments problem. When all things are considered PV powered pumps should be the system utilized on pumped systems in Jamaica.

However, one cannot simply purchase a PV panel of x volt, y watt rating, hook it to a pump of x volt, y watt rating and expect the system to pump

properly, much less double as a controller.

The author has made a study of such systems, and the matching process is covered somewhat in Paper 8-1.

The overall process requires four steps:

1) Determine the pumping requirement of the solar system as covered in Module 10. (Gpm and head at full sun)
2) Select a DC pump that meets the pumping requirement in the "good" efficiency part of its fow curves as in Module 10. Buy the pump.
3) With a variable voltage power supply hook the pump up and develop an I-V load curve for it, noting where the full sun requirement falls on the pumps I-V load curve.
4) Using the PV panels IV curves, design a PV panel configuration that will match the PV panel output to the pump IV load line, such that the pump starts at .2 suns and stops at .3 suns. This may require tilting the PV panel 10^{0} to the East.

Such a PV matched system is ideal for Jamaica where freeze protection is not needed. As a second choice, the author recommends a snap switch control system with a photosensitive cutoff.

160

Professional Paper

Sizing and Matching a Photovoltaic Circulation System with a Solar Domestic Hot Water System

FSEC-PF-29-83

By:
Charles J. Cromer

Florida Solar Energy Center
300 State Road 401
Cape Canaveral, Florida 32920

This paper was presented at the
AMSE Solar Division Conference,
April, 1983 in Orlando, Florida.
Views and opinions expressed here represent
those of the author and not necessarily
those of the Florida Solar Energy Center.

Best Available Document

Sizing and Matching a Photovoltaic Circulation System with a Solar Domestic Hot Water System

Charles J. Cromer

Florida Solar Energy Center
300 State Road 401
Cape Canaveral, FL 32920

Abstract:

Circulation pumps for solar domestic hot water systems require a reliable electrical switching mechanism (controller) and electrical power to utilize fully the available panel heat. The controller has long been termed the weakest mechanism in solar domestic hot water hardware. In some areas, electrical power is not available or the supply is not always reliable. Perhaps the best solution to these problems is the use of photovoltaic (PV) panels to convert sunlight to direct current which drives a DC circulating pump. With PV power output proportional to insolation intensity, a variable flow pumping output is produced which is proportional to absorber heat availability.

Such a PV-pumped system has been constructed with off-the-shelf components at the Systems Test Laboratory of the Florida Solar Energy Center, Cape Canaveral, Fl. Its purpose is to allow comparison on a side-by-side basis of a PV-pumped circulation strategy vs. other circulation strategies (snap switch, differential, proportional flow differential, and thermosiphon). The engineering of such a PV system from components available in the marketplace requires the consideration of PV panel output, PV panel cost, pump output and starting and stopping characteristics, pump cost, solar system pumping requirements, panel performance and piping heat loss. A methodology is provided to allow the solar engineer to select the least costly components necessary for proper operation of such a PV-pumped system. Also provided are actual system operational data taken on a 4' x 10' panel, 82-gallon tank system at the FSEC Systems Test Laboratory.

Introduction:

Unlike thermosiphon systems, typical solar systems used in northern climates have the solar panels mounted above the tank and utilize a circulating pump to circulate the heat removal fluid from the tank to the collectors and back. In most cases, the entire system is pressurized and fluid filled such that a lifting head does not have to be produced by the pump. The pump does only the work needed to overcome the friction forces associated with the panel and piping at the circulation flow rate. As a result, very small circulating pumps can be used with an associated small power requirement.

A conceptual view of such a PV-pumped system as applied to an open solar domestic hot water system is shown in Figure 1.

To design such a system and to have it a viable alternative to the common differential-type control, the following criteria are established:

1. Cost of a PV system should not exceed twice the cost of a comparable operating differential control system. In 1982, a differential control costs around $100, so the PV control should not be more than $200.

2. The system should start and stop pumping when the return water temperature at the tank is slightly greater than the water leaving the tank. The panel inlet and outlet temperatures relate to the leaving and return tank temperatures but, clearly, the system should only pump when the tank has a heat gain.

3. A minimum flow rate of 10 lbm/hr per square foot of collector area should be provided through the collector loop at .75 to 1.0 suns.

Photovoltaic systems have been constructed and tested for domestic hot water circulation [1], [2], [3]. However, none of these systems meet the first requirement established here. They are all too costly. The driving cost is the PV panel itself as 20 watt panels typically cost $25 per watt. Research done at the Florida Solar Energy Center (FSEC) indicates these larger panels are not necessary. A 5 to 7 watt panel can be used, but such use requires that the pump motor and volute's I-V load and pumping characteristics properly match with the PV I-V output characteristics.

FIGURE 1
Conceptual View of a PV Powered Solar System

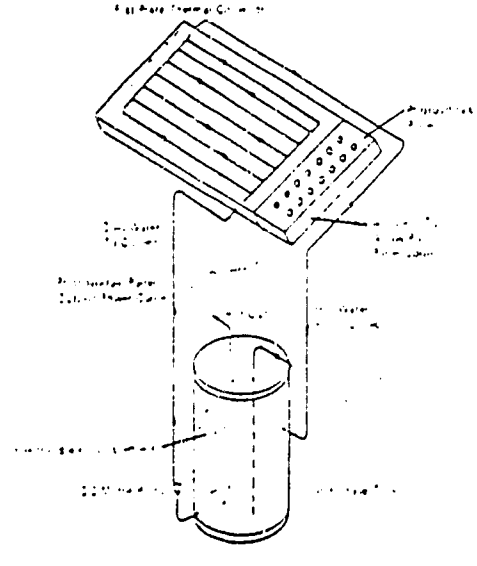

112

Best Available Document

Pump-Motor Power Requirements:

When pumping water from a well, the primary concern of the pump and motor is flow rate vs. head. This is not the primary concern in direct circulation systems. The dynamic flow head measured on four typical hot water systems (82-gallon tank, 60 feet of 1/2" pipe) at 1 gpm was .6 to .8 feet of water. This low head results because no lifting is needed and the flow rate is very small. Optimum flow rate in a direct circulation system is a question that requires further study, however work at FSEC indicates that diminishing returns are reached very quickly at 1.0 to 1.3 gpm on a 40 square foot solar panel. Preliminary results from actual systems presently under study indicate that flow rates above 1.0 gpm may even be detrimental to overall system performance (delivery water heat content) because of the induced mixing and destruction of stratification within the storage tank. For this study with a 40 square foot thermal panel, we utilized a pump requirement of .8 to 1.0 gpm at .6 to .8 feet of dynamic head under full sun.

Four pumps and motors were tested at FSEC for their I-V load lines (Hartell 24V, Micropump 24V, March 12V, Micropump 12V). These results are provided as Figure 2. The load lines were developed by running the pumps through a mock-up solar system while powered by a Lambda LK-2095 variable regulated power supply. Current measurements were made by a HP 3465A digital multimeter and voltage measurements by a HP3438A digital multimeter. Flow measurements were taken with a Flow Technology BM10 turbine flow meter and flow output was read on a Potentiometer 5811A frequency converter. Tests were also run on the Hartell pump with two types of PV modules to assure the voltage regulation of the power supply did not affect the current drawn by the pump and motor. The load lines determined with the power supply for the pump motor combinations identically matched those determined with the PV panels.

The stars on Figure 2 show the locations on each pump motor load line where flow rates of .8 gpm were obtained (the system produced approximately .8 foot head at this rate). Notice that V x I at this circulation rate for pumps 1 through 4 are 2.8 watts, 3.0 watts, 2.4 watts and 3.0 watts respectively. It is not necessary, therefore, to use a 20 watt rated panel to do a 5 watt job.

FIGURE 2 I-V LOAD LINES

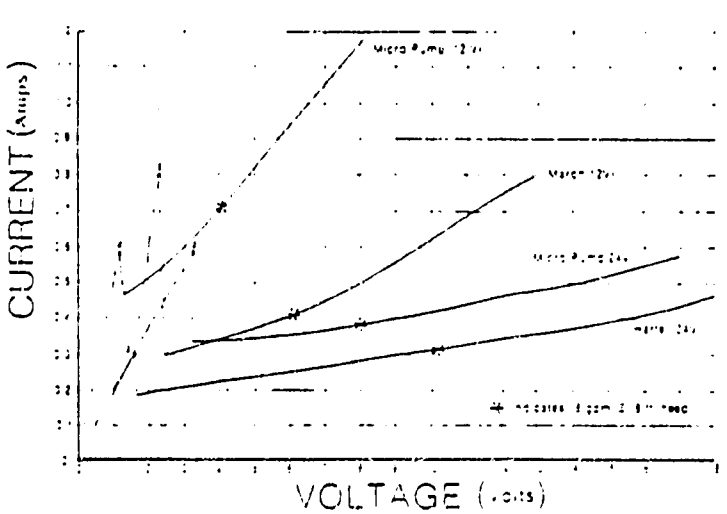

Pump Starting:

All motors tested show that a high current peak was required to the start the motors. This peak for each motor is shown as point a on Figure 2. This starting peak is not furnished in the manufacturer's data and must be experimentally determined. Harmon and Yumma [4] also experienced this high amp starting requirement on a 12-volt March pump they tested. Before the motor begins to turn, the windings provide a low ohm resistance which keeps the voltage output of the PV panel low. Once the pump starts, the induced negative emf of rotation is seen by the PV panel as increased winding resistance and this drives up the PV output voltage.

The experimentally determined IV curves of two commercially available PV panels are shown as Figure 3 and Figure 4. The IV curves were determined using an Eppley PSP pyranometer, the two HP digital multimeters mentioned earlier, and a variable resistance load box built at FSEC for this purpose. Overlayed on these IV curves are the pump load lines for the March and Hartell pumps. Such an overlay is the key tool in properly matching pump and PV power. The pump starting difficulty is clear from the overlay. The smaller 4W panel (published rating of 7 watts) will not start the March pump at full sun. The Hartell pump requires slightly better than .5 sun to start. Since heat gain is available from the thermal panel around .2 to .3 suns, it appears the larger PV panel is needed to extract the maximum heat available. However, once started, the smaller PV panel would provide the power needed for adequate circulation pumping. It should be noted that the Hartell pump rated at 24 volts matches the smaller 12-volt rated panel better than the 12-volt rated March pump. The nominal ratings of pump and panel are of little value in finding the best panel and pump match.

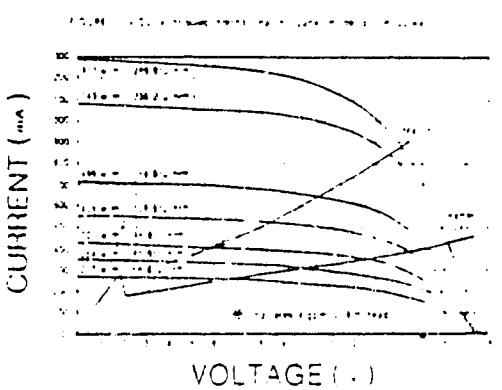

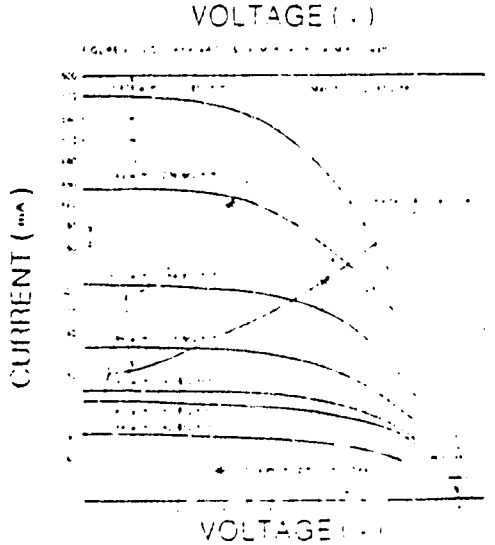

Figures 5 and 6 provide circuits for simple pump starters. A starter of Figure 5 design was tested at FSEC and found to overcome the high current starting difficulty. Capacitor C1 charges until the closing voltage of the relay is reached. When the relay closes, a pulse of sufficient current is delivered to the pump to cause it to rotate. The relay in use closes at approximately 5 volts, yet the relay stays closed until the voltage available from the PV panel drops to about 2 volts. The overlay predicts that the use of such a starter, which can be constructed for less than $20, would allow the smaller PV panel to be utilized in the system, saving approximately $200 in system cost. Using a pump starter eliminates the high initial starting current peak. When the PV output is below point b (2V) shown on Figure 4, the motor should pulse, but not run continuously. At about point b, the relay should stay closed and the motor rotate slowly but continuously. With the starter, one would also expect the pump motor starting and stopping characteristics to show similar behavior.

FIGURE 5 Circuit design of PV pump starter

FIGURE 6 Alternative PV pump starter

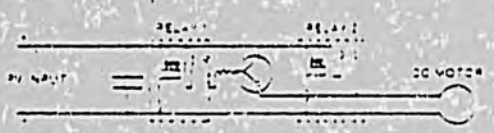

RELAY 1 - Pulses motor through transistor at low outputs
RELAY 2 - Latches for continuous operation

The operating characteristics of the starter/pump-motor/PV panel as predicted by the pump-motor IV load line and PV panel IV curves were tested at the FSEC system laboratory. Typical results of insolation, flow rate through the system, and temperature differences between tank inlet and outlet are shown in Figure 7. Temperature differences were measured via copper-constantan thermocouples. All measurements were taken on a L & N Speedomax W three-channel recorder.

Motor start and stop characteristics matched the predicted insolation rates exactly. However, flows flows did not begin until approximately .40 suns. This is because the centrifugal volute does not begin pumping until a minimum rpm is reached. Also, maximum flow rates of only .85 gpm were obtained at full sun. This is considered acceptable because temperature differences measured across inlet and outlet of the tank did not exceed 10 degrees C.

It is interesting to note that the hysterisis effect of the relay is needed for the pulsing operation of the pump starter. A solid-state switcher using a zenier diode and field effect transistor to provide the switching voltage buildup of the capacitor was also built and tested (schematic not included). Switching was so rapid with the same 4 volt swing that the output simply caused the motor to buzz -- not rotate. It appears that the time delay between pulses that is naturally caused by the motion of the relay arm is also important to the starter's operation. Such a delay (allowing the capacitor to release a larger jolt) could be constructed electronically with a 555 or similar chip, however, simplicity would be sacrificed.

Pump Volute:

Earlier work on PV pumps [5] has recommended centrifugal volutes for the best performance. The ease in getting the impeller rotating (the starting problem) and the more vertical power load line (a better match to the maximum power output of the PV panel) are cited as the rational. However, with the use of a pump starter, the circulation of direct domestic hot water systems seems to have different operational requirements than pumping water where high volume or high heads are important.

Since the pump starter begins to jolt the pump into pulsed rotation at about .15 suns, it would appear that the better pump volute may be one of positive displacement -- each jolt would move a small pulse of water through the system. Such flow would truly match the insolation rates at the low ends as well as at higher rates.

To test this approach, a positive displacement gear type volute (Micropump #042) was attached to the Hertel motor. The results are provided in Figure 8. The gear volute began actual pumping at lower insolation rates

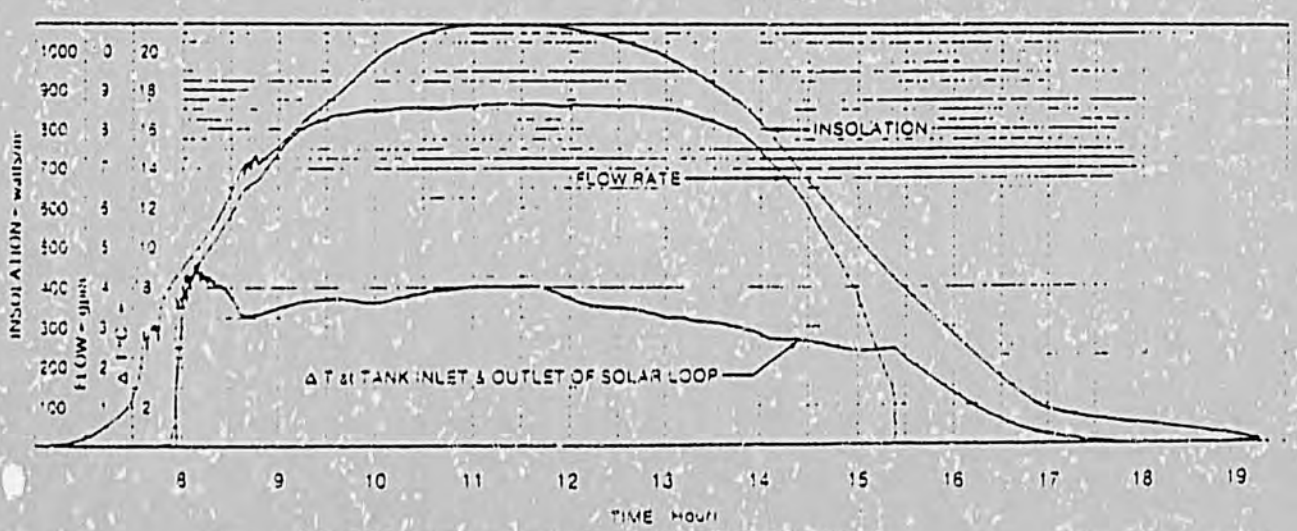

FIGURE 7 Pumping Characteristics With Centrifugal Volute

164

as anticipated, however, the maximum flow obtained of .2 gpm is too low. The micropump volute tested has a very small displacement with each revolution. A larger displacement gear pump has not been tested, however, the results indicate that a good match between displacement and motor RPM at full sun when 1.0 gpm is obtained from the gear volute would provide a better performing volute than the centrifugal type in this low head low volume application.

Tilting the PV Panel:

A problem encountered with larger PV panels (20 watts or more) is that the pump will continue to run in the afternoon beyond the point at which heat is available from the thermal panel. This is easily remedied by tilting the PV panel 5 to 10 degrees to the east which also improves the starting problem. Such tilting is not found to be necessary when the smaller PV module and pump starter is used. On our test units, the lower flow rates at lower insolation rates always provided an increase in return water temperature so tilting the PV panel was not necessary.

Conclusions:

(1) The use of a pump starter is an economical means by which the PV panel size needed for direct domestic hot water circulation can be reduced. Such a system should be competitive with AC differentially controlled systems. The question of operational life of a relay type starter still needs to be answered, as does the question of potential reduction in brush life due to the high current capacitance jolting of the motor.

(2) The operational IV load curves of pumps and motors can be determined experimentally with a variable voltage power supply. Typical flow rates of these pumps and motors for direct systems (40 square feet collector) can be estimated by utilizing a .8- to 1.0-foot head while IV load lines are developed.

(3) The minimum sized PV panel (minimum system cost) that will provide the minimum flow requirement (.8 gpm for 40 square foot panel) at .75 to 1.0 sun can be determined by comparing the pump motor IV load curves to the PV panel IV output curves. Nominal pump and panel voltage ratings are not very useful in this matching process.

(4) It appears that constant volume volutes may provide fluid movement more closely matched to the heat available in the thermal panel than do centrifugal volutes, especially during early morning and late afternoon. If necessary flow is obtained during full sun, this type volute is probably the better choice.

References

[1] Parker, G. J. "A Forced Circulation System for Solar Water Heating" Solar Energy, Volume 18, pp 475-479. Pergamon Press 1976.

[2] Litka, A. H. and Chandra, S. Photovoltaic Powered Solar Domestic Hot Water Heater, Florida Solar Energy Center, 300 State Road 401, Cape Canaveral, Florida, FSEC publication #P-126, August 1979.

[3] Roger, J. A. "Theory of Direct Coupling Between D.C. Motors and Photovoltaic Solar Arrays", Solar Energy. Volume 23 pp 193-198. Pergamon Press 1977.

[4] Hammond, B. and Mumma, S. "A Photovoltaic Powered Circulator Pump". Proceedings of the Annual Conference of the International Solar Energy Society, Philadelphia, PA, May 1981. Volume 4.1, pp 691-695.

[5] Roger, J. A., et al "Calculations and In Situ Experimental Data on a Water Pumping System Directly Connected to a 1/2 KW Photovoltaic Converter Array." 1977 Photovoltaic Solar Energy Conference. Luxembourg (September 1977).

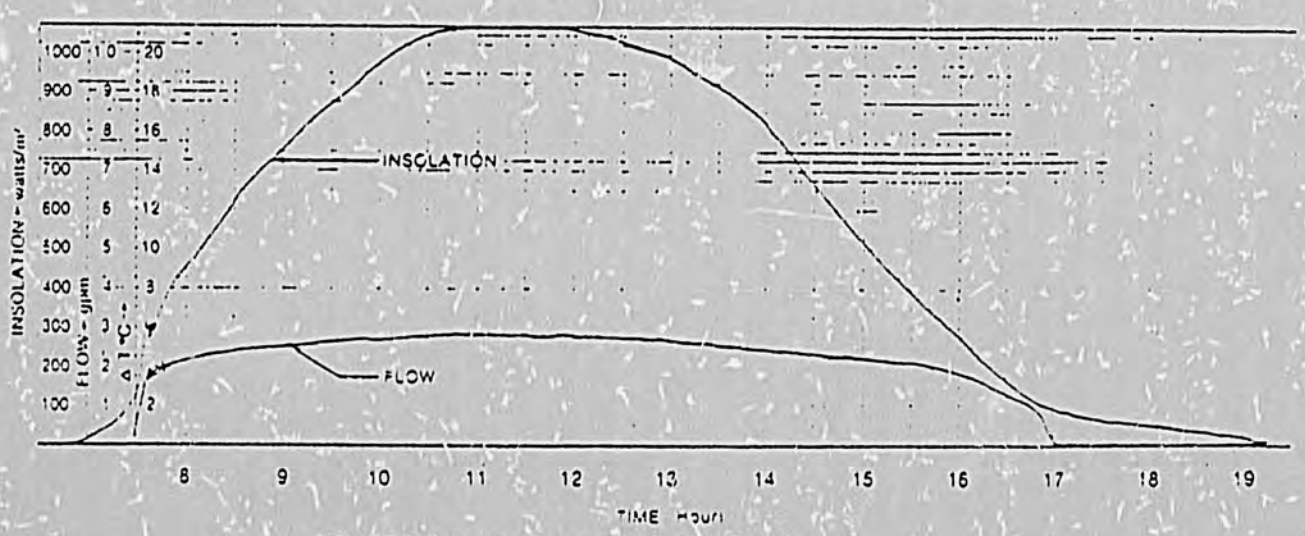

FIGURE 8 Pumping Characteristics With Gear Pump

FIGURE 3 I-V Curve for Solec International Inc. panel, model S3136 (20 watt)

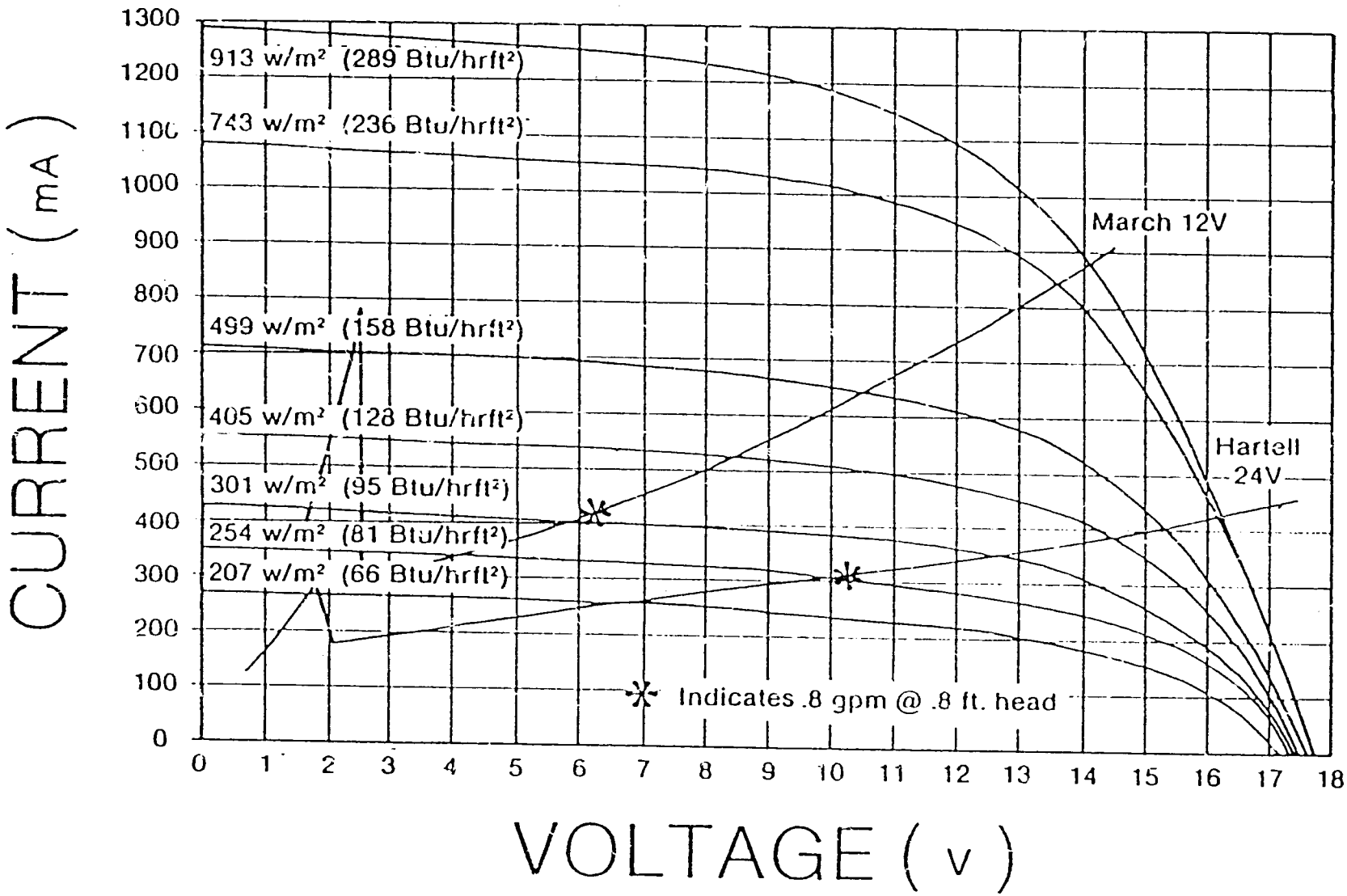

FIGURE 4 I-V Curve for ARCO Solar Module, model M 81 (7watt)

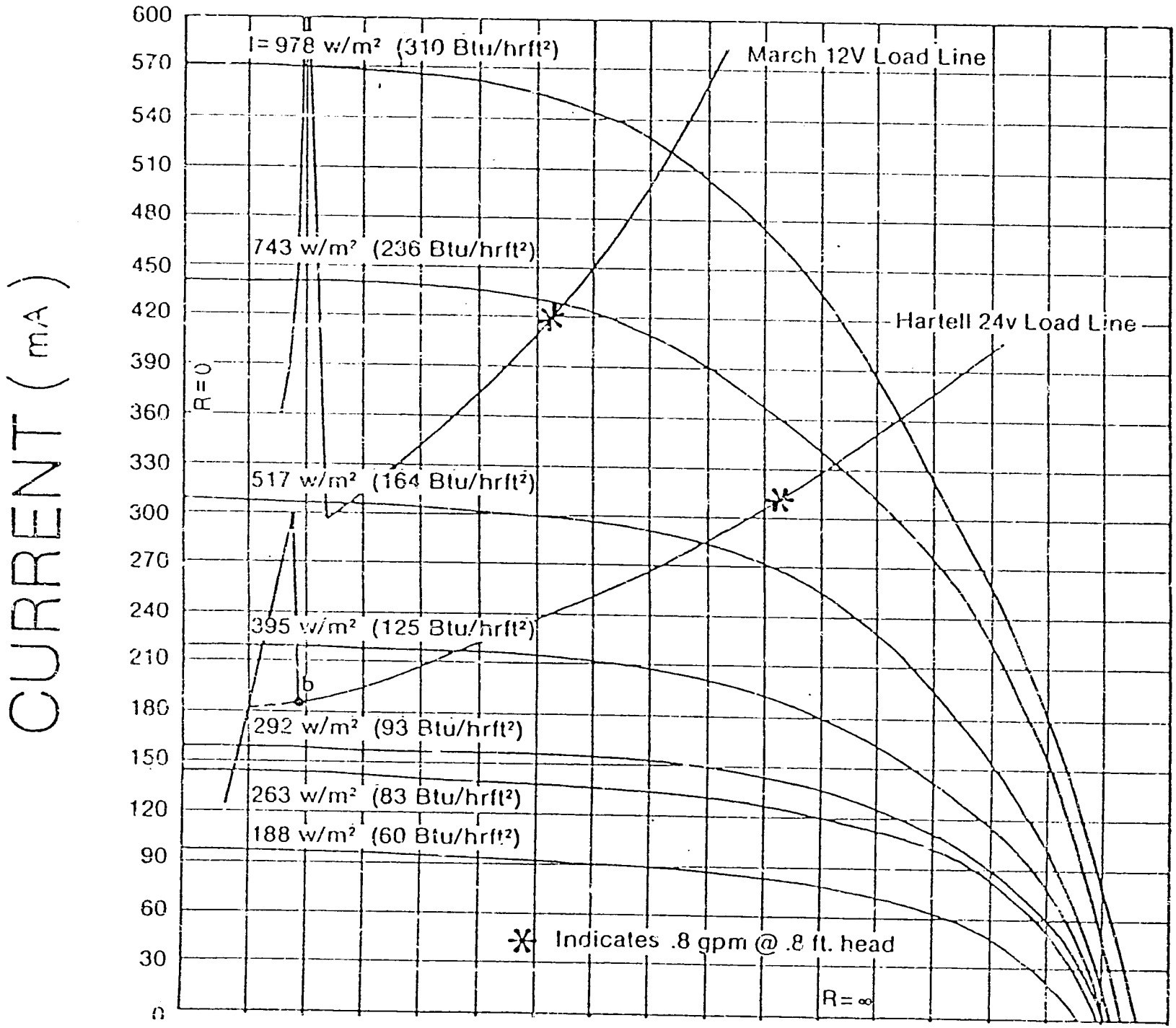

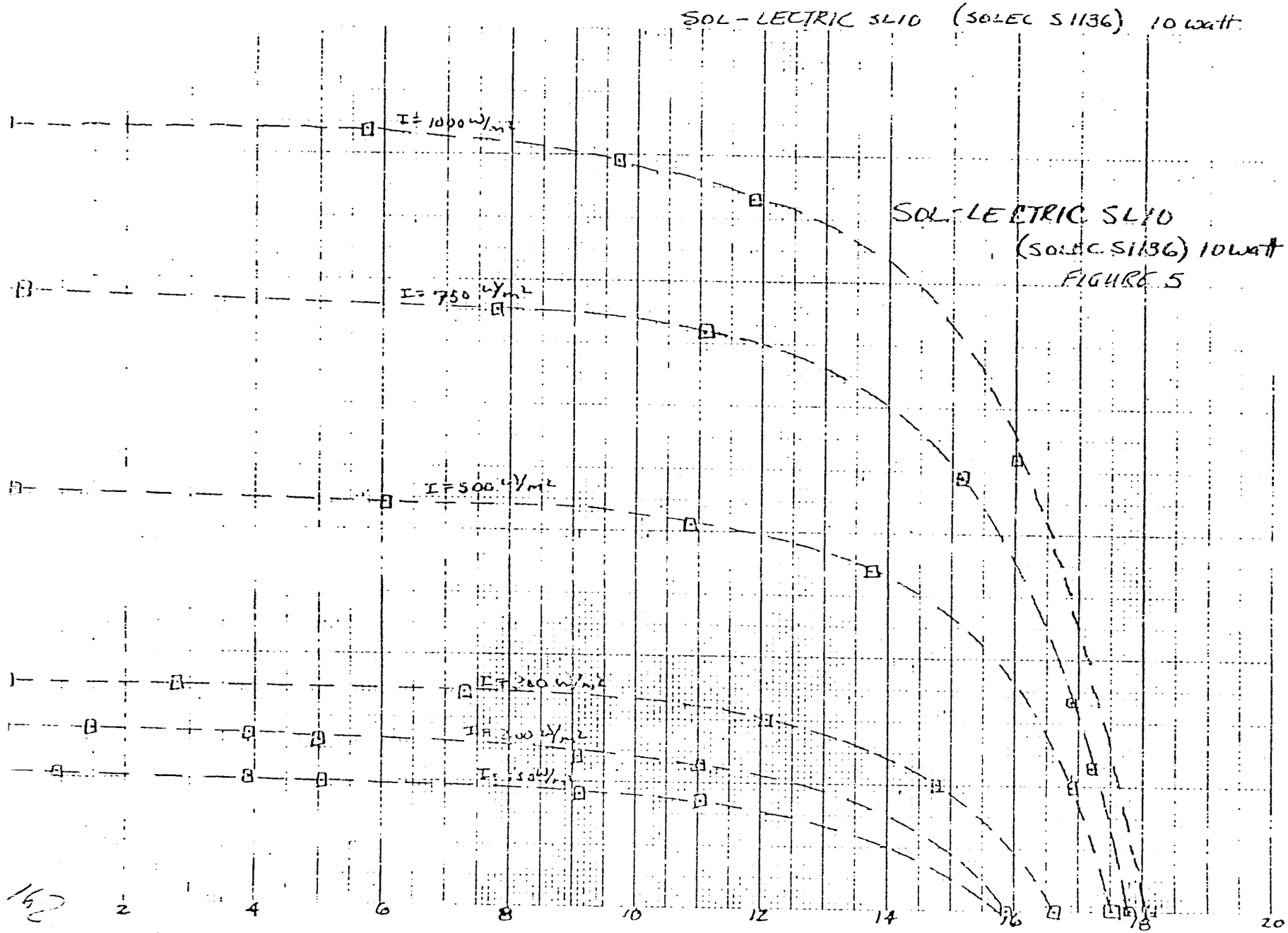

SOL-LECTRIC SL10
(SOLEC S1136) 10 watt
FIGURE 5

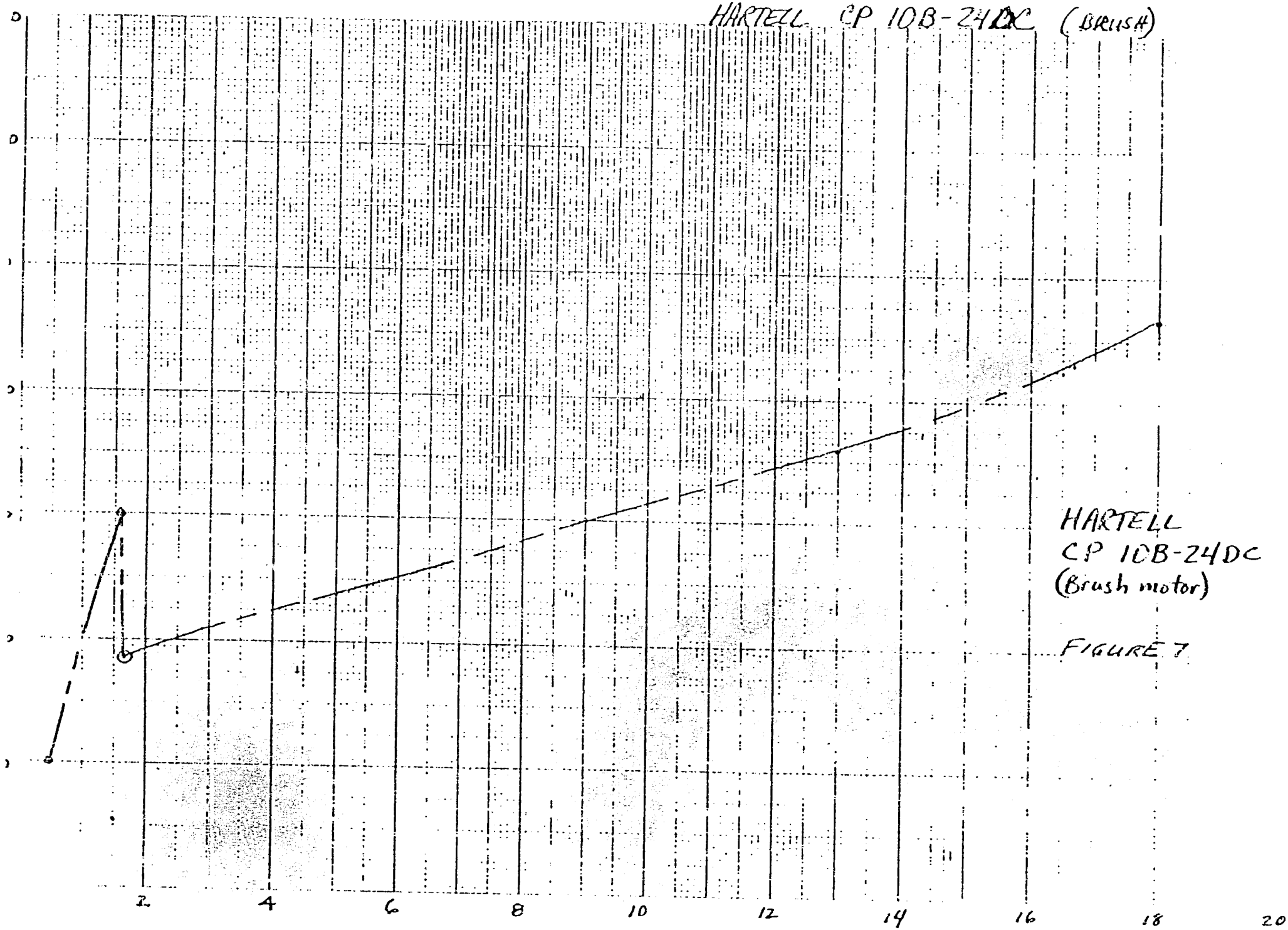

HARTELL
CP 10B-24DC
(Brush motor)

FIGURE 7

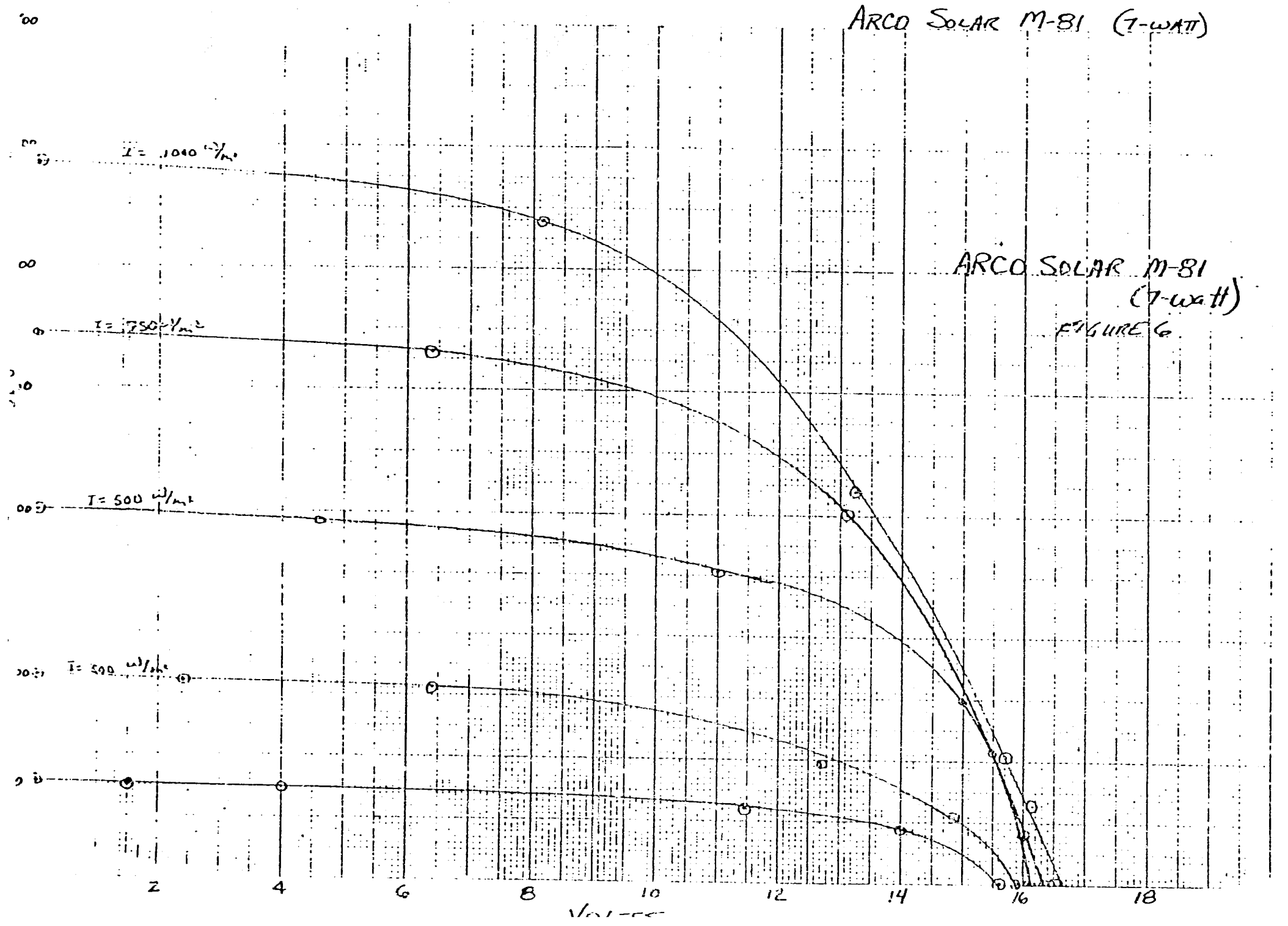

ARCO SOLAR M-81
(7-watt)
FIGURE 6

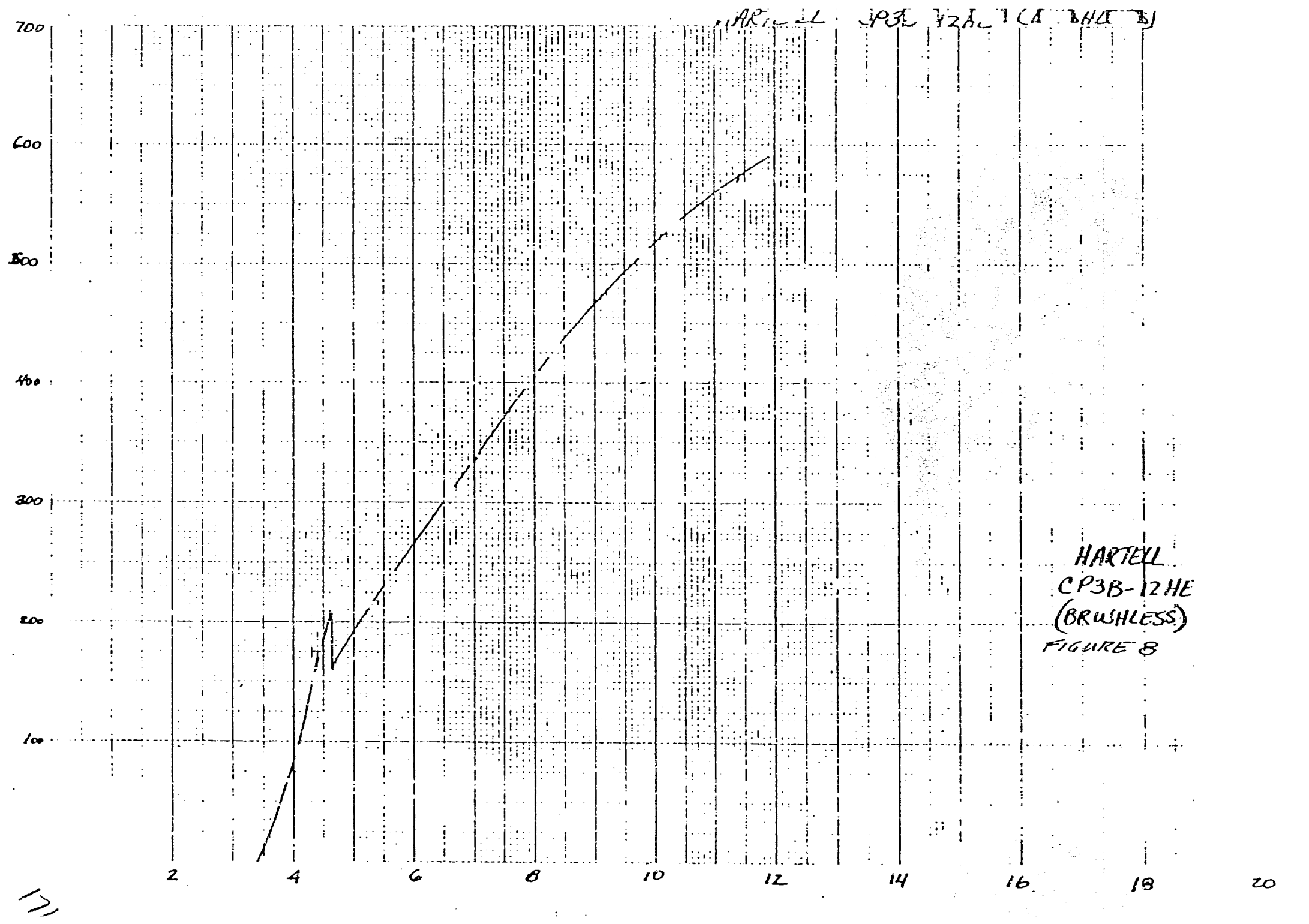
700
600
500
400
300
200
100
2
4
6
8
10
12
14
16
18
20
HARTELL
CP3B-12HE
(BRUSHLESS)
FIGURE 8

ENGINEERING RELEASE

BRUSHLESS DC CIRCULATOR PUMP

THE HARTELL MAGNETIC DRIVE CIRCULATOR PUMP SERIES NOW INCLUDES ELECTRONICALLY COMMUTATED, ULTRA HIGH EFFICIENCY, DC MOTORS, ENGINEERED TO OPERATE FROM LOW WATTAGE PHOTOVOLTAIC PANELS

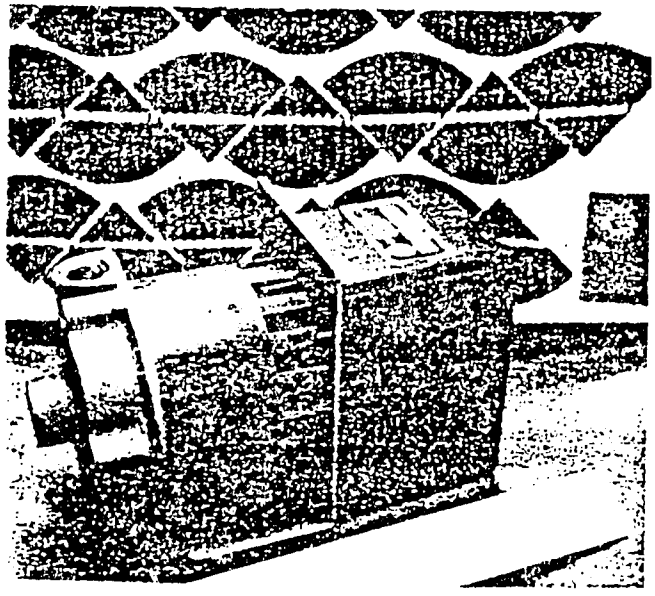

- Brushless DC Motor: Rotor Position Feedback; Electronically Commutated for High Efficiency, Dual Ball Bearing.
- Low Power Start Up.
- Over Voltage Regulator Protected.
- Leak Proof Magnetic Drive Pump with Low Friction Carbon Graphite Pump Bearings
- 30,000 Hours Life Expectancy.
- Engineered for 200°F Fluid and 150 PSI System Pressures.
- Pump Models Available
  - CP-38-12HE 1.2 x 1.2 MPT Inline Pump Hd.
  - CP-48-12HE 3.8 x 3.8 FPT Suction Pump Hd.
- Pump Systems Available

This brushless DC circulator pump has been engineered for photovoltaic powered applications; and is suitable for open or closed loop, water or freeze protected fluid systems.

The ultra high efficiency motor is an electronically commutated design and is truly "brushless". The rotor position sensing feedback electronic field switching is entirely solid state and over voltage protected.

The dual ball bearing motor and graphite bearing impeller design ensures optimum reliability, efficiency, and long life.

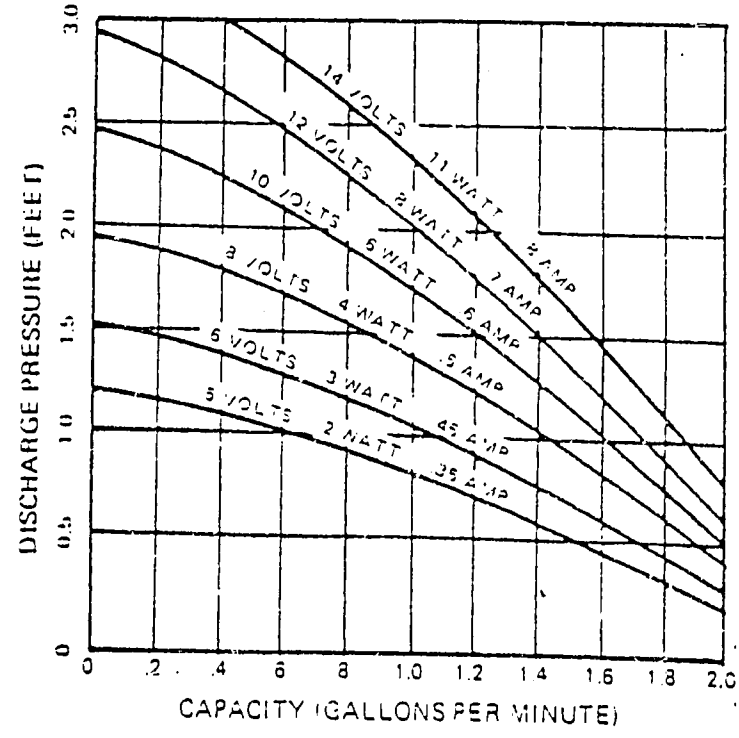

HARTELL DIVISION MILTON ROY COMPANY
70 INDUSTRIAL DRIVE, IVYLAND, PA. 18974
215-322-0730

CP SERIES - BRUSHLESS DC CIRCULATOR PUMP

INSTRUCTIONS

IMPORTANT ! This pump incorporates an electronically commutated motor. The electronic components are susceptable to damage as a result of overvoltage and/or reverse polarity.

Voltage supplied to the pump must be regulated to a maximum of 15 volts or used with Photovoltaic Modules of 7 to 40 watts (maximum) with open circuit voltages not in excess of 22 volts.

Never connect the pump to solar modules that are already in direct sunlight. (Cover the modules while connecting the pump.)

INSTALLATION INSTRUCTIONS FOR PHOTOVOLTAIC MODULE SYSTEMS

1. Mount photovoltaic module and cover against sunlight.
2. Connect Redwire of pump to positive red terminal on module.
3. Connect black wire of pump to negative black terminal on module.
4. Remove cover from photovoltaic module.

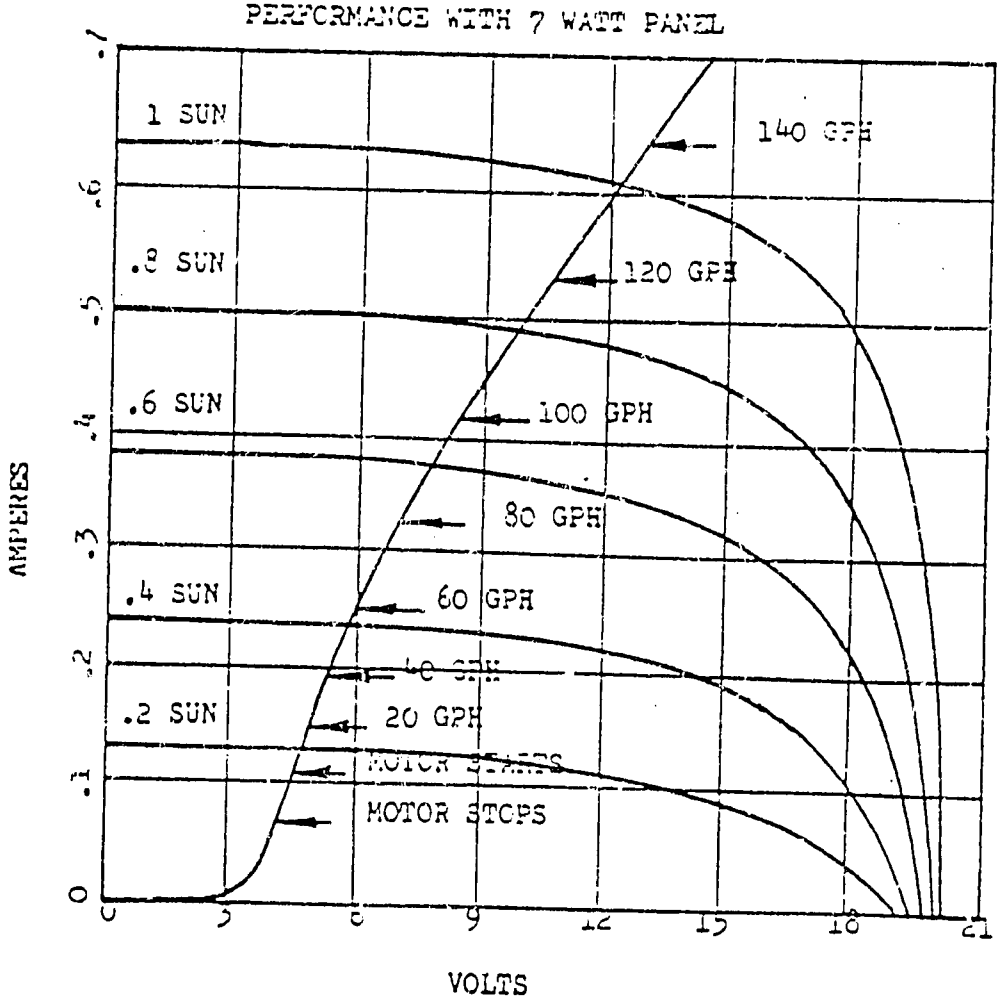

HARTELL DIVISION, MILTON ROY COMPANY
70 INDUSTRIAL DRIVE, IVYLAND, PA. 18974
215-322-0730

8-20

173

CP SERIES DIRECT CURRENT

ENGINEERING RELEASE

THE HARTELL MAGNETIC DRIVE CIRCULATOR PUMP SERIES NOW INCLUDES D.C. MOTORS ENGINEERED TO OPERATE ON PHOTOVOLTAIC POWER IN SOLAR WATER HEATING SYSTEMS.

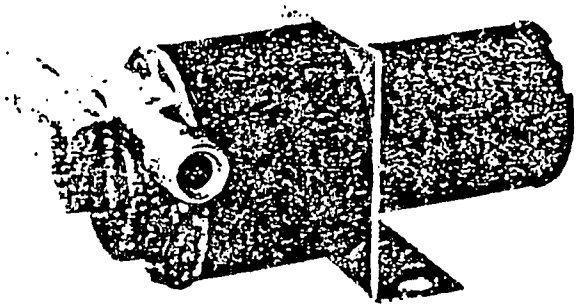

MODEL CP–10 B–12 DC

DESIGN FEATURES

Leak-Proof Magnetic Drive – No Mechanical Seals To Wear and/or Leak.

High Efficiency, Permanent Magnet D.C. Motor–Cool Running Die Cast Bearings–Extremely Low Power Start.

Low Friction, Maintenance Free Carbon Graphite Pump Bearing Ensures Long Trouble Free Life.

Wide Variety of Standard Pump Heads. Special Pump Heads Can Be Provided For Original Equipment Manufacturers.

Designed for Easy Service–Two Screws Remove Motor from Pump Assembly. (No Need To Disturb Fluid System)

Engineered for 200°F Fluid and 150 psi System Pressures.

MAGNETIC DRIVE

HARTELL

70 INDUSTRIAL DRIVE. IVYLAND. PA 18974 PHONE 215-322-073.

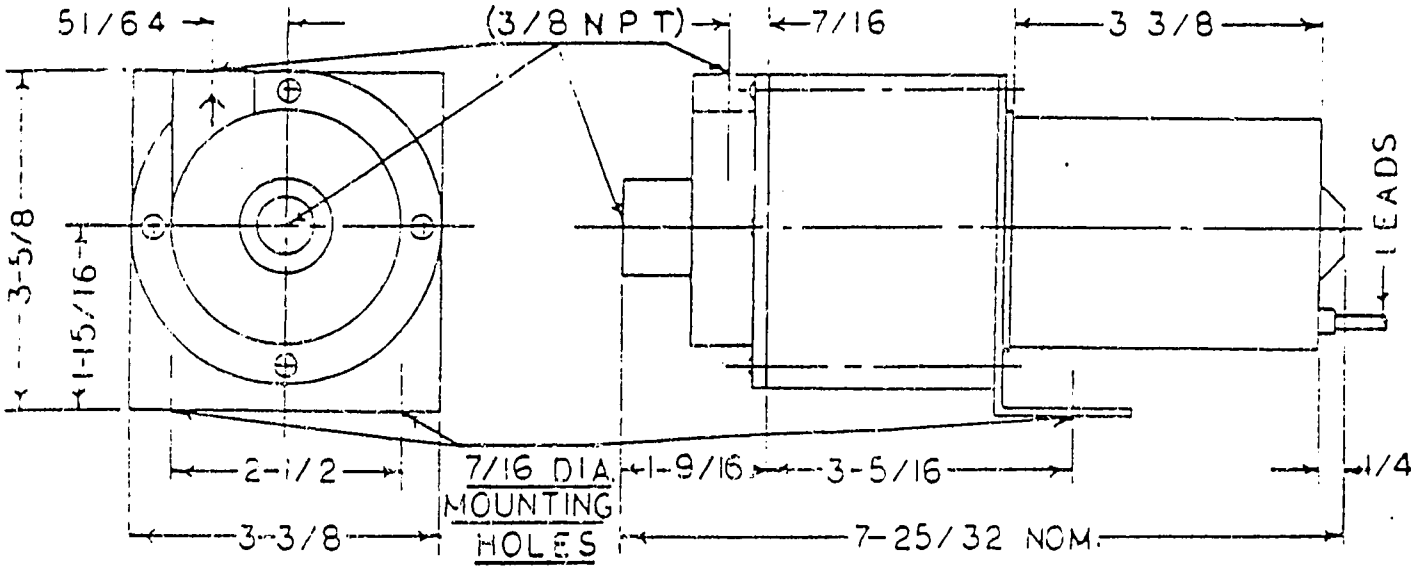

MODELS CP-12B-12DC ; CP-12B-24DC

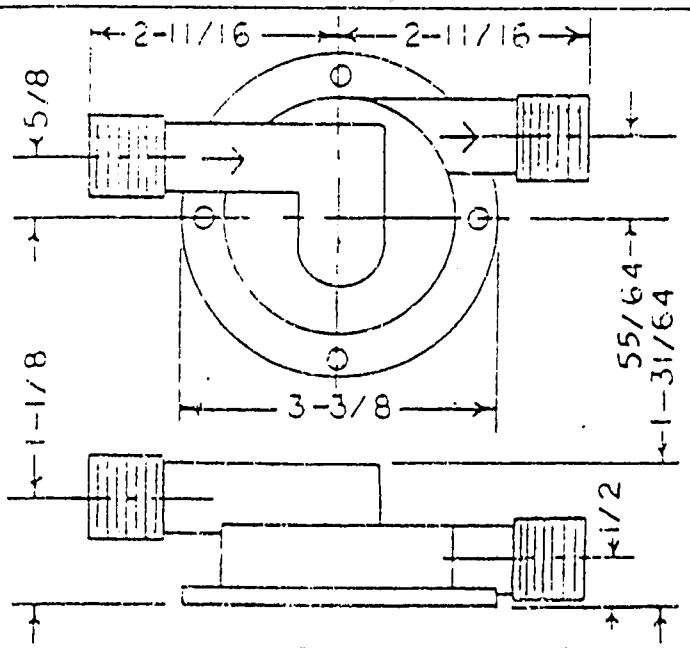

IN-LINE PUMP CASINGS

MODELS AVAILABLE

CP - XX Y - ZZ DC

- DC — DIRECT CURRENT
- ZZ — NOMINAL VOLTAGE
- Y — PUMP CASING MATERIAL
- XX — PUMP CASING STYLE
- CP — MODEL DESIGNATION

XX Y PUMP CASING STYLE-MATERIAL

10 B:	-1/2" M.N.P.T. IN-LINE	BRASS
12 B:	-3/8" F.N.P.T. END SUCTION	BRASS
14 B:	-5/8" FLARE 45° IN-LINE	BRASS
16 N:	-15/16" BALL-COCK IN-LINE	PLASTIC

ZZ NOMINAL VOLTAGE

12:-0 to 14 Volts--:--0 to 36 Watts
24:-0 to 28 Volts--:--0 to 33 Watts

TYPICAL 12-VOLT PUMP CURVE

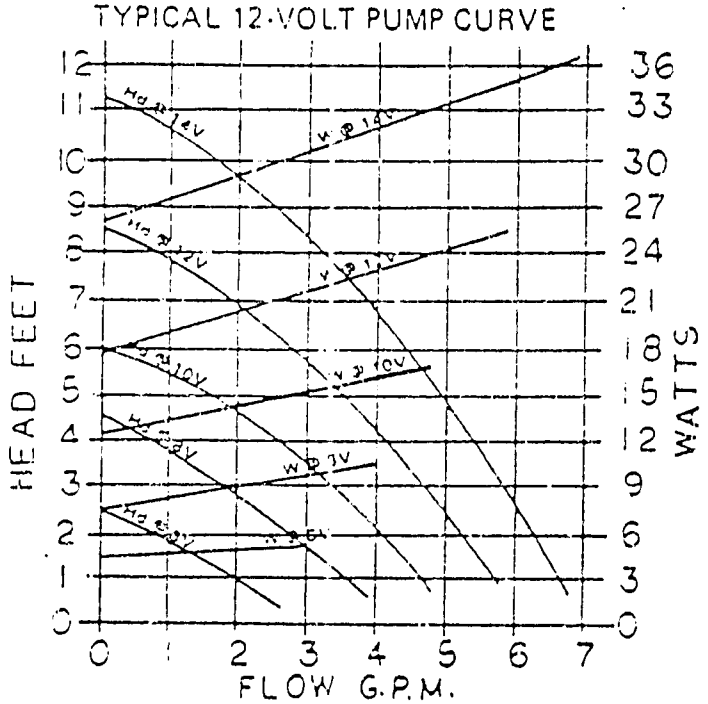

TYPICAL 24-VOLT PUMP CURVE

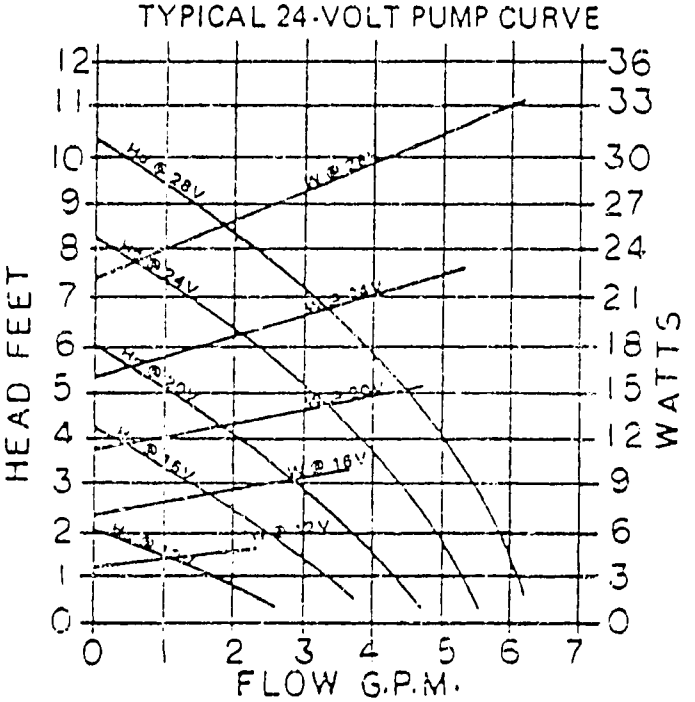

CP SERIES DIRECT CURRENT

CIRCULATOR PUMP

ADDENDUM TO

ENGINEERING RELEASE

24 VOLT UNIT CAN BE USED AS SHOWN BELOW
RANGE:
0 - 14 VOLTS
0 - 7 WATTS

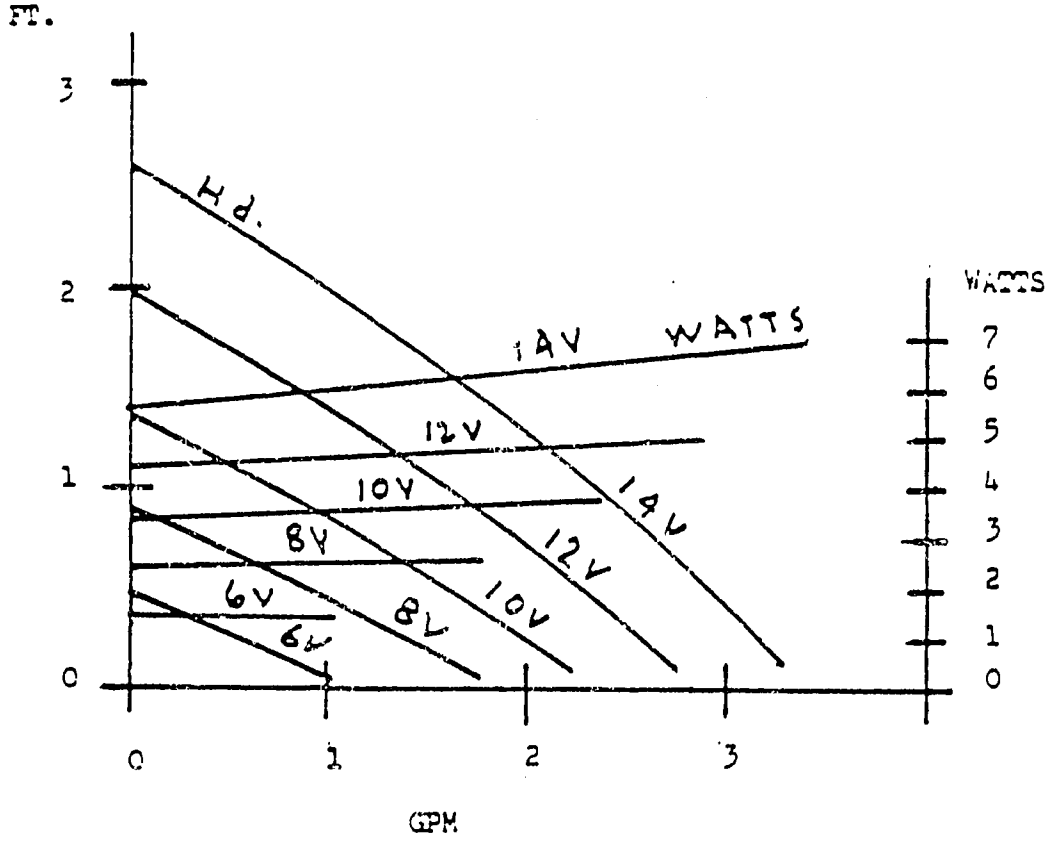

176

MILTON ROY CO. - HARTELL DIV. - 70 INDUSTRIAL DRIVE, IVYLAND, PA. 18974 PHONE: 215-322-0730

Module 9: Plumbing Multiple Collector Arrays

Objective

The objective of this module is for the trainee to obtain a working knowledge of reverse return piping design and of calculating hanger and U bend location.

Module 9: PLUMBING MULTIPLE COLLECTOR ARRAYS

The calculation of pressure drop through a collector array of a particular configuration is covered in Module 10, as is the calculation of pressure drop through the piping.

This module deals with the correct configuration layout of panels in an array and the proper calculation of hanger and U bend location.

Piping Large Collector Arrays. One of the most common errors in installation occurs in the piping of a collector array. If piped incorrectly, some panels will be starved of flow and will not contribute to the energy gain. With their high cost per square foot, all collectors should function at their peak efficiency, and simple piping errors can cripple the performance of a very costly system.

The easiest method of piping to assure proper flow in large arrays uses parallel, reverse return piping (Figure 9-1), which ensures a fairly uniform flow in the array. A parallel connection without reverse return leads to non-uniform flow throughout the collector array and results in reduced heat collection.

Under almost all conditions, reverse return piping is the best choice. It may require additional pipe, but such pipe quickly pays for itself in increased performance.

113

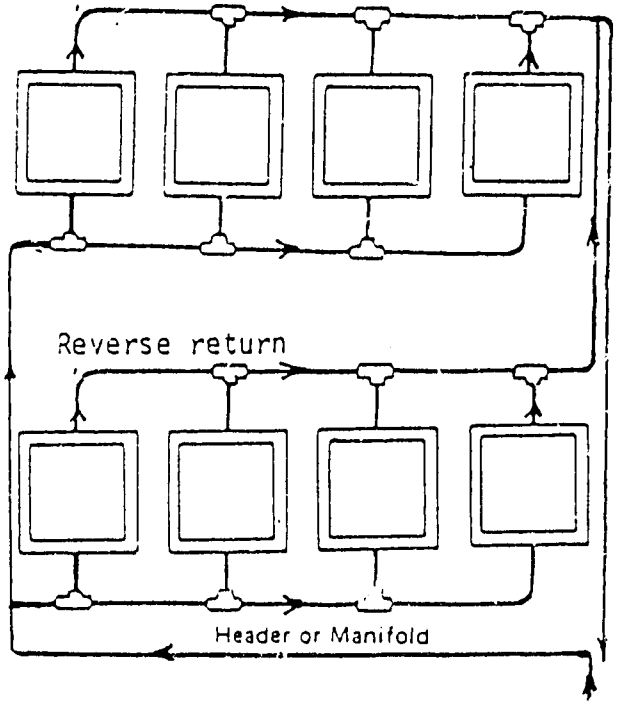

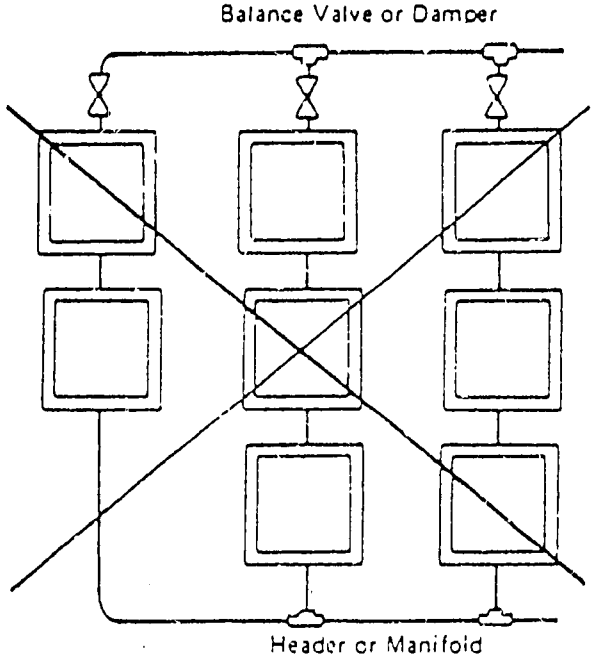

Avoid series connections and balance valves if possible.

Multiple Collector Piping Arrangements
Figure 9-1

If it is not possible to pipe the array in parallel with reverse return, flow-balancing valves should be used. This makes it possible to restrict the flow in channels of highest flow, thereby equalizing the flow rate over the entire array.

A balancing valve is an inexpensive square-head cock. More expensive, calibrated balancing valves are available for use in very large arrays. Simple globe or gate valves have been used but are not recommended, because their sensitivity to changes in adjustment and flow restriction caused by thermal expansion and contraction makes accurate control difficult to attain.

Collectors are usually connected in parallel. Parallel connections are shown in Fig. 9-2a ; series connections in Fig. 9-2b. In the series arrangement, water passes through one collector and then through the next, increasing the pressure required to maintain adequate flow as well as causing some of the collectors to operate at higher, less efficient temperatures. Parallel connections, in which the water is returned directly back to the tank after passing through one collector, are superior because those difficulties are avoided.

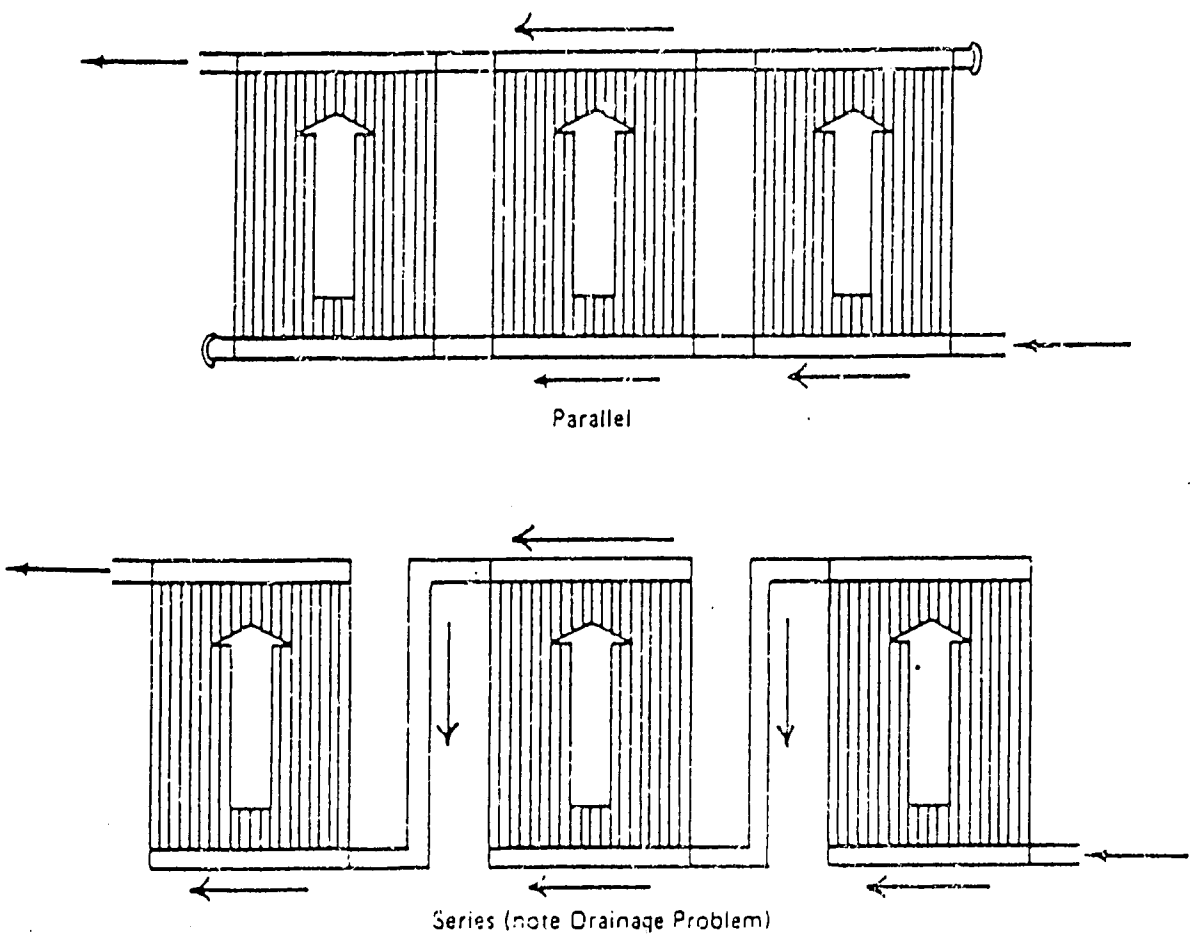

FIGURE 9-2
Collector Connections

The path of fluid flow through any collector should be approximately the same length. Fig. 9-3a illustrates the preferred arrangement, and Fig. 9-3b shows a common, but less efficient, connection where water is short-circuited through the first collector, and those at the end are starved for flow, causing their performance to drop. In Fig. 9-3 a the length of the water path is the same for all collectors, so the flow is evenly distributed. Frequently, plumbing in this fashion will require extra pipe, but improved collector performance compensates for the additional cost.

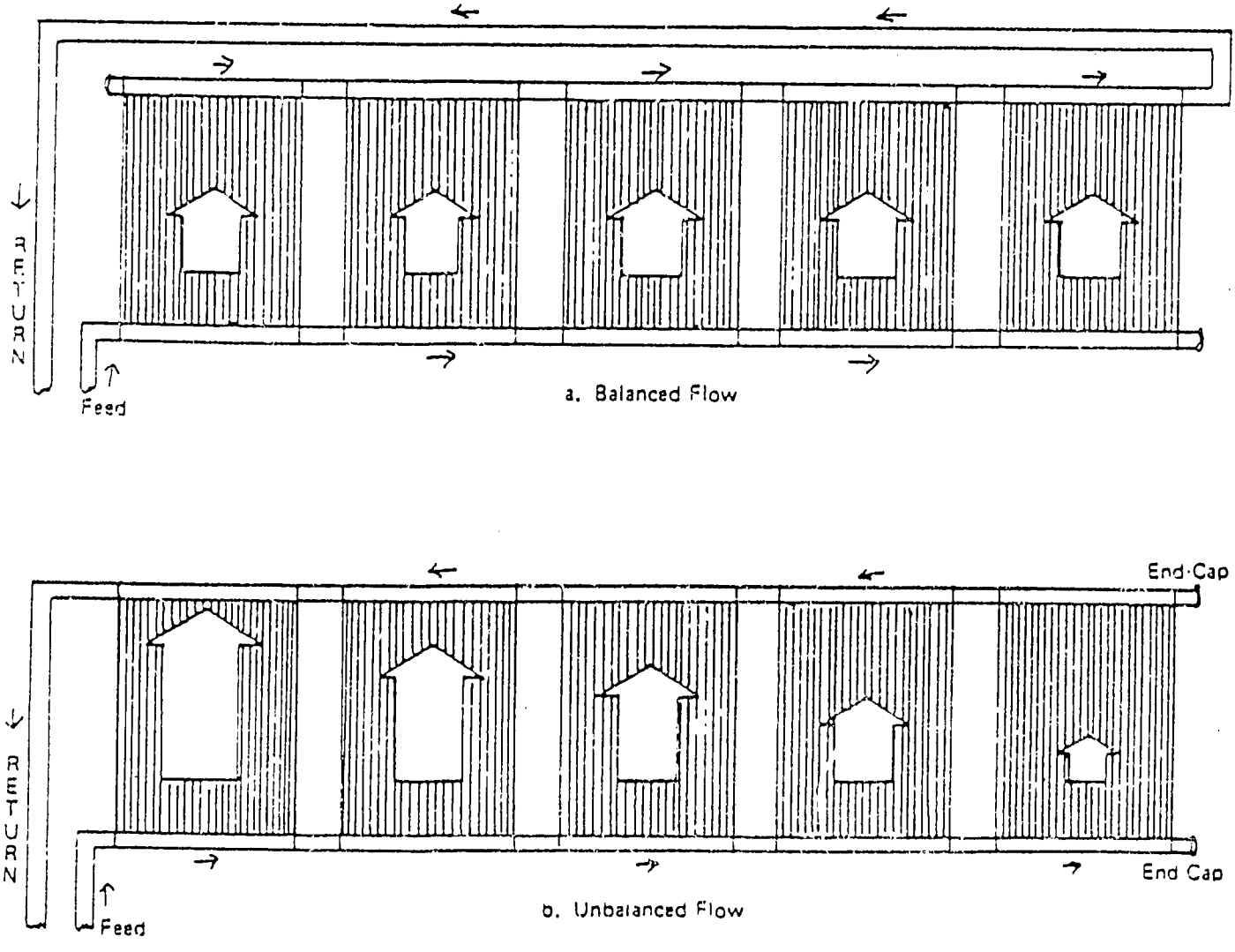

FIGURE 9-3
Flow Balancing in Collector Groups

Groups of collectors at different heights should be plumbed in such a way that they all receive water from the lowest point in the system and return it from the highest point. Fig. 9-4 illustrates a properly plumbed system, and the dashed line indicates a tempting, but unsatisfactory, arrangement. If the return lines do not come from a common height, flow through the panels will be uneven, causing a reduction in performance.

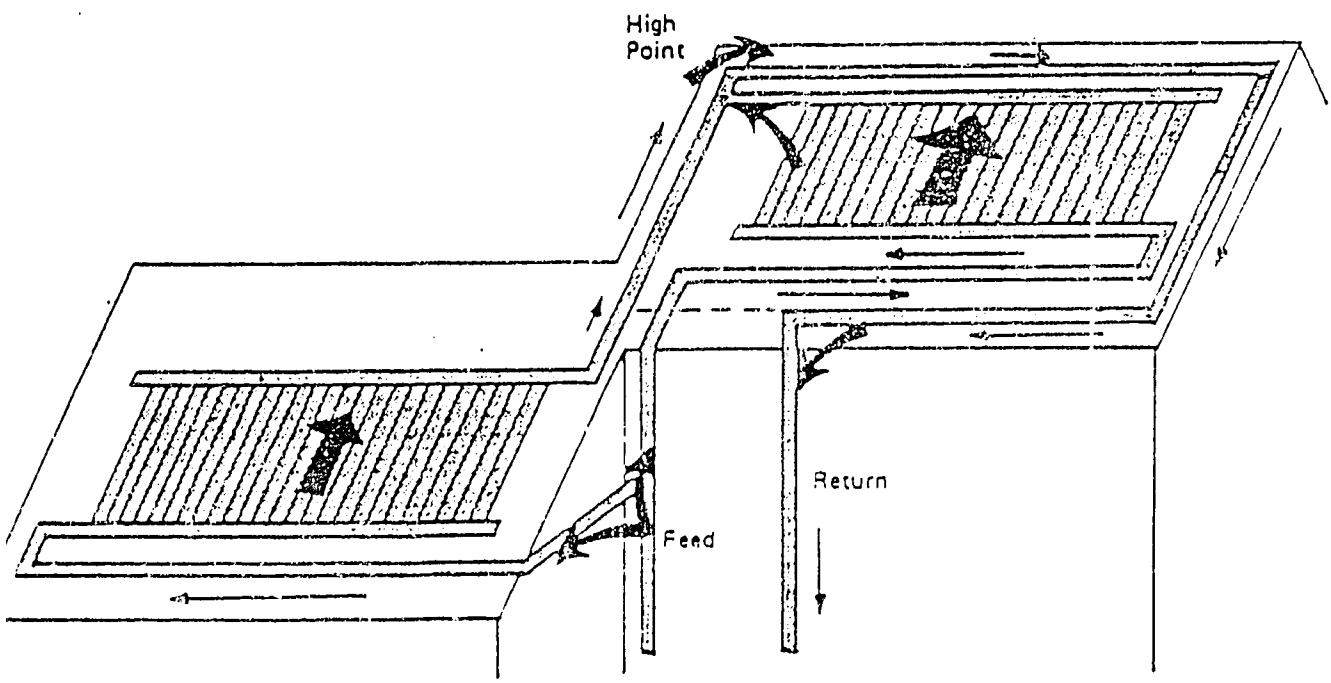

FIGURE 9-4
Plumbing Collectors at Different Heights

Piping Between Collectors. About the same amount of flow should pass through each collector. When it is necessary to divide the solar collecting panels into groups and connect the groups with pipe, care must be taken to ensure that all collectors receive the same flow. Most situations encountered can be satisfied using principles discussed in this section, but for extremely complicated cases it may be desirable to calculate individual flow path pressure drop. (See Module 10).

Flexible connectors from the array header to the individual collectors should be avoided unless the installer has years of satisfactory experience with a particular brand. A U.S. National Bureau of Standards survey of large operational solar systems showed that all those using flexible hoses had experienced system failures because of hose degradation. Flexible hoses are not recommended for systems which are subject to city water pressure.

Collector-To-Storage Runs

Piping from tank to collectors should be as short as possible because it is a major source of heat loss. If the collectors must be mounted relatively far from storage, the installer should consider using larger pipe because of high pressure drops associated with longer runs (see Module 10).

Because pipe expands and contracts considerably as its temperature varies, allowances should be made for change in length. Horizontal "U" bends are typically used to absorb the changes in length produced by long pipe runs. These should be included on the schematic by the design engineer if needed.

Table 9-1 provides typical stress for constrained pipe.

Table 9-1

Thermal Stresses Resulting from Total Constraint

Temperature* Change, F Deg	Thermal Stresses, psi (× 6.89 = kPa)					
	Steel	Wrought Iron	Cast Iron	Brass or Bronze	Copper	Aluminum
20	3900	3800	1428	2760	2980	2700
40	7800	7600	2856	5520	5960	5400
60	11700	11400	4284	8280	8940	8100
80	15600	15200	5712	11040	11920	10800
100	19500	19000	7140	13800	14900	13500

*For temperatures between 32 and 400 F (0 and 204.4°C)

Cast iron, for example, for a temperature change of 100°F (55.6°C), a compressive strength of 7140 psi would be developed. If the pipe were held straight, this stress would be handled easily, if however, the stress were allowed to cause a bending moment, then the pipe might fracture.

The values of stress found in Table 9-1 were found by the equation:

$$F = aEA\,\Delta t$$

where F = force of constraint, lb

a = coefficient of linear expression, in/in

E = modulus of elasticity, psi

A = cross section area of metal in pipe

Δt = temperature change, deg F

Values A and E are given in Table 9-2 for various pipe materials:

Table 9-2

Physical Properties for Determining Thermal Stress*

	Steel	Wrought Iron	Cast Iron	Brass or Bronze	Copper	Aluminum
Coefficient of Linear Expansion, $a \times 10^{-6}$	6.5	6.8	5.95	9.85	9.3	13.5
Modulus of Elasticity, E, psi × 10^6	30	28	12	14	16	10
Product of aE, psi	195	190	71.4	138	149	135

Example: The coefficient of expansion for steel = 0.0000065 in./in. and the modulus of elasticity = 30 000 000 psi. Therefore aE = 195 psi (1344 kPa).

*For temperatures between 32 and 400 F (0 and 204.4°C). Conversion factors: kPa = psi × 6.89; mm = in. × 25.4.

It is interesting to note that length does not enter into the determination of the force of constraint. This is because elasticity forces stress as a unit length function, and so is the expansion; therefore they cancel each other out. The realization that thermal stress is independent of length is important but is often overlooked. This concept explains the feasibility of utilizing the inherent flexibility of pipe to take care of expansion. Regardless of the length of pipe between anchors, it is possible to provide for the expansion by putting the force of expansion into the pipe as internal stress.

Five methods generally used to compansate for pipe expansion are: 1) packless expansion joints (like rubber bellows joints), 2) slip joint with packing, 3) flexible ball joint - this is a special fitting placed at a bending moment location, 4) allowing the flexibility of the pipe to absorb the stress of expansion through a U bend, and 5) allowing the compression strength of the pipe itself to absorb the stress. Option #4 is the preferred choice for solar applications.

The expansion produced by a length of non-restrained pipe is:

$$e = aL\Delta t$$

where: a = coefficient of linear expansion in/in

L = length of pipe run

Δt = temperature change

This is the deformation that must be absorbed by the U bend. The length of the U bend, L, as shown in Figure 9-5 can be calculated by the equation:

$$L = 6.16\sqrt{D_o e}$$

where: L = length of U bend pipe, ft.

D_o = outside diameter of pipe, in

e = deformation to be absorbed, in (Ref. 1)

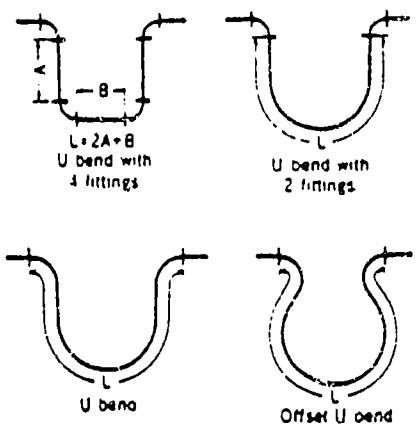

Measurement of L on Various Pipe Bends

Figure 9-5

Hangers and Supports

Typical bending and deflection equations are given in Table 9-3 so that supports can be properly sized, and if necessary, pitched.

Table 9-3

Equations for Bending Stress and Deflection between Supports

Type of Support	Bending Stress, psi (kPa) S	Deflection, in. (mm) Y
Single span (free ends)	$S = \frac{0.75\ WL^2 D_o}{I}$	$Y = \frac{22.5\ WL^4}{EI}$
Continuous line	$S = \frac{0.5\ WL^2 D_o}{I}$	$Y = \frac{4.5\ WL^4}{EI}$

W = total weight (pipe, fluid, and the like) lb/ft (kg/m)
D_o = outside diameter of pipe, in. (mm)
L = length of span, ft (m)
E = modulus of elasticity, psi (kPa)
I = moment of inertia, in.^{4} (mm^4)

$$I = \frac{\pi}{64}\left[(D_o)^4 - (D_i)^4\right]$$

D_i = inside diameter of pipe, in. (mm)

Even with proper support spacing there will be some sagging; this can be determined by deflection, Y, above. In such a case, the supports should be on a gradient to prevent air pockets. This calculation is desirable with pumped systems but is of necessity with thermosiphon systems where a gradient must be maintained throughout the piping and system. Both the recommended maximum spacing of hangers and the minimum diameter of hanger rods are given in Table 9-4.

Table 9-4

Recommended Maximum Spacing of Hangers and Minimum Hanger Rod Size for Steel and Copper Pipe[a]

Nominal Pipe Size, in. (× 25.4 = mm)	Maximum Span, ft (× 0.3048 = m)	Minimum Rod Diameter, in. (× 25.4 = mm)
1	7	3/8
1 1/2	9	3/8
2	10	3/8
3	12	1/2
3 1/2	13	1/2
4	14	5/8
5	16	5/8
6	17	3/4
8	19	7/8
10	22	7/8
12	23	7/8

[a]For 1/2 in. (12.7 mm) copper tube, 5 ft (1.5 m) spacing of hangers is recommended.

There are two types of supports: anchors and hangers. Anchors are used to guide the expansion or fix the pipe. They are needed to take the stress out of the line and translate the stresses to the foundation. In that way, all stress can be taken out of the line before it can be transferred to such equipment as boilers or pumps. By means of solid anchors, the anchors can be used to divide the piping into isolated sections that cannot transmit the stresses to other sections.

Hangers are used to support the piping and take out the bending

181

stresses. They are of the spring, roller, or rod type. Such a support bracket should be constructed so that an expanding pipe will slip in its collar rather than work the support bracket screws loose where they contact the roof or wall's outer surface yet maintain full support. Figure 9-6 shows one such pipe support bracket.

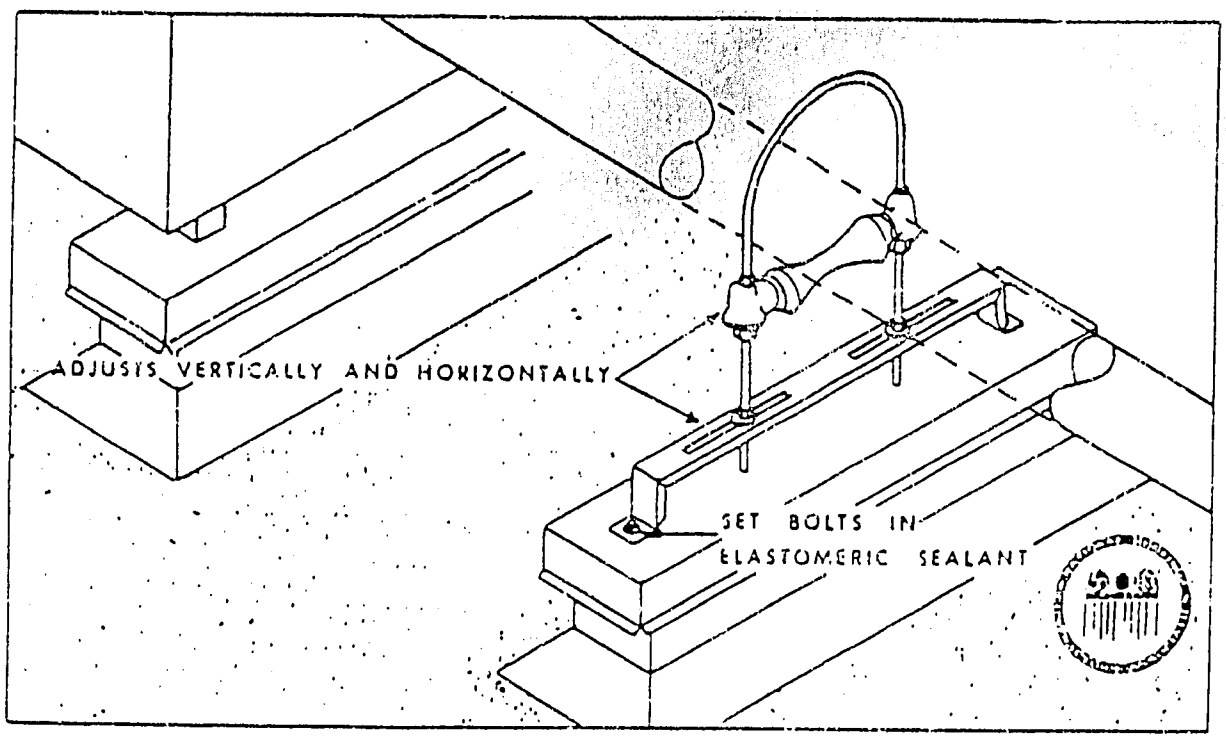

FIGURE 9-6
Pipe Support Bracket

Forces On The Collector Array

A mounted collector is not only exposed to sunlight and the rigors of ultraviolet light but also to wind forces. Possible hurricanes dictate that a collector and its mounting structure must be able to withstand intermittent loads from winds up to 130 miles per hour,which corresponds to a pressure of about 75 lbs. per square foot on a typical collector mounted with a standoff (see Figure 9-6). Such winds may also cause vibrational fatique in mounting brackets and bolts as well as lead to lower panel thermal performance.

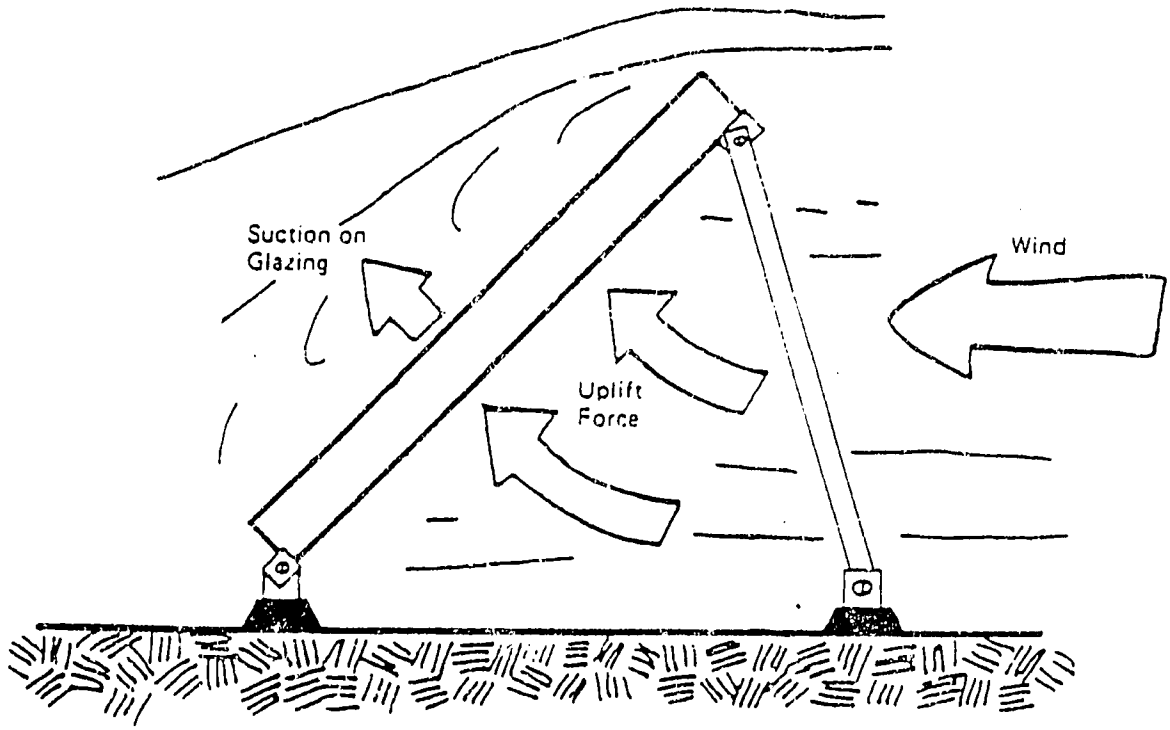

FIGURE 9-6
Conceptual Drawing of Wind Loading

Standard engineering load calculations can be used to calculate the bracket sizes and bolts necessary for a particular array design. The fluid filled load on structures needs to be calculated as well as the distributed lifting load of 75 lbs/ft^2 from wind forces. Typical stand-off detail is shown in Figure 9-7.

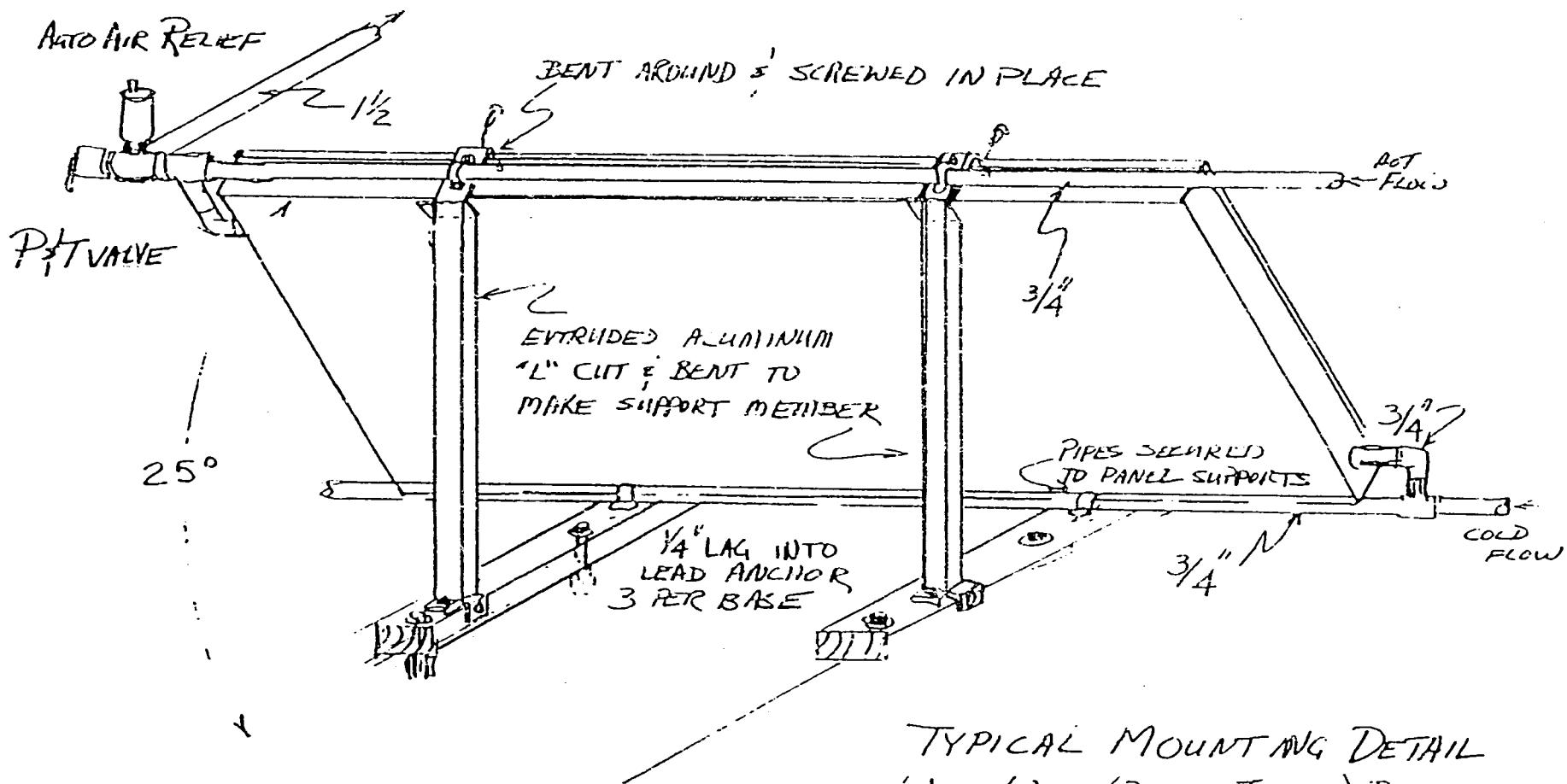

TYPICAL MOUNTING DETAIL
WITH WOOD (PRESSURE TREATED) BASE
AND ALUMINUM STANDOFFS

FIGURE 9-7

Special Array Considerations for Thermosiphon Systems

Thermosiphon systems must be installed such that all piping provides a continuous slope from the collectors to the tank. The collectors used in the array should be ground mounted where possible and mounted flush to the sloping ground level (i.e., within for or five inches from the ground).

Mounting a collector array using the natural slope of a hill is an excellent way to reduce wind effects and loads, provide collector tilt and provide for the sloped piping needed in thermosiphon systems. Figure 9-8 shows a mounting detail when the ground is sloped.

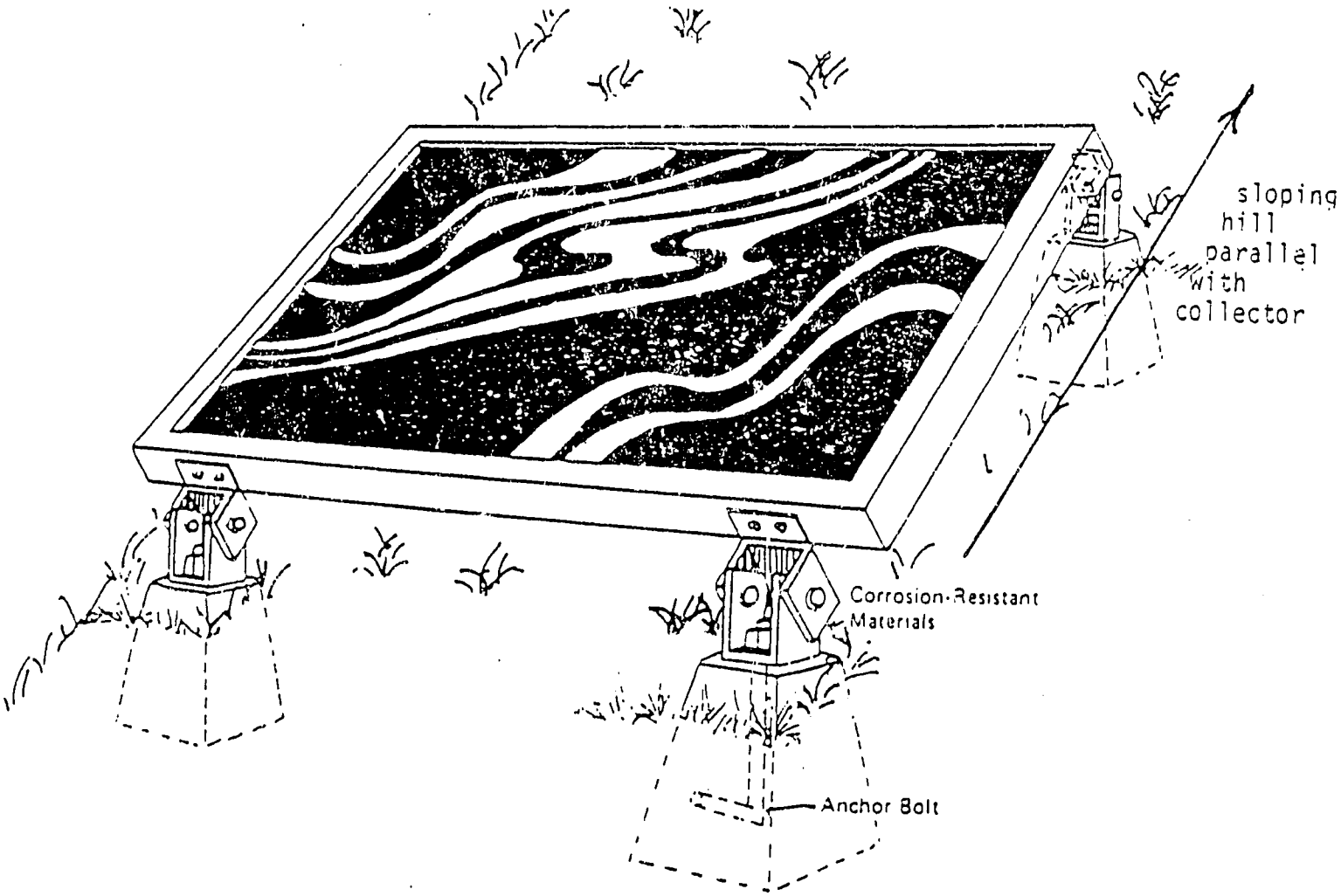

FIGURE 9-8

Conceptual Drawing of a Ground-Mounted Collector On Sloping Hill

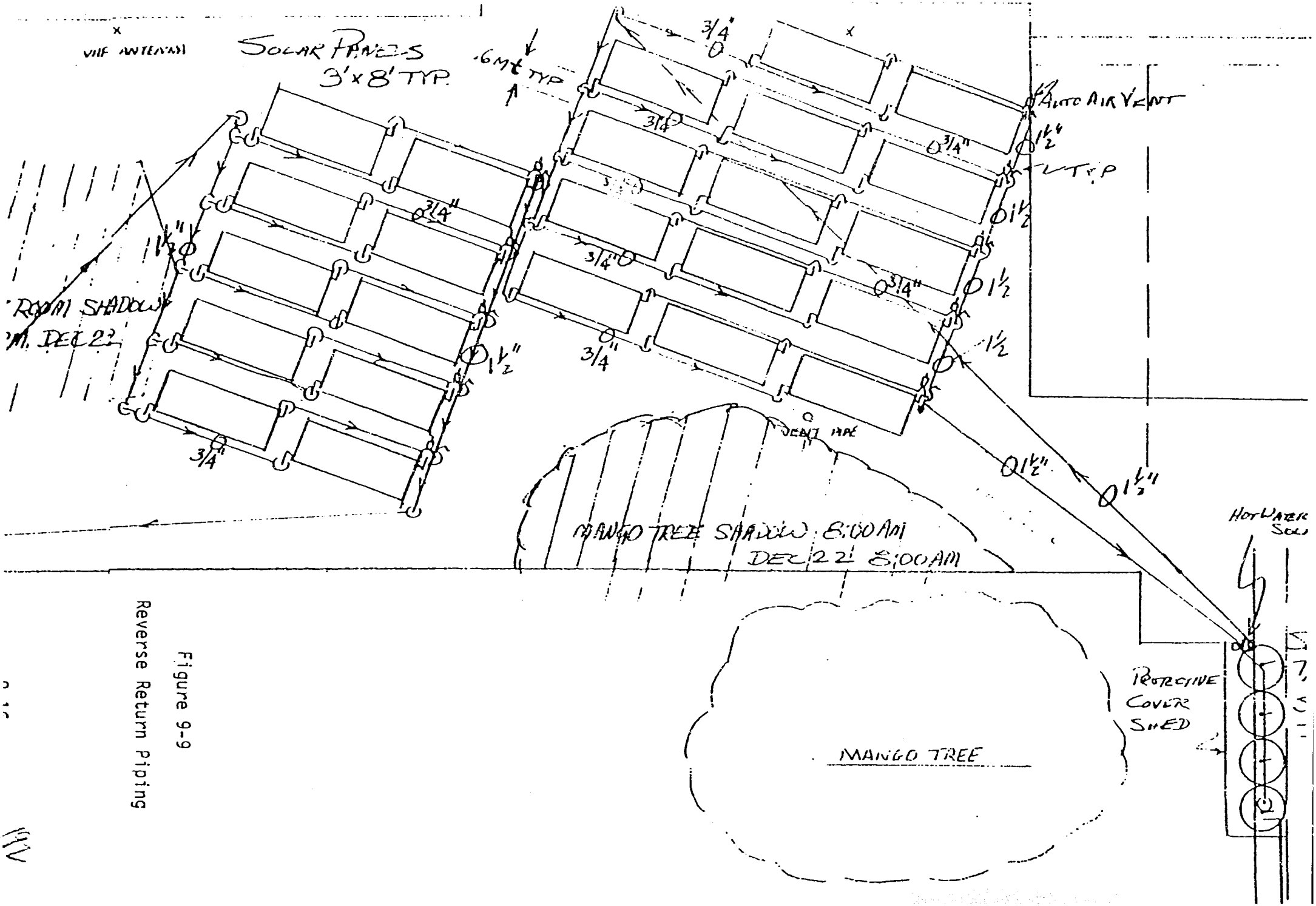

Figure 9-9
Reverse Return Piping

References:

1) H. Ten Bosch: Calculations of Machine Elements, Springer, Berlin, Germany

2) Crocker and King: Piping Handbook, 5th ed. McGraw-Hill Book Company NY, 1967

3) ASHRAE HANDBOOK, American Society of Heating, Refrigerating and Air Conditioning Engineers Inc. 1791 Tulhe Circke, N.E. Atlanta, GA,30329; 1983

Module 10: Sizing the Pipe and Circulation Pump

Objective

The objective of this module is for the trainee to be able to select subsystems for a solar hot water system such as pipe, pump, filters and heat exchangers.

Module 10: Sizing the Pipe and Circulation Pump

PUMPS

The pumps must be selected to provide the required design flow rates. The pumps should be centrifugal type with direct coupled motors. Centrifugal pumps provide two advantages over the positive displacement style pump. Centrifugal pumps offer a safety feature in that they will pump only a small amount above rated pressure if the fluid loop should be blocked. Thus, such an occurrence would neither damage the pump nor burst a fluid line. A second advantage, particularly on the collector loop, is the increase in flow rate as the temperature of the fluid increases. This is due to viscosity changes of the fluid and improves the collector efficiency at high temperatures.

Pumps are rated according to the flow rate they will provide when subjected to a given head pressure. The head pressure is calculated by determining the pressure drop in each component of a loop. For example, consider the loop for pump(3) in Figure 10-1. The pressure drop consists of a Δp in the collectors, a Δp due to pipe friction, a Δp due to elbows, a Δp due to valves, a Δp due to the filter, and a Δp due to the ion getter. In a loop that is kept full, one does not include the head pressure due to pumping the fluid to a higher elevation. However, in a system that is drained, this head would have to be included.

The pressure drop through the collectors will represent a major drop in the system. This will have to be provided by the collector manufacturer or otherwise determined experimentally before the system design can be completed. Typical pressure drops are on the order of .2 lb/in^2 per collector panel. This can be related to feet of water by the relation:

$$1 \text{ ft } H_2O = 0.433 \text{ psi}$$

.Flow Rates Through Collectors. Standard flow rates, as defined by ASHRAE test, are as follows: For liquid type collectors, 0.02kg/(s.m^2), (14.7lbm/(hr.ft^2). For air type collectors, 0.01 m^3/(s.m^2), (2 scfm/ft^2).

However requirements may exist to use different flow rates in applying the collectors to a particular project. In some cases, collectors are used in series, and the solar energy collected will be different than for a single collector.

If flow rate is increased, the temperature range through which the fluid is heated will be less than with standard flow rates, whereas if the flow rate is decreased, the range will be increased. It is also true that for an increased flow rate, the rate of heat transfer between the fluid and the absorber will increase. Conversely if the flow rate is decreased, the rate of heat transfer will also decrease. For nearly all collectors, the change in fluid temperature range has the major effect on rating and the change in heat transfer is a second order effect and can usually be neglected in calculating the difference in performance.

Peter Lunde in attached paper 10-1 uses this concept to calculate the effect of flow rate on performance using the tested ASHRAE performance curve for the calculation. For a typical good flat plate collector:

$$\eta = .705 - .689 \frac{T_i - T_a}{I}$$

Lund found the effect on flow to be a 2.3% reduction in efficiency when the flow is reduced to half of the ASHRAE value (.03 gal/min per ft^2). A 700 square foot system would have a 21 gpm total flow rate requirement

based on the ASHRAE standard. However, very little performance reduction is experienced at a 10.5 gpm total flow. A similar result was obtained by Culham and Saner (Ref 1) using purely simulated data. They found a performance reduction of 5.2% when flow is reduced to (.015 gal/min.ft^2), half the ASHRAE value. For Jamaica, with its high cost of power, the author recommends a flow of .020 gal/min per ft^2 of panel as the flow rate design parameter for utility operated pumps and no panel increase. The author recommends for PV pumped systems, a flow of .015 gal/min per ft^2 panel area with an increase in panel size of 2.5%.

The pressure drop through a collector is a fuction of flow rate and this function should be obtained from the manufacturer.

PIPE

The pressure drop through copper pipes can be determined by referring to Figure 10-2 which gives pressure drop in various sizes of pipe at various flow rates. For example, at a flow rate of 15 gpm through 1 1/4 inch copper pipe, the Δp is 5 feet of water per 100 feet of pipe. Similar charts may be obtained for other types of pipe.

The Δp through elbows, valves, and tees may be determined by referring to Figure 10-3 or by simply adding about 50% to the Δp for the pipes.

The pressure drop through the ion getter is so small that it can be ignored. However, the Δp through the filter can be significant and should be obtained from the manufacturer. In the case of the filter in CSU Solar I the values range between those shown in Figure 10-4.

After determining the individual pressure drops, the total Δ_p may be determined in order to select a pump. For example, in a system with 1000 sq ft of collector area the total pressure drop in the loop was found to be about 27 feet of water. This was made up of the following items.

$$\Delta p_{pipes} = (140 \text{ ft}) \left(\frac{6 \text{ ft } H_2O}{100 \text{ ft}} \right) = 8.4 \text{ ft}$$

$$\Delta p_{elbows} = \left(8 \frac{\text{ft}}{\text{elbow}} \right) (13 \text{ elbows}) \left(\frac{6 \text{ ft } H_2O}{100 \text{ ft}} \right) = 6.24 \text{ ft}$$

$$\Delta p_{valves} = \left(1 \frac{\text{ft}}{\text{valve}} \right) (12 \text{ valves}) \left(\frac{6 \text{ ft } H_2O}{100 \text{ ft}} \right) = 0.72 \text{ ft}$$

$$\Delta p_{ht. exc.} = 20.8 \text{ ft}$$

$$\Delta p_{coll} = 9.2 \text{ ft}$$

$$\Delta p_{filter} = 2.3 \text{ ft.}$$

A typical pump selection chart is shown in Figure 10-5. The pump should be selected to provide the desired flow rate with the Δp calculated.

Notice for this typical system, the pipe, pipe fittings and values account for 57% of the pressure drop. The solar designer should calculate the pressure drop using several sizes of pipe for each system and do a cost trade-off between the additional cost of the pipe and the reduced cost of pump and operating cost, or pump and PV panel.

Air Vents:

Since it is virtually impossible to keep air out of a solar system, it is absolutely essential that air vents be included in the system design. The air vents and valves should be made of the same material as the plumbing that they connect to in order not to add to the corrosion problem if metal pipes are used.

Heat Exchangers:

The use of a heat exchanger in a solar system typically doubles the pressure drop through the system. The engineer/designer must size the heat exchanger and then calculate the pressure drop through it. There are a number of sources that provide this engineering information. Since there is no freeze protection problem in Jamaica, and because of the high cost and efficiency penalty of heat exchangers, use of only direct open loop systems is recommended.

Pressure/Temperature Relief Valves:

Pressure/temperature relief valves should be placed on the hot side of the array with no less than one valve for each five panels. The exit port of these valves must have a blow pipe on them and the pipe must be at least 50 cm in length. The pipe exit should be oriented in such a way as to prevent scaulding of any persons who may be near the collector array if a valve were to discharge. When such valves discharge, they do so with steam under much force so care must be taken to properly pipe the P&T valves on a ground mounted sustem such that they can discharge safely.

Insulation of Piping:

The appendix contains an analysis of pipe insulation for Jamaica. If piping is not insulated, then an additional square foot of collector area would have to be added to the array for each square foot of exposed piping.

Nevertheless, all piping at the top of the solar tank should be insulated for a distance of three feet from the tank. This includes hot water supply lines, cold water inlet lines that may enter the top of the tank, and the tank P&T valve and fittings. Heat loss from this area is significant if not insulated and insulating here is well worth the high cost of insulation even though insulation is not recommended for array and connecting pipes because of its high cost.

Special Piping Considerations for Thermosiphon Systems:

Pipe size in thermosiphon systems is of critical importance since the movement of water through a thermosiphon is induced by temperature related densities between the average temperature of panel water and the average colder water temperature at the bottom of the tank. This difference in density and the heigth of the tank above the panel provides the moving force for circulation. Using efficient measured flows typical of thermosiphon systems (15 lbm/hr/ft sq) and assuming the header to riser distances are under 100 feet in length (50 feet for each leg) then the proper pipe size needed (such that resistance to flow is below induced forces) can be determined for various collector array sizes and tank heights above the array. This data is given in the Figure 10-8 below:

Figure 10-8 Minimum Header-Riser Pipe Sizing

Collector Area	needed gpm in main risers and headers	h=5'	h=10'	h=15'	h=20'	h=25'
330 sq ft	10 gpm	2"	1 1/2"	1 1/4"	1 1/4"	1 1/4"
500 sq ft	15 gpm	2"	2"	1 1/2"	1 1/2"	1 1/2"
670 sq ft	20 gpm	2"	2"	2"	2"	2"
830 sq ft	25 gpm	2 1/2"	2"	2"	2"	2"
1000 sq ft	30 gpm	2 1/2"	2 1/2"	2"	2"	2"

h = height of tank base above center of collector array. Values are given for nominal ID smooth galvanized pipe.

Use of smaller pipe for headers and risers in these larger systems than shown in Figure 10-8 could result in significant loss of performance. Also piping from tank to collectors should be as short as possible because it is a major source of heat loss. If collectors have parallel flow passageways, they must be mounted with these passageways running vertically. The low flow pressures in thermosiphon systems require that water tubes be a minimum 3/4 inch inside diameter (ID) within the panels used.

All piping must have a continuous upward slope to the tank of at least 1 1/4' per foot (10 cm/meter). The greater the piping slope the better the performance. No piping can be allowed that sags to create a negative slope for the fluid flow, as this retards natural circulation.

1 CUTOFF VALVE
2 ISOLATION VALVE
3 PUMP
4 AUTOMATIC AIR VALVE
5 P & T VALVE
6 CHECK VALVE
7 ISOLATION VALVE
8 P & T VALVE
9 DRAIN
10 FILTER
11 ION GETTER

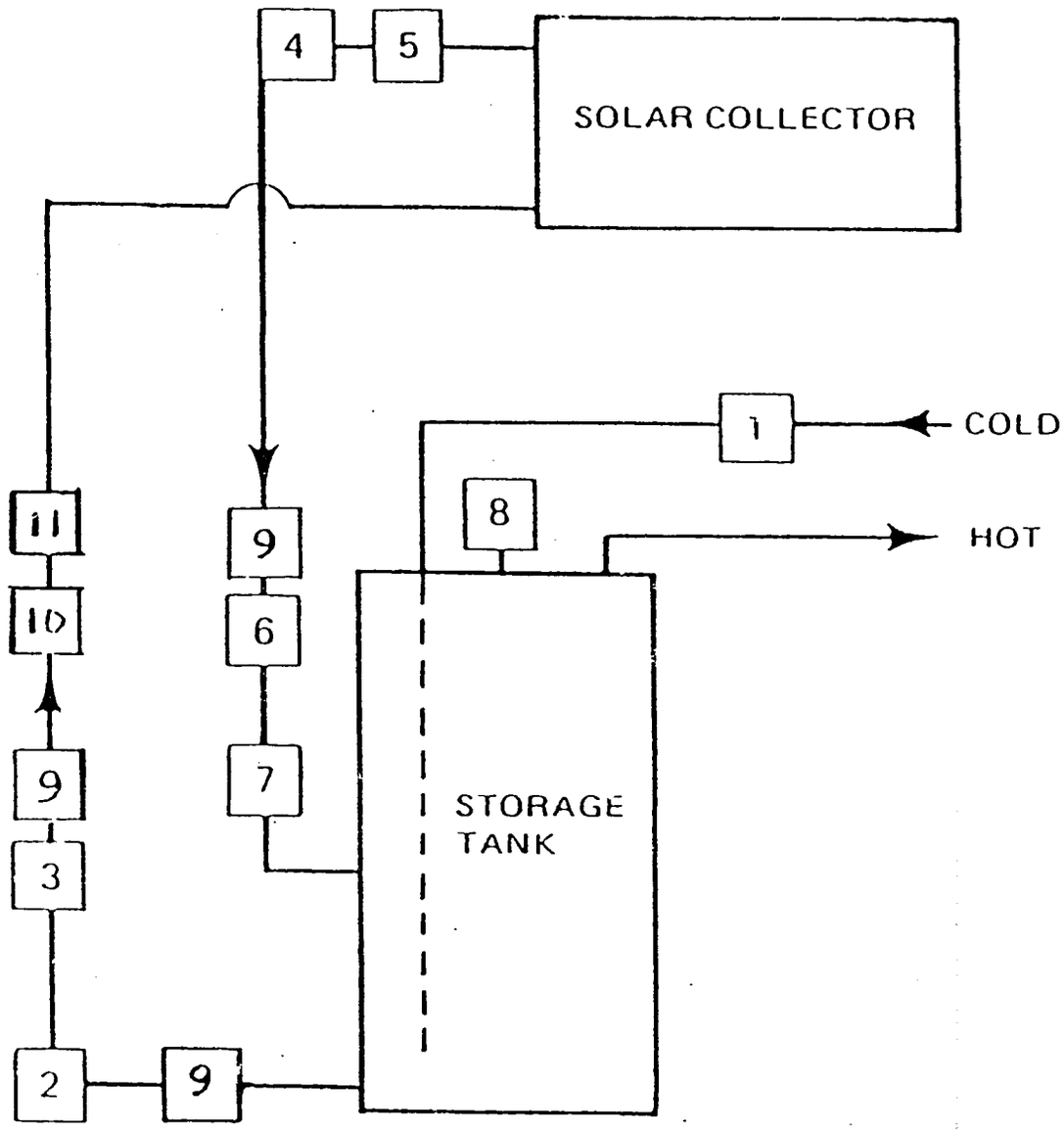

Figure 10-1

Block Diagram of Open Solar Water Heating System

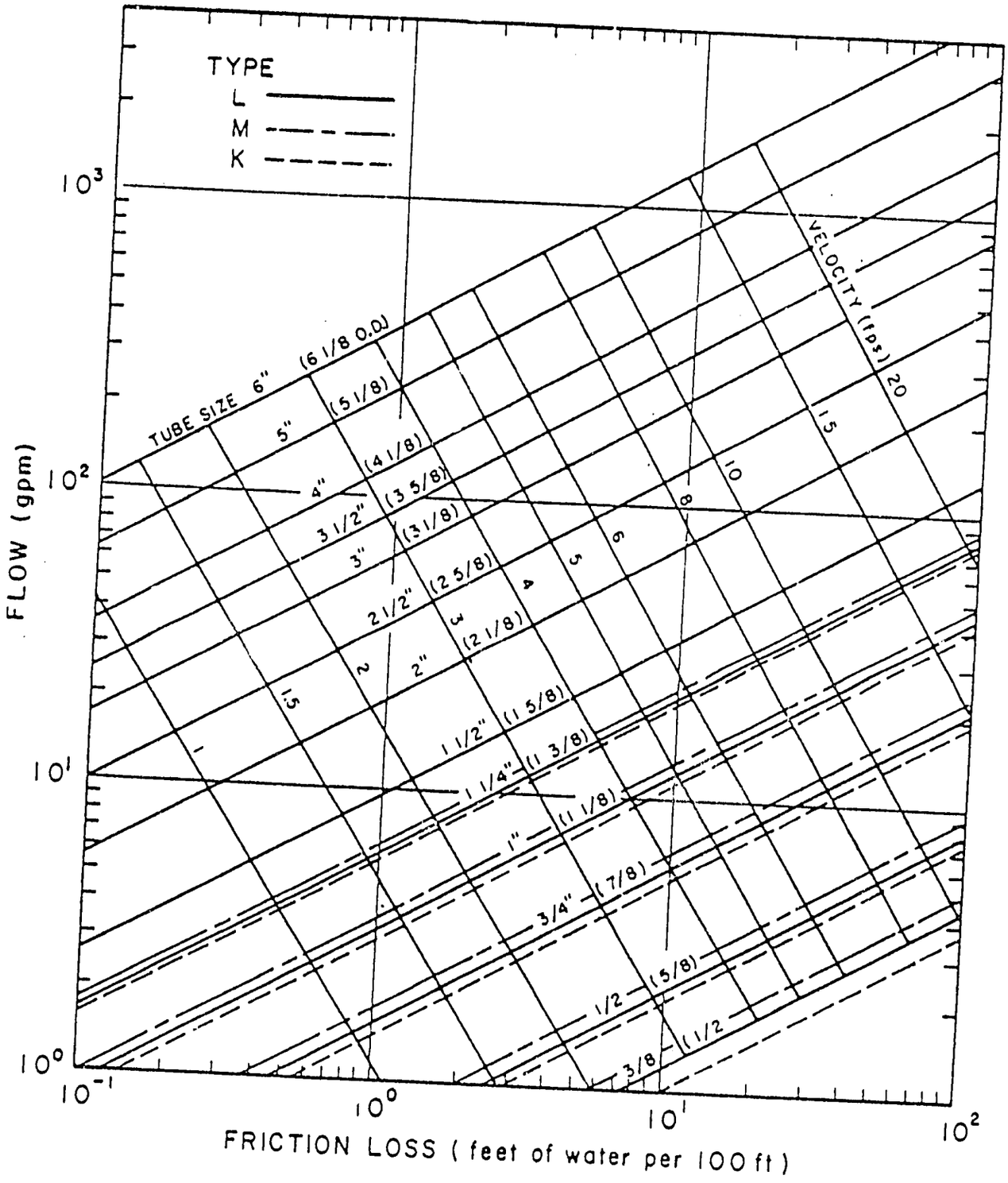

Figure 10-2 Friction Loss in Copper Tubing

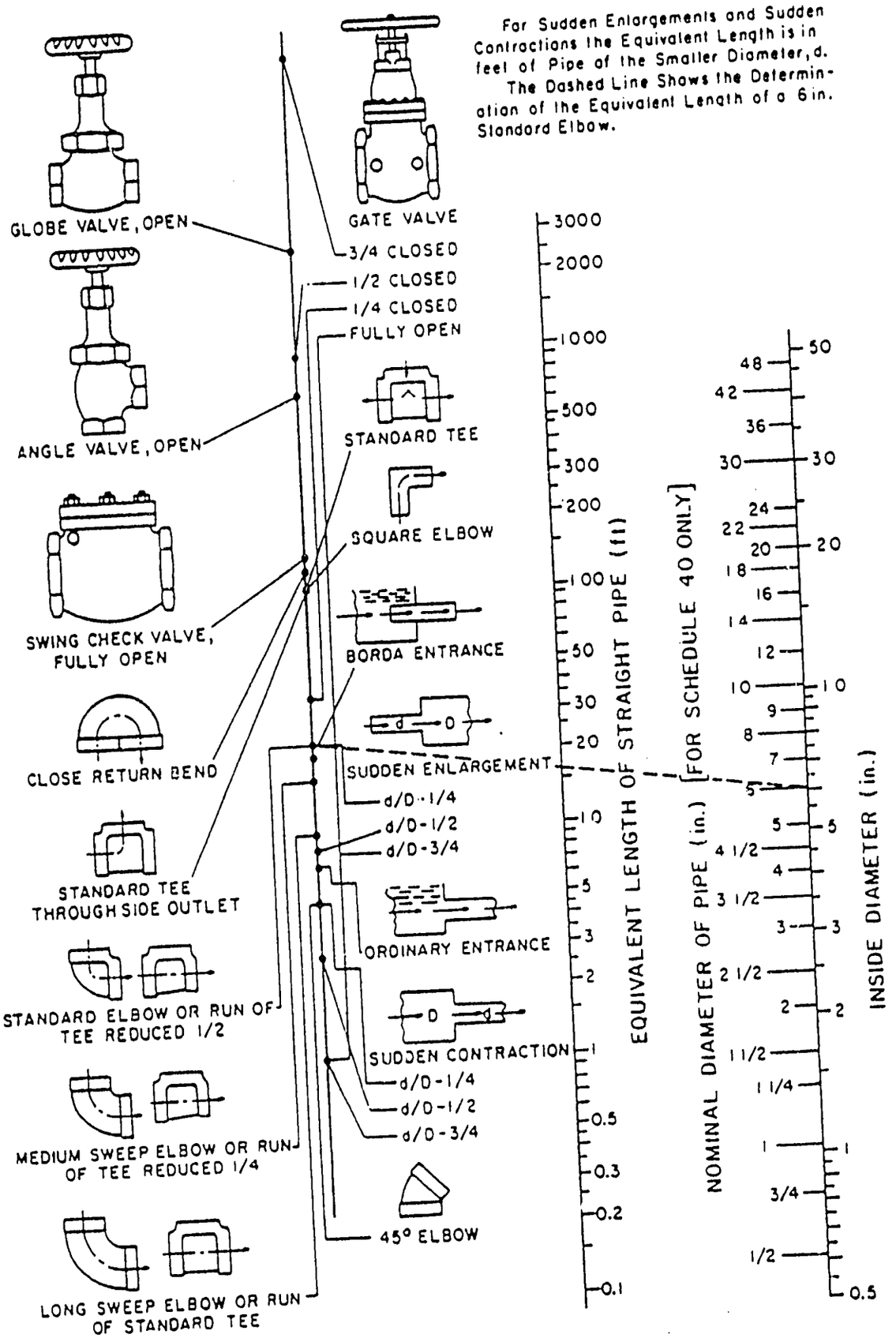

Figure 10-3 Pressure Loss in Various Elements.

204

Figure 10-4 Pressure Drops through Filter in CSU Solar I

	Δp (psi)		
	Fine	Medium	Coarse
16 gpm 205 °F 60% ethylene glycol (in water)	2.10	0.70	0.35
5 gpm 87 °F pure water	0.60	0.20	0.10

FIGURE 10-5

PUMP PERFORMANCE CURVES

Series 60 Pumps can be furnished in bronze-fitted, all iron, or all bronze construction to suit your application

DOTTED-IN CURVES REPRESENT STOCK PUMP SELECTIONS

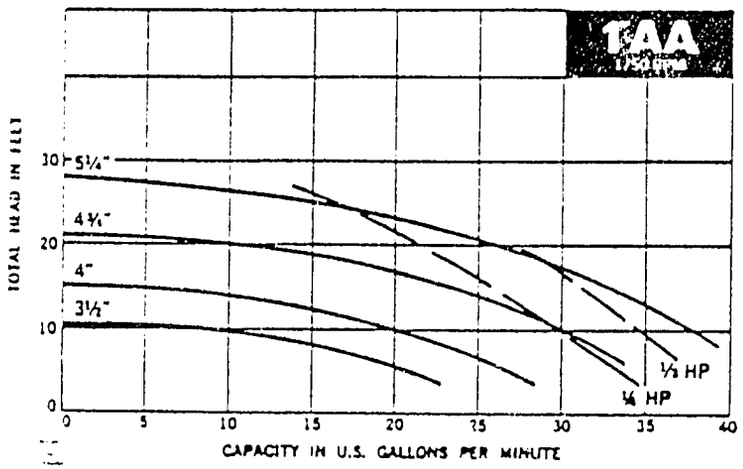

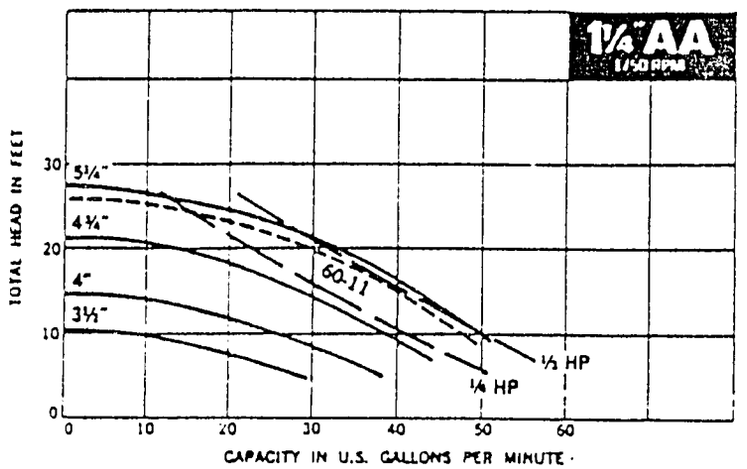

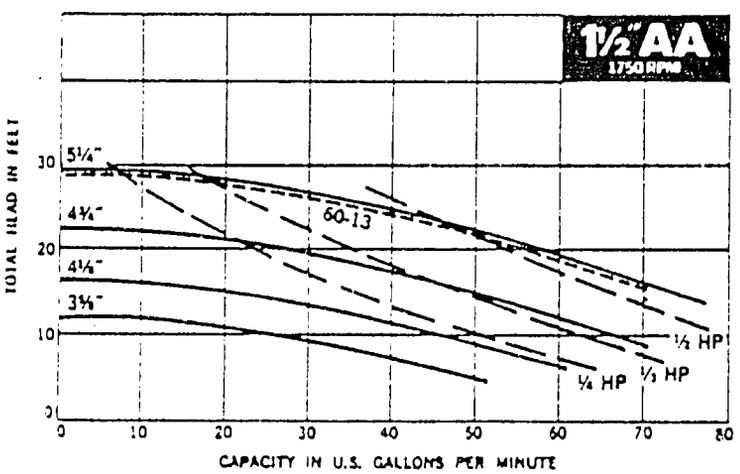

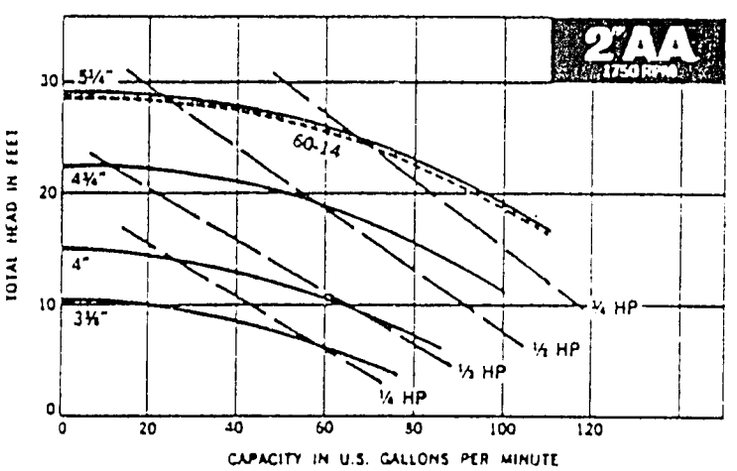

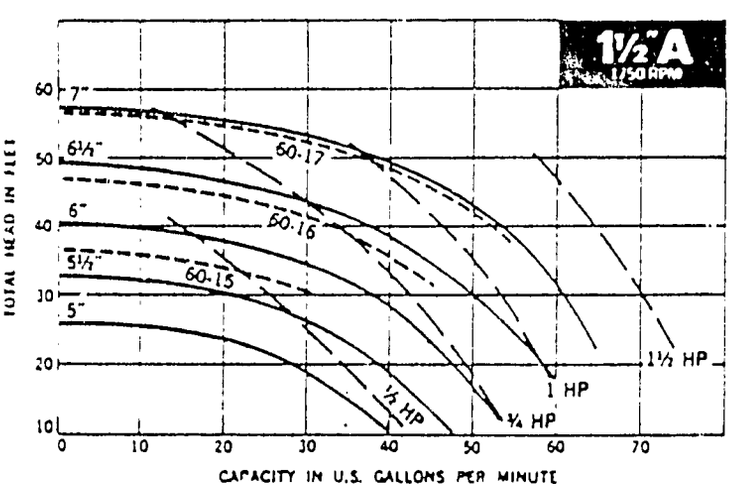

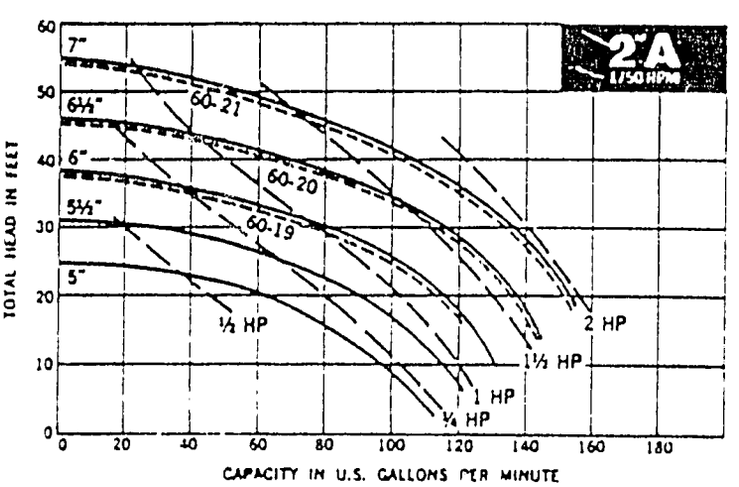

Curves based upon shop test using clear cold water at a temperature of not over 85 F.
Horsepower curves do not include motor service factor.

20b

STA-RITE

FIGURE 10-6

FRICTION LOSS . . . PLASTIC PIPE

1/2" PIPE

FLOW (Gals. Per Minute)	VELOCITY (Feet Per Second)	FRICTION LOSS (Feet Per 100 Feet)
1.0	1.06	1.48
1.5	1.58	3.00
2.0	2.11	5.10
2.5	2.64	7.70
3.0	3.17	10.60
3.5	3.70	13.70
4.0	4.23	17.80
5.0	5.28	22.30
10.0	10.60	76.80

3/4" PIPE

FLOW (Gals. Per Minute)	VELOCITY (Feet Per Second)	FRICTION LOSS (Feet Per 100 Feet)
1.5	903	.69
2.0	1.20	1.12
2.5	1.51	1.68
3.0	1.81	2.35
3.5	2.11	3.00
4.0	2.41	3.90
4.5	2.71	4.70
5.0	3.01	5.80
6.0	3.61	7.70
7.0	4.21	10.00
8.0	4.82	12.40
9.0	5.42	15.30
10.0	6.02	18.80

1" PIPE

FLOW (Gals. Per Minute)	VELOCITY (Feet Per Second)	FRICTION LOSS (Feet Per 100 Feet)
2	.742	.295
3	1.11	.63
4	1.49	1.04
5	1.86	1.49
6	2.23	2.00
8	2.97	3.30
10	3.71	5.15
12	4.46	6.95
14	5.20	9.20
16	5.94	11.40
18	6.68	13.8
20	7.43	17.0

1-1/4" PIPE

FLOW (Gals. Per Minute)	VELOCITY (Feet Per Second)	FRICTION LOSS (Feet Per 100 Feet)
4	.86	.35
5	1.07	.48
6	1.29	.65
7	1.50	.85
8	1.72	1.08
10	2.15	1.60
12	2.57	2.23
14	3.00	2.92
16	3.43	3.70
18	3.86	4.55
20	4.29	5.55
25	5.36	8.20
30	6.43	11.00
35	7.51	14.00

Friction (Head) Loss for Insert Adapters and Insert Couplings

For every ten (10) Insert Adapters used add the number of feet indicated in column "A" to total length of pipe.

For every ten (10) Insert Couplings used add the number of feet indicated in column "B" to total length of pipe.

1-1/2" PIPE

FLOW (Gals. Per Minute)	VELOCITY (Feet Per Second)	FRICTION LOSS (Feet Per 100 Feet)
4	.63	1.50
5	.79	.225
6	.95	.300
7	1.10	.400
8	1.26	.520
9	1.42	.630
10	1.58	.770
12	1.89	1.07
14	2.21	1.39
16	2.52	1.76
18	2.84	2.11
20	3.15	2.58
22	3.47	2.98
24	3.78	3.60
26	4.10	4.20
28	4.41	4.70
30	4.73	5.30
32	5.04	5.85
34	5.36	6.40
36	5.67	7.50
38	5.99	7.85
40	6.30	8.50
42	6.62	9.20
44	6.93	9.80
46	7.25	10.06
48	7.57	10.15
50	7.88	10.24
55	8.67	10.45
60	9.46	10.69

2" PIPE

FLOW (Gals. Per Minute)	VELOCITY (Feet Per Second)	FRICTION LOSS (Feet Per 100 Feet)
7	.67	.12
8	.77	.15
9	.86	.19
10	.96	.23
12	1.15	.34
14	1.34	.44
16	1.53	.56
18	1.72	.68
20	1.91	.83
22	2.10	.98
24	2.29	1.15
26	2.49	1.33
28	2.68	1.56
30	2.87	1.74
35	3.35	2.20
40	3.82	2.86
45	4.30	3.40
50	4.78	4.30
55	5.26	5.00
60	5.74	5.80
65	6.21	6.70
70	6.69	7.50
75	7.17	8.60
80	7.65	9.55
85	8.13	10.7
90	8.61	11.8
95	9.08	13.2
100	9.56	14.4

PIPE SIZES	"A"	"B"
½"	11	5
¾"	15	7
1"	20	10
1¼"	27	13
1½"	34	16
2"	44	20
3"	62	29
4"	90	41
6"	140	62

3" PIPE

FLOW (Gals. Per Minute)	VELOCITY (Feet Per Second)	FRICTION LOSS (Feet Per 100 Feet)
20	.87	.125
25	1.09	.188
30	1.30	.260
35	1.52	.335
40	1.74	.435
45	1.95	.525
50	2.17	650
55	2.39	770
60	2.60	.880
65	2.82	1.01
70	3.04	1.15
75	3.25	1.31
80	3.47	1.45
85	3.69	1.64
90	3.91	1.82
95	4.12	2.01
100	4.34	2.20
110	4.77	2.63
120	5.21	3.20
130	5.64	3.65
140	6.08	4.20
150	6.51	4.65
160	6.94	5.20
180	7.81	6.40
200	8.68	7.80
220	9.55	9.20
240	10.4	10.6
260	11.3	12.2
280	12.2	14.0
300	13.0	15.8
320	13.9	17.5

4" PIPE

FLOW (Gals. Per Minute)	VELOCITY (Feet Per Second)	FRICTION LOSS (Feet Per 100 Feet)
40	1.01	.111
50	1.26	.166
60	1.51	.225
70	1.76	.294
80	2.02	.38
90	2.27	.48
100	2.52	.59
110	2.77	.70
120	3.02	.82
130	3.28	.94
140	3.53	1.09
150	3.78	1.22
160	4.03	1.38
170	4.29	1.52
180	4.54	1.69
190	4.79	1.89
200	5.05	2.04
220	5.55	2.41
240	6.05	2.83
260	6.55	3.30
280	7.06	3.80
300	7.57	4.30
320	8.07	4.80
340	8.58	5.30
360	9.08	5.80
380	9.59	6.70
400	10.1	6.90
440	11.1	8.4
480	12.1	9.6
500	12.6	10.2
550	13.9	12.1
600	15.1	14.0
650	16.4	16.5
700	17.6	18.8

Friction loss charts by courtesy of Carlon Products Corporation, Aurora, Ohio.

FIGURE 10-7

Useful Tables . . . for Sizing and Selecting Sta-Rite Pumps

STA-RITE

CONVERSION TABLE . . . POUNDS PRESSURE . . . FEET OF HEAD

POUNDS PRESSURE	FEET OF HEAD	POUNDS PRESSURE	FEET OF HEAD	POUNDS PRESSURE	FEET OF HEAD
1	2.31	13	30.0	45	103.9
2	4.62	14	32.3	50	115.5
3	6.93	15	34.7	55	127.0
4	9.24	16	37	60	138.6
5	11.6	17	39.3	65	150.1
6	13.9	18	41.6	70	161.7
7	16.2	19	43.9	75	173.2
8	18.5	20	46.2	80	184.8
9	20.8	25	57.7	85	196.3
10	23.1	30	69.3	90	207.9
11	25.4	35	80.8	95	219.4
12	27.7	40	92.4	100	231.0

CONVERSION TABLE . . . INCHES MERCURY . . . FEET OF WATER

INCHES MERCURY	FEET OF WATER	INCHES MERCURY	FEET OF WATER	INCHES MERCURY	FEET OF WATER
1	1.13	11	12.46	21	23.79
2	2.27	12	13.60	22	24.93
3	3.40	13	14.73	23	26.06
4	4.53	14	15.86	24	27.19
5	5.67	15	17.00	25	28.33
6	6.80	16	18.13	26	29.46
7	7.93	17	19.26	27	30.59
8	9.06	18	20.39	28	31.72
9	10.20	19	21.53	29	32.86
10	11.33	20	22.66	30	33.99

FRICTION LOSS TABLE . . . STANDARD STEEL PIPE

GPM	½"		¾"		1"		1¼"		1½"		2"		2½"		3"		4"		GPM
	VEL.	FRIC.	VEL.	FRIC.	VEL.	FRIC.	VEL.	FRIC.	VEL.	FRIC.	VEL.	FRIC.	VEL.	FRIC.	VEL.	FRIC.	VEL.	FRIC.	
5	5.3	41.1	3.0	10.9	1.3	3.2	1.1	.9	.8	.5	.5	.1							5
10	10.5	150.0	6.0	37.5	3.7	11.6	2.2	3.1	1.6	1.5	.9	.4	.6	.2	.4	.1			10
15			9.3	80.2	5.6	24.0	3.2	6.9	2.3	3.1	1.4	.9	1.0	.4	.6	.1			15
20			12.1	136.0	7.4	42.0	4.3	11.2	3.2	5.2	2.0	1.5	1.4	.6	.9	.2	.5	.06	20
25					9.2	62.5	5.4	17.0	3.8	8.0	2.4	2.4	1.7	.9	1.1	.3	.6	.09	25
30					11.1	89.1	6.4	24.0	4.7	11.2	2.8	3.3	2.0	1.4	1.3	.5	.7	.13	30
35							7.6	32.0	5.5	15.2	3.3	4.4	2.4	1.8	1.5	.7	.9	.18	35
40							8.5	40.1	6.4	19.0	3.8	5.7	2.7	2.4	1.7	.9	1.0	.22	40
45							9.6	50.6	7.1	24.1	4.3	6.9	3.0	2.9	1.9	1.0	1.2	.28	45
50							10.6	61.0	7.9	29.0	4.8	8.4	3.3	3.5	2.2	1.3	1.3	.34	50
60							12.8	84.6	9.4	40.0	5.7	11.8	4.0	5.0	2.6	1.9	1.5	.46	60
70									11.1	53.4	6.6	15.6	4.7	6.6	3.1	2.5	1.8	.62	70
80									12.6	68.4	7.6	20.3	5.3	8.4	3.5	3.3	2.0	.79	80
90											8.6	25.2	6.0	10.5	4.0	4.1	2.3	1.0	90
100											9.6	31.0	6.7	12.7	4.4	4.9	2.5	1.2	100
110											10.5	37.0	7.3	15.1	5.0	6.0	2.8	1.4	110
120											11.6	43.5	8.0	17.8	5.2	6.9	3.0	1.7	120
130											12.4	50.1	8.7	20.7	5.6	8.1	3.3	1.9	130
140													9.4	24.0	6.1	9.3	3.5	2.2	140
150													10.0	27.2	6.8	10.6	3.8	2.5	150
175													11.7	36.1	7.6	12.3	4.4	3.4	175
200													13.4	46.4	8.7	18.0	5.1	4.3	200
225															9.8	22.0	5.6	5.5	225
250															10.8	27.0	6.3	6.6	250
275															11.9	32.0	6.9	7.8	275
300															13.0	38.0	7.5	9.0	300
350															15.2	49.0	8.8	11.8	350
400																	10.1	16.0	400
450																	11.3	19.0	450
500																	12.6	24.0	500
550																	14.0	29.0	550
600																	15.0	33.8	600

FRICTION LOSSES IN FITTINGS
Equivalent Length of Straight Pipe, Feet

Size	½"	¾"	1"	1¼"	1½"	2"	3"	4"
Gate Valve (Full Open)	0.6	0.7	0.9	1.2	1.3	1.6	2.0	2.7
Elbow, 90°	3.6	4.5	5.3	6.7	7.5	8.6	11.1	13.1
Elbow, 45°	0.7	0.9	1.4	1.8	2.2	2.8	4.1	5.6
Tee (Straight Thru)	1.8	2.5	3.3	4.7	5.7	7.8	12.1	17.1
Tee (Thru Side)	4.3	5.4	6.7	8.8	10.0	12.1	17.1	21.2
Swing Check Valve	8.1	8.9	11.2	13.1	15.2	19.1	27.1	38.2

PETER J. LUNDE: PRACTICAL ENGINEERING

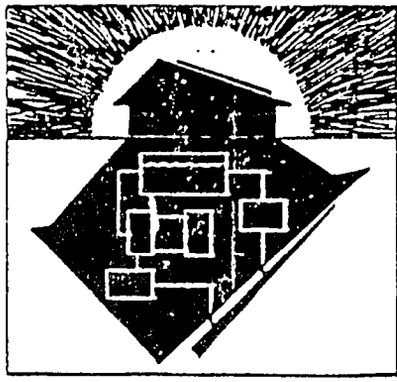

Collector Flowrate

The correct collector fluid flowrate is not always the one recommended by the manufacturer. Indeed, the solar theoretician—who properly wants to keep the collectors cool for minimum heat loss—recommends the maximum flow possible. The practical engineer, however, must balance the cost of a larger pump and additional pumping power against the value of increased thermal performance of the system. If electrical power is projected to become much more costly over the life of the system, a lower flowrate than is usually specified may be desirable.

To properly compare systems after changing the flowrate, we adjust the collector area as necessary to restore the original performance. The increase or decrease in area causes a corresponding change in capital costs.

To do this we must quantitatively predict the way flowrate affects array performance.

The effect of flowrate on performance

Suppose the manufacturer's ASHRAE 93-77 collector test, which is usually run with water, gives an intercept $F_R\tau\alpha$ equal to 0.705 and a slope of F_RU_L equal to 0.689 Btu/hr °F ft². Assume that water is to be used as the system heat transfer fluid, so the results apply directly. The design calls for 700 ft² of collector area.

The transmissivity-absorptivity ($\tau\alpha$) product is calculated (from the manufacturer's data on glass and absorber surface) as $\tau\alpha = 0.901 \times 0.95 = 0.856$. Therefore, the inlet-based heat transfer factor (F_R), which accounts for the flowrate, is $F_R = F_R\tau\alpha \div \tau\alpha = 0.705 \div 0.856 = 0.824$. The actual collector heat loss coefficient is then $U_L = F_RU_L \div F_R = 0.689 \div 0.824 = 0.836$ Btu/hr °F ft².

The inlet heat transfer factor can also be calculated theoretically from:

$$F_R = \frac{1}{\left(\frac{1}{\eta} + \frac{U_LA_c}{U_fA_f}\right) + \frac{U_L}{2Wc/A_c}} \qquad (1)$$

where W = mass flowrate, c = specific heat, η = plate fin efficiency, A_c = gross collector area, and $_f$ = fluid film heat transfer coefficient. The first two terms in the denominator are associated with the heat transfer from the plate to the fluid. Only the third contains Wc/A_c, the area-normalized flow capacity rate. For the ASHRAE test results, this is 15 Btu/hr °F ft².

To bring theory and experiment together, we solve for the unknown terms in equation (1) and use experimental values to evaluate them:

$$\left(\frac{1}{\eta} + \frac{U_LA_c}{U_fA_f}\right) = \frac{1}{F_R} - \frac{U_L}{2Wc/A_c}$$

$$= \frac{1}{0.824} - \frac{0.836}{2 \times 15} = 1.186$$

We can now rewrite equation (1) for this collector as:

$$F_R = \frac{1}{1.186 + \frac{0.836}{2Wc/A_c}} \qquad (2)$$

This equation can predict the effect of flowrate on system performance.

Effect on capital cost

The heat transfer factor F_R appears in the Hottel-Whillier collector heat balance equation when it is written to use the inlet collector fluid temperature (T_i):

$$q = F_R[\tau\alpha I - U_L(T_i - T_a)] \qquad (3)$$

where T_a = ambient temperature and I = incident solar radiation. System performance at any time is predicted by this equation. Even though we may not know the values of all the variables in the brackets, it is clear that the performance is always proportional to F_R. Therefore, if we change from its nominal value of 0.824 by halving the flow, by equation (2) the new value is:

Dr. Peter J. Lunde is president of New Energy Resources, Inc., and principal of 3D Solar Programs. He teaches at the Hartford Graduate Center and is the author of the text Solar Thermal Engineering.

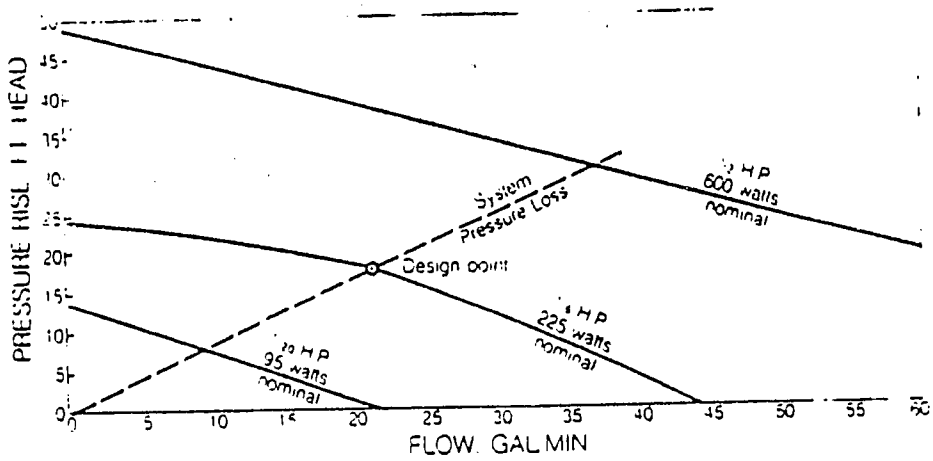

Figure 1. Pressure rise characteristics for a line of centrifugal pumps. The upper line is a 1/2 hp pump using 600 Watts. The middle line represents a 1/4 hp pump with a nominal 225 Watt power consumption. The lower line is an alternative 1/20 hp pump using 95 Watts.

$$F_R = \frac{1}{1.186 - \frac{0.836}{2 \times 15 \times .5}} = 0.805$$

We are thus reduced to 0.805/0.824 = 97.7 percent of the original thermal performance. To keep the same performance for a nominal 700 ft² system, it must be enlarged to 700/0.977 = 716 ft², a 2.3 percent increase in collector area. Assuming a cost of \$35/ft², this means 16 × \$35 = \$560 additional investment. That must be paid back by the savings in pump capital cost and pumping power or the flow shouldn't be reduced.

Effect on system operating cost

The performance curves and electrical characteristics of three solar pumps are shown in Figure 1. The dashed line represents the system pressure drop, conservatively assumed to be linear with flowrate.

The design volumetric flow rate (V) can be calculated from the specified Wc/A_c = 15 Btu/hr °F ft²:

$$V = \frac{15\ \text{Btu}}{\text{hr °F ft}^2} \times \frac{\text{lb °F}}{1\ \text{Btu}} \times 700\ \text{ft}^2 \times \frac{\text{hr}}{60\ \text{min}} \times \frac{\text{gal}}{8.33\ \text{lb}} = 21\ \text{gal/min}$$

If the flowrate is halved from 21 gal/min to 10.5 gal/min, the system pressure drop falls from 16 to 8 ft of fluid head, permitting use of the smaller pump and savings of 130 watts. By use of threshold level radiation tables at Hartford, Conn., I estimate that a hot water water system will operate 2800 hours per year if the average annual threshold level is 45 Btu/hr ft². Therefore, the initial annual savings, if electricity costs, say, 8¢ per kWh, are:

$$\frac{\$0.08}{\text{kWh}} \times 130\ \text{W} \times 2800\ \text{hr} \times \frac{\text{kW}}{1000\text{W}} = \$29$$

To evaluate the power costs, we must know the worth of an annual energy savings that is continued over the life of the system. Calculating this is beyond our present scope, but let us assume that \$1 saved annually is worth \$25 over the life of a system when fuel inflation, interest rate, and tax deductions for interest are taken into account. Combined with, perhaps, \$75 in capital cost savings from using a smaller pump, a present value of (\$29 × 25) − \$75 = \$800 saved over the life of the system. Since the investment to do this was only \$560, the outlay is desirable.

Another alternative, doubling the flow, might also be considered. F_R would increase to 1/[1.186 + 0.836/(2 × 15 × 2)] = 0.833, a 1.1 percent increase in performance, permitting a reduction of only 8 ft² in area. This is a savings of only \$280 in system cost—diminishing returns are clearly setting in. Without redesign of the system piping to handle more flow, the 600 watt pump that is needed would consume an added 375 watts, costing \$0.08 × 375 × 2800/1000 = \$84 per year, worth up to \$84 × 25 = \$2,100 in life-cycle operating costs. Even after a system redesign to the original pressure loss, the pump required (not shown) would consume about 200 extra watts. A flow increase is not called for.

In the case examined, the manufacturer's recommended flow rate is too high and should be reduced. This will not always be true. Lower electric power costs favor larger pumps. And there are other considerations. For instance, in a commercial installation the electric power used for the larger pump is tax deductible, but the extra area needed to compensate for a smaller pump must be capitalized and depreciated over a number of years. Such a tax policy decreases the value of electrical savings, favoring the use of traditional energy instead of renewable resources.

The effects of pump sizing can be evaluated in just a few minutes. It's another part of the practical engineering that lets us design the most economical solar systems for our customers.

References:

Lunde, P.J. Solar Thermal Engineering, Chapters 5 and 12. John Wiley & Sons, New York (1980).

Lunde, P.J. "New Heat Transfer Factors for Flat Plate Solar Collectors." *Solar Energy* 27, 109-114 (1981).

210

MODULE 11 INSTRUMENTATION

OBJECTIVE

The objective of this module is for the trainee to consider the trades-offs between field and laboratory testing as well as become familiar with the common instruments used in simplified field testing.

211

MODULE 11: SOLAR INSTRUMENTATION

For a number of years there have been significant differences of view concerning the relative merits of testing solar systems in the field vs. testing systems in the laboratory. There are many tasks which can be done more easily and more precisely in the laboratory while others are best done in the field. The decision as to which kind of program is best is contingent on the primary objectives for the specific case under consideration. Given below are some of the advantages and disadvantages of both field and laboratory monitoring.

For most larger solar systems, the type of instrumentation and how it is to be installed is up to the designer/engineer and should be called out on the blueprints. As a minimum, major systems should have dial .. reading thermometers installed in the fluid flow stream leading to the collectors and returning to the tank. A dial reading thermometer on the hot water delivery line is also desirable. Reference (1) contains detail information on the installation, use and maintenence of measurement equipment commonly used in the solar field. This module will deal with some of the positive and negative aspects of field monitoring to assist the designer/engineer in the determination of instrumentation need and requirements.

211

ADVANTAGES AND PROBLEMS OF LABORATORY MONITORING

Advantages

- System configuration is precisely known and controllable (e.g. thermal capacitance of piping).
- Parameters and variables are more easily controlled.
- Instruments may be more easily checked and recalibrated as necessary.
- Results are often reproducible.
- Component malfunction can be spotted early and corrected.
- Data inaccuracies during acquisition are less likely.
- "Tinkering" with controls less likely.
- Weather data may be more precisely evaluated.
- Easier validation of computer models.
- Smaller samples can yield acceptable accuracy.

Disadvantages

- Results may not be representative of actual conditions.
- Selected configuration may not be representative of typical systems.
- Typical test sequence unlikely to duplicate actual lifestyles.
- Real world conditions not under under test.
- Common reasons for system failure or under performance may escape notice.
- Need to construct and assemble the test system.
- Much less visibility for most solar experiments.

ADVANTAGES AND PROBLEMS OF FIELD MONITORING

ADVANTAGES

- Test systems usually already available - no need to finance and construct system.
- Test systems are ab initio, representative of the field.
- Effects of common field installation practices are included within the results.
- Reports data based on actual operating conditions. Statistically significant samples yield real world results.
- Represents only way to test reliability of commercially available components and systems.
- Provides real world cost information.
- Results may be more acceptable to system vendors and manufacturers.

DISADVANTAGES

- More difficult to install and maintain proper instrumentation. Recalibration may be difficult.
- Materially increases cost of:
  - . instrumentation
  - . data collection
  - . instrument calibration
  - . verification of data accuracy
- Increase in data retrieval problems.
- Subject to owner induced distortion of data.
- Often requires access to private property.
- Subject to distortions from change in occupancy.
- Cost of removing instrumentation must be included.
- Proper placement of sensors more difficult than for laboratory conditions.

MONITORING OF ACTIVE SOLAR SYSTEMS
LEVELS OF INSTRUMENTATION

Level	Objective	Measurement Required	Instrumentation	Remarks
0	Public Perception of Product	Sample Opinions	Opinion Surveys Interviews	Surveys of Subjective Perceptions
1	Is System Running?	Pump, Blower, or Valve Position Indicator	Indicator light Audible signal	Qualitative Objective
2	Performance	Water Temperature Air Temperature	Thermometers (Permanent or Portable)	Primary Quantitative
3	Performance	Pump Operation Backup Operation	Elapsed Time Meter	Improving level of information concerning performance
4	Performance	Energy Consumption and Working Fluid Flows	Kwh meters Flow meters	More sophisticated measurement devices
5	Performance	Temperature Measurements	ΔT measurements	Performance at peak hours (solar noon)
6	Performance	Integrated Measurements	BTU Meters	Relationship between accuracy, frequency of data and objectives

245

MONITORING OF ACTIVE SOLAR SYSTEMS
LEVELS OF INSTRUMENTATION

Level	Objective	Measurement Required	Instrumentation	Remarks
7	Performance Evaluate Impact Energy Use Profile	Time of Use Solar and Backup	Recording Meters Kwh and Flow	Impact of solar on energy backup
8	Reliability	Component System Reliability		
. . . . .				
.	Precise Performance Analysis	Insolation and Weather Data	PV cells or pyronometers	Tradeoffs of accuracy and cost

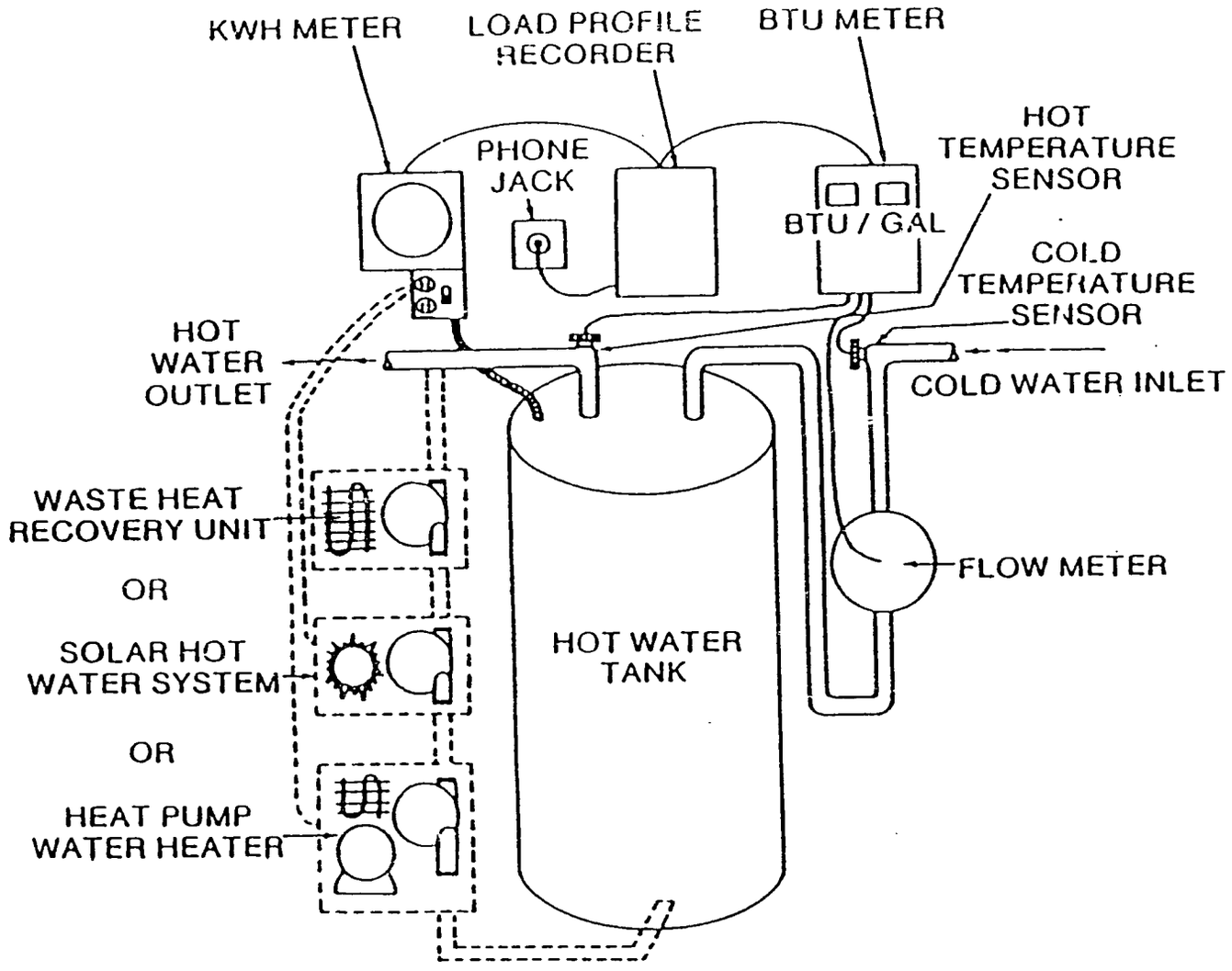

DHW MONITORING INSTRUMENTATION

217

BTU METER

INSTALLATION INSTRUCTIONS

OPERATING INSTRUCTIONS

I INSTALLATION OF FLOW METER

Flow meters may be installed with the included fittings in either a horizontal or vertical position. Flow meters must be installed in the same line in which the temperature sensors are installed.

Plastic flow meters must be installed in the cold water line or where temperature will never exceed 120°F.

Bronze flow meters may be installed where fluid temperatures will not exceed 195°F.

II TEMPERATURE SENSORS

Any of the standard ,provided temperature sensors may be used. The sensor must be well insulated from ambient temperatures. Temperature sensors must be installed in line at the points between which heat transfer measurements are required. Two typical systems are shown in Figures 11-2 and 11-3.

III ELECTRONIC BOX

The electronic box should be installed no further than 100 ft. from the flow meter and temperature sensors. Greater distances may affect the resistance values transmitted by the temperature sensors. Standard electrical practices should be used for the high voltage (110 V.A.C.) power lines. Low voltage flow meter and sensor wires should go through the rubber grommet on the side of the box. The wiring of the box is shown in

Note that the electronic housing is not designed for outdoor use, and must be properly enclosed if this is desired.

IV FLOW METER PLUMBING

For maximum accuracy, the pipe size should match flow meter opening for 10 diameters before the meter and 5 diameters following. See Figure 11-1.

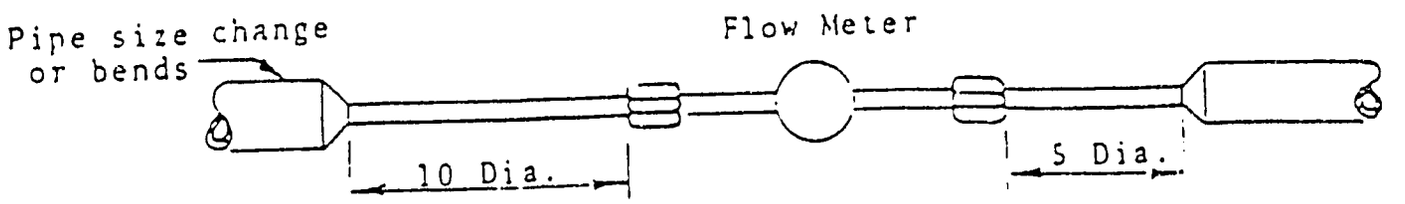

FIGURE 11-1

COLD WATER FLOW METER INSTALLATION (120°F)

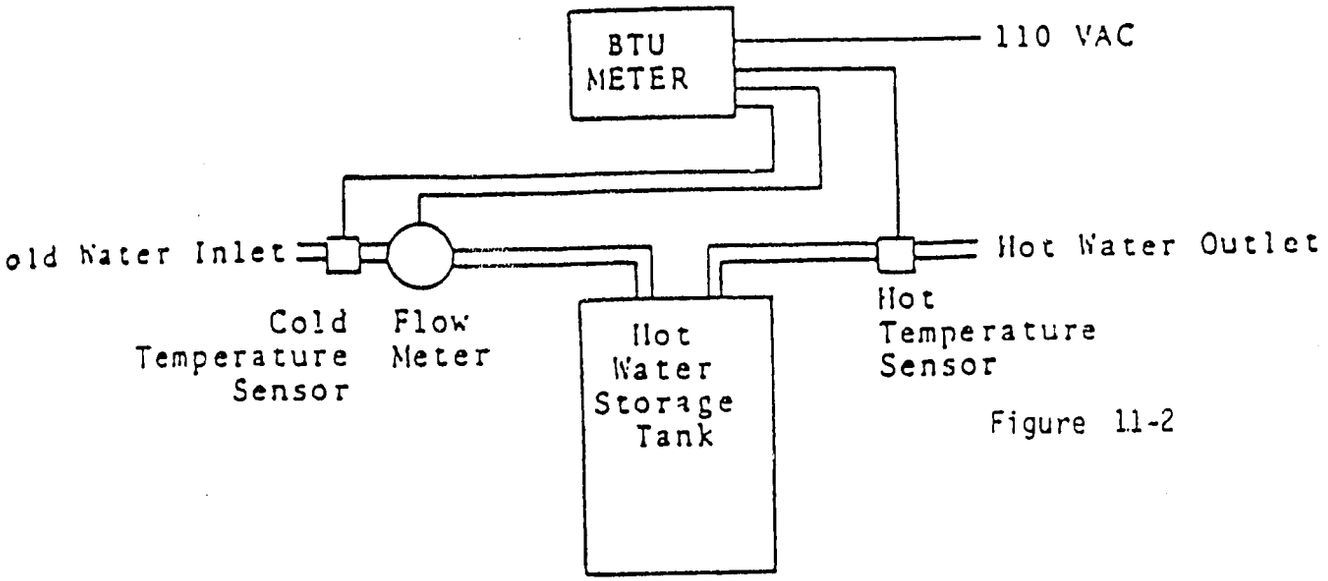

Figure 11-2

BTU METER

See Installation Diagram on inside front cover of BTU Meter Box

---

HOT WATER FLOW METER INSTALLATION (195°F)

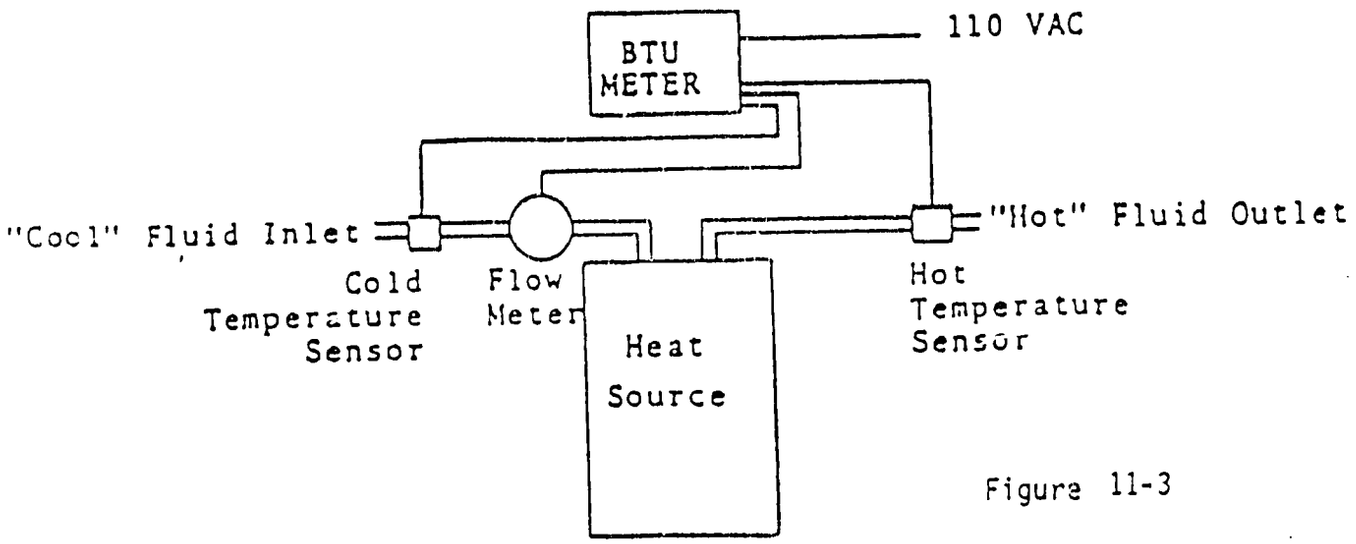

Figure 11-3

BTU METER

See Installation Diagram on inside front cover of BTU Meter Box

RS 805 BTU METER

INSTALLATION DRAWING

Figure 11-4

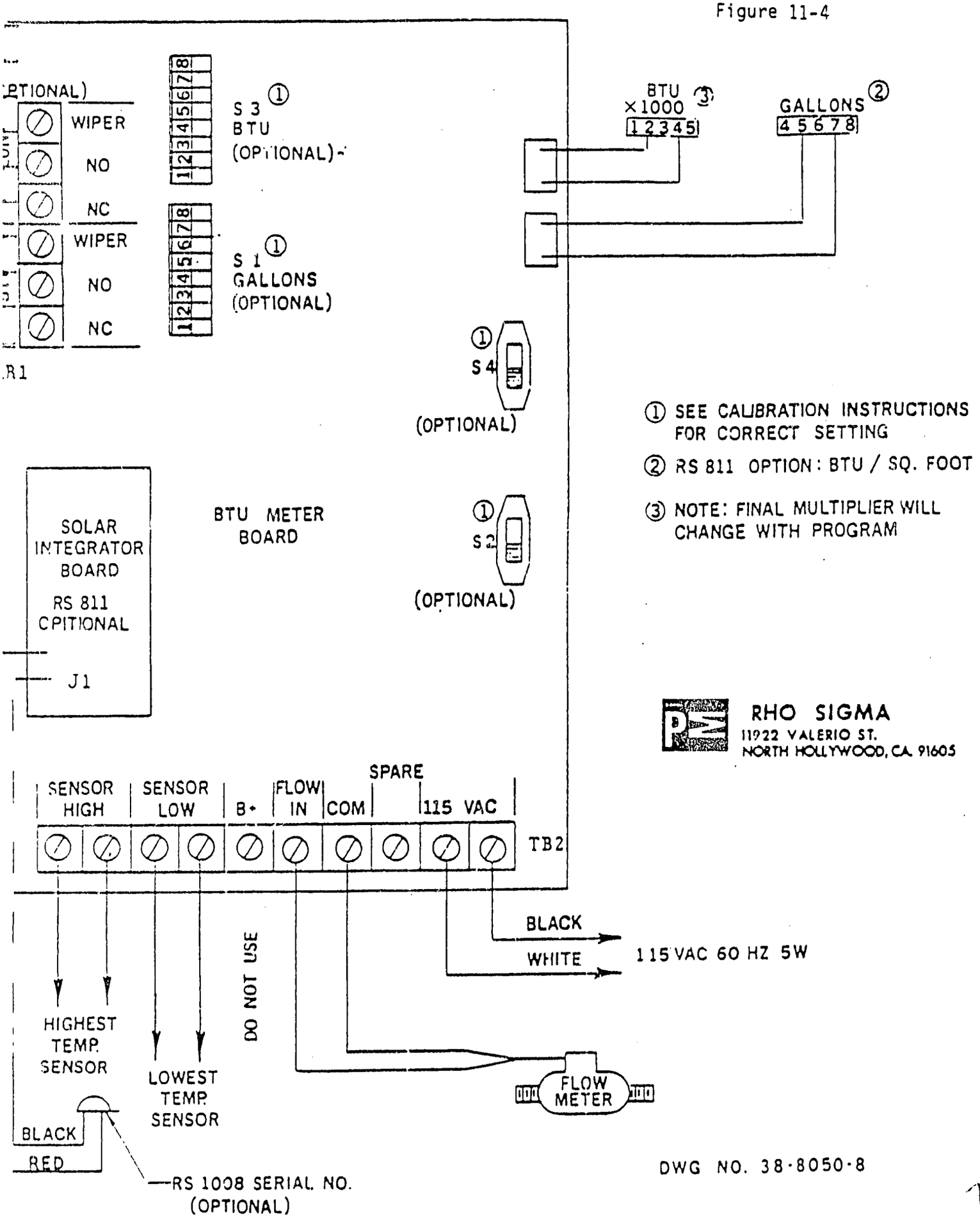

RS805

PRODUCT INFORMATION BULLETIN

RS805 BTU METER

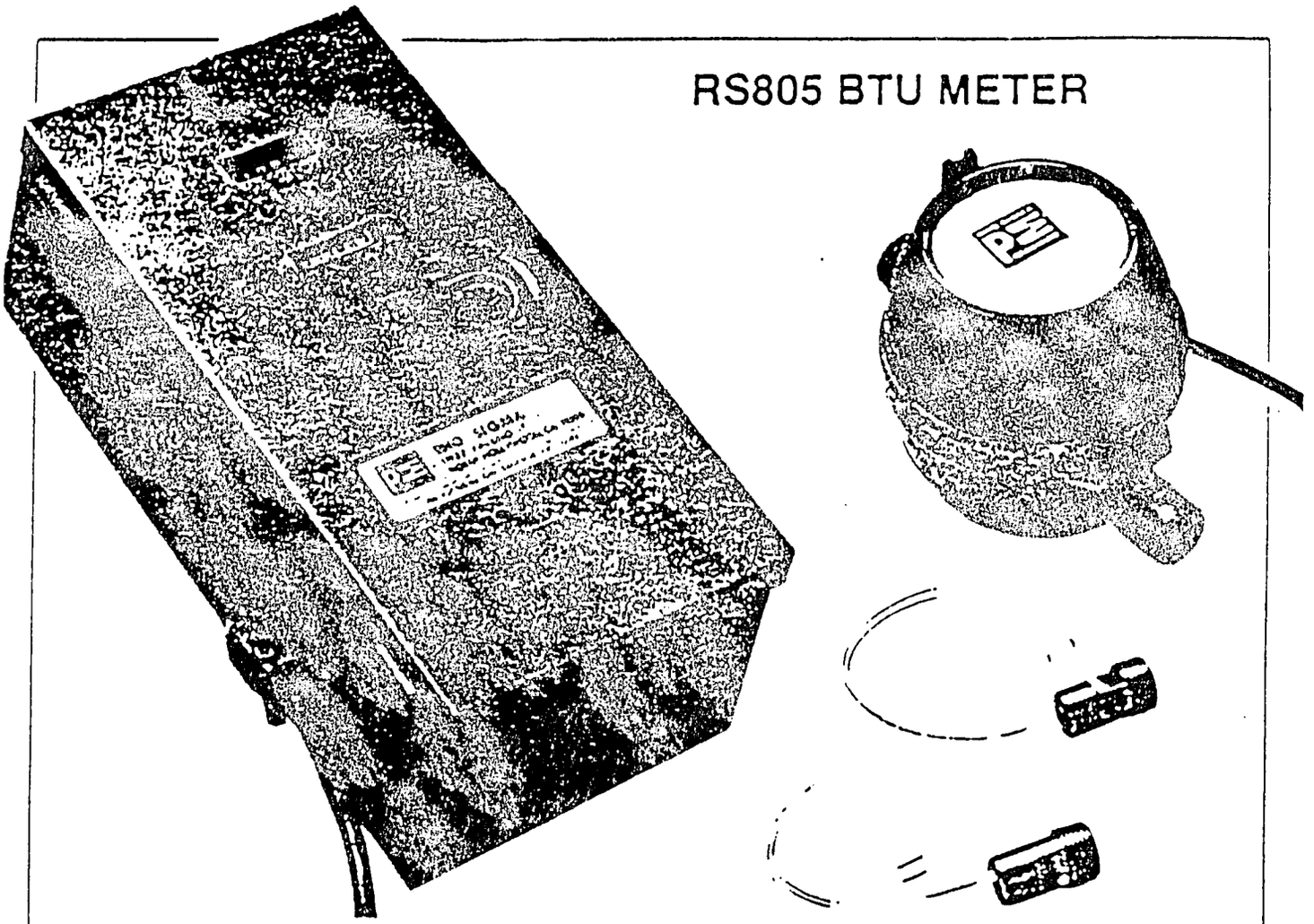

Rho Sigma's BTU meter, Model RS805, is a complete package for measuring and recording thermal energy consumption. It is ideally suited for solar energy, heat recovery, systems monitoring and evaluation, and load shedding.

FEATURES

- Digital readout display of BTUs consumed
- Digital readout display of gallons of water used
- High reliability solid-state circuits
- Compact housing, 4 × 8 × 12 inches
- Integrated circuitry for low power drain
- Overall system accuracy ±1.78% of full scale
- Temperature sensors accurate to ±1°F from 32 to 212°F
- Flow meter accurate to within 1.5% from .25 to 30 gpm
- No loss of data due to power failure

Optional features available:

- integration of available solar energy to measure overall system performance
- tamperproof indicator to prevent unmeasured energy consumption
- temperature output to chart recorder conversion for plotting load profiles vs. time
- non-volatile LED readouts (back-up battery)

RHO SIGMA 11922 VALERIO STREET • NORTH HOLLYWOOD, CA 91605 (213) 982-6800

GENERAL DESCRIPTION

The RS805 provides an economical, reliable means of measuring energy consumption (BTUs) in solar energy systems at the point of use.[1] This is accomplished by comparing temperatures of the inlet fluid and the fluid at its exit (generally from the storage tank); multiplying the temperature differential between these two points by the rate of flow, and integrating the result over time. This provides a reading of the BTUs consumed.

Two output registers are provided; one shows the BTU reading and the other, using the flow rate data, shows total gallons of water consumed.

The RS805 obtains the data for these operations from the flow meter and two temperature sensors included in the RS805 package. The following diagram shows the relationship of the BTU meter, flow meter, temperature sensors, and a typical solar energy system.

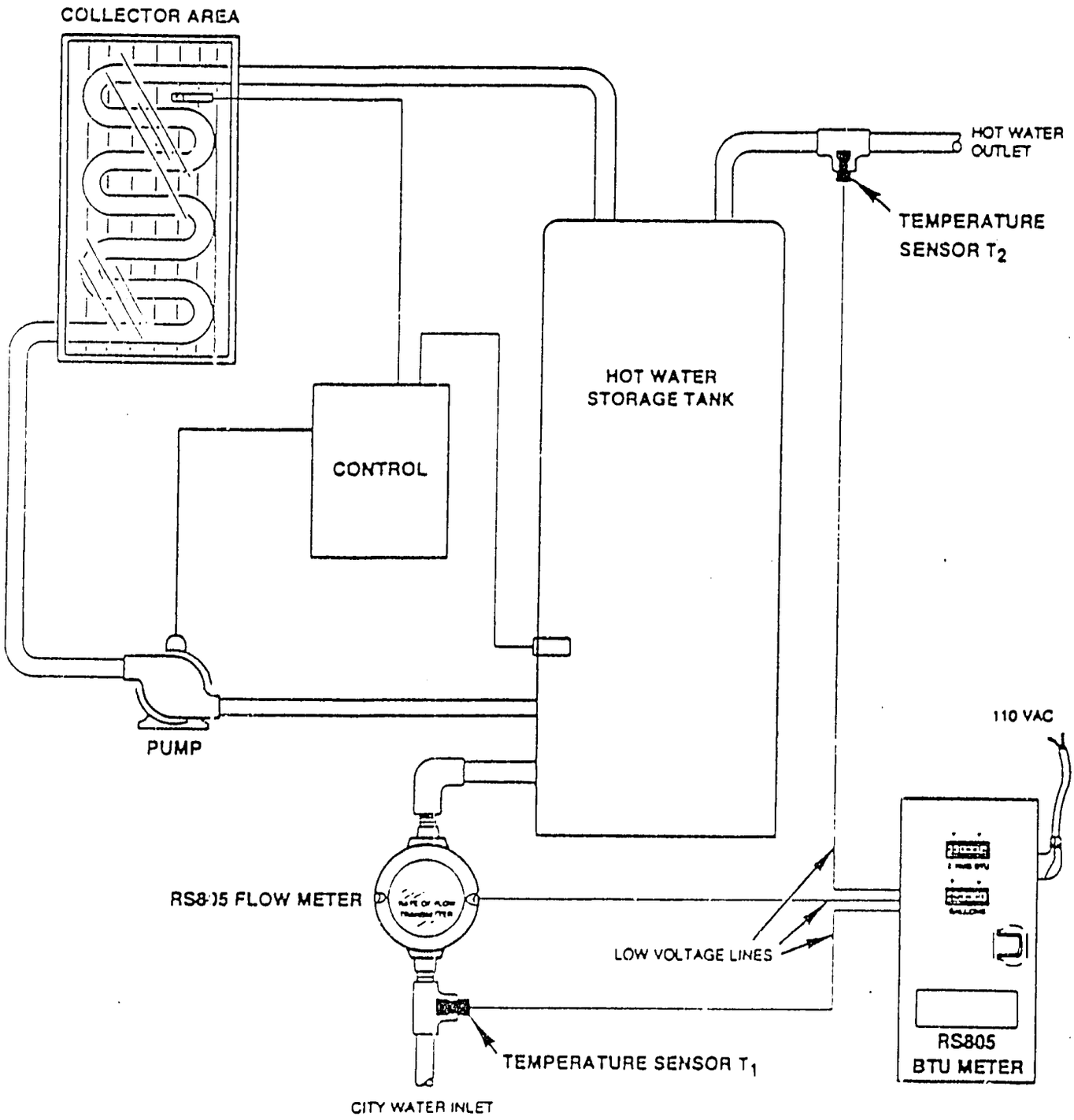

[1] *BTU = British Thermal Unit; the amount of energy required to raise the temperature of 1 lb of water 1°F under conditions of standard temperature and pressure.*

References

1) Meterological Aspects of the Utilization of Solar Radiation as an Energy Source, World Meterological Organization, Technical Note No. 172, 1981; Secretarial of the World Meterological Organization Geneva - Switzerland.

124.

APPENDIX

A. SOLAR SYSTEM SIZING FOR JAMAICA - F-chart.

B. A NOTE ON PIPE INSULATION.

C. SIMPLIFIED SOLAR COLLECTOR TEST PROCEDURES.

APPENDIX A: SOLAR SYSTEM SIZING FOR JAMAICA - F-chart:

F chart 4.0 was used to size the solar system. Table 1 lists the parameters used for sizing. The insolation and ambient temperature data was from the World Meterological Atlas and from the Barbados hospital study respectively. See Table 2 for a sample output.

For sizing, it was assumed that the storage tank would be sized to provide two US gallons of storage per square feet of collector and the pump (or thermosiphon action) would provide a collector flow rate of one gallon per hour per square foot of collector. (Except as noted, all gallons refer to imperial gallons = 1.2 US gallons). Since backup is not recommended, 1.5 US gal/sq ft of collector is the recommended tank size, if it is also close to the hot water demand in gals per day. The remaining parameters to be optimized are collector azimuth, tilt and area.

Collector Azimuth

Collectors should be oriented to ± 15 degrees of south. An orientation of up to ± 45 degrees east or west of south is acceptable if collector area is increased by 15%. These recommendations are based on practical experience in Florida and not from F chart 4.0 which is strictly valid only for south orientations. F chart 4.1 will remove this restriction.

Collector Tilt

To determine the optimal collector tilt, collector areas of 500 and 700 square feet were used and tilt angles varied from 0 to 40 degrees. The resulting optimums were identical for both collector sizes. Table 3 presents the results for the 700 square foot collector.

Table 3. Tilt optimization for 700 square foot collector and a load of 833 gallons per day

Tilt Angle	Solar Fractions Annual	Monthly Best/mo	Monthly Worst/Mo	Δf Between bst & wst mo.
0	0.83	0.94/May	0.67/Jan	0.27
5	0.85	0.93/May	0.72/Jan	0.21
10	0.86	0.93/Apr	0.76/Jan	0.17
15	0.87	0.93/Oct	0.80/Jan	0.13
20	0.87	0.94/Oct	0.83/Jan	0.11
25	0.87	0.95/Oct	0.81/Jun	0.14
30	0.86	0.95/Oct	0.78/Jun	0.17
35	0.84	0.94/Oct	0.74/Jun	0.20
40	0.82	0.92/Oct	0.70/Jun	0.22

The first thing to note is that the extreme insensitivity of annual f to the tilt angle. This points to the minimum tilt angle to minimize structural support costs. However in the range of a 10 degree - 30 degree tilt, there is a significant difference between the best and worst monthly solar fractions. Although a uniform monthly load was used for the analysis, in fact the loads are likely to be higher in the winter months. For this reason, we recomend a tilt angle around 25 degrees. Any higher tilt, although tending to increase the winter performance, will be offset by the higher wind losses, particularly if the headers are external and uninsulated. The wind induced line losses have not been considered in the F chart analysis.

For this study, a typical Jamaican manufacturer's solar collector of moderate performance was used (see Table 1 for collector characteristics). An interesting outcome of this analysis with 120 degree F hot water delivery temperature and 80 degree F cold water inlet is that the FSEC intermediate temperature rating is an accurate predictor of system output in the annual solar fraction range of 0.7 to 0.8. The FSEC rating for this collector would have been 519 Btu/sf/day. The F chart 4.0 output is 502 for an annual f of 0.8 and 533 Btu/sf/day for f = 0.7. So use of the FSEC intermediate temperature rating would permit a rather accurate and easy estimation of the system performance.

Table 4 shows the simple payback for a series of collector sizes.

Table 4. Simple payback for Jamaican solar systems. See Table 1 for thermal data. All $'s are Jamaican $'s. Current prices were obtained from Ministry of Mining and Energy.

Electricity = 25 cents/Kwh = J$73.2/MMBtu @ eff = 1.0
Oil = J$1.58/Imp. gal = J$15.3/MMBtu @ eff = 0.6
LPG (Propane) = J$2.05/Imp. gal = J$24.4/MMBtu @ eff = 0.7
Hot water load = 833 gpd = 125.3 MMBtu/yr

Coll. Area Sq. Ft.	System Cost 1000 J$	f	Simple Payback, Years LPG	Elec	Oil
100	20.0	0.21	31.2	10.4	49.6
200	25.0	0.37	22.1	7.4	35.3
300	30.0	0.50	19.6	6.5	31.3
400	35.0	0.62	18.5	6.2	29.4
500	40.0	0.71	18.5	6.14	29.4
600	45.0	0.80	18.3	6.13	29.3
700	50.0	0.87	18.8	6.3	29.4
800	55.0	0.94	19.2	6.4	30.6
900	60.0	0.98	20.0	6.7	32.0
1000	65.0	1.0	21.3	7.1	33.9
Annual fuel costs with no solar:			3059	9172	1917

Life cycle costing results along with their assumptions are presented in Table 5. This was done using the TI-59 F chart program.

Table 5. Present Value of Life Cycle Savings From Solar Systems

Assumptions are those listed in Table 4 plus the following:

System life	=	25 yr.
Operation and maint. cost	=	1% per yr.
General inflation	=	7% per yr.
Fuel inflation	=	10% per yr.
Discount rate	=	7% per yr.
Salvage value	=	0
Collector area dependent costs	=	J$50 per sq.ft
Collector area independent costs	=	J$15,000

F chart assumes solar costs are additional to a convential system which will be used for backup

Coll. Area Sq. Ft.	System Cost 1000 J$	Area/ Demand	f	P.V. Of Life Cycle Savings From Solar(1000J$) LPG	Elec	Oil
100	20.0	.12	0.21	-3.2	39.3	-11.3
200	25.0	.24	0.37	6.7	81.9	-7.3
300	30.0	.36	0.50	13.8	115.3	-5.2
400	35.0	.48	0.62	19.8	145.7	-3.7
500	40.0	.60	0.71	22.7	166.9	-4.1
600	45.0	.72	0.80	25.7	188.2	-4.6
700	50.0	.84	0.87	26.6	203.3	-6.3
800	55.0	.96	0.94	27.6	218.5	-8.0
900	60.0	1.08	0.98	25.5	224.5	-11.6
1000	65.0	1.20	1.0	21.3	224.4	-16.5
Annual fuel costs with no solar				3059	9172	1917

The optimum collector area to load in terms of the ratio of square feet of collector per gallon of demand depends on the economic criteria used. Table 6 presents the results based on table 4 and 5 results.

Table 6. Optimum collector areas for different fuel

Criteria	Fuel Type Gas (LPG)	Elec	Oil
Maximize LCC savings	0.96	1.08	0.48
Simple payback	0.72	0.72	0.72
(Δsav/Δcost)	0.48	1.08	0.0

Recommended optimum for all sytems = 0.72 sq ft/imp.gal load.

Maximum LCC (life cycle cost) saving and simple paybacks are commonly used criteria. In our view maximization of LCC saving is a poor criteria and it tends to too large a system. The simple payback is not as bad a criteria as it might first seem. This is because in general the fuel inflation rate and the discount rate (for government) are pretty close to the general inflation rate. So the simple payback, usually closely reflects the true payback if operation and maintenance costs are small.

The third criteria is perhaps the best criteria. This is marginal cost effectiveness, i.e., one evaluates whether the increase in LCC savings for the next larger sized array is greater than the cost. e.g. in table 5 we see that under the gas column that increasing the collector area from 400 to 500 square feet, increases LCC savings by only J$2,900 while increasing costs by J$5,000. Therefore the optimum area is 400 square feet or 0.48 square feet/gpd demand. Against oil this criteria indicates that no solar system is the best choice!

Of course this kind of cost benefit analysis does not account for the social and environmental benefits of solar energy viz. increasing local jobs, increased balance of payments and thus reduced inflation, less dependence on foreign technology etc. A true macro economic analysis considering such factors will undoubtedly favor solar energy for Jamaican hospitals against any alternative fuel.

It must be noted that this analysis was done for a low performing collector when compared to current U.S. collectors that use selective surface and iron free glass. Undoubtedly Jamaican technology will produce better collectors in the future. Also since first cost is a real barrier to installation of solar systems, and since these solar systems will probablly be installed without a backup system and mostly in cases where there is currently no hot water; we recommend a system with no backup and a minimum collector area of 0.7 square feet/gpd demand. It must be remembered that in solar systems optimums are never well defined. The major difficulty will be in estimating the demand.

The collector area/gpd demand can be increased as budgets permit.

A note: F Chart 4.0 significantly overpredicts solar system performance when compared to the TI-59 F chart program. This is because the basis of the two programs are different. From the authors' experience in comparing field performance to predictions; it appears F chart 4.0 is a good predictive tool and F chart 4.1 will be even better as it will account for off south collectors and the hot water correlations will be improved.

Table 1. Solar DHW Parameters Used In Sizing

COLLECTOR PARAMETERS		
C1. COLLECTOR AREA	700.00	FT2 (varied)
C2. FR-UL PRODUCT	1.02	BTU/HR-FT2-DEG
C3. FR-TAU-ALPHA (NORMAL INCIDENCE)	0.55	
C6. NUMBER OF COVERS	1.00	
C7. INDEX OF REFRACTION	1.53	
C8. EXTINCTION COEFFICIENT X LENGTH (KL).....	0.04	
C9. INCIDENCE ANGLE MODIFIER CONSTANT	0.15	
C10. COLLECTOR FLOW RATE * SPECIFIC HEAT/AREA	9.67	BTU/HR-FT2-DEG
C12. COLLECTOR SLOPE	0.00	DEGREES (varied)
C13. COLLECTOR AZIMUTH	0.00	DEGREES
C14. GROUND REFLECTANCE	0.20	
STORAGE UNIT PARAMETERS		
S1. TANK CAPACITY/COLLECTOR AREA	17.12	BTU/DEG F-FT2
S2. STORAGE UNIT HEIGHT/DIAMETER RATIO	1.50	
S3. HEAT LOSS COEFFICIENT	0.20	BTU/HR-FT2-DEG
S4. ENVIRONMENT TEMPERATURE (-1000 FOR TENV=TAMB) ..	-1000.00	DEG F
S5. HOT WATER AUXILIARY TANK UA	10.00	BTU/HR-DEG F
S6. HOT WATER AUX TANK ENVIRONMENT TEMPERATURE	80.00	DEG F
LOAD PARAMETERS		
L3. HOT WATER USE	1000.00	GALLONS/DAY(US)
L4. HOT WATER SET TEMPERATURE	120.00	DEG F
L5. WATER MAINS TEMPERATURE	80.00	DEG F
AUXILIARY PARAMETERS		
A3. HOT WATER AUXILIARY FUEL (1=GAS,2=ELEC,3=OIL) ..	2.	
A4. AUXILIARY WATER HEATER EFFICIENCY	1.00	

?

230

Table 2. Sample F Chart Output

******* FCHART ANALYSIS (VERSION 4.0) **********

RUN FOR OPTIMUM TILT ANGLE WITH 700 SQ.FT COLLECTOR

KINGSTON JAM LATITUDE 18.0

**** LOOP AND OPTIMIZATION PARAMETERS ****

C12. COLLECTOR SLOPE ..... 25.00 DEGREES

THERMAL PERFORMANCE

	HT (MMBTU)	TA (DEG-F)	HWLOAD (MMBTU)	QU (MMBTU)	QLOSS (MMBTU)	FDHW
JA	37.45	75.9	10.64	10.55	1.10	0.86
FE	35.19	75.9	9.61	9.59	1.05	0.92
MA	40.71	75.9	10.64	11.13	1.16	0.91
AP	36.68	78.1	10.30	9.85	1.03	0.88
MA	36.79	80.1	10.64	10.09	0.96	0.84
JU	33.13	81.0	10.30	9.00	0.88	0.81
JU	36.25	80.1	10.64	9.95	0.94	0.82
AU	35.52	80.1	10.64	9.70	0.97	0.84
SE	36.50	80.1	10.30	10.36	0.98	0.88
OC	39.29	79.0	10.64	10.99	1.12	0.95
NO	34.16	79.0	10.30	9.88	0.97	0.85
DE	36.51	77.0	10.64	10.26	1.08	0.87
YR	438.19	78.5	125.29	121.37	12.25	0.87

PURCHASED ENERGY SUMMARY

	GAS	ELECTRIC	OIL	TOTAL
USE (MMBTU)	0.00	16.29	0.00	16.29
COST ($)	0.00	102.63	0.00	102.63

APPENDIX B: A NOTE ON PIPE INSULATION

In solar literature one inevitably finds the recomendation of well insulating the solar piping. However in Jamaica, pipe insulation must be imported and is expensive.

On the basis of the following analysis we recommend that solar system piping to provide hot water for hospitals or residences in Jamaica (and for that matter in the entire caribbean) may not need to be insulated if the pipes are protected from the wind, painted black and are exposed to sunlight. It will definitely not be necessary to insulate the piping at all if a galvanized or aluminum sheet metal pipe cover is painted black and installed over the pipe to cut down the wind induced convective loss. The basic reason for this conclusion is that with the plentiful sunshine and warm ambient temperatures there is actually a heat gain into the fluid flowing in black sunlit solar piping for low wind speeds. If the local windspeed is high then there will be a heat loss, and that can be nullified by a black sunlit pipe cover or by providing an extra 40 square foot of collector for every 100 linear feet of uninsulated piping.

Analysis

Case i) Pipe is insulated with 1/2" wall thickness closed cell foam type insulation. The insulation is painted white on the outside for sunlight protection of the insulation.

d = 1 1/2"
t = 1/2"
K (insulation)
= 0.3
Btu in/
hr sq ft degree F

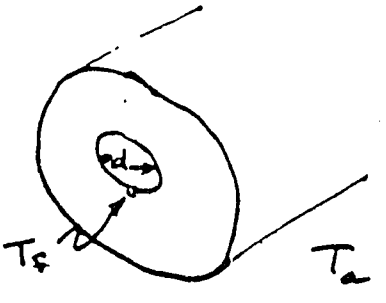

The heat flux per unit area of piping is given by:

$$q/(T_f - T_a) = 1 \Big/ d/2k \ln(1 + 2t/d) \quad \ldots (1)$$

The denominator of the right hand side is the effective R value of insulation in cylindrical geometry.

Substituting the values we obtain:

$$R = 1.28 \quad \ldots (2)$$

For 100 feet of piping the loss rate UA value will be:

APPENDIX B: A NOTE ON PIPE INSULATION

In solar literature one inevitably finds the recomendation of well insulating the solar piping. However in Jamaica, pipe insulation must be imported and is expensive.

On the basis of the following analysis we recommend that solar system piping to provide hot water for hospitals or residences in Jamaica (and for that matter in the entire caribbean) may not need to be insulated if the pipes are protected from the wind, painted black and are exposed to sunlight. It will definitely not be necessary to insulate the piping at all if a galvanized or aluminum sheet metal pipe cover is painted black and installed over the pipe to cut down the wind induced convective loss. The basic reason for this conclusion is that with the plentiful sunshine and warm ambient temperatures there is actually a heat gain into the fluid flowing in black sunlit solar piping for low wind speeds. If the local windspeed is high then there will be a heat loss, and that can be nullified by a black sunlit pipe cover or by providing an extra 40 square foot of collector for every 100 linear feet of uninsulated piping.

Analysis

Case i) Pipe is insulated with 1/2" wall thickness closed cell foam type insulation. The insulation is painted white on the outside for sunlight protection of the insulation.

d = 1 1/2"
t = 1/2"
K (insulation)
= 0.3
Btu in/
hr sq ft degree F

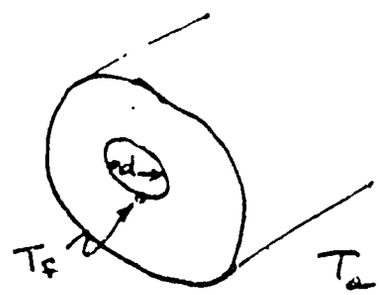

The heat flux per unit area of piping is given by:

$$q/(T_f - T_a) = 1 \Big/ \frac{d}{2k} \ln(1 + 2t/d) \quad \ldots (1)$$

The denominator of the right hand side is the effective R value of insulation in cylindrical geometry.

Substituting the values we obtain:

$$R = 1.28 \quad \ldots (2)$$

For 100 feet of piping the loss rate UA value will be:

32

$UA = 100 \times \pi \times 1.5/12 \times 1/1.28 = 30.7$ Btu/hr per degree F

Case ii) Bare black pipe, which is sunlit.

α = absorptance = 0.9
h = heat transfer coefficient per unit surface area between pipe and ambient
H_t = Incident solar radiation

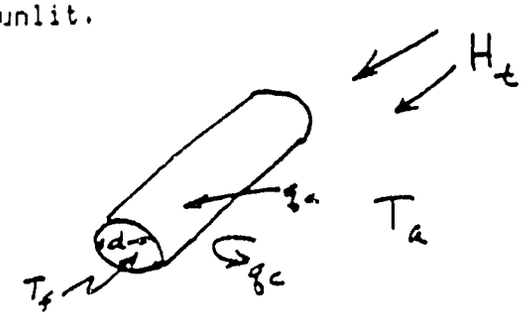

Let us assume the pipe is sunlit over half of its circumference while the heat loss is over the entire circumference. Then

q_a = absorbed solar energy = $H_t A/2$
q_c = heat convected from the pipe by wind = $hA\ (T_f - T_a)$ assuming pipe surface is at fluid temperature
q_g = net heat gain (or lost) into the fluid

In steady state

$$q_g = q_a - q_c$$

$$\text{or } q_g/A = \alpha H_t/2 - h\ (T_f - T_a)$$

Assume that under average operating conditions

H_t = 250 Btu/hr/sq. ft
α = 0.9
T_a = 80 degree F

We solve T_f for $q_g/A = 0$

$$T_f = T_a + \alpha H_t/2h = T_a + 112.5/h$$

The h value for pipes have been calculated from ASHRAE and Eckert & Drake and are shown below for various windspeeds along with the T_f value below which the fluid will actually gain heat from the pipe rather than lose heat.

Table B1 Analysis of sunlit pipe heat loss. T_f indicates that pipe fluid below the value will gain heat.

Windspeed (mph)	h btu/sq ft per degree F	T_f (degree F)
still air	1.0	192.5
3.0 (typical of protected area)	5.4	100.8
7.0 (typical exposed)	8.9	92.6
14 mph (very windy)	13.5	88.3

It is thus seen that if the piping is protected from the wind by careful pipe runs or by a black protective cover there will not be an appreciable heat loss for fluid temperatures around 100 degree F.

However for a 120 degree F fluid temperature the losses at typical exposed condition (7 mph wind) will be

$$q_L/A = 0.9 \times 250/2 - 8.9\ (120-80) = -243.5$$

or for the 40 degree F delta T, the heat loss coefficient is:

$$q_L/A = -6.09 \text{ Btuh/Sq ft per degree F}$$

For 100 feet of 1 1/2" piping (area = 39.2 square feet),

The losses will be:

$$UA = 240 \text{ Btuh/degree F}$$

about eight times the value of insulated piping.

Therefore it is essential to follow the recommended practice stated earlier to reduce this loss. Another alternative, which may be feasible in some cases, will be to provide a square foot of extra collector area for every square foot of exposed uninsulated pipe area.

APPENDIX C

Simplified Solar Collector Test Procedures

Let:

A = Gross area of the collector
H_t = Insolation on the collector plane
τ = Transmittance of cover plate
α = Absorptance of the absorber
T_i = Collector inlet tempereture
T_o = Collector absorber plate temp
$\dot{m}C_p$ = massflowxcapacitance of fluid through collector
F_r = Collector heat removal factor
η = Collector instantaneous efficiency

Then to the first order, under quasi steady state conditions

$$\dot{m}C_p(T_o - T_i) = F_r A\left[H_t \tau\alpha - U_l(T_i - T_a)\right] \quad \cdots (1)$$

This is usually rewritten as

$$\eta = \frac{\dot{m}C_p(T_o - T_i)}{AH_t} = F_r\tau\alpha - \frac{F_r U_l (T_i - T_a)}{H_t} \quad \cdots (2)$$

The factors which need to be known for performance estimation are:

$$F_r\tau\alpha \quad \text{and} \quad F_r U_l$$

The ASHRAE 93-77 test procedure describes a test method using a closed fluid test loop to determine collector efficiency. While accurate, this method is expensive. Although expensive, it is recommended that Jamaica develop and maintain one or two ASHRAE 93-77 test loops; however, some much simpler tests are suggested below which can be used by most government organizations and collector manufacturers for quick determination of collector performance

The F_rU_l test:

Test Setup: (see figure 1)

An open loop indoor test setup, it needs a large insulated tank containing about 130°F water.

A small circulating pump keeps the water in the tank always mixed with special mixing diffusers as shown. The collector is piped as shown. To simulate the night sky, a black cloth is placed one foot above the collector. The flow rate is measured with a bucket and stop watch.

Test Procedure

Water in the tank is heated up and mixing pump is run. The downstream globevalve is opened to desired flow rate. Temperatures are monitored, until steady state is achieved which should not take longer than 30 minutes. Since $H_t = 0$, the outlet will be cooler than inlet and

$$\dot{m} c_p (T_i - T_o) = F_r U_l (T_i - T_a) \quad \cdots (3)$$

From eq. 3 $F_r U_1$ can be determined since everything else is known.

The $F_r(\tau\alpha)_r$ Test:

Test Setup (see figure 2)

Place collector outdoors under noon time sun with water in it and both ends capped with room for water expansion in collector. Tilt collector so that noon time sun will be perpendicular to it.

Test Procedure

Let collector cook in the sun. During noontime, say 1 hour before to one hour after, monitor T_p, H_t and WS. WS should be below 10 mph for glazed collectors and should be measured near the collector cover. Wait until collector's panel temperature is stable. At that point the collector is at stagnation equilibrium, efficiency is zero and

$$F_r H_t \tau\alpha = F_r U_1 (T_p - T_a)$$

Then $F_r \tau\alpha = F_r U_1 (T_p - T_a)/H_t$

and can be determined since $F_r U_1$ has been determined from the night test.

236

This test procedure will be also of great help in determining collector reliability, because the tests can be repeated after letting the collector stagnate for 30-45 days and retesting to see if there is any thermal degradetion. Moreover multiple collector arrays can be tested also.

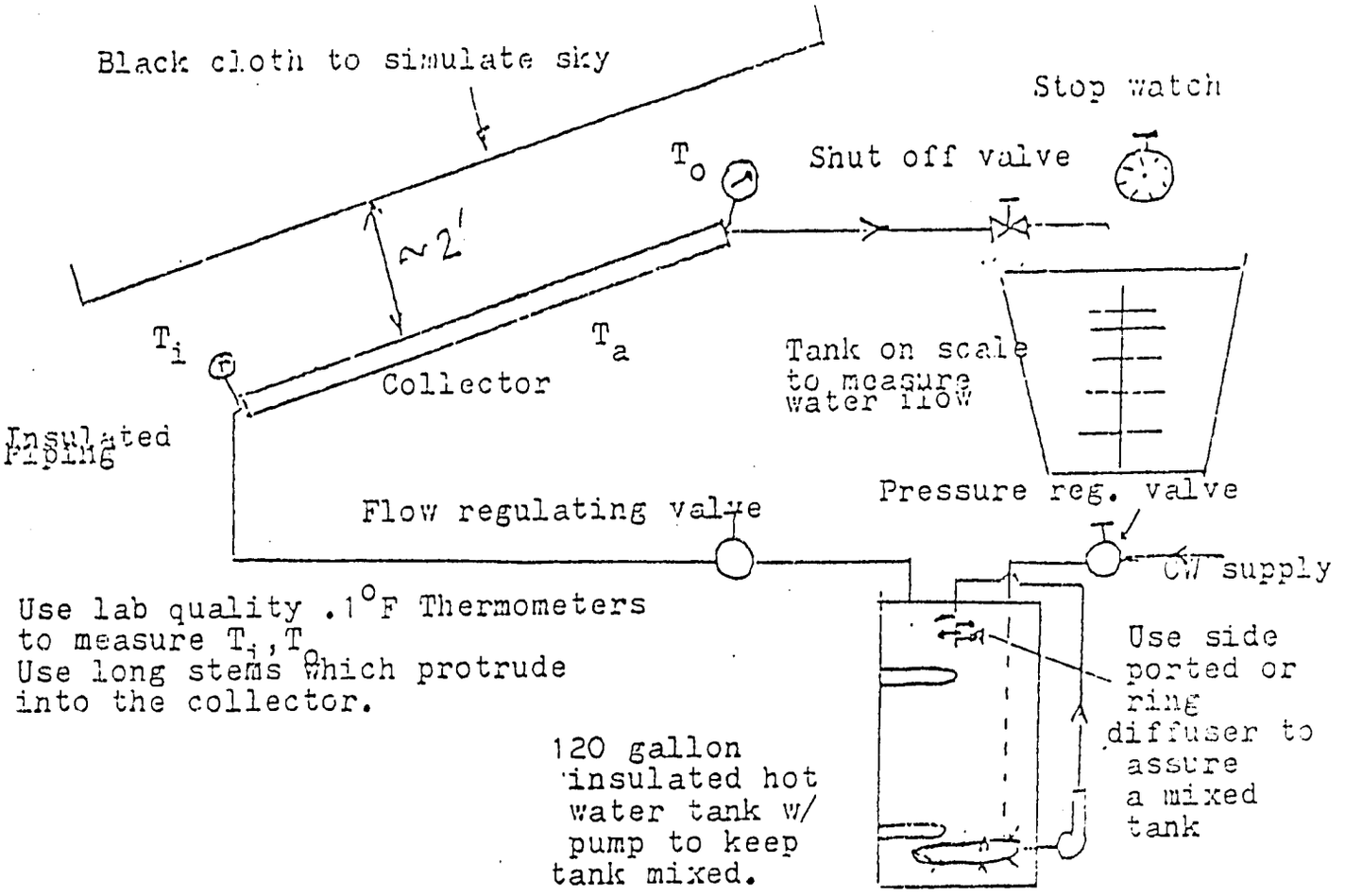

Figure 1 Indoor Test stand for $F_R U_L$ tests

Stagnate collector with water in them and ends capped with room for expansion
At stagnation $T_i = T_o$

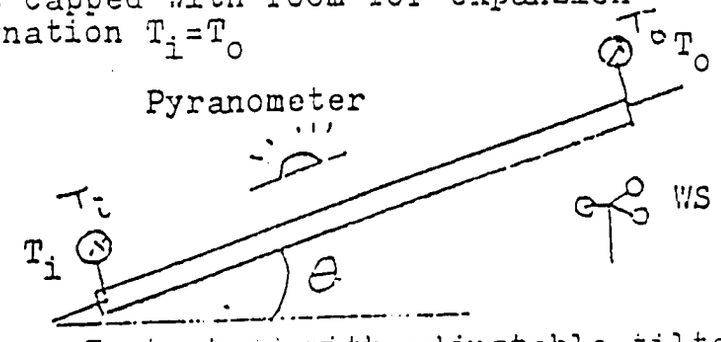

Construct a fence around test area to keep winds below 5 mph

Test stand with adjustable tilts so that collector is normal to noontime sun.

Figure 2 Outdoor test stand for the $F_R \tau \alpha$ tests